Universidade de Aveiro Departamento de Física
2020

Leandro Alves Vaz

Otimização da Exploração de Aquacultura Estuarina: Ferramentas de Modelação

Optimization of Estuarine Aquaculture Exploitation: Modelling Approach

Universidade de Aveiro Departamento de Física
2020

Leandro Alves Vaz

Otimização da Exploração de Aquacultura Estuarina: Ferramentas de Modelação

Optimization of Estuarine Aquaculture Exploitation: Modelling Approach

Dissertação apresentada à Universidade de Aveiro para cumprimento dos requisitos necessários à obtenção do grau de Doutor em Ciência, Tecnologia e Gestão do Mar, realizada sob a orientação científica do Doutor João Miguel Dias, Professor Associado com Agregação do Departamento de Física da Universidade de Aveiro, e do Doutor Ramon Gómez-Gesteira, Professor Catedrático da Faculdade de Ciências de Ourense da Universidade de Vigo

O autor foi financiado pela Fundação para a Ciência e Tecnologia (FCT), através da bolsa de Douroramento com a referência SFRH/BD/103973/2014, no âmbito do Quadro de Referência Estratégico Nacional (QREN) e do Programa Operacional de Potencial Humano (POPH), comparticipado pelo Fundo Europeu e por fundos nacionais do Ministério da Educação e Ciência (MEC). Este trabalho foi também desenvolvido no âmbito do Projecto AquiMap (MAR-02.01.01-FEAMP-0022), co-financiado pelo Programa MAR2020, Portugal 2020 e União Europeia através do Fundo Europeu dos Assuntos Marítimos e das Pescas.

o júri / the jury

presidente / president	**Professora Doutora Ana Isabel Couto Neto da Silva Miranda** Professora Catedrática da Universidade de Aveiro
vogais / examiners committee	**Professor Doutor Ramiro Joaquim de Jesus Neves** Professor Associado com Agregação do Instituto Superior Técnico da Universidade de Lisboa
	Doutor Juan José Taboada Hidalgo Investigador Coordenador da Meteogalicia - Servicio Meteorológico de La Xunta de Galicia
	Doutor João Daniel Lencart e Silva Gestor Sénior de Projetos da Longline Environment, Ltd
	Doutora Magda Catarina Ferreira de Sousa Investigadora Doutorada da Universidade de Aveiro
	Professor Doutor João Miguel Sequeira Silva Dias Professor Catedrático da Universidade de Aveiro

acknowledgements

I would like to thank many people who supported and participated actively during this intensive journey as a PhD student. Thank you all for the help, encouragement and friendship.

In first place, a special thank to my supervisor, Prof. João Miguel Dias, not only for the guidance and good advices during this 4 year journey, but also to be friendship and trust during the last years. To my co-supervisor, Prof. Moncho Gómez-Gesteira, for his scientific supervision, suggestions and recommendations.

To the NMEC (Estuarine and Coastal Modelling Group) working group, in particular to Nuno Vaz for the daily exchange of ideas, and help in the results analysis. A special acknowledgement is also given to Magda Sousa for the help in Delft3D problem-solving. To Ana Raquel Costa for valuable suggestions in the analysis of model performance.

To Marisela Des Villanueva (EPhysLAB, University of Vigo) to help me in organizing data that have become essential for the achievement of the goals proposed in this work.

To Silja Frankenbach for the unfailing help in the laboratory. To Prof. João Serôdio for kindly allowing me to use his lab for sampling processing, providing all the necessary material.

To Rui Ruela and Joana Mendes for the help during the field trips.

Thanks are also due to Prof. Eduarda Pereira and Dr. Pedro Coelho, from Chemistry Departments of University of Aveiro for supplying some of the equipment used in field monitoring.

To my friends, and to the most important and supportive people of my life, my family. To my parents, for your unconditional support and love. You are the reason behind my successes. To my parents-in-law and to Bernardo for the support and affection. The last but not least, to Vanessa for walking by my side in life, giving me all the love and support.

Thank you all.

Palavras-chave Aquacultura, Ria de Aveiro, Rias Baixas, Modelação Numérica, Modelo de Habitat, Hidrodinâmica, Qualidade da Água.

Resumo

A aquacultura é uma das atividades económicas com maior taxa de crescimento. Em 2006, já era responsável por cerca de 40% do consumo total de peixe, e em 2012, consolidou-se como a principal fonte de alimentos de origem marinha. Contudo, este forte e rápido desenvolvimento do setor tende a refletir-se em significativos impactos ambientais, e em novos desafios na gestão e planeamento das zonas costeiras. Neste contexto, este trabalho pretende contribuir para a sustentabilidade do sector, identificando locais preferenciais para a exploração aquícola de forma sustentável, com um impacto ambiental mínimo e um custo relativamente baixo, sob condições ideais de hidrodinâmica e qualidade da água na Ria de Aveiro (Portugal) e Rias Baixas (Espanha), os dois sistemas com maior exploração no NW da Península Ibérica. Este estudo torna-se particularmente relevante porque o mapeamento das localizações mais adequadas à exploração aquícola nunca foi efetuado em nenhuma das áreas de estudo, revelando-se fulcral, não só para demonstrar o potencial da atividade comercial e incentivar o investimento das empresas, mas principalmente para permitir um direcionamento adequado dos investimentos, e contribuir para a sustentabilidade do setor. Para alcançar este objetivo foi aplicada uma metodologia multidisciplinar que compreendeu a realização dos seguintes passos: 1 - caracterização das variáveis hidrodinâmicas, físicas, químicas e biológicas importantes para a aquacultura; 2 - implementação, calibração, validação e aplicação de modelos hidrodinâmicos e de qualidade da água; 3 - desenvolvimento de um modelo de habitat, para transformação dos resultados dos modelos numéricos, num índice de exploração; 4 - aplicação do modelo de habitat, e mapeamento das zonas mais adequados à exploração de peixes e bivalves na Ria de Aveiro e Rias Baixas. Os resultados evidenciam que 22% da Ria de Aveiro é adequada para a produção de peixes (eixo dos principais canais, desde a embocadura até à zona intermédia dos canais), enquanto que a produção de peixes pelágicos nas Rias Baixas não é aconselhável, devido aos gradientes verticais de temperatura da água e de oxigénio dissolvido. Relativamente aos bivalves, o modelo de habitat prevê que 31% da Ria de Aveiro é adequada à sua produção. Nas Rias Baixas, exceptuando algumas zonas marginais e perto das cabeceiras, a adequabilidade para a produção de bivalves é quase total, confirmando a elevada exploração que se verifica na região. A definição das áreas propícias para a exploração aquícola está altamente relacionada com os diferentes processos geomorfológicos, hidrológicos e biogeoquímicos que ocorrem na Ria de Aveiro e nas Rias Baixas, mas também com a estrutura vertical dos sistemas estuarinos: uma coluna de água homogénea (Ria de Aveiro) em oposição a um sistema estuarino parcialmente estratificado (Rias Baixas). Os resultados para a Ria de Aveiro indicam que as cabeceiras dos principais canais são as áreas mais vulneráveis do ponto de vista da qualidade da água, evidenciando a importância da adveção nos processos ecológicos, em oposição à dinâmica das Rias Baixas, onde a estratificação adquire maior relevância.

Nestes estuários, o forte gradiente vertical da temperatura da água e do oxigénio dissolvido impede que os peixes possuam taxas de crescimento sustentáveis. A abordagem de modelação numérica combinada com um modelo de habitat permitiu considerar um elevado número de variáveis, integrando-as de forma a gerar resultados de grande utilidade para gestores e investidores do setor aquícola. Consequentemente, este trabalho mostra que a metodologia aqui desenvolvida é eficaz para a identificação de locais propícios para a exploração de espécies de interesse económico, gerando uma ferramenta que pode ser replicada e/ou adaptada em estudos futuros a realizar noutros sistemas costeiros. Finalmente, este trabalho demonstrou o potencial da modelação hidrodinâmica e biogeoquímica no suporte ao processo de tomada de decisão em futuros planos de ordenamento das zonas costeiras.

Keywords Aquaculture, Ria de Aveiro, Rias Baixas, Numerical Modeling, Habitat Suitability Model, Hydrodynamics, Water Quality.

Abstract Aquaculture is one of the fastest growing activities worldwide. In 2006, it already accounted for around 40% of total fish consumption, and since 2012, aquaculture is the main source of marine food supplies. However, this strong and fast development of the sector tends to be reflected in significant environmental impacts and new challenges in the management and planning of the coastal areas. In this context, this work intends to contribute to the sustainability of the sector, by identifying preferential locations to ensure aquaculture expansion and proper operation in a sustainable manner and with minimal environmental impact under optimal hydrodynamic and water quality conditions in Ria de Aveiro (Portugal) and Rias Baixas (Spain). This study is particularly relevant because the mapping of the most suitable areas for aquaculture exploitation has never been performed in any of the study areas, proving to be crucial, not only to demonstrate the potential in this commercial activity and to encourage investment by companies, but mainly to enable an adequate targeting of investments. To achieve this objective, a multidisciplinary methodology was applied, which comprised the following steps: 1 - characterization of hydrodynamic, physical, chemical and biological variables governing aquaculture activities; 2 - implementation, calibration, validation and exploitation of hydrodynamic and water quality models; 3 - development of a habitat model integrating the numerical model results into an exploitation index; 4 - application of a habitat model and mapping of the suitable and unsuitable areas for fish and shellfish exploitation in Ria de Aveiro and Rias Baixas. The results show that 22% of Ria de Aveiro is suitable for fish production (axis of the main channels, from the inlet to the middle of the channels), while the production of pelagic fish in the Rias Baixas is not recommended due to vertical gradients of water temperature and dissolved oxygen. Concerning to bivalves, the habitat model predicts that 31% of Ria de Aveiro is suitable for production. In the Rias Baixas, except for some marginal areas and upstream areas, the suitability for bivalve production is almost complete, confirming the high exploitation of the region. The definition of suitable areas for aquaculture exploitation is highly related with the different geomorphological, hydrological and biogeochemical processes of Ria de Aveiro and Rias Baixas, but also with the vertical structure of the estuarine systems: homogeneous water column (Ria de Aveiro) in opposition to a partially mixed estuarine system (Rias Baixas). Results of Ria de Aveiro indicate that the upstream areas of the lagoon are the most vulnerable from the water quality point of view, highlighting the importance of the advective processes in the lagoon's water quality, in opposition to Rias Baixas dynamics, where stratification is more relevant. In Rias Baixas, the strong vertical gradient of water temperature and dissolved oxygen disallows fish from having sustainable growth rates.

The numerical modelling approach combined with a habitat model allowed to consider a large number of variables, integrating them in order to generate results that are very useful for coastal managers and investors. Therefore, this work shows that the methodology developed here is effective for the identification of favorable areas for the exploitation of species with economic interest, generating a tool that can be replicated and/or adapted in future studies in other coastal systems. Finally, this work demonstrated the potential of hydrodynamic and biogeochemical modelling to support the decision making process in future coastal plans.

List of Symbols

$\boldsymbol{A}$	Absorption Coefficient of Chlorophyll
$\boldsymbol{C}$	Computed Concentration
$\boldsymbol{c}$	Mass Concentration
$\boldsymbol{C_{2D}}$	2-D Chézy Coefficient
$\boldsymbol{C_d}$	Wind Drag Coefficient
$\boldsymbol{C_B}$	Boundary Condition
$\boldsymbol{C_b}$	Initial Concentration of the Passive Tracer
$\boldsymbol{C_x}$	Concentration
$\boldsymbol{CO_2}$	Carbon Dioxide
$\boldsymbol{D}$	Data
$\boldsymbol{d}$	Threshold defined on Intertidal Criteria
$\boldsymbol{D_h}$	Horizontal Diffusion Coefficient
$\boldsymbol{D_{SGS}}$	Diffusion due to the Sub-Grid Scale Turbulence Model
$\boldsymbol{D_v}$	Vertical Diffusion Coefficient
$\boldsymbol{D_{3D}}$	Diffusion due to the Turbulence Model in Vertical Direction
$\boldsymbol{D_H}^{\boldsymbol{back}}$	Horizontal Diffusion Coefficient
$\boldsymbol{D\%\ O_2}$	% Deviation of Oxygen Concentration
$\boldsymbol{E}$	Non-local Source Term of Evaporation
$\boldsymbol{N_2}$	Nitrogen in the Form of Inert Gas
$\boldsymbol{f}$	Coriolis Parameter
$\mathbf{F}_\xi$ and $\boldsymbol{F}_\eta$	Unbalance of Horizontal Reynold Stresses
$\boldsymbol{g}$	Acceleration Resulting from Gravity
$\boldsymbol{H}$	Total Water Depth
$\boldsymbol{K}$	Factor to Equate the Reduction in Absorbance
$\boldsymbol{L}$	Path Length of the Cuvette
$\boldsymbol{M}$	Model Estimations
$\boldsymbol{M_n}$	Manning Coefficient
$\boldsymbol{M_i}^{\boldsymbol{t}}$	Mass at Each Time Step
$\mathbf{M}_\xi$ and $\boldsymbol{M}_\eta$	Contributions Due to External Sources or Sinks of Momentum

$\boldsymbol{N}$	Total Number
$\boldsymbol{NH_3}$	Ammonia
$\boldsymbol{NH_4^+}$	Ammonium
$\boldsymbol{NO_2^-}$	Nitrite
$\boldsymbol{NO_3^-}$	Nitrate
$\boldsymbol{P}$	Non-local Source Term of Precipitation
$\boldsymbol{P_{atm}}$	Atmospheric Pressure
$\boldsymbol{PO_4^{3-}}$	Phosphate
$\boldsymbol{Q}$	Contribution per Area Unit of the Discharge
$\boldsymbol{Q_{an}}$	Net Incident Atmospheric Radiation
$\boldsymbol{Q_{br}}$	Back Radiation
$\boldsymbol{Q_{co}}$	Convective Heat Flux
$\boldsymbol{Q_{ev}}$	Evaporative Heat Flux
$\boldsymbol{Q_{sn}}$	Net Incident Solar Radiation
$\boldsymbol{q_{in}}$	Local Sources per Unit of Volume
$\boldsymbol{q_{out}}$	Local Sinks per Unit of Volume
$\boldsymbol{S}$	Source and Sink Terms per Unit Area
$\boldsymbol{SiO_2}$	Silica
$\overline{T}$	Absolute Temperature
$\boldsymbol{t}$	Time
$\boldsymbol{T}$	Water Temperature
$\boldsymbol{T_a}$	Air Temperature
$\boldsymbol{T_{th}}$	Thatcher-Harleman Time Lag
$\boldsymbol{r}$	Reflection Coefficient
$\boldsymbol{U,\ V}$	Depth-Averaged Velocity Components
$\boldsymbol{u,\ v}$ ***or*** $\boldsymbol{w}$	Velocity Components
$\boldsymbol{U_{10}}$	Wind Speed at 10 meters
$\boldsymbol{V_l}$	Volume of Filtered Water
$\mid \vec{U} \mid$	Magnitude of the Depth-Averaged Horizontal Velocity
$\mid \vec{u}_b \mid$	Magnitude of the Horizontal Velocity in the First Layer
$\boldsymbol{w_i}$	Relative Weight
$\xi,\ \eta$ ***or*** σ	Directions
$\boldsymbol{z}$	Depth
β	Threshold Concentration
ϕ	Potential Energy Anomaly
ρ	Density of Sea Water

ρ_0	Sea Water Reference Density
ρ_a	Air Density
σ_{sb}	Stefan-Boltzmann's Constant
σ_d	Standard Deviation of the Data
σ_{mol}	Molecular Prandtl Number
υ_t	Temperature Dependency Constant
υ_a	Acetone Volume
υ_{mol}	Kinematic Viscosity of Water
υ_v	Vertical Eddy Viscosity Coefficient
τ_b	Bottom Shear-Stress
τ_s	Wind Shear-Stress
∇z_b	Distance to the Computational Grid Point Closest to the Bed
θ	Angle Between the Wind Stress Vector and the Local Direction
ε	Emissivity Factor of the Atmosphere
λ_d	First Order Decay Process
ζ	Free-Surface Water Elevation
$\sqrt{G_{\xi\,\xi}}$, $\sqrt{G_{\eta\,\eta}}$	Coefficients Used to Transform Coordinates

List of Acronyms

BOD	Biochemical Oxygen Demand
CF	Cost Function
Chl *a*	Chlorophyll *a*
DO	Dissolved Oxygen
EU	European Union
FAO	Food and Agriculture Organization of the United Nations
GIS	Geographic Information System
HS	Habitat Suitability
IH	Portuguese Navy
IRT	Integral Renewal Time
INE	Portuguese National Statistic Institute
LRT	Local Renewal Time
ME	Nash Sutcliffe Model Efficiency
NNE	North-Northeast
NR	Natural Reserve
NW	North-West
PAR	Photosynthetically Active Radiation
POT	Percentage of Time
PSOEM	Portuguese Maritime Spatial Planning Situation
RMS	Root Mean Square
RNAP	National Network of Protected Areas
SI	Suitability Index
SCI	Site of Community Importance
SMHI	Swedish Meteorological and Hydrological Institute
SNAC	National System of Classified Area
SPA	Special Protection Area
SSE	Sea Surface Elevation
SSW	South-Southwest

SW	Southwest
TFG	Phytoplankton Growth as Function of Water Temperature
TRIX	Trophic Index
UI	Upwelling Index
USA	United States of America
VSF	Variable Suitable Functions
W	West
WFD	Water Framework Directive
WRT	Water Renewal Time
1-D	One Dimension
2-D	Two Dimension
3-D	Three Dimension

Publications and Communications During the Period of this Thesis

Some publications in peer reviewed journals and presentations at national and international conferences resulted from the research developed in the scope of this dissertation.

Papers in international journals indexed in Web of Science

- Lopes, J.F., Vaz, N., **Vaz, L.**, Ferreira, J.A., Dias, J.M. (2015). Assessing the state of the lower level of the trophic web of a temperate lagoon, in situations of light or nutrient stress: A modeling study. Ecological Modeling, 313, 59-76.

- **Vaz, L**., Mateus, M., Serodio, J., Dias, J.M., Vaz, N. (2016). Primary production of the benthic microalgae in the bottom sediments of Ria de Aveiro lagoon. Journal of Coastal Research, SI75, 178-182. (Chapters 5, 6)

- **Vaz, L**., Frankenback, S., Serôdio, J., Dias, J.M. (2019). New insights about the primary production dependence on abiotic factors: Ria de Aveiro case study. Ecological Indicators, 106.

- Vaz, N., **Vaz, L**., Serôdio, J., Dias, J.M. (2019). A modeling study of light extinction due to cohesive sediments in a shallow coastal lagoon under well mixed conditions. Science of the Total Environment, 694.

- Frankenbach, S., Azevedo, A.A., Reis, V., Dias, D., **Vaz, L**., Dias, J.M., Serodio, J. (2019). Functional resilience of PSII, vertical distribution and ecosystem-level estimates of subsurface microphytobenthos in estuarine tidal flats. Continental Shelf Research, 182, 46-56.

- **Vaz, L.**, Sousa, M. C., Gómez-Gesteira, M., Dias, J.M., (submitted to Aquaculture). Water Renewal Estimation for Sustainable Aquaculture Development in Ria de Aveiro and Rias Baixas. (Chapter 7)

- Frankenbach, S., Ezequiel, J., Plecha, S., Gossling, J., **Vaz, L.**, Kulh, M., Dias, J.M., Vaz, N., Serôdio, J., (submitted to Frontiers in Marine Science). Synoptic spatio-temporal variability of the photosynthetic productivity of microphytobenthos and phytoplankton in a tidal estuary.

- **Vaz, L.**, Gómez-Gesteira, M., Dias, J.M., (*in prep*). A habitat suitability model for aquaculture site selection: Ria de Aveiro and Rias Baixas. (Chapter 8)

Conferences Abstracts, Proceeding and Communications

- **Vaz, L.**, Sêrodio, J., Mateus, M., Dias, J.M., Vaz, N. (2016). Primary production of the benthic microalgae in the bottom sediments of Ria de Aveiro Lagoon. 13th International Coastal Symposium, 6-11 March 2016, Sydney, Australia.

- **Vaz, L.**, Dias, J.M., Vaz, N. (2016). Light attenuation in a shallow lagoon: dependence on SLR and extreme freshwater discharge. ECSA56, 4-7 September 2016, Bremen, Germany.

- **Vaz, L.**, Dias, J.M. (2018). Optimal Conditions for Aquaculture Exploitation in Ria de Aveiro: a Numerical Modelling Approach. Encontro Ciência '18, 2-4 July 2018, Lisbon, Portugal.

- **Vaz, L.**, Dias, J.M. (2019). Optimal Conditions for Aquaculture Exploitation in Ria de Aveiro: a Numerical Modelling Approach. CESAM contributions for Environmental Management and Spatial Planning, 3 May 2019, Aveiro, Portugal.

- **Vaz, L.**, Dias, J.M. (2019). Optimal Conditions for Aquaculture Exploitation in Ria de Aveiro: a Numerical Modelling Approach. Research Summit, 5 July 2019, Aveiro, Portugal.

- **Vaz, L.**, Vaz, N., Gómez-Gesteira, M., Dias, J.M. (2019). Time and Spatial Distribution of Water Column Stratification in Rias Baixas: Influence on Aquaculture. International Society for Ecological Modelling, 1-5 October 2016, Salzburg, Austria.

- Vaz, N., **Vaz, L.**, Mateus, M., Dias, J.M. (2019). A model study of time and spatial distribution of nutrients in the Tagus estuary coastal continuum. International Society for Ecological Modelling, 1-5 October 2016, Salzburg, Austria.

Contents

List of Figures

List of Tables

Chapter 1

Introduction

1.1 Motivation

Aquaculture is the farming of aquatic organisms including fish, molluscs, crustaceans and aquatic plants. Nowadays, about 580 aquatic species are currently farmed all over the world, representing a wealth of genetic diversity both within and among species, being practiced by some of the poorest farmers in developing countries and by multinational companies.

According with the World Bank Organization (`http://www.worldbank.org/`), aquaculture is projected to be the prime source of seafood by 2030, as demand grows from the global middle class and wild capture fisheries approach their maximum take. When practiced responsibly, fish farming can help provide livelihoods and feed a global population that will reach nine billion by 2050.

Despite the main purpose for human feeding, aquaculture may have other motivations such as: re-population of the natural environment, re-population of species of interest for sport fishing, algae species for organic effluents treatment, production of bait for artisanal or industrial fish farming, fish production for ornamental purposes and also for the production of fertilizers, pharmaceutical products and pearls (Tabuada, 2009).

In Figure 1.1 is depicted the temporal evolution of aquaculture and captured fisheries productions worldwide (Figure 1.1 A), and in Portugal and Spain (Figure 1.1 B and C), where this study is focused. The evolution rate per year is also represented in Figure 1.1 D. In the case of Figure 1.1, aquaculture production specifically refers to output from aquaculture activities, which are designated for final harvest for consumption, while capture fisheries production measures the volume of fish catches landed by a country for all commercial, industrial, recreational and subsistence purposes.

The analysis of Figure 1.1 A evidences that the contribution of aquaculture world-

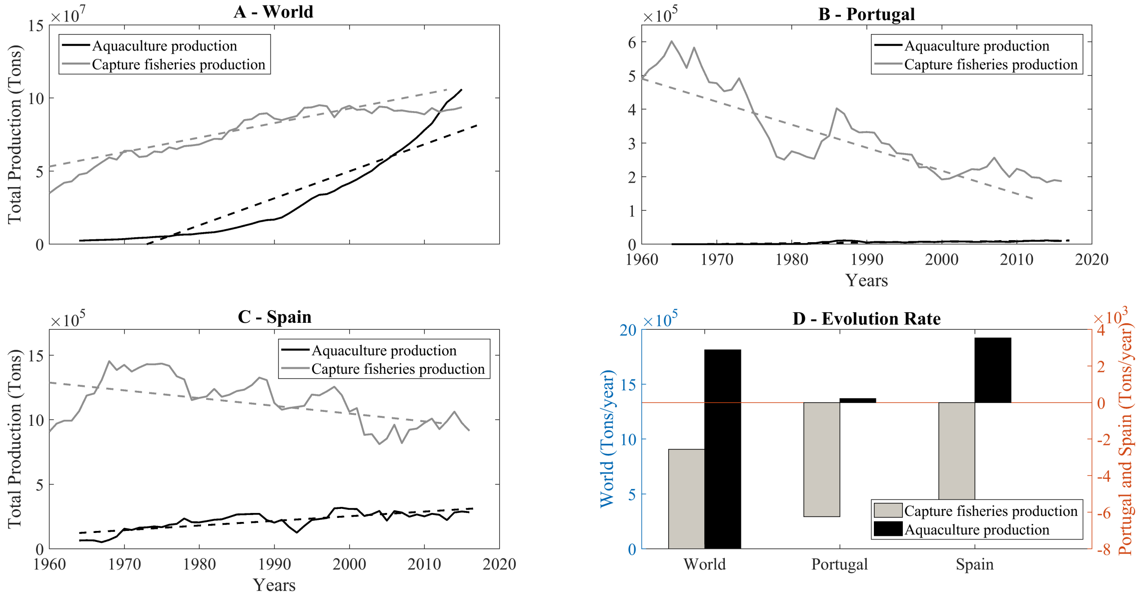

Figure 1.1: Time series of annual total aquaculture production and capture fish production worldwide (A), in Portugal (B) and Spain (C), in tons. Dashed lines corresponds to the mean yearly evolution between 1960 and 2016. Evolution rates of aquaculture production and captured fish, in million tons/year, are also depicted (D).

wide to the supply of fish, crustaceans, molluscs and other aquatic animals has increased significantly over the years, mainly since 1990's. For example, in 2006, fish coming from aquaculture represents 40% of the total consumption (6.2×10^7 tons of a total of 15.2×10^7 tons). Despite the increase in capture fisheries production, since 2012, aquaculture is the main source of marine food supplies worldwide, becoming increasingly important its environmental, economic and social sustainability, which varies with species, location, societal norms and the state of knowledge and technology.

The temporal evolution in Portugal (1.1 B) does not follow the world trend. The captured fisheries production decreased 61% since 1960 until 2015, from 4.9×10^5 tons to 1.8×10^5. On the other hand, the aquaculture production was almost non-existent until 1982, however since 1983, the production increased about 288%. Despite the increasing efforts to aquaculture development, the production is negligible and not enough to compensate the decrease of the captured fisheries, which encourages imports.

Indeed, according with Food and Agriculture Organization of the United Nations (FAO) (`http://www.fao.org/`), Portugal is one of the countries with higher fish consumption in world, with an average consumption per capita of around 60 kg/year, which is above the world average (19.2 kg/year). In response to the growing demand, Portugal has a high rate of fish import, affecting negatively the country trade balance, which according with Portuguese National Statistic Institute (INE) has a deficit of around 641 million Euros.

In Spain (1.1 C), the balance between aquaculture and capture fish production seems to be more sustainable comparing with Portugal. Despite, the higher volume of capture fish due its higher population, the aquaculture is responsible for 23% of the total fish consumption. The aquaculture production revealed an increase of 337% while the capture fisheries decreased 24%, since 1960's until 2017.

The patterns previously described are summarized in Figure 1.1 D, in which is observed that the evolution of aquaculture production is the double of the capture fisheries production evolution (left panel of Figure 1.1 D). The figure also depicts that the decreasing rates of Portugal and Spain are similar (about 6×10^4 tons per year), however the aquaculture production in Spain tends to compensate the decrease of captured fish, in opposition to what occurs in Portugal.

Estuaries and coastal lagoons presents a high potential for the development of the activity, since they are commonly rich in nutrients and phytoplankton, which favours the growth and productivity of species with high demand and significant commercial value. In addition, according to FAO, these coastal regions usually presents acceptable salinity, water temperature and oxygen conditions, which favours the aquaculture sector.

Taking the example of Portugal, in the early 1990s, aquaculture was limited to the production of two species: trout and clams. Thereafter, in response to the increasing consumption, aquaculture has shown a strong growth and modernization, focusing on the production of other valuable species such as sea bass, sea bream and oysters (`http://eaquicultura.pt`).

According to information collected on the website of the General Directorate for Natural Resources, Safety and Maritime Services of Portuguese government (`http://eaquicultura.pt/`), the production of fish in brackish and marine waters represents 47.7% of the production, in which the great majority (91.0%) is sea bream and turbot. The bivalve molluscs represent 45% of the total production, standing out the clams as the most relevant species, followed by the mussels. The production of oyster (1085 tons produced) increased by 36.6% in 2014 due to a new investment paradigm that has been observed in Portugal, in which spaces that were previously used for fish production, are now under oysters production, due to its high demand and commercial value, particularly at international level.

In this context, Ria de Aveiro and the Rias Baixas, where this study is focused, are the main locations for fish and bivalve cultures in the North of Iberian Peninsula (Chapter 2), despite being contrasting coastal systems, in their geomorphology, hydrodynamic, hydrologic and ecological features. Therefore, the assessment and the comparison of their biogeochemical functioning is very relevant and will contribute to bring new insights about aquaculture sustainability in both coastal systems.

Additionally, there is no prior information supporting the development of aquaculture activity in Ria de Aveiro and Rias Baixas, in particular by identifying the areas of greatest potential for the exploitation of each commercial valuable species. This limitation is identified by Portugal and Spain, which establishes the need to identify and evaluate new areas with high aquaculture potential. This mapping is indispensable, not only to demonstrate the potential of this commercial activity and to encourage investment by companies, but mainly to enable an adequate targeting of investments, and to the sustainability of the sector.

Furthermore, the fast evolution of aquaculture industry in the last decades observed in Figure 1.1, leads to important environmental impacts (Sapkota et al., 2008; Vezzulli et al., 2008), making essential the existence of tools and scientific knowledge that help the coastal planners and managers to promote aquaculture development in an environmental, economical and social sustainable manner.

The response to these concerns seeks to align with the strategic objective defined for the period 2014-2020 by European Union, to increase and diversify the production in Portugal and Spain, in order to satisfy the growing demand and local development, promoting sustainable aquaculture production in estuarine and coastal systems. Therefore, this study aims to contribute to enhance the conditions for the expansion of this sector through the development and application of methodologies that clearly and unequivocally identify and evaluate new estuarine or lagoonal areas with high aquaculture potential.

1.2 Aims

Attending the concerns referred in previous subsection, the main aim of this work is to identify preferential sites to ensure aquaculture expansion and proper operation in a sustainable manner and with minimal environmental impact under optimal hydrodynamic and water quality conditions in Ria de Aveiro (Portugal) and Rias Baixas (Spain). Besides this, the present work aims to:

- Develop and implement high resolution hydrodynamic and water quality models for Ria de Aveiro and Rias Baixas;

- Calibrate and validate the hydrodynamic and water quality models, to guarantee the accurate reproduction of the hydrodynamic and biogeochemical processes in Ria de Aveiro and Rias Baixas;

- Characterize and assess the temporal and spatial evolution of the main biophysical variables;

- Determine the eutrophication level and the water quality status of Ria de Aveiro lagoon and Rias Baixas;

- Produce high resolution maps of the descriptors considered essential by the sector: current velocity, salinity, water temperature, dissolved oxygen, pH, trophic status, primary production indicators;

- Develop a habitat model and the concept of *Suitability Index*;

- Produce high resolution maps of the suitable and unsuitable locations for fish and bivalves production in Ria de Aveiro and Rias Baixas;

The approach used to accomplish the specific objectives listed above involves the implementation of 2-D and 3-D models and *in situ* data analysis, allowing to research the biogeochemical dynamics of the study areas, and especially to deep the knowledge about the preferential areas to ensure aquaculture exploitation.

1.3 Literature Review

1.3.1 Ria de Aveiro

Ria de Aveiro lagoon has been widely studied during the last 20 years, in a extensively variety of scientific branches, from physics, chemistry, geology and biology, resulting in several publications regarding bacterioplancton, zooplankton, benthic biodiversity, pollution impacts, fisheries, among several others issues (e.g. Morgado et al. (2003); Lopes et al. (2010); Pereira et al. (2011); Anjum et al. (2012)).

As this study is focused on identifying preferential areas to aquaculture exploitation through the development and analysis of hydrodynamic and water quality models results, the literature research is based on lagoon's hydrodynamic and water quality models applications.

One of the first steps in this task is the study made by Dias et al. (1999). The authors concluded that the tide in the Ria de Aveiro is semi-diurnal and is the main forcing agent, and M_2 and S_2 are the most important constituents in the lagoon, representing approximately 90% of the tidal energy in Ria de Aveiro. The model application using a structured grid model SIMSYS2D was the base for several other studies (Dias et al., 2000; Lopes et al., 2001; Dias et al., 2003) to study tidal dynamics processes.

MOHID numerical model was also applied by Vaz et al. (2009) to study the stratification processes within Ria de Aveiro lagoon, being later used for several studies (Mendes et al., 2011; Valentim, 2012).

The first application of an unstructured grid model (MORSYS2D) to Ria de Aveiro was performed by Oliveira et al. (2006), in order to study the morphodynamics of Ria de Aveiro inlet. Later, Plecha (2011) used this application to assess the sedimentary processes in the inlet area, concluding that Ria de Aveiro inlet morphodynamics is influenced mainly by tides and coastal waves; Lopes et al. (2011) also applied this model to study the influence of mean sea level rise on inlet morphodynamics, depicting an intensification of sedimentary fluxes and sedimentation rates under future scenarios of sea level rise.

The model developed by Oliveira et al. (2006) has been adapted in numerous works, in the last years. Picado et al. (2010) introduce to the grid developed by those authors, the complex net of small and narrow channels located in the central area of the lagoon, aiming to study the tidal changes induced by the flooding of abandoned salt pans, finding an intensification of the tidal currents, tidal prism and tidal asymmetry due to the increase of the flooded area. Later on, Vaz (2012) increased the grid resolution in the offshore and inlet areas, and coupled the hydrodynamic model ELCIRC with the wave model SWAN, to study the influence of coastal waves on Ria de Aveiro inlet hydrodynamics, concluding that the lagoon sea level remains above offshore sea level during storm wave periods. Azevedo (2018) used a Delft3D - Flow structured model as a basis to develop a biological model considering the seasonal dynamics of intertidal seagrass *Zostera noltei*.

One of the first steps towards modelling the water temperature and salinity distributions in Ria de Aveiro lagoon was performed by Dias et al. (1999). These authors characterize Ria de Aveiro from a hydrological point of view, concluding that it should be considered vertically homogeneous, with exception to periods of important rainfalls. These hydrological characteristics were later confirmed by Vaz and Dias (2008) and Dias and Lopes (2006). Lopes et al. (2007a) studied the nutrient dynamics and seasonal succession of phytoplankton assemblages in Ria de Aveiro, through seasonal measurements of dissolved inorganic nitrogen, dissolved phosphate, dissolved silica and chlorophyll *a* at eight stations. This study increased the knowledge about the spatial and temporal dynamics of nutrients, suggesting phosphorous limitation at the system level.

Some preliminary modelling works aiming to analyse biological or chemical processes in Ria de Aveiro were performed using particle-tracking modules coupled to hydrodynamic models, which allow to study the dispersion processes in coastal waters, estuaries and lagoons. For example, Cerejo and Dias (2007) applied this tool to evaluate the dispersion of marine toxic microalgae in the lagoon. More recently, Santos et al. (2014) implemented an identical procedure designed to assess the importance of the freshwater inflow in bacteria displacement. However, with the development of sophisticated and reliable water quality models, new horizons arise that allow the achievement of deeper studies and processes analysis.

Therefore, water quality models are essential tools for the assessment of ecosystem interactions occurring within the coastal systems. Despite Ria de Aveiro's biology and chemistry has been widely explored, the application of numerical water quality models, based on physical processes, is understudied. Nevertheless, there were a few previous studies based on the implementation of models developed and applied to investigate the lagoon's biogeochemical processes. The first was due to Lopes et al. (2005) and was based on a Mike21-HD water quality model implementation, aiming to compute the major water quality features under the influence of different forcing conditions. These authors state that the main vulnerable areas of the lagoon, from the water quality perspective, are the far end of the main channels, where low dissolved oxygen concentration and high BOD concentrations are observed. Later on, using the same model, Lopes and Silva (2006) characterized the temporal and spatial distribution of dissolved oxygen, concluding that the circulation patterns inside the lagoon are responsible for the high level of oxygen in the water column. A new study from Lopes et al. (2010) predicted the lagoon ecological patterns in a spring season, suggesting that nutrient inputs from the freshwater tributaries support the uptake and growth of phytoplankton, reflecting high chlorophyll *a* and dissolved oxygen concentration. Finally, Lopes et al. (2015) assessed the state of the lower level of the trophic web, showing that changes in light or nutrients availability may seriously modify the actual lower level state of the lagoon trophic level. A very similar study was performed by Rodrigues et al. (2009), which also modelled the lower trophic level in Ria de Aveiro, but in this case using the Eco-Selfe water quality model. Results show that the model implemented was able to reproduce the dynamics of the ecosystem for the period in analysis, fitting the model results inside the range of data variation. MOHID model was recently applied to study the trophic processes in this lagoon (Vaz et al., 2016), in which a new methodology to compute microalgae in the bottom sediments was presented. This study revealed that an increase of nutrients concentration in the water column favours the phytoplankton growth, which increases biomass, leading to an attenuation of the light intensity reaching the bottom sediments, resulting in a decrease of benthic primary production.

Delft3D - WAQ was the most recently model applied to study biological processes at Ria de Aveiro (Stalnacke et al., 2016; Azevedo, 2018). In the scope of LAGOONS project, which aimed to develop science-based strategies and decision support frameworks for the integrated management of 4 lagoons around Europe (including Ria de Aveiro), a book was published (Stalnacke et al., 2016). In chapters 13 and 16, the application of Delft3D - WAQ was performed in order to evaluate the impacts of the climate change on lagoons and their catchments, and to assess the response of the lagoons to different integrated scenarios, respectively. Chapter 13 shows that the variations of water temperature and salinity induced by climate change, imposed in Ria de Aveiro open boundary, will affect the distribution of those variables along the lagoon, decreasing their gap between the lagoon and the adjacent shelf. The results of Chapter 16 allow to draw an important conclusion: in the future, the lagoon's water chemical status is not expected to change, since the scenarios projected will not influence the lagoon's nutrient balance and chlorophyll *a* patterns.

Following the work performed in LAGOONS project, Azevedo (2018) studied the seasonal dynamics of intertidal seagrass *Zostera noltei*, resulting in a very important knowledge to lagoon's fauna conservation: the most favourable areas for seagrass presence in the future are located mainly in the south-central and northwest central areas of the lagoon.

According to this literature revision, there is a lack of studies exploring the use of water quality models to ensure the most appropriate locations for human intervention in the lagoon. In this context, this thesis intends to contribute to the state of the art about lagoon's water quality models development, biogeochemical processes, developing an innovative methodology to ensure aquaculture exploitation, which may be used for other purposes (outfall diffuser site, implementation of wind turbines, etc.). Moreover, the lagoon limiting factors affecting the phytoplankton growth needs to be clarified, which is also performed in this thesis.

1.3.2 Rias Baixas

Rias Baixas were also extensively studied through the analysis of field data and numerical model results. Prego and Fraga (1992) developed a stationary model to calculate residual flows and mixing rates in Ria de Vigo, predicting residual currents between 4 and 8 cms^{-1} during winter, and classified Ria de Vigo as a partially mixed estuary. Doval et al. (1998) carried out a hydrographic sampling along Ria de Vigo main axis, from May 1994 to September 1995, in order to characterize the spatio-temporal evolution of hydrographic and biogeochemical properties along the water column, under two different period: upwelling and non-upwelling seasons. During upwelling events, Ria de Vigo behaves like an extension of the shelf, while a partially mixed estuary is depicted during non-upwelling season. A similar study was performed by Alvarez et al. (2013), analysing the influence of upwelling events at Ria de Vigo thermohaline properties, from October 2003 to September 2004. Eastern North Atlantic Central Water was observed during spring-summer at the southern mouth of Ria de Vigo.

DeCastro et al. (2000) measured hydrodynamical and thermohaline properties from February to July 1998 at 10 stations distributed along Ria de Pontevedra, concluding that wind velocities higher 4 ms^{-1} are the main driver of surface layers currents, even against tidal effect. Prego et al. (2001) carried out a systematic investigation between October 1997-98 about Ria de Pontevedra hydrography. Four distinct water bodies penetrating in Ria de Pontevedra during a year were observed: autumnal shelf water; seawater depicting features of the poleward current, in winter; subsurface shelf water from May to September when upwelling relaxes; and the Eastern North Atlantic Central Water in summer. During the same period, Gómez-Gesteira et al. (2001) depicted a unusual two layered tidal circulation induced by stratification and wind in Ria de Pontevedra, which depends on the summer stratification conditions and on the presence of easterly winds inside the estuary. The vertical stratification generated by solar heating and favourable upwelling conditions on the adjacent shelf reinforces the estuarine positive circulation and promotes the inflow of typical upwelling water through bottom layers. Three years later, deCastro et al. (2004) measured an estuarine negative circulation, in which the two layered circulation pattern was generated by the existence of two different water masses at intermediate depths. The water presented in the inner area of the Ria de Pontevedra was a mixture of estuarine water and Eastern North Atlantic Central Water, which had entered in the estuary some days before, as result of an intense upwelling event. The water in mid-estuary was a mixture of estuarine and fresh waters coming from the river discharge. This water mass distribution gave rise to the existence of denser water in the inner part of the estuary than in the middle, generating the observed negative circulation pattern. This negative circulation pattern was also observed in Ria de Arousa by Álvarez-Salgado et al. (1996).

Concerning to Ria de Arousa, Rosón et al. (1997) state that, during the summer, the local dynamics is mainly controlled by wind. Heat exchanges with the atmosphere and river discharges play a minor role during this period. From November to March, due to intense rainfall and freshwater discharges, stratification of the water column is maintained by salinity, generating a positive circulation in the estuary. Density differences in Ria de Arousa mouth not only depends on the freshwater plume, but also on wind direction. During episodes of predominant SW wind, a negative circulation is observed, retaining water within the estuary (Rosón et al., 1997). On the other hand, when the wind changes direction to NE quadrant, an outflow of water from the surface layer is promoted (Álvarez-Salgado et al., 2000). Bermúdez et al. (2013) studied the short-scale physical processes in the Ria de Arousa, highlighting along-channel wind forcing, through the application of Delft3D - Flow model. The authors concluded that onshore wind seems to induce water column mixing and hence a reduction of the water stratification. On the other hand, moderate offshore wind appears to increase stratification, in spite of the mixing effect of the wind. For both wind directions, the higher wind speeds tends to reduce the water column stratification.

Regarding to Ria de Muros, its circulation was studied for the first time by Iglesias et al. (2008) using a numerical model, depicting that the tide is the main driving forcing of the local hydrodynamics. Nonetheless, this study also reveals that wind plays a major role on Ria de Muros water circulation, mainly in certain zones of the estuary middle and outer areas. Carballo et al. (2009) used a Delft3D - Flow model to predict the residual circulation in the Ría de Muros. They conclude that residual velocity magnitudes are maximum in the upstream area of the estuary due to river action, followed by wind and tide, respectively. In a situation of high freshwater inflow, the river-driven residual circulation prevails. Contrarily, in the absence of important river run-off, the residual circulation is mainly dominated by the wind. The importance of the tide is limited to the inner Ria de Muros. In the same year, Iglesias and Carballo (2009) used the same model to study the seasonality of the circulation in the Ría de Muros, finding that, during summer, the circulation consists in two-layer flow, with inflow of shelf water in the bottom layer and outflow of estuarine and river water in the surface layer. The wind is responsible for the intensification of the circulation in the surface layers of the water column. During winter, Ria de Muros is characterized by a three layers circulation instead of the usual two layers estuarine circulation. One year later, Iglesias and Carballo (2010) applied the same Delft3D - Flow model in order to understand how high winds affect Ria de Muros circulation, reinforcing the results achieved by Iglesias and Carballo (2009). The results showed that the NNE wind significantly strengthens the positive estuarine circulation, while the SSW wind turns the two-layer pattern into a three-layer circulation, with water inflowing in the surface and bottom layers and outflowing in the intermediate water column.

Several studies comprising more than one estuary of Rias Baixas have been performed during the last decades. The inter and intra annual evolution of water temperature and salinity of Ria de Vigo, Pontevedra and Arousa were analysed from October 1997 to October 2002 by Alvarez et al. (2005), measuring thermal inversion from November to February, intense upwelling events from April to September, and the input of a warm water mass in October, in all Rias. These authors state that Ria de Vigo and Ria de Pontevedra are very similar from a hydrological point view, differing from Ria de Arousa mainly in its northern mouth - here, lower salinity is observed in winter, and upwelling events are less frequent in summer. These authors attribute this phenomenon to the different orientation of Ria de Arousa comparing with remaining rias, higher river discharge, and the shallowness of its mouth. Alvarez et al. (2006) studied the hydrographic behaviour of Rias Baixas under the influence of Minho River outflow, in a period when Minho River discharge and wind patterns are favourable to spread the river plume northward. The intrusion of Minho River water into Rias Baixas reverses the normal salinity gradient in the along axis direction in Ria de Vigo and Pontevedra, while there were no changes observed in Ria de Arousa.

This subject has been studied until nowadays. Sousa et al. (2014a) researched the main factors driving an unusual pattern on Rias de Vigo and Pontevedra circulation - the reversion of the normal circulation pattern inside the Rias Baixas affecting the exchange between the estuaries and Atlantic ocean caused by Minho river intrusion. They conclude that Minho River discharge is the main driving agent in the establishment of the negative circulation, while Rias Baixas tributaries slightly attenuate this circulation. The propagation and influence of Minho estuarine plume in Rias Baixas circulation and hydrography was assessed by Sousa et al. (2014b), through application of MOHID numerical model. They found that a moderate Minho river discharge combined with southerly winds is enough to reverse the circulation pattern of Ria Baixas, reducing the importance of the occurrence of specific events of high runoff values. More recently, the work of Des et al. (2019) comes in sequence of studies of Sousa et al. (2014b,a), and intends to answer the following questions: (1) How often is the occurrence of Minho intrusions?; (2) The events duration?; (3) How long is the relaxation period between consecutive events?; and (4) What is the importance of the freshwater discharge from inside of Ria de Vigo. Based on *in situ* measurements, Minho River intrusion was detected in Ria de Vigo with a percentage of occurrence of 8.9%, 8.4% in Ria de Pontevedra, and in Ria de Arousa in only 4.5% of the cases. The numerical simulations allowed to determine these events duration - approximately 1.5 days. The intrusion events were characterized by the authors in three different phases: initial positive estuarine circulation pattern; intrusion development; relaxation of the intrusion and recovery of the initial positive circulation.

Due to the importance of the water quality status in a coastal embayment occupied by mussel farms, the ecology, the trophic status and the anthropogenic impacts on Rias Baixas were highly investigated by scientific community in the last decades. Torres-López et al. (2005) developed a 1-D model to evaluate offshelf fluxes and fractionated mineralization of particulate phytogenic materials in Rias Baixas, concluding that under strong upwelling events, an important offshelf flux is verified, with a low effect of mineralization on net community production; in case of weak upwelling conditions, particulate organic matter is significantly reduced while mineralization is promoted. Castro et al. (2006) evaluated the hydrological, chemical and biological changes in Ria de Pontevedra water column due to Minho river dams discharges on 12-13 May, 1998. These authors state that when nutrient-rich Minho river water reaches Ria de Pontevedra is pumped through surface layers due to the formation of cross-axis density gradients. Therefore, the induced bloom generated at the shelf is pumped to Ria de Pontevedra, leading to the development of high concentrations of ammonium (NH_4^+), and the typical spring bloom of phytoplankton.

The phytoplankton dimension and seasonal and short-time scale variability of primary production in Ria de Vigo was assessed by Cermeno et al. (2006). During upwelling season, the respiration represented a minor fraction of gross primary production, evidencing the large organic matter export. On the other hand, during downwelling, respiration strongly outweighs the production, suggesting that most of the photosynthesised organic matter was re-mineralised within the ecosystem. In 2010, the effects of suspended mussel culture on benthic–pelagic interactions in Ria de Vigo was investigated (Alonso-Pérez et al., 2010). This subject was studied in more detail three years later by Seeyave et al. (2013). Vertical particular organic carbon fluxes underneath the mussel raft were 3 times higher than the fluxes obtained between raft sand, and 10 times higher than in the main channel reference site. Dissolved oxygen, ammonia (NH_3), silica (SiO_2) and phosphate (PO_4^{3-}) benthic fluxes were significantly higher under the rafts than at the inner Ria de Vigo. More recently, Froján et al. (2018) carried out a similar work, in which the impact of mussel farming on the primary production and the metabolic balance in Ria de Vigo was assessed. The mussels cause a decrease of chlorophyll *a* concentration and on carbon fixation. Mussel culture also changes the metabolic balance of the microbial community at Ría de Vigo. This influence basically occurs through the decrease of gross primary production due to phytoplankton consumption by mussels and through the light attenuation caused by raft structures. Using ecological modelling with Ecopath software, Outeiro et al. (2018) calculated the current ecological carrying capacity and production carrying capacity of Ria de Arousa, concluding that current mussel aquaculture biomass has exceeded ecological carrying capacity, however it is below production carrying capacity. They classified Ria de Arousa as a mature ecosystem, since its resilience to cope with the temporal changes and to the intensification of food production and human activity.

From a taxonomic point of view, Aneiros et al. (2015) study the epibenthic megafauna in order to describe the spatial distribution, testing possible differences between inner and outer areas of Ria de Vigo. Suspension-feeding molluscs dominated the innermost part of the estuary, and were substituted by echinoderms in the external zones.

Additionally, several studies related with mussel farms in Rias Baixas were performed (Alonso-Pérez et al., 2010; Piedracoba et al., 2014; Froján et al., 2018; Outeiro et al., 2018). However, the identification of the proper locations for aquaculture development was never assessed. Consequently, the present study comprises the first implementation of Delft3D-WAQ in Rias Baixas. Moreover, this study is the first implementation of a water quality model encompassing the 4 estuaries in an integrated manner.

1.3.3 Geographic Information Systems (GIS) Application and Modelling Tools to Aquaculture Development

Although planning is commonly quoted as a priority for aquaculture development (Ross et al., 1993), the identification of new sustainable aquaculture areas is a very demanding spatial and temporal problem which requires a full knowledge about marine ecosystems, mainly their geomorphology, hydrodynamics, hydrology, water quality, social, economic and civil factors.

Geographic Information Systems (GIS) application to assess aquaculture development has focused a wide range of species and geographic scales. One of the first steps in this subject was performed by Ross et al. (1993), where a GIS methodology was developed for site selection for a salmonide cage culture development in Argyll, Scotland. They used data of bathymetry, current velocity, shelter and water quality variations to determine the suitability of the site. Two year later, Aguilar-Manjarrez and Ross (1995) use a geographical information system to construct environmental models for land-based aquaculture development in the State of Sinaloa, Mexico. The methodology enabled multi-criteria and multi-objective decision making concerning site selection and location. In assessing site considerations, these general models identified wider resource management options and solved conflicts of land allocation and land use between aquaculture and agriculture. Later on, Katavić and Dadić (2000) used GIS in order to optimize site selection by identifying the zones which are unsuitable for mariculture development in Adriatic Sea, Croatia coast. Meanwhile several studies were addressing this issue (Arid et al., 2005; Guneroglu et al., 2005; Corner et al., 2006; Handisyde et al., 2014). Arid et al. (2005) developed a methodology for delimitation of the optimal zones for the installation of aquaculture farms, integrating satellite data and *in situ* measurements. Guneroglu et al. (2005) performed a similar study analyzing water temperature, salinity and current velocity data of Surmene Bay, Black Sea. Corner et al. (2006) developed a GIS-based model of particulate waste distribution from marine fish-cage sites.

Arnold et al. (2000) and Zeng et al. (2003) used a GIS multi-criteria technique to develop aquaculture management in New South Wales (Australia) fisheries. The technique consists in the conversion of raw data to standardised aquaculture suitability scores (normalised values between 0 and 1) through the use of parameter specific suitability functions.

Vincenzi et al. (2006) used a similar methodology to identify areas of different clam yield potential within the Sacca di Goro lagoon, by using a GIS-based habitat suitability model that explores the relationship between occurrence and abundance of *Manila* clam and key hydrodynamic and biogeochemical features for clams survival and growth, that can be sampled or estimated at a fairly low-cost. These authors state that the methodology adopted may be considered as a valid screening methodology to plan and design clam concessions in a fairly objective and equitable way. Later on, Longdill et al. (2008) and Silva et al. (2011) used identical methodology to ensure the long-term sustainability of aquaculture in New Zealand, and to develop and test an integrated approach of GIS and farm-scale modelling to site selection of shellfish aquaculture in Valdivia estuary (Chile), respectively.

More recently, Gimpel et al. (2018) integrated, assessed and mapped 30 indicators reflecting economic, environmental, inter-sectorial and socio-cultural risks and opportunities for proposed aquaculture systems in a marine environment, in Northern Europe. Jayanthi et al. (2018) explored the impact of shrimp aquaculture on land use changes in India's coastal wetlands using GIS techniques, but also Landsat satellite data and field measurements. They conclude that mudflats, scrublands, saltpan, and waterbodies ecosystems suffers side effects through the aquaculture expansion. Specific studies have included the proper areas selection for target species, such as bivalves (Arnold et al., 2000), fish (Perez et al., 2005) and crustaceans (Alarcon and Villanueva, 2001).

Regarding the use of numerical modelling approaches, several circulation models based on mathematical equations governing fluid motion provide a practical solution to the problem of understanding water mixing and renewal in aquaculture exploitation areas. Several authors assess the circulation (Trites, 1995), flushing time (Koutitonsky et al., 2004) and oxygen depletion (Culberson and Piedrahita, 1996). Koutitonsky et al. (2004) developed a numerical model to predict residence times in Richibucto estuary (Canada), where the largest American oyster aquaculture operation in eastern Canada is located, while Culberson and Piedrahita (1996) developed a water temperature and dissolved oxygen model in that provides a framework into which may be added characterizations of pH, alkalinity, nutrient dynamics, and finally, fish yield.

Duarte et al. (2003) developed a 2-D coupled physical–biogeochemical model to assess the carrying capacity for multi-species culture of Sungo Bay, China, concluding that this system is being exploited close to the environmental carrying capacity for suspension-feeding shellfish. Ferreira et al. (2007) developed a 3-D model to simulate tidal, wind and ocean currents in Carlingford Lough, Strangford Lough, Belfast Lough, Larne Lough and Lough Foyle (Ireland), in order to develop a dynamic ecosystem-level, in order to predict carrying capacities for shellfish culture. A coupled 3D physical, chemical and biological ocean model was applied by Skogen et al. (2009), aiming the investigation and documentation of the environmental effects of fish farming, with a particular focus on eutrophication on the Norwegian fjords. They concluded that the effect on the primary production was the largest if the fish farms were located quite far inside the fjord. The best localization to the fish farms was found to be near the mouth of the fjord, where the water exchange with the coast is higher.

Plew (2011) evaluated changes to tidal circulation in Pelorus Sound (New Zealand) induced by shellfish farm, evidencing a decrease of the mean current speed of about 7%. The use of FDC, a 3-D finite difference hydrodynamic model, was explored by O'Donncha et al. (2017) in order to investigate the impacts of suspended aquaculture farms on flows and material transport, depicting low impacts on flushing rates of Cobscook Bay (USA). These authors concluded that aquaculture practices leads to a decrease of the flushing rates less than 6%.

1.3.4 Environmental Conditions to Aquaculture Development

In this section, the most important morphological, hydrodynamic, physical, biological and chemical parameters are assessed in order to understand the standard values for the development of fish and bivalves cultures, according with the literature.

Later in this thesis, the data analysis, the numerical simulations, the establishment of the environmental ranges for aquaculture development, and consequently, the settlement of the proper locations to production, are based on the information collected in this specific sub-section.

1.3.4.1 Bathymetry

The water depth, in combination with the average current speed, is determinant in the aquaculture site selection, since determines the concentration of waste sediments and pollutants around cages (Cardia and Lovatelli, 2015). According with Cardia and Lovatelli (2015), water depth may have the following impacts:

- Environmental footprint: The environmental footprint is directly related to the water depth, since the length of the mooring is three to five times the location depth;

- Mooring design: site depth may influence the equipment and materials used for moorings, which increase the implementation and maintenance costs;

- Diving inspections: If necessary, diving inspections at deep sites may present a problem, requiring specific training, and professional and expensive gear for working at greater depths.

Although the influence of the depth can not be dissociated from surrounding environment conditions, Baluyut and Balnyme (1995) defined an ideal range between 1 and 10 meters depth to the best sites for finfish and molluscs culturing.

1.3.4.2 Current Velocity

Current speed has a major influence on finfish and molluscs culture, since it affects the water exchange in the cages, feed dispersion, net shape and rearing volumes, cage movements and fish transfers.

According with Cardia and Lovatelli (2015), optimal current speed varies with the cultured fish species. For example, in the Mediterranean Sea, the optimal current speed in aquaculture cage is generally between 0.1 and 0.2 ms^{-1} and not exceeding 0.6 ms^{-1}. Norway, which is the country with the strongest investment in aquaculture, settles a minimum of 0.5 ms^{-1} for determining the size of the mooring system.

The criteria adopted by Katavić and Dadić (2000) for current speed, defines a suitable range for finfish culture between 0.2 and 0.6 ms^{-1}, medium suitability between 0.05 and 0.2 ms^{-1}, and defined less suitable areas with current velocity lower than 0.05 ms^{-1} and higher than 0.6 ms^{-1}. Laing and Spencer (2006) defined that sheltered areas with velocities between 0.5 and 1.0 ms^{-1} usually provide the best conditions, and will assure enough water exchange to supply the molluscs bivalves with an adequate supply of food and oxygen and for the removal of waste.

1.3.4.3 Water Temperature

Sea water temperature has a major effect on the seasonal growth of fish and bivalves health and growth and may be largely responsible for any differences in growth between sites. For fish, breathing, embryonic development and growth are some of the vital functions that are strongly affected by water temperature. Additionally, fast increases in water temperature are usually problematic for some fish species, since they greatly increase their metabolism, decreasing dissolved oxygen and increasing the activity of pathogenic bacteria (Lawson, 2013). In Table 1.1 is depicted the minimum and maximum water temperatures bearable for the 3 most explored fish species in Portugal and Spain, as well as their optimal temperature to growth and breathing.

Table 1.1: Optimal, minimum and maximum temperatures supported by some of the most cultivated species. Source: Egna and Boyd (1997).

Species	Optimal Temperature	Min Temperature	Max Temperature
Dicentrarchus labrax	18-24°C	1°C	34°C
Sparus aurata	25°C	3°C	35°C
Anguilla anguilla	22-25°C	5°C	30°C

Regarding to bivalves, their growth usually begins when sea water temperatures rise up to 8-9°C, reaching the maximum growth rate typically around 16-18°C. In case of high water temperature events, in combination with high stocking density, limited food availability and low water exchange, the bivalves are under biological stress. Despite many bivalves species can tolerate water temperatures of 25°C or even more, in the above circumstances, temperatures above 20°C can be stressful and may result in mortalities, even after the animals have been transferred to ideal conditions (Laing and Spencer, 2006).

On the other hand, some bivalves such as oysters, clams, scallops and mussels are tolerant to water temperature below 3-5°C. For examples, mussels (very commercialized in Ria de Aveiro and Rias Baixas) are very resistant to low temperatures, being able to ingest food particles and grow even during low water temperature events (Laing and Spencer, 2006).

Salinity has a major influence on the bivalves tolerance to low temperatures. For example, scallops may survive to temperatures below 3°C if the salinity is above 30, but they may die at temperatures below 5°C if salinity drops to less than 26 (Laing and Spencer, 2006). The effect of salinity on fish and bivalves is discussed in the next sub-section.

1.3.4.4 Salinity

Salinity is one of the most important environmental factors for fish and bivalves. The fish species commonly farmed in Portugal and Spain, such as *Dicentrarchus labrax*, *Sparus aurata* and *Anguilla anguilla*, are euryhaline species, i.e., they are able to adapt to a wide range of salinities, living in estuaries/lagoons, or in the ocean (Nebel et al., 2005). For that reason, water temperature may be more important in Ria de Aveiro and Rias Baixas farmed species than salinity. However, when salinity decreases down to 10, organisms use more dissolved oxygen for respiration indicating an increase in their metabolic rates.

As mentioned above, these species can adapt to changes in salinity and survive both in seawater and brackish water. The osmotic pressure can be controlled by the skin, kidneys, and intestines of these fishes, but the main osmolality control occurs in the gills. In these organs, the ion concentration in the blood can be controlled to adapt to changes in salinity and minimize damage caused by salinity differences (Hwang et al., 2018). For that reason, higher salinity fluctuations in a short period can be dangerous, since the animals may not have time to adapt to the new conditions.

Salinity fluctuations do not affect the growth and breeding of bivalves as much as water temperature variations, even though most bivalves usually only feed at high salinity water, so is advisable that the bivalves rafts should be placed where salinity is within their optimum range, for as long as possible. Oysters and clams are comfortable with seawater salinities, while scallops are very intolerant to salinities lower than 30, therefore areas with high freshwater inflow are not suitable for the cultivation of these species. Mussels have good growth rates above 20 (Laing and Spencer, 2006).

1.3.4.5 Dissolved Oxygen

All marine organisms use the oxygen dissolved in the sea water for respiration. The oxygen concentration of sea water is usually enough to breathe at normal rates. However, in some circumstances, such as high water temperature or calm weather (no rearation), the dissolved oxygen levels in sea water may become very low. These periods are usually of short duration, not constituting a major problem, depending on the time of exposure.

According to Lawson (2013), dissolved oxygen is the most important variable in aquaculture production. In estuaries and coastal lagoons, the photosynthesis is the main source of oxygen, therefore the phytoplankton has to produce, at least, the same oxygen than it is consumed by fish and other animals, bacteria, chemical reactions and bottom sediment.

Problems with the limited supply of dissolved oxygen (DO) in water are usually aggravated in lagoons and estuaries, due to the high rates of biological activity that can rapidly deplete oxygen concentration. The natural replenishment of dissolved oxygen from the atmosphere is relatively slow. For that reason, the aquaculture farms resort to a supplement to the natural aeration of dissolved oxygen using mechanical aerators (Tabuada, 2009). Figure 1.2 indicates the effect of dissolved oxygen concentration on fish condition.

Generally, fish do not grow when dissolved oxygen decreases below 25% of saturation. It is commonly accepted by aquaculture producers and researchers that fish species are healthier when DO concentration is close to saturation. Summerfelt et al. (2008) and Lawson (1995) recommend that DO concentration in aquaculture systems

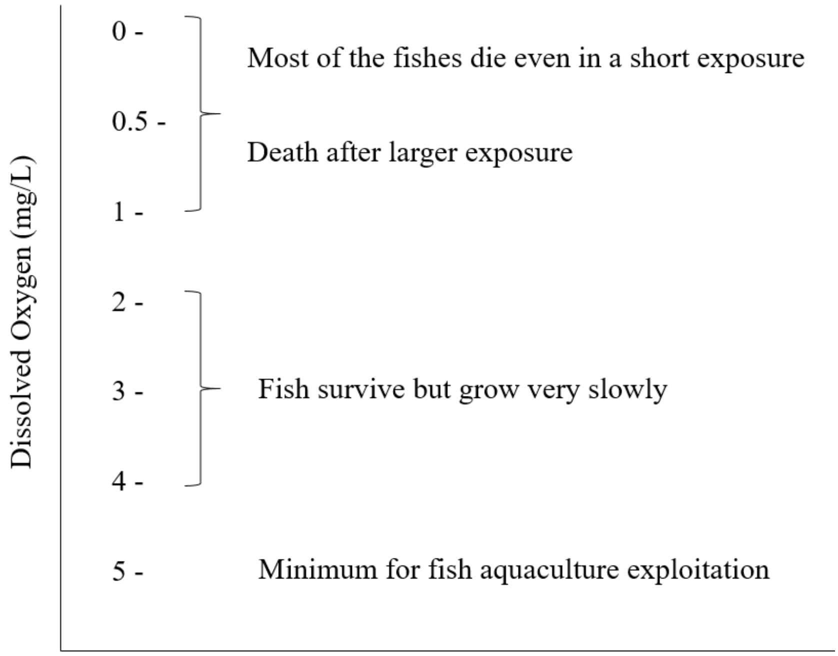

Figure 1.2: Effect of dissolved oxygen concentration on fish condition. Source: Boyd and Tucker (2012).

should be maintained at around 90% saturation, as a minimum, at all times, for optimum performance.

Regarding to the bivalves, they are quite tolerate to low DO concentrations, adapting their metabolic activity according with the environmental conditions, using anaerobic respiration to provide energy needs. However, prolonged periods of very low oxygen, particularly at high water temperature, can stress bivalves, causing them to gape and possibly to die (Laing and Spencer, 2006).

1.3.4.6 pH

Due to the large buffering capacity of the ocean, the pH of the seawater has a very low variability, evidencing a typical value of 8.3 at the surface. However, in estuaries and lagoons, where phytoplankton and other aquatic plants are abundant, using CO_2 for photosynthesis, the pH has a daily variability, increasing during the day and decreasing during the night (Tabuada, 2009).

Fish and bivalves can adapt to gradual changes in pH, however they do not tolerate rapid pH variations, which can cause death. In general, according with Randall and Tsui (2006), fish do not tolerate pH values outside the range between 5 and 9. Figure 1.3, adapted by Lawson (2013), represents the effect of pH on fish condition.

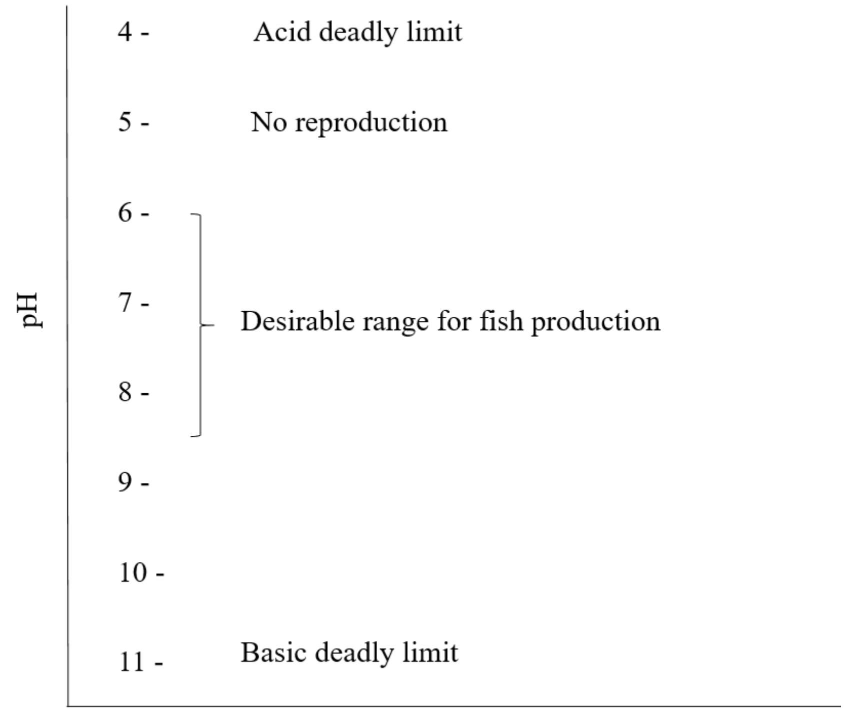

Figure 1.3: Effect of pH on fish condition. Source: Lawson (2013).

1.3.4.7 Microalgae Biomass and Nitrogen Compounds

According to Fiúza et al. (1998) and Trainer et al. (2010), aquaculture production can be positively or negatively affected by microalgae biomass. The main advantage is that phytoplankton is the main food source for fish and bivalves, keeping them free from harmful effects of chemical feed and reducing the production costs. However, algae may also cause problems in aquaculture as documented by Díaz et al. (2019) in Chile, as they may deteriorate the cultures of farmed organisms by oxygen depletion at night or after death (Dahms, 2014), and by producing toxins that threaten both the health of the cultured organisms and the health of consumers. Since, it is difficult to define a biomass range, eutrophication conditions should be avoid.

Regarding to bivalves, they feed by filtering mainly phytoplankton, but also some other organic detritus. It has been estimated by Asokan et al. (2011), that when bivalves are growing under similar environmental conditions at different sites, more than 85% of any difference in growth observed between sites can be attributed to water temperature and primary production rates. Shepard et al. (2010) have shown that the growth of small scallop spat is positively co-related with the concentration of chlorophyll in the water. This proves the importance of primary production for healthy growth of cultivated bivalves species.

Nitrogen is the major nutrient that affects the aquatic ecosystem because it is one of the constituents of proteins and an important component of cellular protoplasm.

The nitrogen may be in the form of inert gas (N_2), organic nitrogen, ammonia (NH_3), ammonium (NH_4), nitrite (NO_2^-), nitrate (NO_3^-), etc. Aquatic animals find their need for nitrogen in food intake. Aquaculture depends on natural food to support the growth of animals, and nitrogen is important because it is the key to the growth of plants in aquaculture (Lawson, 1995).

On the other hand, nitrogen from animal excretions can contribute to the overgrowth of phytoplankton, and consequent accumulation of nitrite and ammonia. The presence of these compounds may be toxic to aquatic animals at relatively low concentrations. The nitrogen in the discharge of the tanks enriched with organic and inorganic nitrogen can degrade the quality of the receiving water (Tabuada, 2009).

Regarding to these biological and chemical variables, there is no standardized values for aquaculture practices. Therefore, it is important to predict the trophic status of the coastal systems, that can be assessed by using information about the concentration of the limiting nutrients and chlorophyll *a*.

1.4 Structure of the Work

This thesis is divided in 9 chapters. The current Chapter 1 is an introduction in which the motivation of the study is presented, as well as the contextualization of the importance of this study for scientific knowledge. Are presented in this chapter, the main goals and the literature review concerning the development of hydrodynamic, hydrologic and water quality models to study Ria de Aveiro and Rias Baixas; the international background about the application of GIS techniques and modelling tools contributing to the sustainable development of aquaculture; finally, a literature review of the suitable and unsuitable ranges of environmental conditions to aquaculture development. Chapter 2 presents a detailed description of the study areas, from the geomorphological, hydrodynamic and ecological points of view. In this chapter is also highlighted the location, characteristics and species cultivated in Ria de Aveiro and Rias Baixas. Chapter 3 presents the analysis of *in situ* measurements to assess the influence of the water column stratification in mussels production in Rias Baixas. The seasonal and vertical variability of some hydrographic and chemical variables is also discussed in this chapter. Chapter 4 presents the general overview of Delft3D - Flow and Delft3D - WAQ numerical models, while in Chapter 5 the setup of hydrodynamic and water quality model is presented, as well as the calibration and validation procedures of the estuarine models. Chapter 6 presents the methodology, results and discussion of *in situ* data collected from field surveys, which were used in the Ria de Aveiro water quality validation procedure presented in Chapter 5. Here, is also presented a combination between measurements and predictions to estimate new insights about primary production dependence on environmental conditions in Ria de Aveiro. Chapter 7 presents the hydrodynamic characterization and suitability to aquaculture development in Ria de Aveiro and Rias Baixas, highlighting the estimation of water renewal. In Chapter 8 a GIS-based habitat suitability model is developed and applied to accomplish the main goal of this thesis: to identify preferential sites to ensure fish and bivalves aquaculture expansion and proper operation in a sustainable manner in Ria de Aveiro and Rias Baixas. Chapter 9 presents the main conclusions of this study and suggestions for future work.

Chapter 2

Study Areas

2.1 Ria de Aveiro

Ria de Aveiro (Figure 2.1) is a shallow coastal lagoon located on the Portuguese northwest coast, being separated from the Atlantic Ocean by a sand dune barrier. It has an irregular geometry, and is connected with Atlantic Ocean through an artificial channel, constructed in 1808 (Dias, 2001; Dias and Mariano, 2011). The lagoon has a maximum width of 8.5 km and a length of 45 km, being constituted by four main channels: Mira, São Jacinto, Ílhavo and Espinheiro. The Mira channel is an elongated shallow arm, with 14 km length, S. Jacinto channel is about 29 km long, and Ílhavo and Espinheiro have 15 and 17 km, respectively (Dias, 2001).

The Ria de Aveiro's area is characterized by large variability due to the tidal influence in its hydrodynamics. During spring tide, the lagoon area reaches a maximum area of 89.2 km^2 at high tide, which is reduced to 64.9 km^2 at neap tide (Lopes et al., 2013). Despite the inlet channel can exceed 30 meters deep due to dredging operations, Ria de Aveiro's average depth is about 1 meter relative to local datum. The physical and hydrodynamic description of the lagoon is described in detailed.

2.1.1 Physical and Hydrodynamic Description

The tide is the main forcing agent driving water circulation in Ria de Aveiro, with an average tidal amplitude at the inlet of 2 meters, and amplitudes of 0.6 meters in neap tides and 3.2 in spring tides (Dias, 2001; Araujo, 2006). Several authors, using different numerical models and considering different bathymetries, predicted the lagoon's tidal prism, resulting in the achievement of different values.

For maximum spring tide, Dias (2001) and Lopes et al. (2006) estimated 136.7×10^6 m^3, Picado et al. (2010) 86.3×10^6 m^3 and Lopes et al. (2010) estimated 87.5×10^6

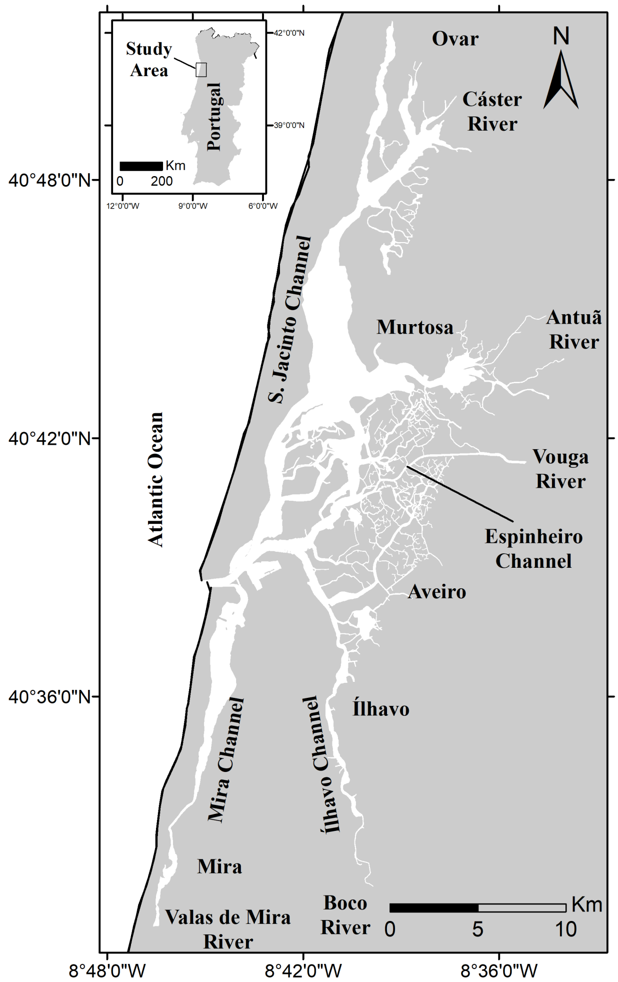

Figure 2.1: Map of Ria de Aveiro lagoon, and its location in Portuguese coast.

m^3 for intermediate tides, and for minimum neap tide Dias (2001) and Lopes et al. (2006) estimated 34.9×10^6 m^3, Picado et al. (2010) 31.0×10^6 m^3 and Lopes et al. (2010) 28.9×10^6 m^3. The tidal prism of each channel relative to it its value at the mouth is: 35.4% for S. Jacinto channel, 25.6% for Espinheiro channel, 10.0% for Mira channel and 13.5% for Ílhavo channel (Dias and Picado, 2011).

Additionally, Ria de Aveiro dynamics is also driven by freshwater input from five rivers discharging in the main channels: Vouga, Antuã, Cáster, Boco and Valas de Mira. According to the Ria de Aveiro Polis Litoral program, which considered the data from the Plano de Bacia Hidrográfica (`www.arhcentro.pt`), the mean freshwater inflows are 60.0 m^3s^{-1} for Vouga river, 4.5 m^3s^{-1} for Antuã, 1.6 m^3s^{-1} for Cáster, 1.0 m^3s^{-1} for Boco and 3.6 m^3s^{-1} for Valas de Mira river. According with Moreira et al. (1993), the total mean river discharge of 1.8×10^6 m^3 during a tidal cycle is considerably lower than the tidal prism at the lagoon mouth.

As mentioned before, the lagoon hydrodynamics is dominated by tide, which is semi-diurnal (Dias, 2001). The Ria de Aveiro is ebb dominated at the inlet and surrounding areas and flood dominant at the upstream areas close to the rivers mouths (Dias, 2001; Oliveira et al., 2006; Picado et al., 2010), resulting in a tendency to export proprieties as sediments, pollutants and algae blooms from the Ria de Aveiro to the ocean. The lagoon is considered by Dias et al. (2000) and Vaz et al. (2009) as vertically homogeneous, except in case of very high freshwater inflows, when a vertical stratification can be found in some upstream lagoon areas.

According to Dias (2001), the influence of wind on lagoon hydrodynamics is residual comparing with the tidal and riverine driving forces. Actually, this influence was assessed by Fortunato et al. (2013), finding that the wind stress may induce water elevations lower than 0.05 meters during storm surge events.

The influence of wind waves in the lagoon hydrodynamics is also residual comparing with the tidal forces. Vaz (2012) concluded that coastal storms events, with waves higher than 4 meters, might induce a maximum over-elevation of the sea surface of 0.22 meters at inlet area.

2.1.2 Ecological Description

According to Almeida et al. (2005), Ria de Aveiro is considered as a mesotrophic shallow lagoon, being characterized by its rich biodiversity encompassing 64 fish species, 12 of amphibians, 8 of reptiles, 173 species of birds and 21 mammal species (Rebelo, 1992).

Ria de Aveiro ichthyofauna can be divided into four ecological groups (AMRia/CPU, 2006):

- Marine stragglers, species occasionally entering the lagoon with the tides (e.g., *Sardina pilchardus*, *Sparus aurata*);

- Marine migrants, including the marine species dependent on the lagoon environment for food, shelter and nursery (e.g., *Lisa aurata*, *Dicenthrachus labrax*, *Platichthys flesus*);

- Estuarine species, including the resident species (e.g., *Atherina presbyter*, *A. boyeri*);

- Fish that are born in seawater, then migrate into fresh or brackish waters as juveniles where they grow into adults, such as catadromous (e.g., *Anguilla Anguilla*, *Alosa alosa*) and anadromous species (*Lampetra planeri*, *Petromyzon marinus*)

Attending to this high biodiversity, the Ria de Aveiro integrates the National System of Classified Area (SNAC), which is constituted by the National Network of Protected Areas (RNAP), the Natura 2000 classified areas and other areas classified under international protection. Due to lagoon's importance for the shelter, feeding and reproduction of many birds species, the Ria de Aveiro is classified as a Special Protection Area (SPA) under the Birds Directive. More recently, it was also classified as a Site of Community Importance (SCI). Furthermore, between the downstream area of S. Jacinto channel and the Atlantic Ocean, is located a protected area classified as Natural Reserve (NR) of S. Jacinto Dunes, covering an area of approximately 700 ha. This protected area was established with the objective of preserving the coastal dunes and its associated flora and fauna. The reserve was divided into three areas depending on their degree of protection: the strict natural reserve which includes the stabilised dune zone and heron-breeding area; the partial natural reserve with limited access, which covers the whole forest area; and the leisure reserve, which includes the beach and woods areas.

The exact location of Natural Reserve (NR) of S. Jacinto Dunes is shown in Figure 2.2(A), as well as the lagoon main habitat designations. In addition to the main water bodies, about 45% of lagoon is constituted by intertidal areas, comprising saltmarshes, mud and sand flats and seagrass meadows, that play a major role on the Ria de Aveiro ecosystem balance.

Saltmarshes play a very important role in ecosystem functioning, because they provide habitat for several fish species, nutrient cycling and margin protection against floods. In addition, saltmarshes are colonized by halophyte plants constituting a source for primary production (Lopes, 2016). The mycrophytobenthos that colonize mud and sand flats constitute the lagoon's main source of primary production. Vaz et al. (2016) predicted a total biomass of $5{\times}10^6$ g(Chl a), more than 100 times comparing with water column production. Furthermore, this habitat is crucial for protection against erosion, feeding for several birds and nutrient cycling.

Regarding seagrass meadows, *Zostera noltii* is the dominant species colonizing those habitats, that are restricted to S. Jacinto and Mira channels (da Silva and Duck, 2001). Similarity to the saltmarshes, mud and sand flats, seagrasses present important ecological services, such as high primary production, carbon and nutrient cycling, sediment stabilization, protection against erosion, habitat and nursery areas for fish species. Silva et al. (2004), and more recently Azevedo et al. (2013), reported a decrease of seagrass meadows due to an increase of tidal amplitude and consequently tidal currents, changing the turbidity patterns and sediment dynamics. Saltpans, which suffered a marked decrease in last decades, occupies about 7% of total lagoon area, and accord-

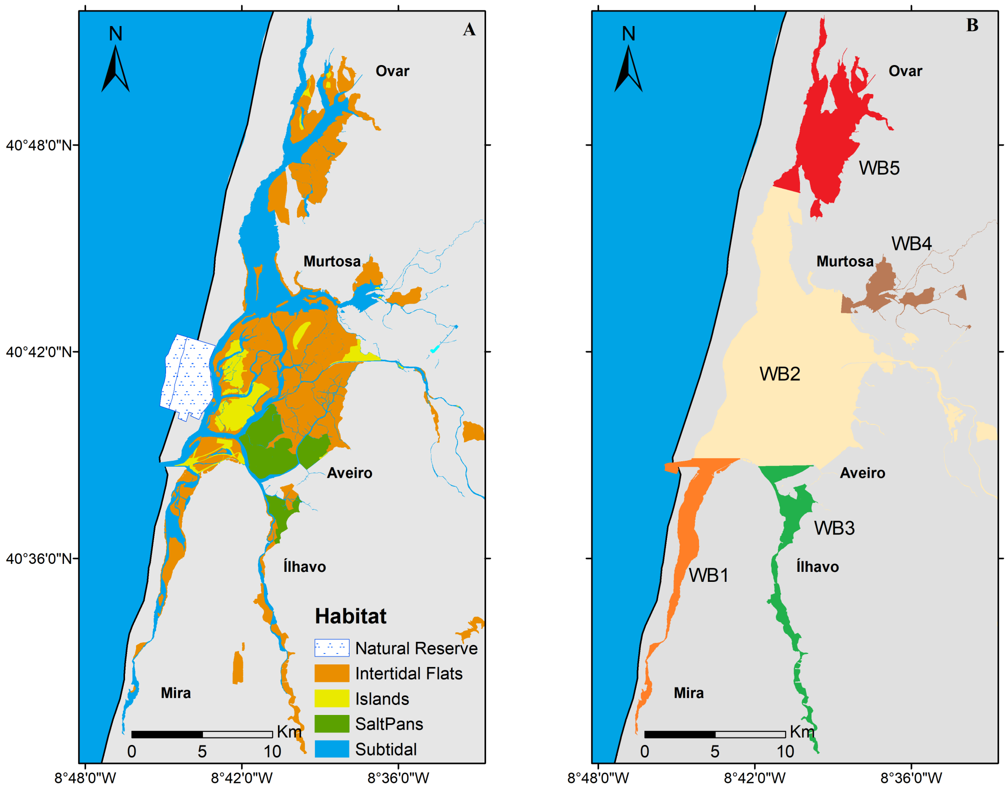

Figure 2.2: Charts of Ria de Aveiro showing, (A) the distribution of the main lagoon habitats; and (B) the lagoon classification according with their water quality status (Raposo et al., 2012).

ing with Rodrigues et al. (2011), they play a crucial role in the ecological health of the ecosystem because several resident and migratory birds species included in the Birds Directive, use those areas for feeding and breeding.

Despite this natural richness, Ria de Aveiro is also characterized by an increasing anthropogenic pressure near its margins, such as land occupation, agricultural and industrial activities. Pollution problems are mainly due to eutrophication associated with nitrates from agricultural activities, flowing from the water course to lagoon water. Additionally, main anthropogenic sources of pollution as domestic and industrial discharges should also be considered (Lopes et al., 2005). Therefore, the water quality of Ria de Aveiro results from a complex balance between natural processes and anthropogenic activities, as well as from the lagoon auto-depuration capacity.

Ferreira et al. (2003) reported that Ria de Aveiro had a moderate degree of eutrophication and low overall human influence in comparison to other coastal/estuarine systems. Furthermore, Lopes et al. (2007b) concluded that, despite the improvement of the multi-municipality sanitation waste water treatment plant system, the upstream lagoon areas still present high concentrations of dissolved inorganic nutrients, especially nitrogen.

In accordance with Water Framework Directive (WFD), Ria de Aveiro is divided in five transitional water bodies according to their water quality status (Figure 2.2B), with the following description and classification (Raposo et al., 2012):

- WB1 – A natural (unmodified) water body that includes Barra and Mira Channel - water ecological status is 'Good';

- WB2 – A heavily modified water body corresponding to the central area of the lagoon - water ecological status is 'Moderate';

- WB3 – A natural (unmodified) water body corresponding to Ílhavo Channel - water ecological status is 'Good';

- WB4 – A natural (unmodified) water body that includes the Murtosa Channel and the Laranjo Basin - water ecological status is 'Moderate';

- WB5 – A natural (unmodified) water body corresponding to the upstream area of S. Jacinto channel - water ecological status is 'Poor';

2.1.3 Ria de Aveiro Marine Cultures

Historically, the local population living around Ria de Aveiro depends on lagoon's natural resources and capital to improve their well-being. In this context, the population has developed several traditional activities such as fisheries, salt production, harvest of seagrasses and macroalgae named "moliço". These were used as agriculture fertilizers for the harvest of reeds in order to use as cattle bedding. More recently, in order to supply food for a growing local population, marine cultures producing fish and molluscs has been rising in Ria de Aveiro. The abandoned saltpans areas mentioned in the previous subsection, are now being used for aquaculture production.

According to MAOT/INAG (2012), Ria de Aveiro provides appropriate environmental conditions for aquaculture and production of species with commercial importance, such as fish and bivalves. The authors also reported that the main fish species produced in extensive or semi-intensive regime is seabass (*Dicentrarchus labrax*). Regarding bivalves, relevant examples of aquaculture production are the Japanese oyster (*Crassostrea gigas*), the clam *Ruditapes decussates* and the blue mussels (*Mytilus spp.*).

Ria de Aveiro is defined by 4 main aquaculture zones with the codes RIAV1 (São Jacinto channel), RIAV2 (Mira channel), RIAV3 (central zone) and RIAV4 (Ílhavo channel entrance). The first two areas are classified as a Class B bivalve estuarine-lagoon area, while the remaining areas are classified as Class C. According to the site `www.eaquicultura.pt`, there are several aquaculture units dedicated to the group of

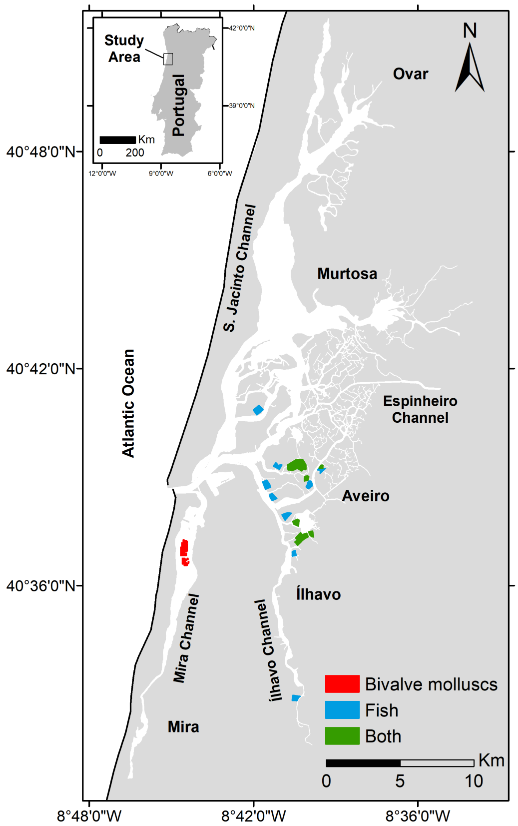

Figure 2.3: Map of Ria de Aveiro lagoon, showing the aquaculture exploitation sites.

bivalve molluscs, especially in the RIAV2 and RIAV3 zone (Figure 2.3). Most of the aquaculture facilities are located in the central area of the Ria de Aveiro, close to the city of Aveiro. On the other hand, RIAV1 region is under-explored, although two units dedicated to oyster cultivation are under construction.

According to the Portuguese government aquaculture portal (`www.eaquicultura.pt`), the total area exploited in Ria de Aveiro is about 1.8 km^2, of which 0.30 km^2 (17% of the total area) is occupied by bivalve production in Mira channel (RIAV2 area). Fish production occupies 0.68 km^2 (38%) of the exploited area, while infrastructures that simultaneously produces fish and bivalve occupies about 0.82 km^2 (45%) of the total production area.

In Table 2.1 are listed the species exploited in Ria de Aveiro marine cultures, divided by taxonomic classes. Therefore, the different aquaculture companies produce 10 molluscs species (including 9 species of bivalves molluscs and 1 species of gastropod molluscs), 8 fish species and 11 algae species. Beyond the species presented in Table 2.1, the species *Paracentrotus lividus* (echinoderm) and *Salicornia europaea* (plant) are also produced. Contrarily to the molluscs and fish species, that are distributed by the different aquaculture companies, the algae production is performed by only one company, located in Ílhavo channel.

Table 2.1: List of the species produced in Ria de Aveiro marine cultures.

Molluscs	**Fish**	**Algae**
Bivalve		
Ruditapes decussatus	*Sparus aurata*	*Ulva rigida*
Venerupis corrugata	*Anguilla anguilla*	*Porphyra dioica*
Ensis siliqua	*Dicentrarchus labrax*	*Porphyra*
Ostrea spp	*Mugil spp*	*Umbilicalis*
Crassostrea gigas	*Solea solea*	*Palmaria*
Crassostrea angulata	*Psetta maxima*	*Palmata*
Cerastoderma edule	*Pleuronectes platessa*	*Chondrus Crispus*
	Scophthalmus rhombus	*Gracilaria sp*
Scrobicularia plana		*Fucus Vesiculosas*
		Codium Tomentosum
Gastropod		*Grateloupia Turuturu*
Littorina littorea		

2.2 Rias Baixas

Rias Baixas are four estuaries located south of Cape Finisterre (between 42°N and 43°N), in the northwestern coast of the Iberian Peninsula: Ria de Vigo, Ria de Pontevedra, Ria de Arousa and Ria de Muros, as mapped in Figure 2.4. These coastal systems are characterized by a V shape, narrowing progressively from the estuaries mouths towards upstream. They are connected to the Atlantic Ocean by more than one entrance due to presence of islands in outermost part. Freshwater contributions come from 5 rivers distributed by the four estuaries: Verdugo-Oitaben River at Ria de Vigo head; Lérez River at Ria de Pontevedra; Umia e Ulla Rivers at Ria de Arousa; and finally, Tambre River at Ria de Muros head.

Socially, important Spanish cities are located on Rias Baixas margins, such as Vigo, conferring to the Ria de Vigo the highest population among the Rias. The Ria de Arousa is the one with higher water surface, followed by Ria de Pontevedra. The Ria de Arousa, due to two main tributaries discharge, is the estuary with the highest freshwater inflow, in addition to being the shallowest of Rias Baixas. In Table 2.2, adapted from Sousa (2013), is shown a summary of the fundamental dimensions of Rias Baixas.

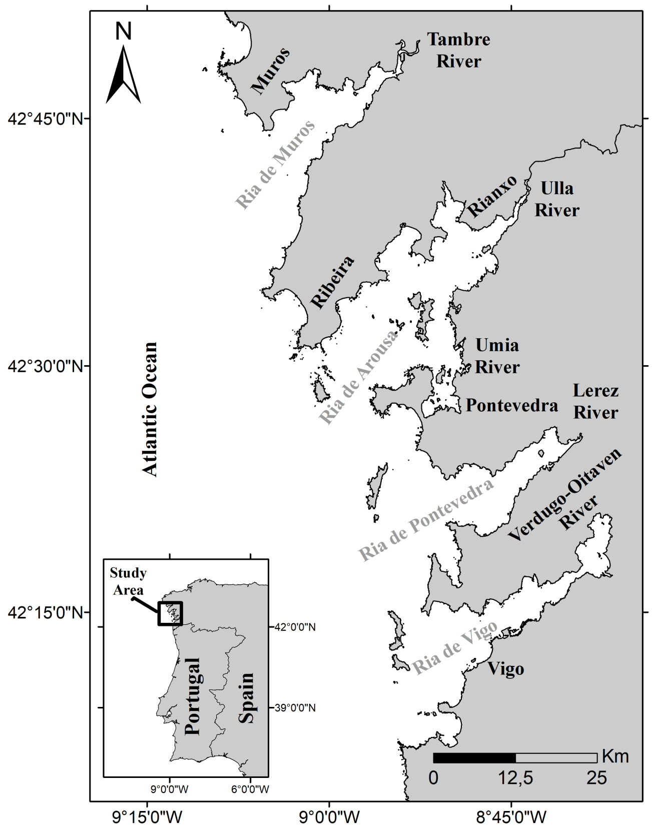

Figure 2.4: Map of Ria Baixas, and its location in NW coast of the Iberian Peninsula.

Table 2.2: Rias Baixas characteristics.

	Vigo	**Pontevedra**	**Arousa**	**Muros**
Location	42°(06'-21')N	42°(15'-25')N	42°(27'-41')N	42°(35'-45')N
	8°(36'-54')W	8°(39'-56')W	8°44'- 9°01'W	9°(04'-06')W
Surface (km^2)	156	141	239	90
Volume (km^3)	3.12	3.47	4.34	2.06
Mean width (km)	4.80	3.80	9.00	3.42
Mean depth (m)	21	31	19	25
Number of Inlets	2	2	2	1
Mouth width (km)	south: 5.10 north: 2.80	south: 7.30 north: 3.60	south: 4.60 north: 3.70	6.3
Mouth depth (m)	south: 45 north: 25	south: 60 north: 15	south: 55 north: 5	45

2.2.1 Physical and Hydrodynamic Description

2.2.1.1 Ria de Vigo

Ria de Vigo's tidal forcing is semi-diurnal, presenting a tidal range between 2 and 4 meters, therefore being classified as a mesotidal estuary (Alvarez et al., 2005). Ria de Vigo is considered a partially mixed estuary, showing a stratification which is normally maintained throughout the year, with positive residual circulation and a two layer circulation pattern, in which the water flows into the estuary from the surface, and outflows close to the bottom layers (Alvarez et al., 2013). Ria de Vigo presents and outgoing flux to the ocean of about 6×10^5 kgs^{-1} (Prego and Fraga, 1992).

According to Pérez et al. (1992), Ria de Vigo is divided in three distinct areas due to the important influence of the oceanic and river forcings: the innermost, middle and outer zones. The outer zone is under oceanic influence, comprising the area between Cíes islands and Cape Mar. The Cíes islands protect the estuary from the Atlantic swell. The middle area is the mixing zone, which is under both oceanic and continental actions, spreading from the Cape Mar to Rande Strait. Finally, the innermost area present a strong influence of Verdugo-Oitaben river, however the effects of tides is also important (3 meters tidal range, in average).

The Verdugo-Oitaben river, the main tributary of Ria de Vigo, has an annual average discharge of 13 m^3s^{-1}, and a catchment area of about 333 km^2 (Sousa, 2013). During dry season, the discharge may be less than 3 m^3s^{-1}, while in winter, river flows higher than 120 m^3s^{-1} are observed (Prego and Fraga, 1992).

2.2.1.2 Ria de Pontevedra

The physical and hydrodynamic features of Ria de Pontevedra are similar to those observed in Ria de Vigo. The tide is semi-diurnal and mesotidal, with an average tidal range of around 2.5 meters. According to Ruiz-Villarreal et al. (2002), a slightly longer duration of flood is observed, and typical mean tidal velocities between 0.05 and 0.1 ms^{-1} are found, with maximum velocities around 0.3 ms^{-1}. Wind forcing can induce higher velocities in surface layers. Similarity to Ria de Vigo, Ria de Pontevedra is a partially mixed estuary during most time of the year. Freshwater flows seawards in the surface layer, while water coming from Atlantic Ocean flows into the Ria through the bottom layers (Ruiz-Villarreal et al., 2002).

The Lerez river is responsible for about 80% of the total river discharge into the Ria de Pontevedra (Ibarra and Prego, 1997). The monthly mean discharge varies between a maximum of 80 m^3s^{-1} in winter and a minimum of 2 m^3s^{-1} in dry season. Due to these relative low run-offs periods, the estuary circulation is mainly baroclinic, and not advective (Ruiz-Villarreal et al., 2002). However, under some intense rainfall events, the runoff can exceed 300 m^3s^{-1}.

2.2.1.3 Ria de Arousa

Ria de Arousa is also a partially mixed estuary, with a two-layered positive residual estuarine circulation (Margalef and Fraga, 1979). The tidal range, during neap and spring tides, is 1.1 and 3.5 meters, respectively, therefore, classifying the estuary as mesotidal (Hanson et al., 1986).

The Ulla river is responsible for more than 80% of the total freshwater into the estuary, with a catchment area close 3000 km^2, and an annual mean runoff of about 76 m^3s^{-1}, ranging from a maximum of 150 m^3s^{-1} in winter, to 5 m^3s^{-1} during the dry season (Otto, 1975). Umia River discharges an average flow of 16 m^3s^{-1} into Ria de Arousa.

According to Rosón et al. (1995), the estuary middle area has intermediate hydrographic characteristics depending on the river discharge, but mainly on the wind regime over the shelf, which is the main factor governing Ria de Arousa hydrodynamics.

2.2.1.4 Ria de Muros

Ria de Muros presents very similar tidal features (semidiurnal and mesotidal tidal range of 2.5 meters). Typical depth-averaged tidal velocities are in order of magnitude of 0.05 - 0.2 ms^{-1} in the outer and middle estuary. Higher tidal currents (up to 1.5 ms^{-1}), are restricted to the shallow and inner areas (Iglesias et al., 2008).

The largest freshwater inflow is provided by the Tambre River, with an annual average discharge of 54 m^3s^{-1}. Tines River, the other tributary, has an annual mean flux of 0.6 m^3s^{-1}, and only influences the area close to its mouth (Carballo et al., 2009).

2.2.2 Ecological Description

Rias Baixas, submerged unglaciated river valleys (García-Moreiras et al., 2019), are very sensitive to climate and oceanographic oscillations affecting the North Atlantic region (DeMenocal et al., 2000). These ecosystems hold a very productive and miscellaneous habitats, providing an immeasurable socio-economic and ecological value (Figueiras et al., 2002). However, fauna, hydrology and ecosystems are very vulnerable to natural and anthropogenic disturbances, highlighted on changes on sea level (Sobrino et al., 2014).

The coastal upwelling and downwelling events induced by wind are the main processes driven the biogeochemistry, ecology and primary production rates in Rias Baixas.

Indeed, the seasonal coastal upwelling induced by favourable winds in spring-summer months is the main recognized source of primary production (Fiúza et al., 1998). Upwelled waters are characterized by considerable variability in the vertical distribution of nutrients and phytoplankton (Brown and Hutchings, 1987).

However, in these type of ecosystems with high productivity rates, harmful algal events due to toxic phytoplankton species and/or high-biomass blooms may cause an increasing threat for aquaculture and fishing operations, ecological health and diversity, resulting in possible implications for human health and activities (Trainer et al., 2010).

These type of events are documented in the literature since 1950s, describing the favourable conditions to the development of harmful algal blooms, studying their origin, dynamics, distribution and toxicity levels (Margalef, 1956; Figueiras et al., 1994; Pitcher et al., 2010). More concretely, Figueiras and Ríos (1993) established a relationship between spring and summer upwelling events in Rias Baixas and the appearance of a specific potentially toxic diatom species (*Pseudo-nitzschia* spp.).

Figueiras et al. (1996) state that the advection of warm water from the shelf into the Rias Baixas at the end of the upwelling season coincides with the highest abundances of *G. catenatum*, a dinoflagellate known to be responsible for paralytic shellfish poisoning, a neurotoxic poisoning syndrome which affects human consumers of contaminated shellfish.

Therefore, as mentioned before, upwelling events enrich the Rias Baixas water with nutrients and phytoplankton, being the most important driver of primary production rates, contrarily to what occurs in Ria de Aveiro. However, this high productivity may develop a bloom of some patogenic species of diatoms or dinoflagellates that may harm bivalves aquaculture in the estuaries, which is described in detail in the next sub-chapter.

2.2.3 Rias Baixas Marine Cultures

According to FAO, Rias Baixas are considered as one of the most important phytoplankton deposits worldwide. The physical and ecological conditions, such as water temperature and the high primary production, make Rias Baixas an excellent development seafood place.

In this context, according to data provided by Galician Fishing Technology Platform (`https://www.pescadegalicia.gal/`) and depicted in Table 2.3, the total marine aquaculture production in 2018 was more than 289 tons distributed among algae, bivalves, cephalopods, gastropods and fish productions. Table 2.3 highlights three important features: (i) fish production is unimportant in the global context of aquaculture in Rias Baixas; (2) from the total fish production weight (8.48 tons), 98.7%

Table 2.3: Marine species produced in Rias Baixas in 2018, including the production weight (in kg and %). Source: `https://www.pescadegalicia.gal/`.

	Weight (kg)	**%**
Algae	**411**	**0.00**
Phaeophyceae	376	0.00
Saccorhiza polyschides	35	0.00
Bivalves	**281 293 611**	**97.07**
Venerupis corrugata	247 428	0.09
Ruditapes decussatus	144 190	0.05
Venerupis philippinarum	1 090 486	0.38
Cerastoderma edule	348 780	0.12
Mytilus galloprovincialis	278 707 763	96.18
Ostrea edulis	325 256	0.11
Crassostrea gigas	428 567	0.15
Aequipecten opercularis	1 140	0.00
Cephalopods	**842**	**0.00**
Octopoda	842	0.00
Gastropods	**2 685**	**0.00**
Haliotis discus	2 685	0.00
Fish	**8 475 103**	**2.92**
Solea solea	401 745	0.14
Pagellus bogaraveo	108 077	0.04
Scophthalmus rhombus	7 965 281	2.75
Total	**289 772 651**	**100**

corresponds to benthic fishes (*Solea solea* and *Scophthalmus rhombus*), which may mean that the farmers consider that the water column conditions are not appropriate for this practices; (3) bivalves comprises more than 97% of the total sea food production, in which *Mytilus galloprovincialis* is responsible for 96.2% of the total marine production, and 99.1% of the total bivalves production in Rias Baixas. Due to this high importance, details about *Mytilus galloprovincialis* production will be provided in the next sub-section.

2.2.3.1 *Mytilus galloprovincialis*

Following the previously mentioned, Rias Baixas are the largest production area of mussel *Mytilus galloprovincialis* in Spain, with more than 90% of the total country production. Rias Baixas comprises 3266 mussel rafts, differently distributed around the estuaries, as depicted in Figure 2.5. Ria de Arousa has the larger number of rafts

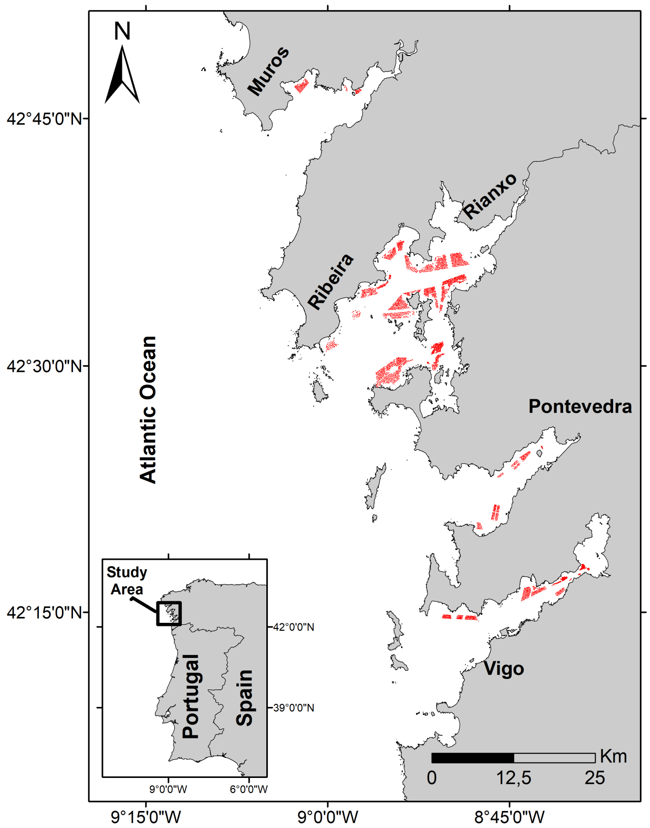

Figure 2.5: Map of Rias Baixas, showing the *Mytilus galloprovincialis* rafts sites.

(2318 rafts, corresponding to 69%). Then, Rias de Vigo and de Pontevedra have similar number of rafts (15% and 12%, respectively), followed by Ria de Muros, with only 122 mussel rafts (around 4%).

The Galician Mussel Regulatory Council (`https://www.mexillondegalicia.org/`) states that the Galician Mussel gets its commercial size (70-95 mm) in about 17 months, which is considerably lower than in other producing countries, where the cultivation period is much longer (all across the Europe, the mussels needs 2 to 6 times more time to reach this size). Indeed, Rias Baixas presents the highest mussel production in Europe - 250 $\times 10^6$ kg year^{-1}, which is 41% of the European and 15% of the world production. More concretely, Ria de Arousa is the one with higher production rate per raft (75.91 $\times 10^6$ kg raft^{-1} year^{-1}), followed by Ria de Pontevedra and Ria de Vigo with 75.51 and 72.18 $\times 10^6$ kg raft^{-1} year^{-1}, respectively. Ria de Muros has a slightly lower production - 69.70 $\times 10^6$ kg raft^{-1} year^{-1} (Figueiras et al., 2002).

Figure 2.6, which shows the monthly evolution of *Mytilus galloprovincialis* production in Rias Baixas, shows that production increases from May to October, when upwelling occurs on the northwest coast of the Iberian peninsula (Sousa, 2013). In October, a mean value of 30.2 tons was produced in Rias Baixas, which is lower than

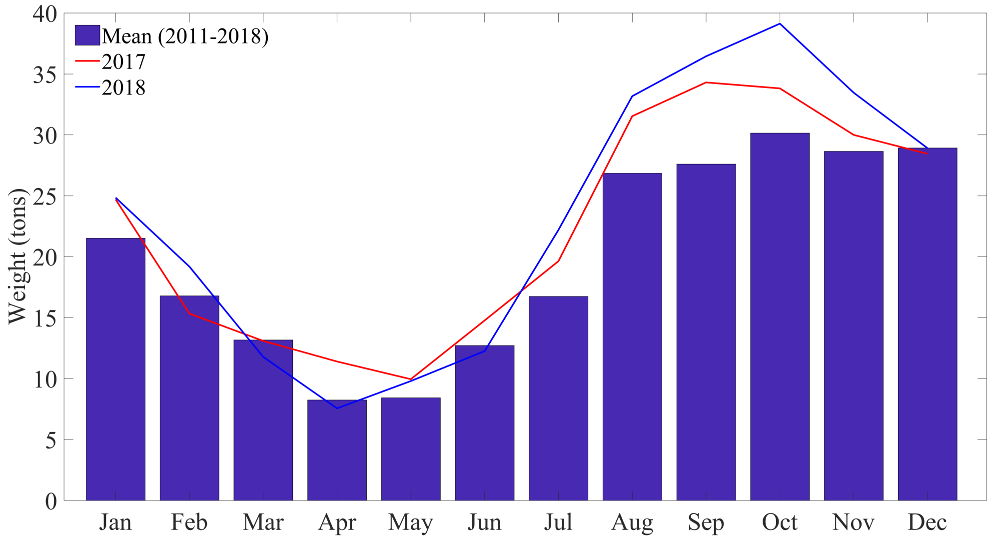

Figure 2.6: Monthly evolution of *Mytilus galloprovincialis* production in Rias Baixas. Red and blue lines corresponds to 2017 and 2018 production, while the bars represent the monthly average production between 2011 and 2018.

the production for the two most recent years (33.8 and 39.12 in 2017 and 2018, respectively), which indicates that production increased over the last decade. During winter, from January to April, the lower food availability leads to lower mussels production (lower mean value of 8.2 tons).

In fact, according with Figueiras et al. (2002), high yield production of mussels in Rias Baixas is highly related with seston characteristics, which depends on the interaction between coastal upwelling and water circulation in rias. The phytoplankton response to upwelling provides high quality food for mussels, determining the efficiency of its absorption . Therefore, chlorophyll *a* concentration and total particulate matter influence the mussel physiology response and consequently the mussel growth rates (Fernández-Reiriz et al., 2001).

Physiognomically, *Mytilus galloprovincialis* has a large number of parallel filaments allowing to filter food particles from the water, feeding from phytoplankton and organic matter. Indeed, according with FAO, a mussel with 5 cm length is capable to filter 5 litres of water per hour. Due to the good environmental conditions, such as continuous upwelling of cold water rich in nutrients, the mussels reproduction may take place at any time of the year.

The *Mytilus galloprovincialis* cultivation process may be divided in three different stages:

- obtaining the seed;
- growing the seed;

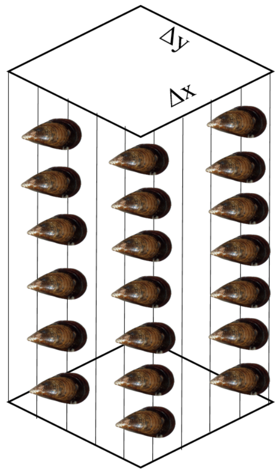

Figure 2.7: Simplified scheme of a mussel raft, adapted from Duarte et al. (2008).

- thinning out the juveniles and growing them until adult size to be commercialized.

According to Duarte et al. (2008), mussel rafts are fixed to the bottom by one or two anchors, allowing rotation with the tides, as illustrated in Figure 2.7. Each mussel raft has an approximate area of 500 m^2, with 500 hanging ropes 12 m long (Figueiras et al., 2002).

Based on this information, the vertical processes and the vertical variation of the environmental conditions that make bivalves grow, feed and reproduce gain relevance, and will be assessed in the next chapter.

Chapter 3

Time and Spatial Distribution of Water Column Stratification in Rias Baixas: Influence on Aquaculture

3.1 Introduction

As described in subsection 2.2, Rias Baixas are the location of important inshore shellfish production. Due to the large areas of sheltered and productive waters in Rias Baixas, the aquaculture activities have considerable economic potential. According to Duarte et al. (2008), phytoplankton is the most important primary producer within Rias Baixas ecosystem, in which its seasonal and inter-annual variations in biomass may affect the productivity of filter-feeding invertebrates under exploitation, such as *Mytilus galloprovincialis*, which comprises 97% of the total annual aquaculture production in Spain (Chapter 2).

Apart of water temperature, which has a major effect on the seasonal growth of bivalves and may be largely responsible for any differences in growth between sites, there are other environmental variables affecting the health and growth of bivalves. *Mytilus galloprovincialis* feed by filtering mainly microscopic algae (phytoplankton), but also some organic detritus from sea water. Additionally, the oxygen content of sea water is usually enough for bivalve to breathe at normal rates. They also have a high tolerance to low dissolved oxygen concentrations, reducing the metabolic rate due to the capability to use anaerobic respiration to provide energy. However, prolonged periods of very low oxygen, can stress bivalves, letting them to decrease their growth rate. Moreover, they may become more susceptible to diseases, or cause death depending on the exposure time (Laing and Spencer, 2006).

The variations in phytoplankton productivity magnitude and dissolved oxygen concentration plays a major role in the recruitment success (Platt et al., 2003), timing and success of invertebrate spawning, larval survival and settlement (Arsenault and Himmelman, 1998). These variations are commonly linked to physical and biochemical variables, such as tidal propagation, freshwater inflow, input of nutrients from river discharges, zooplankton grazing, but also thermohaline dynamics and consequently the water column stratification processes.

The relation between the production and growth of phytoplankton and dissolved oxygen, and the conditions of the different filter feeders, are commonly linked with their location within the water column. For instance, according to Gibbs et al. (1991), flagellate phytoplankton biomass present from the mid to upper water column layers may benefit the mussels that are extended in long-line areas. On the other hand, benthic filter feeders such as scallops may benefit most from high productivity rates of the benthic micro-algae organisms (MacKenzie and Gillespie, 1986).

In this context, according with Duarte et al. (2008), mussel rafts are fixed to the bottom by one or two anchors, allowing their rotation with the tides. As depicted in the sub-section 2.5, the mussels are disposed vertically in water column, making essential the knowledge about the vertical processes and the vertical variation of the environmental factors that make bivalves to proliferate.

Therefore, this chapter aims to assess the influence of the water column stratification in *Mytilus galloprovincialis* production, examining the factors governing the seasonal variation of the water column stratification. For such purpose, the spatial and temporal distributions of water temperature, salinity, dissolved oxygen and irradiance (as photosynthesis indicator) are analysed. These were found to be highly relevant to plan aquaculture development and the sustainability of fisheries enhancement in Rias Baixas.

This chapter was based on the analysis of field measurements collected by Intecmar (`http://www.intecmar.gal/`), during 1 year at 12 stations distributed through the 4 coastal systems under research.

Stratification and destratification processes play a major role in the physics and biogeochemistry of coastal areas. Therefore, it is essential to measure the stability of the water column, which can be quantified from field observations, as well as from the analysis of numerical models results.

Due to the high importance of the stratification and destratification processes for the marine and estuarine ecosystems, this subject has been intensively studied during the last decades. Simpson et al. (1977) were the first to propose the potential density of the water column derived from density vertical profiles as a measure for water column stratification. Later on, Simpson et al. (1981) defined the potential energy anomaly as shown in Equation 3.1 in the next section.

This assumption was used by several authors for quantifying the relative contributions of different processes of stratification in coastal seas, estuaries and coastal lagoons. For example, Simpson and Bowers (1981) analysed field data from the Irish Sea and the British Channel in order to study the stratification of the coastal sea. Rippeth and Simpson (1996) investigated the occurrence of such complete vertical mixing events in Clyde Sea, United Kingdom. They concluded that the persistence of the completely mixed state is largely the result of convection caused by intense surface cooling, sustained by the large pre-existing heat reservoir in the deep water.

Wiles et al. (2006) studied the physical regime of Limfjorden, Denmark, aiming to define its role in controlling the food supply to a community of benthic filter feeders, studying the balance of empirical source terms in the potential energy anomaly equation. They concluded that the competition between the stratificational effects of estuarine circulation, surface heating and the mixing due to wind, waves and surface cooling, leads to episodic stratification in summer with potentially hazardous consequences for benthic filter feeder populations.

MacKenzie and Adamson (2004) evaluate the water column stratification and the spatial and temporal distribution of phytoplankton biomass in Tasman Bay, New Zealand, and its implications for aquaculture. They concluded that variations in water column stability (the result of freshwater inflows, insolation, and tidal mixing) play a major role in determining the spatial and temporal distribution of phytoplankton biomass within Tasman Bay.

3.2 Methodology

Water temperature, salinity, dissolved oxygen and irradiance (as photosynthesis indicator) dataset were downloaded from Intecmar website (`http://www.intecmar.gal/`). The sampling stations (Figure 3.1) were chosen according to their hydrological characteristics, in which M1, A1, P1 and V1 are locations dominated by ocean water; M3, A3, P3 and V3 are riverine stations, and M2, A2, P2 and V2 are typical estuarine stations under the influence of both forcing agents. The coordinates of the sampling stations selected are depicted in Table 3.1.

The water column potential energy anomaly (ϕ=Jm^{-3}) is indicative of the energy required to complete homogenise the water column, and therefore is directly proportional to the strength of the water column stratification (Simpson et al., 1981). This stratification index was calculated from the measured vertical density distribution at

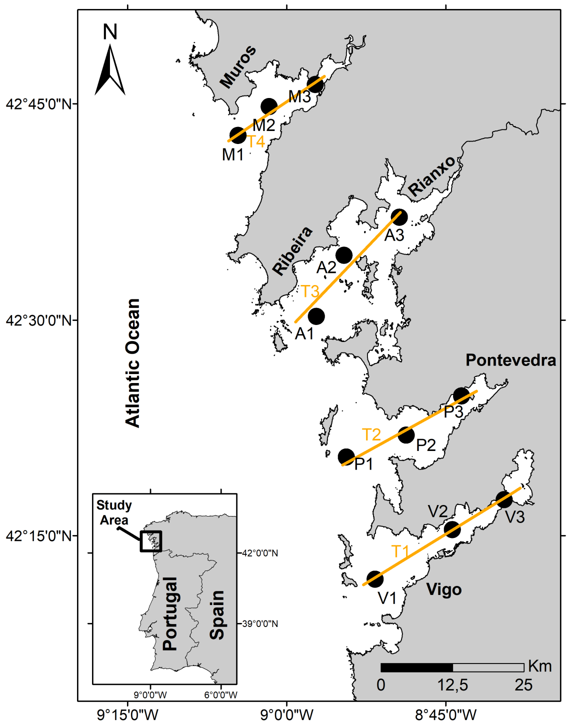

Figure 3.1: Map of Ria Baixas, and its location in Northwest Iberian coast. Black dots correspond to the sampling stations. Orange lines correspond to the transects defined for water column profiles.

each station using the equation:

$$\phi = \frac{1}{h}\int_{-h}^{0} gz(\overline{\rho} - \rho)dz \tag{3.1}$$

where,

$$\overline{\rho} = \frac{1}{h}\int_{-h}^{0} \rho dz \tag{3.2}$$

in Equations 3.1 and 3.2, h is the water column depth in metres, ρ is the density of sea water (kgm^{-3}) at depth z (m), and g is acceleration resulting from gravity (9.8 ms^{-2}).

The relative importance of salinity and water temperature on the strength of water column stability is determined by performing a modification on Equation 3.1. Stratification establishment caused by water temperature gradients (ϕ_t) is given by:

$$\phi_t = \frac{1}{D}\int_{-h}^{0} gz(\overline{\rho'} - \rho')dz \tag{3.3}$$

where ρ' is the density at depth z calculated using the observed water temperature and the mean salinity of the water column. The contribution of salinity to water column stratification can be determined by subtracting ϕ_t from total ϕ. By definition ϕ is

Table 3.1: Location of the sampling stations.

Station	Coordinates
V1	42°10'43"N; 8°52'26"W
V2	42°16'30"N; 8°41'26"W
V3	42°17'29"N; 8°38'47"W
P1	42°21'00"N; 8°51'13"W
P2	42°21'10"N; 8°46'07"W
P3	42°24'31"N; 8°42'55"W
A1	42°30'02"N; 8°55'06"W
A2	42°33'15"N; 8°54'31"W
A3	42°36'32"N; 8°50'16"W
M1	42°42'52"N; 9°03'30"W
M2	42°45'28"N; 9°01'15"W
M3	42°46'41"N; 8°57'06"W

depth independent, but it varies in time. If there is no vertical density variation in the column, ϕ is 0 representing a fully-mixed water column, while ϕ is positive for a stable stratification.

Although ϕ explains the instant state of water column in terms of mixing and stratification, the temporal change of ϕ may explain the interaction processes related to mechanical mixing (wind and tidal propagation) and stratifying mechanisms such as the solar heat flux and the freshwater inflow (Simpson et al., 1991).

Therefore, a year of data of water temperature, salinity, water density, dissolved oxygen and irradiance were analysed and the seasonal variability of ϕ was computed. Additionally, the annual evolution of water temperature, salinity oxygen and irradiance was also plotted. The data were measured weekly from January 2016 to December 2016, from the surface to the bottom.

The annual variability was evaluated for 2016 for two main reasons: firstly, because the year of 2016 is analysed throughout this thesis; secondly, there were no gaps in data for this period. In this context, it is essential to frame 2016 into the historical average, in order to understand if the stratification patterns observed in 2016 are representative of the typical seasonal variability of ϕ, avoiding the analysis of an atypical year. Therefore, Figure 3.2 shows the comparison between the monthly average of ϕ between 2006 and 2018 (blue dots) and their deviation, with the monthly average for 2016 (black dots). The mean value variability of water column potential energy anomaly evidences that

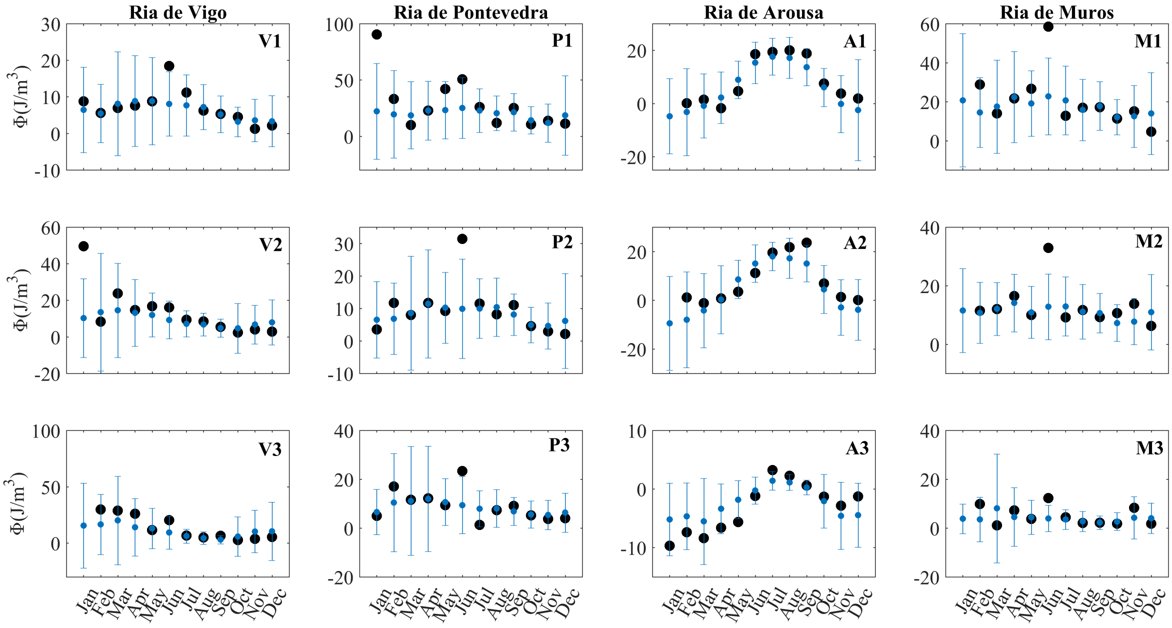

Figure 3.2: Comparison of the historical data of water column potential energy anomaly (ϕ), and monthly average for 2016 (black dots).

2016 is within the average of historical values, being representative of the thermohaline seasonality and stratification events for Rias Baixas.

3.3 Results and Discussion

3.3.1 Seasonal Variability of the Biotic and Abiotic Variables

Temporal series regarding to seasonal variability of water temperature, salinity, irradiance and dissolved oxygen concentration are presented in this subsection. The variability of surface water temperature (Figure 3.3) shows a typical seasonal pattern, characterized by high water temperature during spring and summer, decreasing gradually during autumn, followed by a replenish in late winter. As expected, surface water temperature increase from oceanic to riverine stations, mainly due to the depth decreasing and effects of river action. The results show that Ria de Pontevedra is the coastal system with higher mean surface temperature (15.38°C), followed by Ria de Arousa (15.24°C), Ria de Vigo (15.11°C), and Ria de Muros (14.71°C).

Vertically, water temperature shows different patterns according to the season. During winter (December, January and February), the water temperature is higher in bottom than in the surface. This pattern was also observed by Alvarez et al. (2005), and is justified by the seasonal variability of upwelling and downwelling events. When solar radiation becomes stronger (from March to August), the pattern reverses revealing high

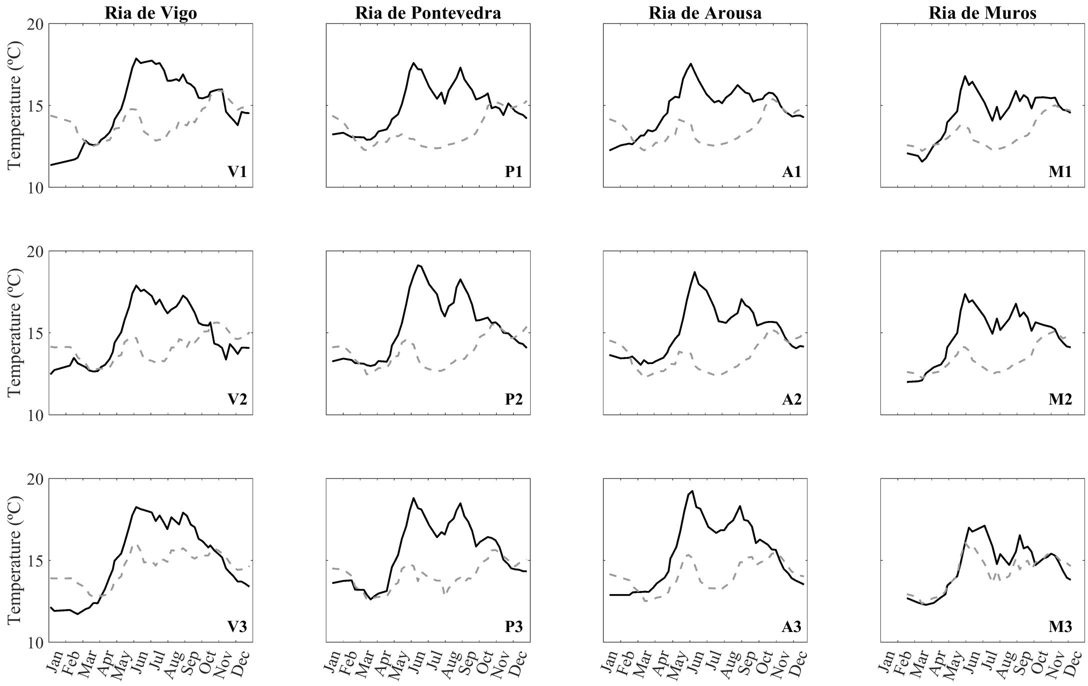

Figure 3.3: Annual evolution of observed water temperature at different stations. Black line corresponds to the surface water, while grey dashed line corresponds to the bottom.

differences between surface and bottom water temperature, indicating water column stratification (more than 5°C). This period is also characterized by winds favourable to the generation of coastal upwelling, introducing cold water into the bottom layers of Rias Baixas, and increasing the vertical stratification in the area under its influence (Otero et al., 2008). Actually, in many stations, the bottom temperature in January or December is higher than in August. From Figure 3.3, it is also depicted that the bottom temperature presents very low seasonal variability comparing with surface temperature.

In Figure 3.4 is depicted the monthly average of upwelling index (UI) for 2016. Positive or negative UI values indicate favourable (northerly winds) or unfavourable (southerly winds) upwelling conditions, respectively. In 2016, the upwelling season occurred from June (31.9 $m^3s^{-1}km^{-1}$) to September (23.5 $m^3s^{-1}km^{-1}$). For the rest of the year, winds are predominantly from the south and southwest, favouring the predominance of downwelling conditions. Figure 3.4 reinforces the statements of the last paragraph, showing that coastal upwelling favours the establishment of a stratified water column, and that downwelling events are responsible for the winter thermal inversion (maximum thermal inversion occurred in January, which coincides with the highest predominance of downwelling conditions (599.5 $m^3s^{-1}km^{-1}$)).

The salinity (Figure 3.5) fluctuates according to the hydrological conditions of each coastal system. Regarding to temporal variability, surface and bottom salinity presents

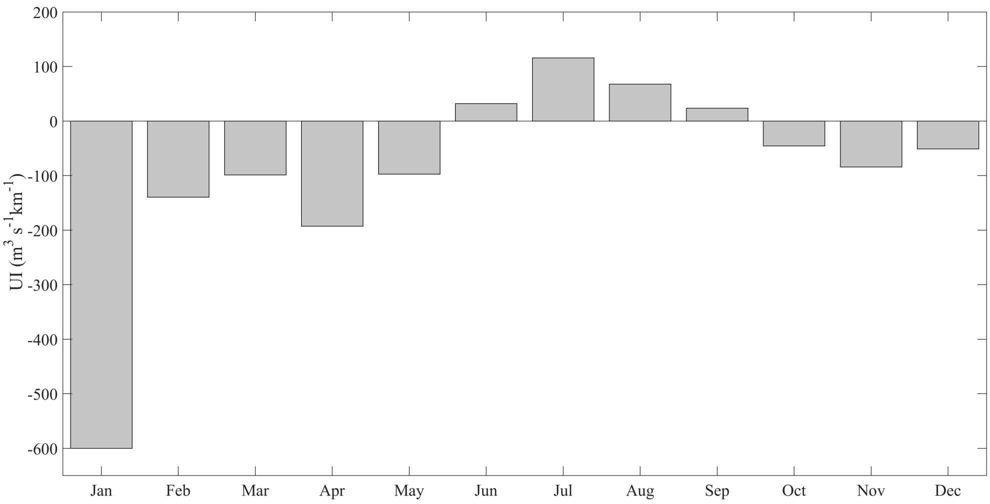

Figure 3.4: Monthly mean of upwelling index.

the expected pattern, characterized by higher salinities measured during summer. As expected, the salinity at the bottom is higher than at the surface.

There are two main variables governing water density and consequently, water stratification: water temperature and salinity. In this context, it is important to know the variations of these variables, and their influence on photosynthesis and dissolved oxygen concentration. Therefore, in Figures 3.6 and 3.7 the time series of irradiance and dissolved oxygen concentration are presented. Irradiance results provides a measure of photosynthetically active radiation (PAR) by measuring the number of photons in the incident radiation (for wavelengths between 400 and 700 nm), per unit of surface and unit of time (quanta/cm^{2}sec).

Irradiance time series reflect the development of characteristic phytoplankton spring and summer blooms along the estuary. Yet, the magnitude and the time of maxima irradiance coincides along the estuaries, what suggests that is not ruled by hydrodynamic processes. The less productive estuary is clearly Ria de Vigo, with an average irradiance value of 769.5 quanta/cm^{2}sec. On the other hand, in Ria de Arousa was observed the highest average value (2427.1 quanta/cm^{2}sec), but also the highest peak (5160.2 quanta/cm^{2}sec), recorded in August. This high productivity measured in Ria de Arousa may reflect on the number of mussel rafts present in this estuary. Regarding to the vertical structure, a clear gradient is observed, with higher surface irradiance than those recorded near the bottom. There is a resemblance between the patterns observed in Figures 3.3 and 3.6, where the higher water temperature difference between the surface and the bottom leads to higher irradiance vertical gradient.

Dissolved oxygen (DO) concentrations (Figure 3.7) at selected locations along the estuaries did not show a clear seasonal trend. Nevertheless, DO concentrations are

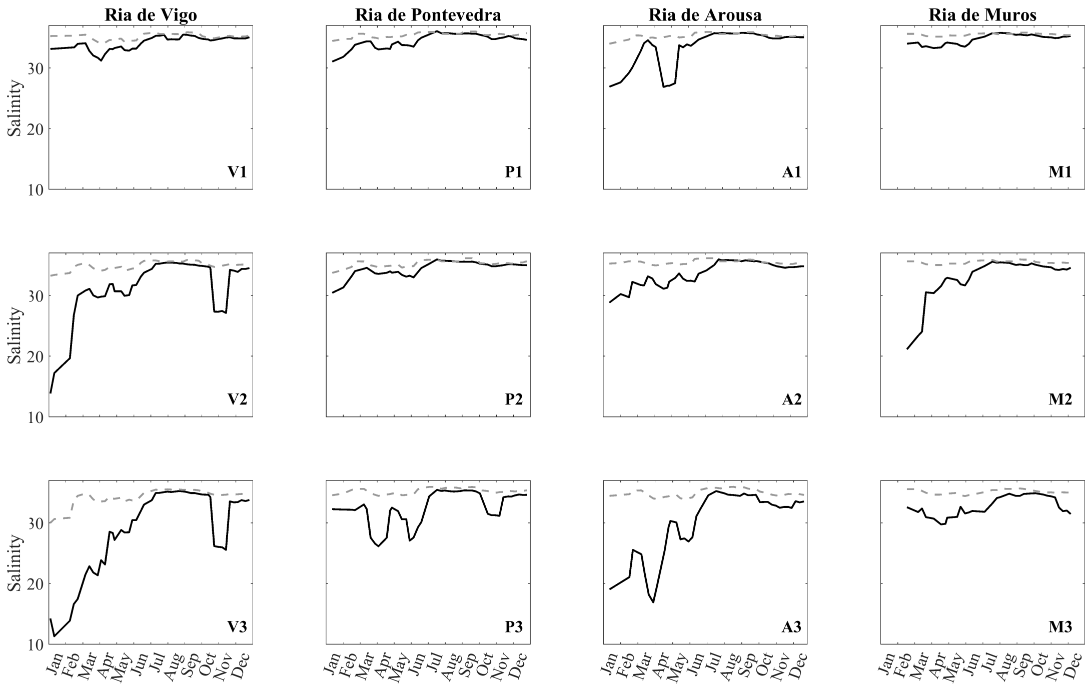

Figure 3.5: Annual evolution of observed salinity at different stations. Black line corresponds to the surface water, while grey dashed line corresponds to the bottom.

generally lower at the upstream limit of the estuaries, when generally nitrification and respiration rates exceed the uptake capacity of oxygen from the atmosphere. In downstream direction, an intensification of mixing processes progressively improves water column oxygenation. Later in the year, concentrations decrease to lower values due to enhanced respiration rates induced by the increased availability of fresh organic matter from the declining phytoplankton blooms (Arndt et al., 2011). Vertically, DO concentrations reveals a strong deplection from the surface to the bottom, which may induce harmful effects on the ecosystem or in the aquaculture production in the bottom layers of Rias Baixas. This pattern can be explained through two different processes: the lowest concentration of phytoplankton in the bottom layers leads to less oxygen production, suggesting that phytoplankton is the main responsible for oxygen production in Rias Baixas; or the oxygen uptake from the atmosphere and produced by phytoplankton in the surface layers can not migrate to the bottom layers due to the strong stratification.

Therefore, in the next sub-section, the stratification and destratification processes, and their influence in biogeochemistry and in aquaculture exploitation are evaluated.

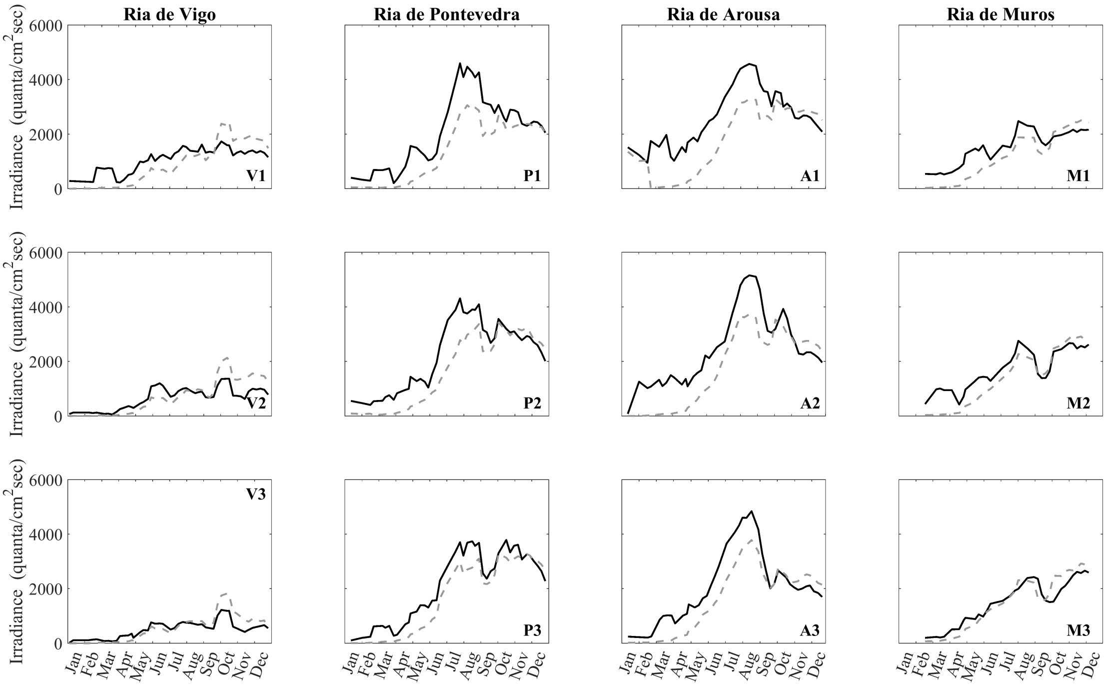

Figure 3.6: Annual evolution of observed irradiance at different stations. Black line corresponds to the surface water, while grey dashed line corresponds to the bottom.

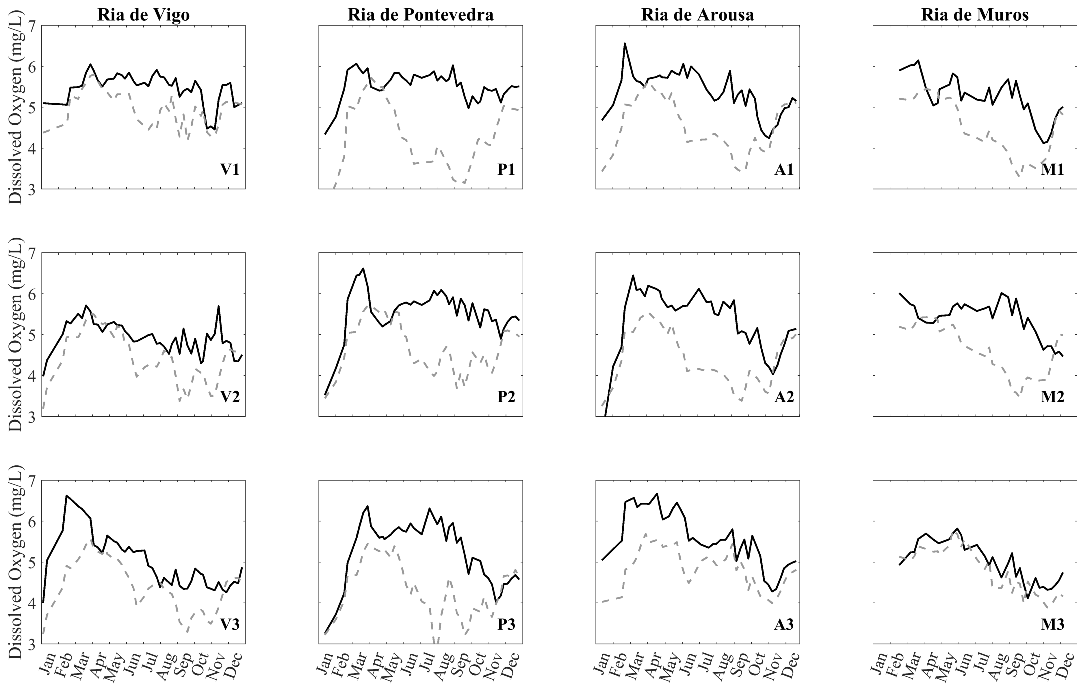

Figure 3.7: Annual evolution of observed dissolved oxygen at different stations. Black line corresponds to the surface water, while grey dashed line corresponds to the bottom.

3.3.2 Simpson's Potential Energy Anomaly: Influence in Aquaculture Production

Plots of Simpson's potential energy anomaly (Figure 3.8) along the four Galician estuaries show a characteristic curve, resulting from the incident heat flux seasonal variability. During winter months, cooling at the water surface induces convective mixing, leading to a ϕ decrease. The exceptions, where maximum ϕ is depicted in winter, are Stations V2 and V3, due to very low salinity values at the surface layer (Figure 3.5). Significant stratification starts to develop in May when the solar radiation at the surface increases. The main difference between estuaries is that Ria de Arousa develops stratification later than the others (maximum stratification occurs in September).

The relative importance of vertical patterns of salinity (red line) and water temperature (blue line) on the strength of water column density stratification also varied seasonally. During strongly stratified periods (summer), with low freshwater inflow and high solar radiation, water temperature contributed up to 90% of total ϕ at some sampling stations. During winter, river run-off is responsible for the establishment of water column stratification. Indeed, the winter thermal inversions (up to 3°C) depicted in Figure 3.3 are responsible for the negative contributions of water temperature to the potential energy anomaly. The stratification at stations with index 3 (riverine stations) is mainly ruled by salinity. In these stations, where river discharge dominates, the vertical variations of salinity are more important than temperature vertical gradients (Figures 3.3 and 3.5).

Pearson's correlations between annual evolution of ϕ, ϕ_t and ϕ_s and the vertical gradient of dissolved oxygen and irradiance were computed and presented on Table 3.2. The analysis of the table reveals significant correlations between the vertical gradients of dissolved oxygen and irradiance with ϕ_t. In fact, positive correlations were found between ϕ_t and vertical gradient of dissolved oxygen for all stations analysed, except for A3 and M3. However, low correlations were found at stations V2, V3, A3 and M1, corresponding to stations where high vertical salinity gradients were observed (Figure 3.5). In the remaining stations, where seasonal variability of stratification is ruled by water temperature, the correlation between ϕ_t and the vertical gradient of dissolved oxygen is significant, from the statistical point of view (p-value < 0.05). Regarding to irradiance, the correlations between ϕ_t are even more significant, excepting in V3 and M2. These correlations also reveal that photosynthesis is inhibited at the bottom when water column stratification is established.

In this context, since the relationship between thermal stratification and vertical gradients of oxygen and irradiance is proven, the vertical structure of $\sigma_{S,T,p}$ density,

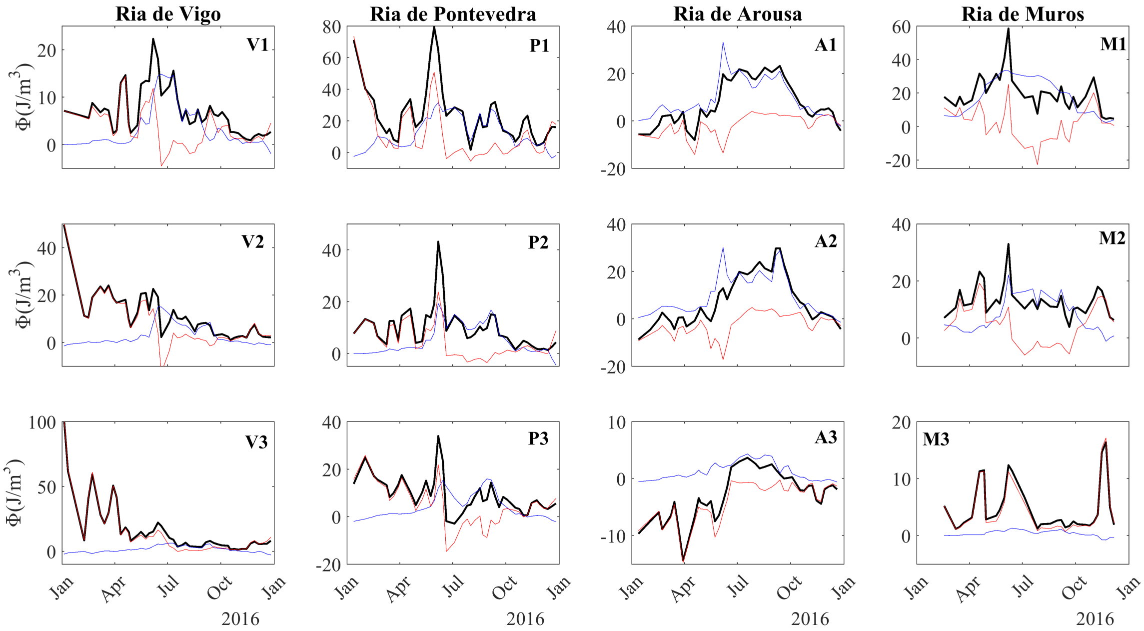

Figure 3.8: Temporal change of the potential energy anomaly (black line), and relative importance of vertical salinity (red line) and water temperature (blue line).

dissolved oxygen concentration, and irradiance along the four transects illustrated in Figure 3.1 were analysed in two different periods: maximum and minimum thermal stratification (Figures 3.9 and 3.10, respectively).

During high stratification periods induced by water temperature there is a vertical decay of irradiance in all estuaries, mainly in Ria de Arousa and Ria de Muros (transects 3 and 4, respectively). In transect 3 (Figure 3.9 K), a high vertical gradient is depicted close to the inlet, where is found a high vertical density variation (Figure 3.9 B), varying from 3182 quanta/cm^{2}sec at the surface to 911 quanta/cm^{2}sec near the bottom. The vertical gradient of irradiance decreases towards the estuary head. Regarding to Ria de Muros (Figure 3.9 L), a maximum irradiance is observed close to Tambre River (1678 quanta/cm^{2}sec), while a minimum value of 672 quanta/cm^{2}sec is verified near the bottom at the inlet area. High irradiance values are depicted in Ria de Pontevedra (Figure 3.9 J), always exceeding 4000 quanta/cm^{2}sec near the surface. The pattern in Ria de Vigo (Figure 3.9 I) is slightly different, since the longitudinal gradient is more pronounced than the vertical one, ranging from 1807 quanta/cm^{2}sec at the inlet to 438 quanta/cm^{2}sec close to Vertugo-Oitaven river.

During low stratification periods, the irradiance apparently does not respond to stratification processes, specifically along transect T4 (Figure 3.10L). Although there is a vertical gradient in transects T1 and T2, corresponding to Ria de Vigo and Ria de Pontevedra, it is much less pronounced comparing to periods of high thermal stratification. In Ria de Arousa (Figure 3.10K), a longitudinal gradient is observed.

Table 3.2: Correlation coefficients between ϕ, ϕ_t and ϕ_s and the vertical gradient of dissolved oxygen and irradiance. The values marked with an asterisk (*) have a significance level higher than 95% (p-value < 0.05).

Station	Dissolved Oxygen			Irradiance		
	ϕ	ϕt	ϕs	ϕ	ϕt	ϕs
V1	0.22	0.55*	-0.34	0.57*	0.41*	0.25
V2	-0.17	0.25	0.24	0.54*	0.51*	0.30*
V3	0.31*	0.06	0.29*	0.42*	0.17	0.38*
P1	0.25	0.59*	-0.07	-0.02	0.56*	-0.36*
P2	0.06	0.59*	-0.47*	0.40*	0.61*	-0.07
P3	-0.09	0.67*	-0.51	0.1	0.50*	-0.22
A1	0.65*	0.73*	0.03	0.35*	0.55*	-0.24
A2	0.72*	0.73*	0.21	0.29	0.45*	-0.18
A3	-0.55	-0.11	-0.60*	0.09	0.72*	-0.19
M1	-0.13	0.27	-0.43*	0.50*	0.65*	-0.14
M2	-0.19	0.66*	-0.72*	0.23	0.13	0.07
M3	-0.12	-0.46*	-0.06	0.22	0.45*	0.17

The vertical structure of dissolved oxygen during high stratification periods shows a clear oxygen stratification along all transects analysed, depicting vertical oxygen depletion. Indeed, the patterns observed in the $\sigma_{S,T,p}$ density are very similar to those depicted in dissolved oxygen, which indicates the effect of water column stratification on vertical structure of O_2 concentration. In transects T1 and T2 (Figures 3.9E and F), surface oxygen concentrations above 5 mg/L are found along the estuaries (maximum of 7.5 and 6.3 mg/L, respectively). In the bottom, hypoxia condition are observed in both estuaries, with minimum values of 3.87 mg/L at 33 meters depth, and 2.27 mg/L at 15 meters depth, in Ria de Vigo and Ria de Pontevedra, respectively. In transect T3 (Figure 3.9G), the maximum values of 6.3 and 6.1 mg/L are observed near shore and close to Ulla river, respectively. In mid-estuary area, the dissolved oxygen drops to 4.2 mg/L at the bottom. Ria de Muros evidences lower vertical oxygen depletion, decreasing from 6.0 to 4.7 mg/L at inlet area. In all transects analysed, the vertical oxygen depletion does not occur gradually in the water column, but a fast concentration decrease is observed at mid-water column. For example, a decrease of 3.1 mg/L from 6 to 10 meters depth.

In autumn and winter, when the mixing processes destroys stratification (Figure

3.10), the vertical oxygen variability is very low, and the concentrations are similar in the four estuaries, ranging between 4.3 and 5.7 mg/L.

Thus, the establishment of a highly stratified water column during the summer season is one of the most important hydrodynamic and hydrological characteristics of Ria Baixas, which may have influence on *Mytilus galloprovincialis* or other cultivable species nutrition and health.

During this time of year, the bottom layer is isolated from the surface cutting off a normal resupply of oxygen from the atmosphere. This stratified period encompasses the period when salinity is maximum and with low vertical gradient. Therefore, the water column is stratified as a result of water temperature gradients. Moreover, during this period, the nutrient concentrations are at their minimum due to phytoplankton uptake, that grows, feeds and dies, sinking down. As bacteria on the estuaries bottom decompose the abundant carbon in the phytoplankton that sinks down, oxygen is consumed. Due to the high water column stratification, oxygen consumption rates at the bottom can easily exceed the supply rates, causing hypoxia, or at least, low dissolved oxygen concentration. This state of hypoxia exposure can persist several weeks or months until there is strong mixing of the estuarine waters.

It is exactly this persistent hypoxia exposure that may cause bivalve stress or even death, in certain cases. In this context, for example in station P1 (Figure 3.8), the water column remains stratified from May to August, which can generate conditions for deep low oxygen concentrations. Actually this event is visible in oxygen concentration time series represented in Figure 3.7. Similar patterns can be observed at stations A2 and M1.

As mentioned in the introduction section of this chapter, and outlined in Figure 2.7, the bivalve rafts are vertically disposed, from the surface to the bottom. Therefore, according to the measurements, the conditions of the mussels *Mytilus galloprovincialis* in top of the raft may be different from those in the bottom, mainly during periods of high water column stratification. The longitudinal and vertical gradients of irradiance (photosynthesis indicator), show differences that may influence the nutrition and growth of bivalves. Therefore, the *Mytilus galloprovincialis* individuals that are located in the deepest zone of the rafts are susceptible to summer hypoxia events combined with low food access. This can cause differentiated growth between the top and bottom located specimens, biological stress, diseases or even death, depending on the exposure time.

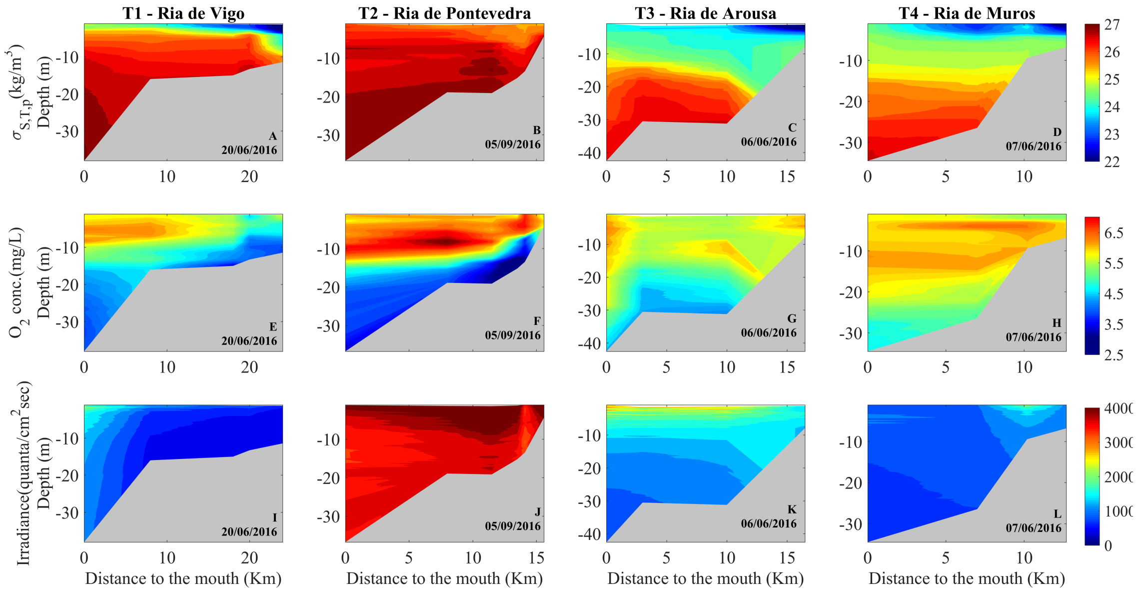

Figure 3.9: Water column profiles of $\sigma_{S,T,p}$ density, dissolved oxygen concentration, and irradiance on transects T1, T2, T3 and T4 during periods of high stratification.

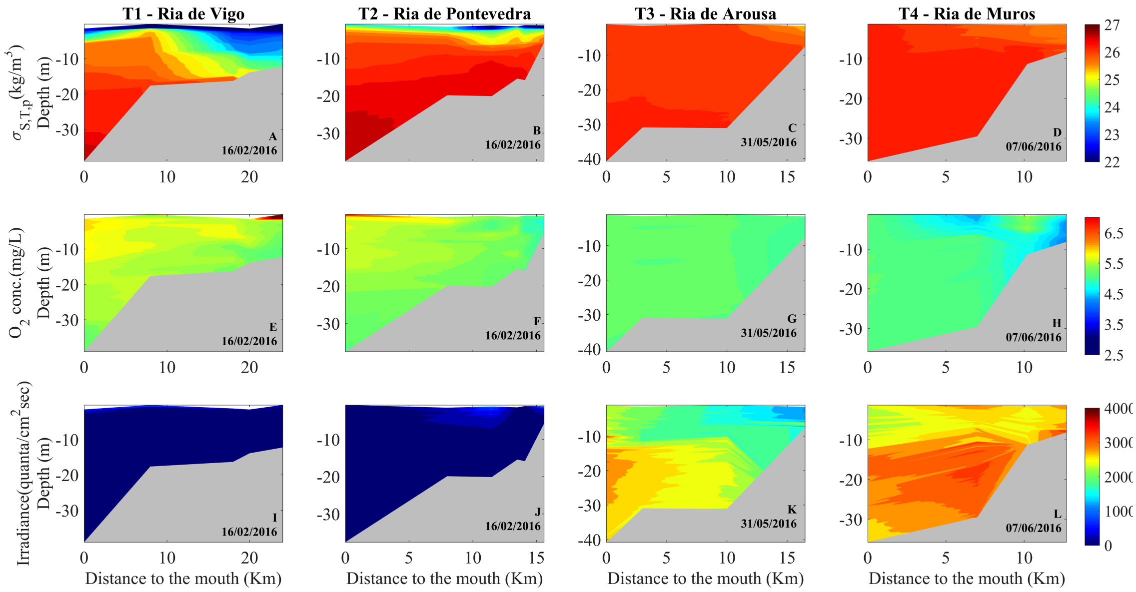

Figure 3.10: Water column profiles of $\sigma_{S,T,p}$ density, dissolved oxygen concentration, and irradiance on transects T1, T2, T3 and T4 during periods of low stratification.

3.4 Conclusions

The main objective of this chapter was to understand the influence of the water column stratification in *Mytilus galloprovincialis* production, based on field measurements during 1 year at 12 stations distributed through the Rias Baixas. The *in situ* data analysis suggest the following:

- During summer, the water temperature is responsible for the vertical density gradients, while vertical salinity distribution promotes stratification during winter;

- Despite the strong vertical variations of water temperature and salinity, both variables are within suitable limits along the vertical for bivalve growth. The deep and cold Rias Baixas water has temperatures above 10°C during the entire year (bivalve growth begins up to 8-9°C). Salinity changes do not affect bivalves growth as much as variation in water temperature (Laing and Spencer, 2006);

- Rias Baixas water column stratification has a significant influence on the vertical profiles of DO concentration and on phytoplankton communities, leading to summer hypoxia events in the bottom layers, combined with low irradiance concentrations, which suggests low food availability;

- If those events are prolonged in time, and coincide with high water temperatures, the bivalves can suffer biological stress, reducing their growth;

- During the summer, the high productivity and oxygen production occurring in the surface layers of the water column, do not interact with the deeper layers;

- To avoid environmental conditions that may harm bivalves *Mytilus galloprovincialis*, shellfish stocks should be located between 2 meters deep and mid-water column. Close to the surface, the low salinity values may cause biological stress, while close to the bottom, the hypoxia may inhibit bivalves growth;

- In fact, mussels are within the range of depths refered, once the ropes maximum length allowed by law is 12 meters, and measurements shows that low oxygen and irradiance concentrations are mainly for depths higher than 20 meters.

This chapter provides a first insight to estimate aquaculture quality at Rias Baixas based only on field measurements. The seasonal and the vertical patterns of variables essential to aquaculture exploitation were assessed, contributing to the knowledge about Rias Baixas ecology. To complement the analysis of these datasets, the development and appliance of modelling tools to estimate the suitability of aquaculture is performed in this work, providing results with higher spatial and temporal resolution. In this context, the next chapter depicts the description of the numerical models used in this research, as well as their governing equations.

Chapter 4

Numerical Models

4.1 Introduction

The numerical simulations for Ria de Aveiro lagoon were performed with the Delft3D Flexible Mesh Suite. In particular, the hydrodynamic D-Flow FM model (Deltares, 2018) and the D-Water Quality modules (Deltares, 2006b) were used. In this case, due to the geomorphological characteristics of the Ria de Aveiro, with narrow and shallow channels and constant and fast variations in the horizontal directions, it was considered a best option to develop a model with high spatial resolution with an irregular grid. As previously mentioned, Ria de Aveiro is a very shallow lagoon, considered vertically homogeneous, where the horizontal length scales are significantly larger than the vertical scales. Therefore, as widely applied for Ria de Aveiro (Lopes et al., 2015; Vaz et al., 2016), a twodimensional model implementation was developed to simulate the local processes.

To study the hydrodynamic and biogeochemical processes in Rias Baixas, the hydrodynamic module Deflt3D-Flow (Deltares, 2006a), and the water quality module, Delft3D-DWAQ (Deltares, 2006b) were used. Comparing to Ria de Aveiro lagoon, Rias Baixas have a regular geomorphology and, for that reason, a regular numerical grid was developed. Additionally, vertical gradients of the different physical, chemical and biological variables are established (Chapter 3), which makes the development of a 3-D model essential to reproduce local processes.

The flow model is used to predict the hydrodynamics of shallow seas, coastal areas, estuaries, lagoons, rivers and lakes, while the water quality module solves the advection-diffusion reaction equation on a predefined computational grid and for a wide range of model substances. D-Water Quality allows great flexibility in the substances to be modelled, as well as in the processes to be considered. This module uses the hydrodynamic information derived from D-Flow FM (Ria de Aveiro) and Deflt3D-Flow (Rias

Baixas) modules, namely the flow fields.

This chapter presents a brief description of the numerical model suite (Delft3D) used, particularly focused on the modules extensively explored in the scope of this study: Flow (hydrodynamics) and WAQ (water quality) modules. The basic conceptual and numerical aspects of the model are also presented, as well as the main features that contributed to select this model suite to conduct this work.

4.2 Hydrodynamic Model

The hydrodynamic modules simulate two-dimensional (2-D, depth-averaged) or three-dimensional (3-D) unsteady flow and transport phenomena resulting from tidal and/or meteorological forcing, including the effect of density differences due to a non-uniform water temperature and salinity distribution (density-driven flow). The flow model can be used to predict the flow in shallow seas, coastal areas, estuaries, lagoons, rivers and lakes. It aims to model flow phenomena when the horizontal length and time scales are significantly larger than the vertical scales (Deltares, 2006a).

If the fluid is vertically homogeneous, such as Ria de Aveiro lagoon, a depth-averaged approach is appropriate. The hydrodynamic model is able to run in two-dimensional mode (one computational layer), which corresponds to solving the depth-averaged equations. Three-dimensional modelling is of particular interest in transport problems where the horizontal flow field shows significant variation in the vertical direction, as Rias Baixas case of study.

4.2.1 Numerical Aspects

Despite the structured and unstructured grid models own identical governing equations for mass and momentum conservation, they present some discrepancies in numerical aspects, according to the illustrated in Figure 4.1.

Therefore, a computational cell in a D-Flow FM grid is composed by corner nodes and edges connecting the corner nodes. The following topological conventions are used in the D-Flow FM grid, as illustrated in Figure 4.1 (A) (Deltares, 2018):

- netnodes: corners of a cell (triangles, quadrangles, etc.);
- netlinks: edges of a cell, connecting netnodes;
- flownodes: the cell circumcentre, in case of the triangles the exact intersection of the three perpendicular bisectors and hence also the centre of the circumscribing circle;

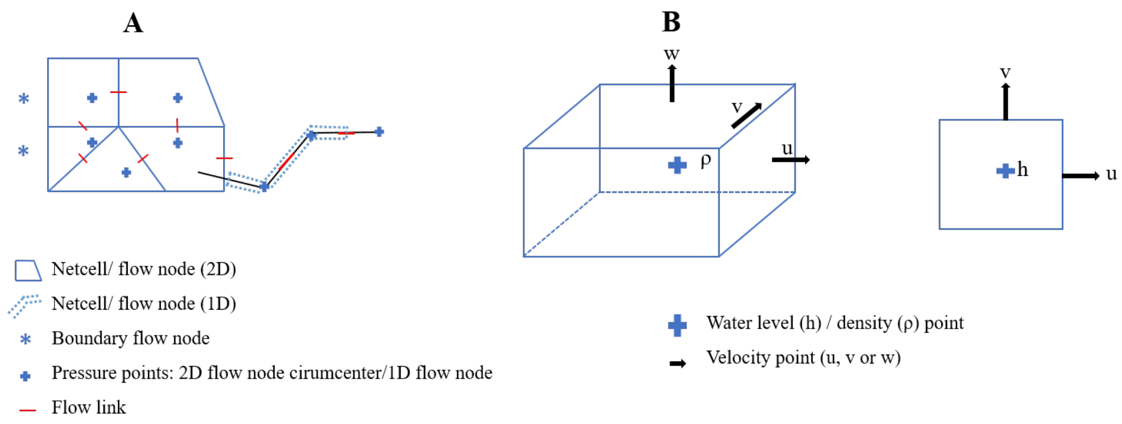

Figure 4.1: Numerical aspects of D-Flow FM (A) and Delft3D-Flow (B).

- flowlinks: a line segment connecting two flownodes.

D-Flow FM uses the circumcenter as the basis of the definition of the elementary flow parameters, water level and flow velocity. The water level is calculated at the circumcenter, while the flow velocity is predicted at the orthogonal projection of the circumcenter onto the cell face, i.e, the midpoint of the cell face (Deltares, 2018).

Regarding to Delft3D - Flow module (Figure 4.1 B), which is based on finite differences method, the description provided here is applied for the vertical σ coordinate system (σ-model) or for the vertical z coordinate system (Z-model). In this case, the grid coordinates can be defined by cartesian or spherical coordinate system.

In order to discretise the 3-D shallow water equations, the variables are organized in a specific way on the grid, as illustrated in Figure 4.1(B), named as staggered grid pattern. In this application, the rearrangement of the variables are performed according with the Arakawa C-grid, in which the water level points (pressure points) are defined in the centre of a (continuity) cell, while the velocity components are perpendicular to the grid cell faces where they are located.

As mentioned above, both hydrodynamic modules (Delft3D - Flow and D-Flow FM) solves the same equations to compute water level and current velocities. Therefore, hence forward, the numerical aspects of the hydrodynamic model will be addressed, without specifying any of them.

4.2.2 Governing Equations

In this sub-section, the governing equations for mass and momentum conservation are presented (continuity equation and momentum equations). Therefore, the Delft3D flow modules (structured and unstructured grid models) solves the depth-averaged continuity equation, derived by integration the continuity equation for incompressible fluids (∇.u=0) over the total water column depth, comprising the boundary conditions both in the water surface and in bed level, and given by Equation 4.1:

$$\frac{\partial \zeta}{\partial t}+\frac{1}{\sqrt{G_{\xi\xi}}\sqrt{G_{\eta\eta}}}+\frac{\partial((d+\zeta)U\sqrt{G_{\eta\eta}})}{\partial \xi}+\frac{1}{\sqrt{G_{\xi\xi}}\sqrt{G_{\eta\eta}}}\frac{\partial((d+\zeta)V\sqrt{G_{\xi\xi}})}{\partial \eta} \\ =(d+\zeta)Q \tag{4.1}$$

with U and V the depth averaged velocities, given by:

$$U=\frac{1}{d+\zeta}\int_{d}^{\zeta}udz=\int_{-1}^{0}ud\sigma \tag{4.2}$$

$$V=\frac{1}{d+\zeta}\int_{d}^{\zeta}vdz=\int_{-1}^{0}vd\sigma \tag{4.3}$$

and Q, which represents the contribution per area unit of the discharge or water withdrawal, precipitation and evaporation, and given by Equation 4.4:

$$Q=\int_{-1}^{0}(q_{in}-q_{out})d\sigma+P-E \tag{4.4}$$

where ζ is the free-surface water elevation; t is the time; $\sqrt{G_{\xi\xi}}$ and $\sqrt{G_{\eta\eta}}$ are the coefficients used to transform curvilinear to rectangular coordinates; d is water depth; q_{in} and q_{out} are the local sources and sinks of water per unit of volume (s^{-1}), respectively; P is the non-local source term of precipitation and E is the non-local sink term due to evaporation.

The momentum equations in eastward and northward directions are given by Equations 4.5 and 4.6:

$$\frac{\partial u}{\partial t}+\frac{u}{\sqrt{G_{\xi\xi}}}\frac{\partial u}{\partial \xi}+\frac{v}{\sqrt{G_{\eta\eta}}}\frac{\partial u}{\partial \eta}+\frac{w}{d+\zeta}\frac{\partial u}{\partial \sigma}-\frac{v^2}{\sqrt{G_{\xi\xi}}\sqrt{G_{\eta\eta}}}\frac{\partial\sqrt{G_{\eta\eta}}}{\partial \xi} \\ +\frac{uv}{\sqrt{G_{\xi\xi}}\sqrt{G_{\eta\eta}}}\frac{\partial\sqrt{G_{\xi\xi}}}{\partial \eta}-fv=-\frac{1}{\rho_0\sqrt{G_{\xi\xi}}}P_\xi+F\xi+\frac{1}{(d+\zeta)^2}\frac{\partial}{\partial \sigma}\left(\upsilon_v\frac{\partial u}{\partial \sigma}\right)+M_\xi \tag{4.5}$$

$$\frac{\partial v}{\partial t} + \frac{u}{\sqrt{G_{\xi\xi}}}\frac{\partial v}{\partial \xi} + \frac{v}{\sqrt{G_{\eta\eta}}}\frac{\partial v}{\partial \eta} + \frac{w}{d+\zeta}\frac{\partial v}{\partial \sigma} + \frac{uv}{\sqrt{G_{\xi\xi}}\sqrt{G_{\eta\eta}}}\frac{\partial\sqrt{G_{\eta\eta}}}{\partial \xi}$$
$$- \frac{u^2}{\sqrt{G_{\xi\xi}}\sqrt{G_{\eta\eta}}}\frac{\partial\sqrt{G_{\xi\xi}}}{\partial \eta} + fu = -\frac{1}{\rho_0\sqrt{G_{\eta\eta}}}P_\eta + F\eta + \frac{1}{(d+\zeta)^2}\frac{\partial}{\partial \sigma}\left(\upsilon_v \frac{\partial v}{\partial \sigma}\right) + M_\eta \tag{4.6}$$

where u, v and w are the velocities in ξ, η and σ directions, respectively; f is the Coriolis parameter; ρ_0 is the reference density of water; υ_v the vertical eddy viscosity coefficient; P_ξ and P_η are the gradient hydrostatic pressure; F_ξ and F_η represent the unbalance of horizontal Reynold's stresses; M_ξ and M_η represent the contributions due to external sources of sinks of momentum.

The vertical velocity (w) in the adapting σ co-ordinate system is also computed from the derivation of continuity equation, expressed by:

$$\frac{\partial \zeta}{\partial t} + \frac{1}{\sqrt{G_{\xi\xi}}\sqrt{G_{\eta\eta}}}\frac{\partial((d+\zeta)u\sqrt{G_{\eta\eta}}}{\partial \xi} + \frac{1}{\sqrt{G_{\xi\xi}}\sqrt{G_{\eta\eta}}}\frac{\partial((d+\zeta)v\sqrt{G_{\xi\xi}}}{\partial \eta}$$
$$+ \frac{\partial w}{\partial \sigma} = (d+\zeta)(q_{in} - q_{out}) \tag{4.7}$$

The vertical velocity (w) is defined at the iso σ-surfaces, and is the vertical velocity relative to the moving σ plane. The effect of precipitation and evaporation is taken into account in the water surface.

Under the shallow water assumption, the vertical momentum equation (Equation 4.7) is reduced to a hydrostatic pressure equation resulting in Equation 4.8, in which vertical accelerations due to buoyancy effects and to sudden variations in the bed topography are considered.

$$\frac{\partial P}{\partial \sigma} = -\rho g H \tag{4.8}$$

After an integration, the hydrostatic pressure is given by Equation 4.9:

$$P = P_{atm} + gH\int_\sigma^0 \rho(\xi, \eta, \sigma', t)d\sigma' \tag{4.9}$$

where, H the total water depth, given by $d + \zeta$; and P_{atm} is the atmospheric pressure.

For a constant density water, and taking into account the atmospheric pressure, gradients of the free surface level are included, called barotropic pressure gradients. The atmospheric pressure is included in the system for storm surge simulations. The atmospheric pressure gradients dominate the external forcing at peak winds during storm events. Space and time varying wind and pressure fields are especially important when simulating storm surges.

In case of a non-uniform density the pressure gradients includes not only barotropic pressure gradient, but also vertical pressure gradient, the so called baroclinic pressure gradient. The baroclinic pressure gradient is the result of variable distribution of density and water temperature in the vertical direction.

In the horizontal gradient, a vertical derivative is introduced by the σ co-ordinate transformation. In estuaries and coastal seas, the vertical grid may deteriorate strongly in case of steep bed slopes. In order to avoid artificial flow the numerical approximation of the baroclinic pressure terms requires a special numerical approach.

4.2.3 Boundary Conditions

A set of boundary conditions for water levels and/or horizontal velocities must be specified in order to reproduce accurately the local hydrodynamics. The following sub-sections describe the two different types of boundaries: the open and the closed boundaries. The open boundaries are also called as "water-water" boundaries. In a numerical model, open boundaries are introduced to restrict the computational area and the computational effort. The closed boundaries are the "natural" boundaries of the study area, for example coast lines and river banks (Deltares, 2006a).

The hydrodynamic model assumes that the flow at the open boundaries is sub-critical, which means that the magnitude of the flow is smaller than the velocity of wave propagation. Sub-critical flow means that the Froude number is smaller than 1, and is given by:

$$Fr = \frac{U}{\sqrt{gH}} \tag{4.10}$$

4.2.3.1 Vertical Boundary Conditions

4.2.3.1.1 Kinematic Boundary Conditions

In the σ co-ordinate system, the free surface (σ=0, or z=ζ) and the bottom (σ=-1 or z=-d) are σ co-ordinate surfaces. w is the vertical velocity relative to the σ-plane. The impermeability of the surface and the bottom is taken into account by prescribing the following kinematic conditions:

$$w|_{z=-1} = 0 \text{ and } w|_{\sigma=-0} = 0 \tag{4.11}$$

For the Z-grid the kinematic conditions read:

$$w|_{z=-d} = 0 \text{ and } w|_{z=\zeta} = 0 \tag{4.12}$$

4.2.3.1.2 Bed boundary condition

At the sea bottom, the boundary conditions for the momentum equations are:

$$\left.\frac{\nu_V}{H}\frac{\partial u}{\partial \sigma}\right|_{\sigma=-1} = \frac{1}{\rho_0}\tau_{b\xi} \tag{4.13}$$

$$\left.\frac{\nu_V}{H}\frac{\partial v}{\partial \sigma}\right|_{\sigma=-1} = \frac{1}{\rho_0}\tau_{b\eta} \tag{4.14}$$

where $\tau_{b\xi}$ and $\tau_{b\eta}$ are the bottom shear-stress for ξ and η directions.

For two-dimensional depth-averaged flow (case of Ria de Aveiro implementation), the shear-stress at the bed induced by a turbulent flow is assumed to be given by a quadratic friction law:

$$\vec{\tau}b = \frac{\rho_0 g \vec{U}\left|\vec{U}\right|}{\mathrm{C}_{2D}^2} \tag{4.15}$$

where $|\ \vec{U}\ |$ is the magnitude of the depth-averaged horizontal velocity; C_{2D} is the 2-D Chézy coefficient, which in this application is determined according to the Manning formulation, given by Equation 4.16:

$$C_{2D} = \frac{\sqrt[6]{H}}{M_n} \tag{4.16}$$

where M_n is the Manning coefficient.

In case of three-dimensional models (case of Rias Baixas implementation), a quadratic bed stress formulation is used, which is quite similar to the one for depth-averaged computations. The bed shear stress in 3-D is related to the current just above the bed:

$$\vec{\tau}_{b3D} = \frac{g\rho_0 \vec{u}_b\left|\vec{u}_b\right|}{\mathrm{C}_{3D}^2} \tag{4.17}$$

where $|\ \vec{u}_b\ |$ is the magnitude of the horizontal velocity in the first layer just above the bed. The contribution of the vertical velocity component to the magnitude of the velocity vector is neglected. The first grid point above the bed is assumed to be situated in the logarithmic boundary layer:

$$\vec{\tau}_b = \frac{\vec{u}_*}{k} ln\left(1 + \frac{\nabla z_b}{2z_0}\right) \tag{4.18}$$

where ∇z_b is the distance to the computational grid point closest to the bed and z_0 is user-defined. In the numerical implementation of the logarithmic law of the wall for a rough bottom, the bottom is positioned at z_0. The magnitude of the bottom stress is defined as:

$$|\vec{\tau}_b| = \rho_0 \vec{u}_* |\vec{u}_*| \tag{4.19}$$

Using Equation 4.17 to 4.20, C_{3D} can be expressed in the roughness height of the bed (z_0):

$$C_{3D} = \frac{\sqrt{g}}{k} ln\left(1 + \frac{\nabla z_b}{2z_0}\right) \tag{4.20}$$

Three dimensional calculations are often preceded by depth-averaged calculations. Then, the Chézy coefficients C_{2D} may be used for calibration of the 3-D model. Under the assumption of a logarithmic velocity profile, equality of bottom stress and the assumption $z_0 \ll H$, the magnitude of the depth-averaged velocity is given by:

$$|\vec{U}| = \frac{|\vec{u}_*|}{k} ln\left(1 + \frac{H}{ez_0}\right) \tag{4.21}$$

The Chézy coefficient (C_{2D}) can be converted into the bed roughness height (z_0) using the relation:

$$z_0 = \frac{H}{e^{1+\frac{kC_{2D}}{\sqrt{g}}} - e} \tag{4.22}$$

The depth H in Equations 4.21 and 4.22 denotes the actual water depth. Consequently, the roughness height (z_0) depends on the horizontal co-ordinates and time. Equality of the bed stress in 2-D lead to the relation:

$$C_{2D} = \frac{\sqrt{g}}{k} ln\left(1 + \frac{H}{ez_0}\right) \tag{4.23}$$

4.2.3.1.3 Surface boundary condition

At the free surface the boundary conditions for the momentum equations are:

$$\left.\frac{\upsilon_v}{H}\frac{\partial u}{\partial \sigma}\right|_{\sigma=0} = \frac{1}{\rho_0}|\tau_s| cos(\theta) \tag{4.24}$$

$$\left.\frac{\upsilon_v}{H}\frac{\partial v}{\partial \sigma}\right|_{\sigma=0} = \frac{1}{\rho_0}|\tau_s|sin(\theta) \tag{4.25}$$

where θ is the angle between the wind stress vector and the local direction. Without wind, the stress at the free surface is zero. The magnitude of the wind shear-stress is defined as:

$$|\vec{\tau}_s| = \rho_0 \vec{u}_{*s}|\vec{u}_{*s}| \tag{4.26}$$

The magnitude is determined by the following widely used quadratic expression:

$$|\vec{\tau}_s| = \rho_a C_d \mathrm{U}_{10}^2 \tag{4.27}$$

where ρ_{a} is the air density; U_{10} is the wind speed at 10 meters; and C_d is the wind drag coefficient, dependent on U_{10}.

4.2.3.2 Open Boundary Conditions

Open boundaries are virtual "water-water" boundaries. They are introduced to obtain a limited computational area and so to reduce the computational effort. At an open boundary, the water level, the normal velocity component or a combination should be defined to get a well-posed mathematical initial-boundary value problem. The data needed for the boundary conditions can be obtained from measurements, tidal data or from regional models.

Depending on the study objectives, the modelling systems presented in this study have several ways to impose the boundary conditions (Deltares, 2006a). In the framework of this work, the oceanic water level boundary condition is defined by Equation 4.28:

$$\zeta = F_\zeta(t) + \delta_{atm} \tag{4.28}$$

where:

$$F_\zeta(t) = \zeta + \alpha\frac{\partial}{\partial t}(U \pm 2\sqrt{gh}) \tag{4.29}$$

where:

$$\alpha = T_d\sqrt{\frac{H}{g}} \tag{4.30}$$

and,

$$\delta_{atm} = \frac{P_{average} - P_{atm}}{\rho g} \tag{4.31}$$

In the rivers boundaries, the freshwater is defined by:

$$Q = F_Q(t) \tag{4.32}$$

4.2.4 Intertidal Criteria

Since one of the main goals for hydrodynamic model implementation is to provide hydrodynamic basis for the water quality module, the Delft3D-Flow accuracy to simulate drying and flooding dynamics in intertidal flats is very important. Therefore, in order to evaluate if a grid cell is covered or uncovered by water, a set of model input parameters needs to be defined. From Equation 4.33, the thickness of the water layer of a dry cell (retention volume) is dependent on the threshold d, which is user defined. Therefore, the threshold value d must fulfil the following condition:

$$\delta \geq \frac{\partial \zeta}{\partial t} \frac{\delta t}{2} \tag{4.33}$$

In this application, a value of 0.1 meters for d was assumed.

4.3 Transport Model

The flows often transport dissolved substances, salinity and/or heat. In this modelling system, the transport of properties and heat is modelled by an advection-diffusion equation in three co-ordinate directions. Source and sink terms are included to simulate discharges. Also first-order decay processes are considered. A first-order decay process corresponds to a numerical solution which is exponentially decreasing.

The transport equation is formulated in a conservative form in orthogonal curvilinear coordinates in the horizontal direction and σ coordinates in the vertical direction, and is given by:

$$\begin{aligned}
&\frac{\partial (d+\zeta)c}{\partial t} + \frac{1}{\sqrt{G_{\xi\xi}}\sqrt{G_{\eta\eta}}}\left\{\frac{\partial[\sqrt{G_{\eta\eta}}(d+\zeta)uc]}{\partial \xi} + \frac{\partial[\sqrt{G_{\xi\xi}}(d+\zeta)vc]}{\partial \eta}\right\} + \\
&\frac{\partial wc}{\partial \sigma} = \frac{d+\zeta}{\sqrt{G_{\xi\xi}}\sqrt{G_{\eta\eta}}}\left\{\frac{\partial}{\partial \xi}\left(D_H \frac{\sqrt{G_{\eta\eta}}}{\sqrt{G_{\xi\xi}}}\frac{\partial c}{\partial \xi}\right) + \frac{\partial}{\partial \eta}\left(D_H \frac{\sqrt{G_{\xi\xi}}}{\sqrt{G_{\eta\eta}}}\frac{\partial c}{\partial \eta}\right)\right\} + \\
&\frac{1}{d+\zeta}\frac{\partial}{\partial \sigma}\left(D_V \frac{\partial c}{\partial \sigma}\right) - \lambda_d (d+\zeta)c + S
\end{aligned} \tag{4.34}$$

where c is the mass concentration; D_H is the horizontal diffusion coefficient; D_V is the vertical diffusion coefficient; λ_d is the first order decay process; and S is the source and sink terms per unit area due to the discharge (q_{in}) or withdrawal of water (q_{out}).

The total horizontal (D_H) and vertical (D_V) diffusion coefficients are defined by Equations 4.35 e 4.36, respectively:

$$D_H = D_{SGS} + D_V + D_H^{back} \tag{4.35}$$

$$D_V = \frac{\nu_{mod}}{\sigma_{mol}} + max\Big(D_{3D}, D_V^{back}\Big) \tag{4.36}$$

where D_{SGS} is the diffusion due to the sub-grid scale turbulence model; ${D_H}^{back}$ is the horizontal diffusion coefficient defined by the user; D_{3D} is the diffusion due to turbulence model in vertical direction; ν_{mol} is the kinematic viscosity of water; and σ_{mol} is the molecular Prandtl number for heat diffusion or the Schmidt number for diffusion of dissolved matter.

4.3.1 Boundary Conditions

The transport of dissolved substances such as salt, sediment or heat is described by the advection-diffusion equation, as previously mentioned. The horizontal transport is advection dominated and the equation is of hyperbolic type. At inflow, one boundary condition is needed and the concentration is specified. The concentration is determined by pure advection from the inner area:

$$\frac{\partial C}{\partial t} + \frac{U}{\sqrt{G_{\xi\xi}}}\frac{\partial C}{\partial \xi} = 0 \tag{4.37}$$

where C is the computed concentration.

The dispersive fluxes through the open boundaries at both inflow and outflow are zero, as expressed in the following equation:

$$\frac{D_H}{\sqrt{G_{\xi\xi}}}\frac{\partial C}{\partial \xi} = 0 \tag{4.38}$$

The vertical diffusive flux through the free surface and bed (Equations 4.39 e 4.40, respectively) is zero, with exception of the heat flux through the free surface. The mathematical formulations for the heat exchange at the free surface are given in next sub-section.

$$\left.\frac{D_V}{H}\frac{\partial c}{\partial \sigma}\right|_{\sigma=0} = 0 \tag{4.39}$$

$$\left.\frac{D_V}{H}\frac{\partial c}{\partial \sigma}\right|_{\sigma=-1} = 0 \tag{4.40}$$

4.3.2 Heat Flux

The heat exchange at the free surface is modelled by taking into account the separate effects of solar (short wave) and atmospheric (long wave) radiation, and heat loss due to back radiation, evaporation and convection. The selected heat flux model for both coastal systems was Heat flux model 2. In this formulation, the combined net (short wave) solar and net (long wave) atmospheric radiation is prescribed (the first two terms of Equation 4.41). The terms related to heat losses due to evaporation, back radiation and convection are computed by the model.

The total heat flux through the free surface reads:

$$Q_{tot} = Q_{sn} + Q_{an} - Q_{br} - Q_{ev} - Q_{co} \tag{4.41}$$

where Q_{sn} is net incident solar radiation (short wave); Q_{an} is net incident atmospheric radiation (long wave); Q_{br} is back radiation (long wave); Q_{ev} is the evaporative heat flux (latent heat); and Q_{co} is convective heat flux (sensible heat).

The short-wave radiation (Q_{sn}) emitted by the sun that reaches the earth surface under a clear sky condition is evaluated applying Stefan-Boltzmann's law for radiation from a black-body, expressed by:

$$Q_{sn} = \sigma_{sb}\overline{T}^4 \tag{4.42}$$

in which σ_{sb} is the Stefan-Boltzmann's constant $= 5.67\times10^{-8}\mathrm{J/(m^2sK^4)}$ and $\overline{T}$ is the absolute temperature in Kelvin.

Atmospheric radiation (long wave radiation) is primarily due to emission of absorbed solar radiation by water vapour, carbon dioxide and ozone in the atmosphere. The emission spectrum of the atmosphere is highly irregular. The amount of atmospheric radiation that reaches the earth is determined by applying the Stefan-Boltzmann's law that includes the emissivity coefficient of the atmosphere (ε). Taking into account the effect of reflection by the surface and reflection and absorption by clouds, the relation for the net atmospheric radiation Q_{an} is expressed by:

$$Q_{an} = (1-r)\varepsilon\sigma_{sb}\mathrm{T}_a^4 \tag{4.43}$$

where T_a is the air temperature in Kelvin; r is reflection coefficient (r=0.03). The emissivity factor of the atmosphere (ε) may depends both on vapour pressure and air temperature. The emissivity of the atmosphere varies between 0.7 and 1.0 for clear sky and low temperature. The presence of clouds increases the atmospheric radiation.

4.4 Water Quality Model

Water quality model solves the equations for transport and physical, biochemical and biological processes, defining substances and processes to simulate. For that reason, the user should be familiar with the basic concepts in order to understand the functioning of D-Water Quality and to make optimal use of the multiple simulation possibilities.

The Water Quality module works coupled to the Flow module, therefore Delft3D-WAQ needs hydrodynamic information from the flow module simulations previously performed. This process is named coupling. In this process, the Delft3D-WAQ reads the information from the hydrodynamic simulation, establishing as starting point the predictions of water level, velocity, density, salinity, water temperature, vertical eddy viscosity and vertical diffusivity.

4.4.1 Governing Equations

In this sub-chapter, will be introduced the mathematical advection-diffusion-reaction equation, which is the basis of the water quality model. As the model makes use of discrete computational elements and discrete time steps, this analytical equation can not be applied directly. Therefore, below will be introduced the numerical discretisation of D-Water Quality and the underlying principles of how to describe transport and water quality processes.

4.4.1.1 Mass Balances

Water quality module administrates the mass balance of several selected state variables, for each computational cell. Mass transported by flowing water from one cell to the next serves as a negative term in the mass balance in the first computational cell and as a positive term in the second computational cell. By combining computational cells in one, two or three dimensions, each water system can be represented and substances can be transported through computational cells and hence through the water system.

To proceed one step in time ($t+\Delta t$), D-Water Quality solves Equation 4.44, which is a simplified representation of the advection-diffusion-reaction equation, for each computational cell and for each state variable.

$$\mathrm{M}_i^{t+\Delta t} = \mathrm{M}_i^t + \Delta t \times \left(\frac{\Delta M}{\Delta t}\right)_{Tr} + \Delta t \times \left(\frac{\Delta M}{\Delta t}\right)_P + \Delta t \times \left(\frac{\Delta M}{\Delta t}\right)_S \tag{4.44}$$

where M_i^t is the mass at the beginning of a time step; $M_i^{t+\triangle t}$ is the mass at the end of a time step; $\left(\frac{\triangle M}{\triangle t}\right)_{Tr}$ are the changes by transport; $\left(\frac{\triangle M}{\triangle t}\right)_P$ are the changes by physical, biochemical or biological processes; $\left(\frac{\triangle M}{\triangle t}\right)_S$ are the changes by sources such as waste loads and river discharges.

4.4.2 Model Kinetics

The water quality module was applied to Ria de Aveiro and Rias Baixas to simulate local water quality and ecological conditions. This provides a framework for a wide range of substances and processes, allowing greater flexibility in model application.

The selection of the modelled kinetics depends on the study goals as well as on the availability of field data. In this context, Figure 4.2 shows a simplistic schematic representation of the water quality model designed for Ria de Aveiro and Rias Baixas water column, although the interactions water-sediment and water-air are also taken into account. The main kinetics in the water column includes the heat and salt transport, phytoplankton growth and mortality, the corresponding cycles of oxygen, carbon, nitrogen and phosphorus.

It should be pointed out that the general mass transport equation (Equation 4.44) is used for all chemical and biological variables in water column, of which the only difference is that each variable has different process formulations. In Table 4.1 is depicted a brief description of the kinetic processes involved in Figure 4.2.

In D-Water Quality, the constituents of a water system are divided in functional groups. A functional group includes one or more substances that display similar physical and/or biochemical behaviour in a water system. For example, the nutrients, such as nitrate, ammonium, phosphate and silicon are a functional group as they are required to compute primary production. Functional groups can interact with each other directly, as in the previous example (Figure 4.2), or indirectly as inorganic suspended matter influences the light availability for primary production. In Table 4.2 are presented the substances and the processes associated considered in the model configurations.

Since the water quality module has several numerical discretization schemes available, the integration method 15 (Iterative solver, backward differences) was applied,

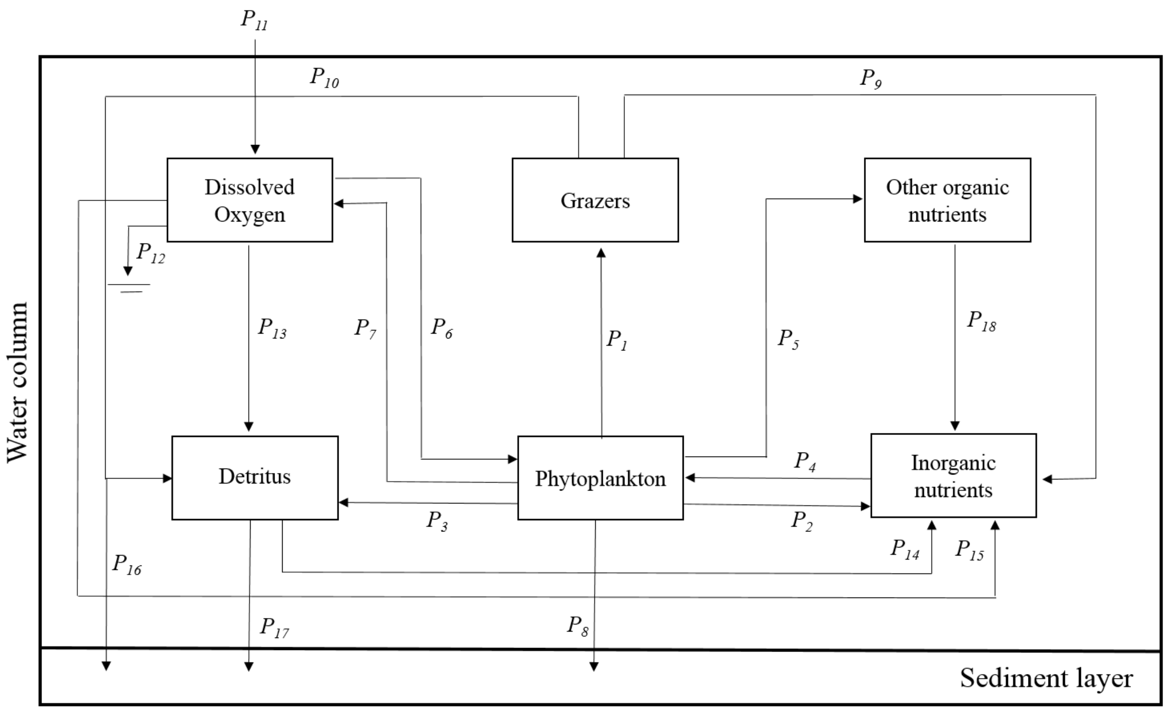

Figure 4.2: Schematic diagram of the water quality model kinetics. P_1 to P_{18} are the processes involved in the water quality model, described on Table 4.1.

due to:

- efficiency for simulations with a high number of substances;
- larger times-steps may be used;
- There are no negative concentrations in the calculus cells.

4.4.3 Boundary Conditions

4.4.3.1 Open Boundaries

Open boundaries are required to obtain the solution of the advection-diffusion equation. Without specification of the open boundaries the model is not able to compute any variables or concentrations. Concentrations of all substances and dispersion coefficients must be specified at all open boundaries for all time-steps, since the flows and volumes are automatically inputted from hydrodynamic model. As a consequence of the equations governing the Water Quality model, downstream boundaries do have an effect on the solution of the Water Quality model:

- If the advection term is computed by a 'central method', the concentration at the interface between the last model segment and the downstream boundary

Table 4.1: Main processes involved in the water quality model.

Process	Description	Process	Description
P1	Phytoplankton losses by grazing	*P10*	Production of detritus by grazers
P2	Return of inorganic nutrients by phytoplankton metabolism and mortality	*P11*	Atmospheric re-aeration
P3	Detritus by phytoplankton mortality	*P12*	Sediment oxygen demand
P4	Uptake of inorganic nutrients by phytoplankton	*P13*	Oxygen consumed by dissolution of detritus
P5	Return of organic nutrients by phytoplankton metabolism and mortality	*P14*	Dissolution of detritus in water
P6	Oxygen consumed by phytoplankton respiration	*P15*	Oxygen consumed by nitrification and mineralization
P7	Oxygen production by phytoplankton photosynthesis	*P16*	Sedimentation or biodeposition of feces
P8	Sedimentation of phytoplankton	*P17*	Sedimentation of detritus
P9	Release of inorganic nutrients by grazers mortality	*P18*	Conversion of organic nutrients to dissolved inorganic nutrients

is computed as the average between the concentration in the last segment and the downstream boundary concentration. Therefore, the downstream boundary concentration affects the advective transport in this case;

- For the computation of the dispersive term, the concentration gradient at the interface between the last model segment and the downstream boundary is computed as the difference between the concentration in the last segment and the downstream boundary concentration divided by the distance between the two. Therefore, the downstream boundary concentration affect the dispersive transport.

4.4.3.2 Closed Boundaries

Closed boundaries are those boundaries that have zero flow and dispersion for all time steps. No transport is associated with these exchange surfaces. Sometimes exchanges are defined anyway for these boundaries in order to keep the grid layout completely structured. In such cases the grid has some permanently dry cells. For closed

Table 4.2: Processes and substances selected.

Substances	**Processes**
Dissolved Oxygen	Horizontal dispersion in 1-D model Horizontal dispersion velocity depend Uptake of nutrients by growth of algae Denitrification in water column Nitrification of ammonium Reaeration of oxygen Variation of primary production within day Sediment oxygen demand Net primary production and mortality Limitation Potential minimum dissolved oxygen concentration Grazing
Inorganic Matter	Composition Sedimentation Secchi depth for visible light Total of transport in sediment for inorganic matter
Ammonium	Uptake of nutrients by growth of algae Composition Nitrification of ammonium Nutrient release of algae Grazing
Nitrate	Uptake of nutrients by growth of algae Composition Denitrification in water column Nitrification of ammonium
Ortho-phosphate	Uptake of nutrients by growth of algae Composition Nutrient release of algae Grazing Ad[De]Sorption ortho phosphorus to inorg. matter
Alkalinity	Simple calculation of pH Uptake of nutrients by growth of algae Denitrification in water column Nitrification of ammonium Nutrient release of algae Grazing
Algae (non-Diatoms)	Net primary production and mortality Limitation Potential minimum dissolved oxygen concentration Sedimentation green algae Grazing

boundaries no concentrations are required as input.

4.4.3.3 Time Lags and Return Time

If water crosses a boundary, it may be assumed that the concentration immediately outside of the model area is influenced by the previous outflows. If the flow changes sign and inflow takes place again, it may be assumed that part of the water flowed out previously, enters again. As inflow proceeds, the boundary conditions, may become more and more effective. This so-called Thatcher-Harleman time lag uses the inner concentration if outflow occurs and starts with the latest outflow concentration to reach the specified boundary concentration within the user specified time lag. Mathematically is given by Equation 4.45:

$$C(t_0 + t) = C(t_0)\left(0.5 + 0.5cos\left(\frac{\pi t}{2T}\right)\right) + C_B(t)\left(0.5 - 0.5cos\left(\frac{\pi t}{2T_{th}}\right)\right) \tag{4.45}$$

where t_0 is the time that outflow changes to inflow; t is the time after t_0; C is the simulated boundary concentration; C_B is the boundary condition imposed; and T_{th} is Thatcher-Harleman time lag.

Chapter 5

Models Implementation on Ria de Aveiro Lagoon and Rias Baixas

5.1 Introduction

In order to study the biogeochemical and water quality processes along Ria de Aveiro and Rias Baixas, coupled hydrodynamic and biogeochemical modes were implemented, which are very valuable tools to complement observational gaps and to provide continual estimation of estuarine water properties. This task proved to be the most challenging and the most time-consuming, due to the the frequent lack of the necessary data, high spatial and temporal variability of properties and the massive number of processes involved and interrelated. Moreover, properties to be simulated strongly depend on each other and on several environmental factors, such as tidal propagation, rivers inflow, nutrients loads, water-air interaction and trophic processes.

Here, the main objective is to describe the implementation and validation of coupled circulation and biogeochemical configurations with Delft Flow and Water Quality modules along the Ria de Aveiro and Rias Baixas. As mentioned in sub-chapter 2.1.1, Ria de Aveiro is a very shallow lagoon, considered vertically homogeneous, where the horizontal length scales are significantly larger than the vertical scales. Therefore, as widely applied for Ria de Aveiro (Lopes et al., 2015; Vaz et al., 2016) a two-dimensional model implementation was developed to simulate the local processes. According with the conclusions achieved in Chapter 3, Rias Baixas are vertically stratified, therefore a three-dimensional model was developed for this coastal system.

Thus, in this chapter, the methodology developed to reproduce the biogeochemical dynamics of the study areas is described, as well as the calibration and validation of the hydrodynamic and biogeochemical models.

5.2 Methodology

To ensure the best reproduction of the hydrodynamic and biochemical processes within Ria de Aveiro and Rias Baixas, several numerical simulations were performed in order to achieve the best model accuracy in predicting the local estuarine processes. For this purpose, a final model configuration was obtained for both coastal systems (section 5.2.1). The hydrodynamics and water quality model calibration and validation procedures are presented in sections 5.2.2 and 5.2.3, respectively.

The stations used for model calibration and validation procedures in both systems are represented in Figure 5.1.

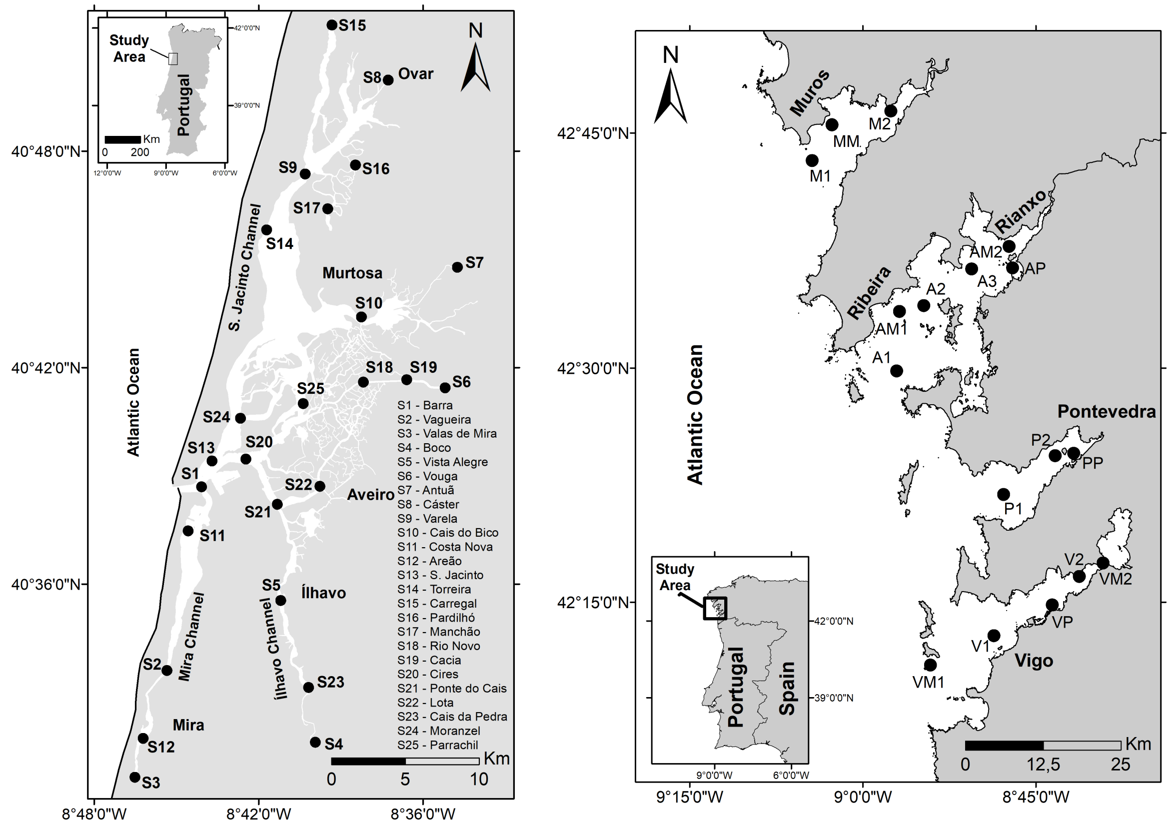

(A) Ria de Aveiro (B) Rias Baixas

Figure 5.1: Map of Ria de Aveiro lagoon (A) and Rias Baixas (B), and the sampling stations used for models calibration and validation procedure.

5.2.1 Models Configuration

5.2.1.1 Hydrodynamic Models

5.2.1.1.1 Ria de Aveiro

One of the key factors in the simulation of tidal flows in lagoons like Ria de Aveiro is the numerical grid generation and depth interpolation in order to generate an accurate numerical bathymetry. It controls the spatial variability of currents magnitude and direction, constituting a key feature that guarantees the realism of the numerical model (Dias and Lopes, 2006). The domain used in this study, which comprises the entire area of Ria de Aveiro and near coastal zone, was discretized in a triangular grid with a variable spatial resolution, due to the complex geometry of the area. Ria de Aveiro has short and narrow channels, where water properties changes significantly in a short horizontal scale. The grid areas with the coarser resolution (1.5 km) are presented in offshore zone, close to the ocean boundary. The spatial resolution increases from this area to the inner channels, where a maximum resolution of 1 m is adopted, in the narrow lagoon channels. The final grid has 103515 elements and 74094 nodes.

The numerical bathymetry (Figure 5.2) was generated from a data set resulting from a general lagoon survey carried out in 1987/88 by the Hydrographic Institute of Portuguese Navy (IH), updated in 2011 for the main channels of the lagoon (Mira, Ílhavo, S. Jacinto and Espinheiro) by Polis Litoral Ria de Aveiro (`http://www.polisriadeaveiro.pt/`) and in 2012 for the inlet region by the Aveiro Harbour Administration, SA (`http://www.portodeaveiro.pt/`).

At the open ocean boundary, which is located outside Ria de Aveiro at a longitude of 8°50'30"W, the hydrodynamic model was forced by 36 harmonic constituents, determined by harmonic analysis of sea surface elevation measured at the lagoon inlet, performed through T_Tide package routines (Pawlowicz et al., 2002). The freshwater input for the five main rivers discharging in Ria de Aveiro (Vouga, Antuã, Cáster Boco, and Valas de Mira) corresponds to time series predicted by the SWIM model (Krysanova et al., 2000), since the rivers discharge is not currently monitored. The time step of the model was set to 15 seconds and a horizontal viscosity of 5 m^2s^{-1} was considered. For the bottom roughness, a Manning coefficient dependent on the depth was used, varying from 0.019 in the deepest areas to 0.025 in intertidal zones.

Time series of relative humidity, atmospheric pressure, air temperature, wind velocity (magnitude and direction) and solar radiation are also applied as atmospheric boundary conditions. These atmospheric data were measured at the University of Aveiro meteorological station with a time resolution of 10 minutes.

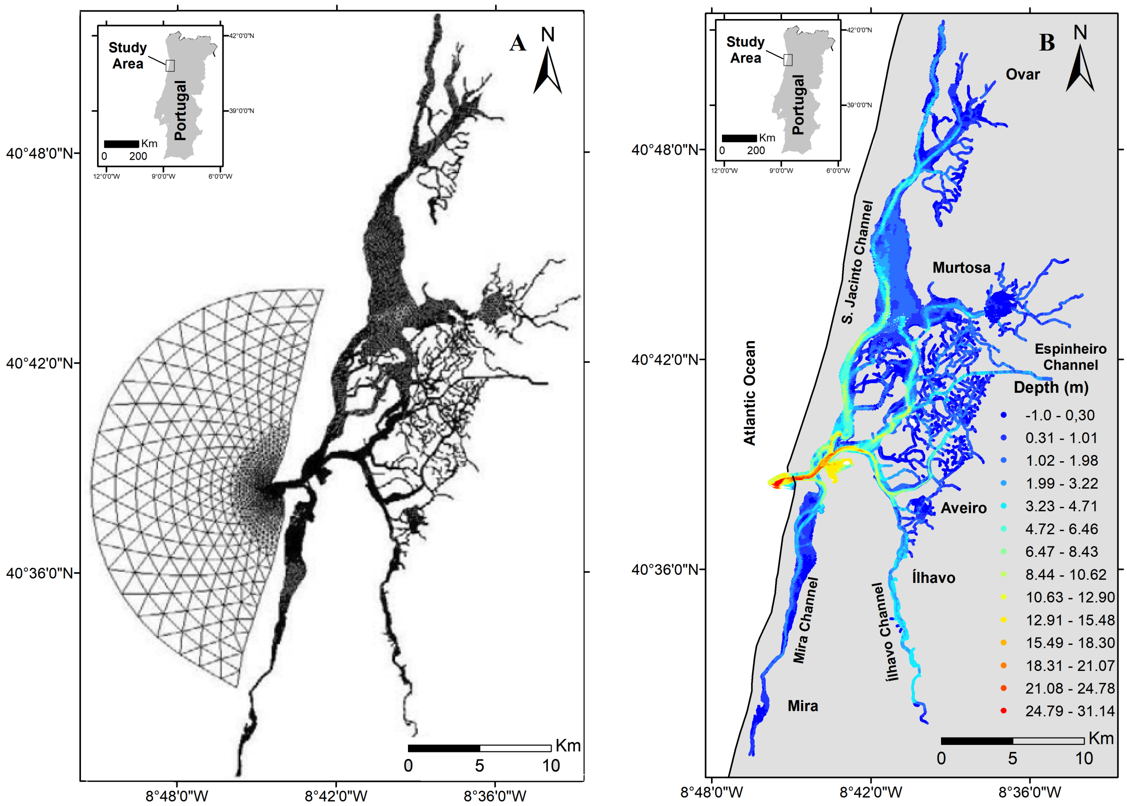

Figure 5.2: Numerical grid (A) and bathymetry (B) of Ria de Aveiro.

5.2.1.1.2 Rias Baixas

Contrarily to Ria de Aveiro model configuration, Rias Baixas model implementation comprises a three-dimensional application. This configuration is based on the curvilinear irregular grid developed by Sousa et al. (2018), that was refined inside the rias in order to better represent the local processes. Therefore, the present configuration (Figure 5.3) presents 371 $\times$ 172 cells, with maximum resolution of 100 meters in the upstream estuarine areas, and 650 m in the offshore area.

The numerical bathymetry was interpolated from General Bathymetric Chart of the Oceans dataset (`https://www.gebco.net/`), and is presented in Figure 5.4. Thirteen vertical sigma layers with refined surface layers were used, since most of the thermohaline processes occur near surface.

The model is forced by tidal harmonic constituents at the offshore open boundary and by river flows at the upstream areas of Rias Baixas estuaries. At the open boundary, the model uses tidal data from the global tidal model TOPEX/POSEIDON (Ray, 1999), which consists in sea surface elevations determined from thirteen constituents with a spatial resolution of about 1/4°. The river discharges for the five tributaries flowing in the Rias Baixas (Verdugo-Oitaben, Lérez, Umia, Ulla and Tambre rivers)

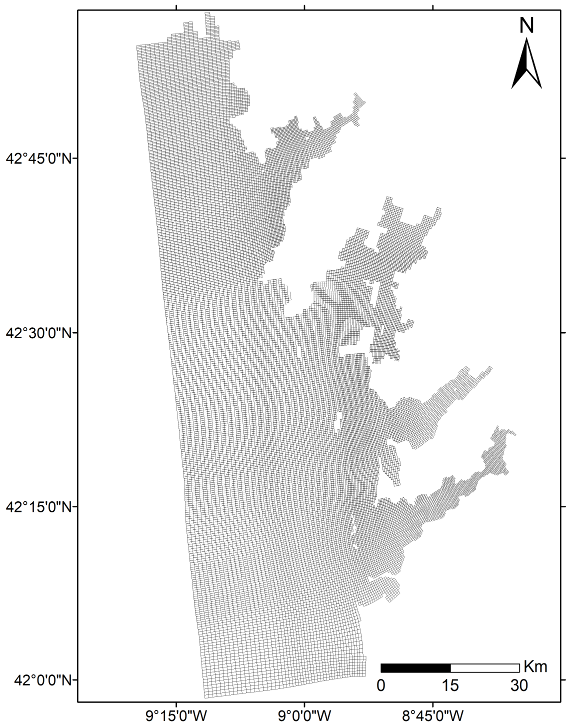

Figure 5.3: Numerical grid developed for Rias Baixas implementation.

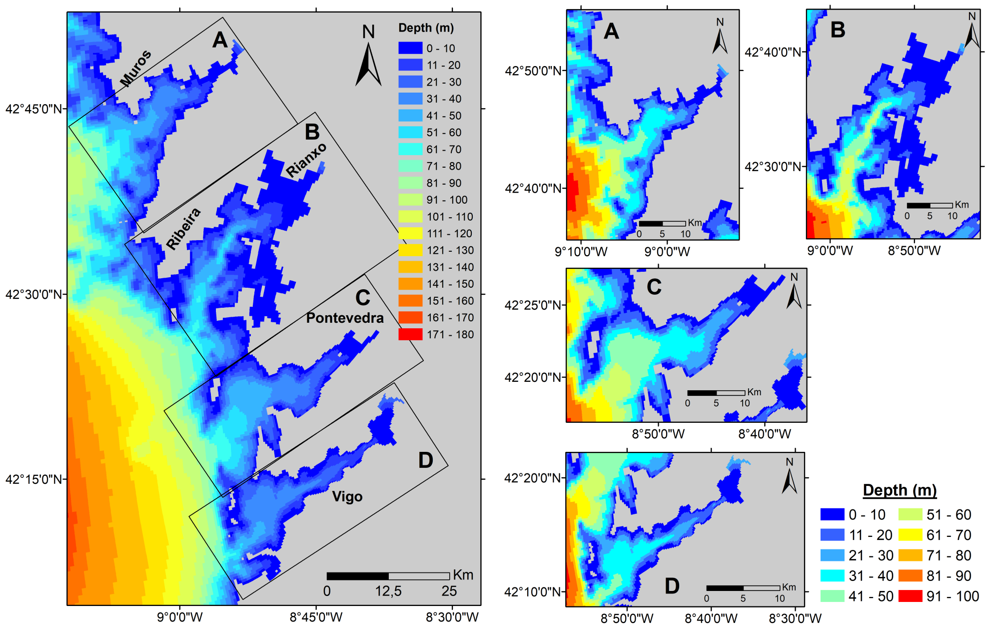

Figure 5.4: Charts of Rias Baixas showing general bathymetry of Rias Baixas and adjacent coast. (A) Ria de Muros; (B) Ria de Arousa; (C) Ria de Pontevedra; (D) Ria de Vigo.

were imposed as time series with a time resolution of 10 minutes, obtained from Meteogalicia (`http://www.meteogalicia.gal`).

In case of Rias Baixas implementation, the heat fluxes and salt transport are calculated coupled to the hydrodynamic model, constituting an input to water quality model. Daily thermohaline properties (salinity and water temperature) from the operational Atlantic-Iberian Biscay Irish-Ocean Physics Reanalysis, with a horizontal resolution of 1/12° and a vertical resolution of 50 sigma coordinates levels, were used as oceanic boundary conditions (`http://marine.copernicus.eu`). The water temperature and salinity of rivers inflows were considered constant, with typical water temperature values for the season and a constant value of 0 for the salinity.

Atmospheric data from the ERA Interim (`https://www.ecmwf.int/`) was used as surface boundary conditions. The heat flux model uses air temperature, combined net solar (short-wave), net (long-wave) atmospheric radiation, relative humidity, and wind speed to calculate heat losses due to evaporation, back radiation and convection.

The time step defined for this application is 30 seconds, the horizontal eddy viscosity and diffusivity is $10^2 s^{-1}$, the vertical eddy viscosity is $10^{-4} s^{-1}$, and a constant value of 0.024 is assumed for bottom Manning roughness coefficient. The k-ε model was used for 3-D turbulence.

5.2.1.2 Water Quality Models

Following the implementation, calibration and validation procedures of the hydrodynamic models, the next step of this study is the implementation of the water quality models. Since the conceptual description and the model kinetics was depicted in the previous chapter, in the next sub-sections are explained the specific features of each coastal system.

5.2.1.2.1 Ria de Aveiro

At the open boundaries previously mentioned in sub-section 5.2.1.1.1, the model was forced with several properties: water temperature, salinity, ammonium, nitrate, phosphate, alkalinity (as function of pH) and microalgae concentrations. The salinity at sea boundary was considered 36.5, while in river boundaries was defined as 0. Water temperature, nitrate, ammonium and phosphate concentrations were imposed according with the daily values predicted by SWIM model (Krysanova et al., 2000).

The algae and alkalinity concentrations were setup from the measurements performed in field surveys (presented in the next chapter). In detail, the chlorophyll *a* values measured in sampling stations S1, S3, S4, S6, S7 and S8 (regarding to the ocean and rivers boundaries), in the scope of the Chapter 6, were converted to $g(C)m^{-3}$ and interpolated to a daily temporal resolution. An identical procedure was followed to alkalinity concentration imposition. The pH values measured were converted to alkalinity concentration (g(HCO^{3-})m^{-3}) and equality interpolated.

5.2.1.2.2 Rias Baixas

The open boundary conditions for the Delf3D-WAQ inputs (chlorophyll *a* concentration, orthophosphate's, ammonium, nitrate and dissolved oxygen concentration) were supplied from the operational Atlantic-Iberian Biscay Irish-Ocean Biogeochemical Analysis and Forecast model system, with a horizontal resolution of 1/35° and a 50 sigma coordinates vertical resolution.

From landward boundaries, monthly mean nutrients concentrations (nitrogen and phosphorous compounds) were provided by the Swedish Meteorological and Hydrological Institute (SMHI) (`https://hypeweb.smhi.se/`) for the period between 2000 and 2010, for the rivers considered. Once simulation period (2015 and 2016) is not included in the data provided, the imposed nutrients resulted from the monthly average of this long term data. For oxygen and chlorophyll *a* concentration, seasonal typical values were imposed and slightly adapted in order to obtain the better possible calibration and validation results.

5.2.2 Hydrodynamic Models Calibration and Validation

The calibration and validation procedures followed to get reliable and accurate numerical results are presented in this section.

The hydrodynamic models performances was firstly evaluated visually, comparing the simulated and observed time series of sea surface elevation SSE, and after quantified by Root Mean Square (RMS) errors and Skill parameter assessment, expressed by Equations 5.1 e 5.2:

$$RMS = \sqrt{\frac{1}{N}\sum_{i=1}^{N}(\eta_{oi} - \eta_{pi})^2} \tag{5.1}$$

$$Skill = 1 - \frac{\sum_{i=1}^{N} |\eta_{pi} - \eta_{oi}|^2}{\sum_{i=1}^{N}[|\eta_{pi} - \overline{\eta_o}| + |\eta_{oi} - \overline{\eta_o}|]^2} \tag{5.2}$$

where η_o is the data; η_p is the model estimations; the overbar indicates the mean of the data set for the chosen variable, N is the total number of model data matches.

Based on Dias et al. (2009), the RMS errors should be compared with the local tidal amplitude and if are lower than 5% of the local amplitude, the agreement between model simulations and observations should be considered excellent; if they range between 5% and 10% the agreement should be considered very good. The model predictive Skill, a method developed by Willmott (1981) and used initially by Warner et al. (2005) and Li et al. (2005), yield a Skill of one for a perfect agreement between model simulations and observations and zero for a complete disagreement. Skill values higher than 0.95 should be considered representative of an excellent agreement between model results and observations (Dias et al., 2009).

Additionally, harmonic constants (amplitudes and phases) determined from simulated and observed SSE time series for the main tidal constituents were also compared using Pawlowicz et al. (2002) harmonic analysis package, in order to quantify the model accuracy in reproducing the tidal wave propagation along the coastal systems under analysis.

5.2.2.1 Ria de Aveiro

The calibration of Ria de Aveiro hydrodynamic model was based on the adjustments of parameters to which the model is most sensitive, in order to optimize the agreement between model simulations and observations. According to Dias and Fernandes (2006), the magnitude of the bottom friction coefficient, which is strongly dependent on the water depth, induces modifications in the tidal wave propagation within the Ria de Aveiro. Therefore, based in previous works (Dias et al. (2009); Picado et al. (2011); Vaz (2012)), it was used a Manning coefficient dependent of the depth as calibration parameter, varying from 0.019 in the deepest areas to 0.025 in intertidal zones.

The Manning coefficients were adjusted using as guideline that an increase in the bottom friction induces a decrease in the tidal wave amplitude, and vice-versa. Moreover, an increase in the bottom friction leads to an increase in the phase lag for high tide and a decrease for low tide (Fry and Aubrey, 1990).

The model was calibrated through comparison between model simulations and observed sea surface elevation data recorded in 18 stations (S1, S2, S5, S8, S10, S11, S12, S13, S14, S15, S16, S17, S18, S19, S20, S21, S22 and S23) within the lagoon in 2003/04 (Araujo, 2006) (Figure 5.1 (A)).

The validation procedure was carried out without any change in the tidal input and in the Manning coefficients. The data used to perform this task corresponds to a period of January of 2018, where model performance was evaluated by comparing RMS errors between simulated and observed SSE time series, for stations S2, S5, S9, S10 and S18.

5.2.2.2 Rias Baixas

The Rias Baixas hydrodynamic model calibration was done comparing observed (`http://www.puertos.es/`) and simulated SSE at three sampling stations represented in Figure 5.1 (B) (Stations AP, PP and VP). The period used to calibrate the hydrodynamic model was from March 1^{th} 2018 to March 31^{th} 2018, while for validation were compared measurements and simulations for August 2018.

5.2.3 Water Quality Models Calibration and Validation

Some of the water quality model parameters were adjusted to obtain a reasonable reproduction of the observed data, while others were obtained directly from the range reported in the literature (Cerco and Cole, 1993; Wool et al., 2006). Water temperature, salinity, nitrate, ammonia, phosphate, alkalinity, total inorganic carbon, dissolved oxygen concentration and microalgae biomass were adjusted in the model open boundaries. To compute this major model substances, more than 300 parameters were kept as a default value given by the model or set considering values found on the literature review.

The water quality models were calibrated and validated through comparison between observations and model simulations for water temperature, salinity, pH, dissolved oxygen and chlorophyll *a* concentration. The water quality model was calibrated comparing measurements and predictions for a short period, based on a data with high temporal resolution. For the validation procedure, the accuracy of the models to reproduce the seasonal variability of the biogeochemical variables was assessed. In this procedure, a simulated year time series of water temperature, salinity, pH, chlorophyll *a* concentration (only for Ria de Aveiro) and dissolved oxygen (only for Rias Baixas) is compared with measurements.

To evaluate the model performance in reproducing the annual variability of the variables, RMS error, model efficiencies, percentage model biases and cost functions are determined following Allen et al. (2007), on the basis of tidally-averaged predictions and observations for Ria de Aveiro's lagoon.

The physical meaning of RMS error and Skill value were previously explained (Sub-Chapter 5.2.2). The Nash Sutcliffe Model Efficiency (ME) (Equation 5.3) of a model variable measures the ratio between the model error and the variability of the data (Nash and Sutcliffe, 1970).

$$ME = 1 - \frac{\sum_{n=1}^{N}(\eta_o - \eta_p)^2}{\sum_{n=1}^{N}(\eta_o - \overline{\eta_o})^2} \tag{5.3}$$

Performance levels are categorised as follows: >0.65 excellent, 0.65–0.5 very good, 0.5–0.2 good, <0.2 poor.

The percentage model Bias (Equation 5.4) measures whether the model is systematically underestimating or overestimating the observations. The closer the value is to zero the better the model results (Maréchal, 2004).

$$BIAS = \frac{\sum_{n=1}^{N}(\eta_p - \eta_o)}{\sum_{n=1}^{N}\eta_o} \tag{5.4}$$

Finally, the cost function (CF) (Equation 5.5) gives a non-dimensional value that assesses the "goodness of fit" between two sets of data; it quantifies the difference between predictions and observations.

$$CF = \frac{1}{N}\sum_{n=1}^{N}\frac{|\eta_p - \eta_o|}{\sigma_D} \tag{5.5}$$

where σ_D is the standard deviation of the data. It is a measure of the ratio of the model data misfit to a measure of the variance of the data; the closer the value is to zero the better the model.

5.2.3.1 Ria de Aveiro

The water quality model was calibrated comparing observations and model simulations for water temperature, salinity, pH and chlorophyll *a* concentration.

For the water temperature and salinity calibration, was used a data set available from field monitoring performed in summer of 1996 on 7 stations distributed along Ria de Aveiro channels (Stations S5, S9, S12, S13, S21, S24 and S25 of Figure 5.1). For pH and chlorophyll *a* concentrations, the observed data was recorded through field work carried out in summer of 2013 in three stations of the lagoon.

The water quality validation was performed comparing model simulations with observations for a different period along a tidal cycle, using data sampled in the scope of BioChanger project leaded by the University of Aveiro. Additionally, this process also includes the validation of the annual variability of the variables under study, as this constitutes one of the major goals of this study. In detail, tidal variability of water temperature and salinity were compared with data observed for January 2017. The annual variability was also evaluated comparing model predictions and the data collected in this study, for 2016. Due to data availability limitations, the pH and chlorophyll *a* concentration were only validated by comparing the model simulations with the seasonal variability of the variables, using the data obtained within the scope of this study (Chapter 6).

5.2.3.2 Rias Baixas

The water quality model application for Rias Baixas was calibrated and validated comparing the model results with data-sets from two different sources: a data-set from Meteo-Galicia website (`https://www.meteogalicia.gal/`); and another from Intecmar website (`http://www.intecmar.gal/`). Since the Rias Baixas water quality application is three-dimensional, the calibration was carried comparing observations and simulations of time series and vertical profiles of water temperature, salinity, pH, dissolved oxygen and chlorophyll *a* concentration.

The water temperature and salinity calibration was carried out comparing data from MeteoGalicia website (stations MM, AM1, AM2, VM1 and VM2 of Figure 5.1 (B)) and model results for March of 2018. The vertical profiles of water temperature, salinity, dissolved oxygen and pH were performed comparing the observed data and model simulations for March, 21^{th} and 22^{th} 2016.

As performed in Ria de Aveiro, the water quality model was validated assessing the model performance to reproduce the seasonal variations of water temperature, salinity, dissolved oxygen and pH, for surface and bottom layers, using all the parameters described in previous sections.

5.3 Results

5.3.1 Hydrodynamic Models Calibration and Validation

5.3.1.1 Ria de Aveiro

In Figure 5.5 is depicted the visual comparison between SSE observations and simulations, in which the blue line presents model results, while the red corresponds to observations. The RMS values ranges from 2% to 16% of the local tidal amplitude for the stations under analysis. For stations S1, S2, S5, S10, S11, S12, S13, S14, S18, S19, S20, S21 and S22 (13 of 18) the RMS values are comprised between 0 and 10% of local tidal amplitude. Therefore, the model accuracy in most of the stations ranges from very good to excellent.

At inlet area (S1), the simulated and observed data comparison should be considered as perfect. The RMS is approximately 7 cm, which represents an error of 2% comparing with local tidal amplitude. In stations S11, S13, S20 and S21, the disagreement is also lower than 5% of tidal range. Generally, the model disagreement increases from the inlet towards the head of the channels.

Excluding stations S8, S15, S16 and S17 (0.88, 0.89, 0.85 and 0.89, respectively),

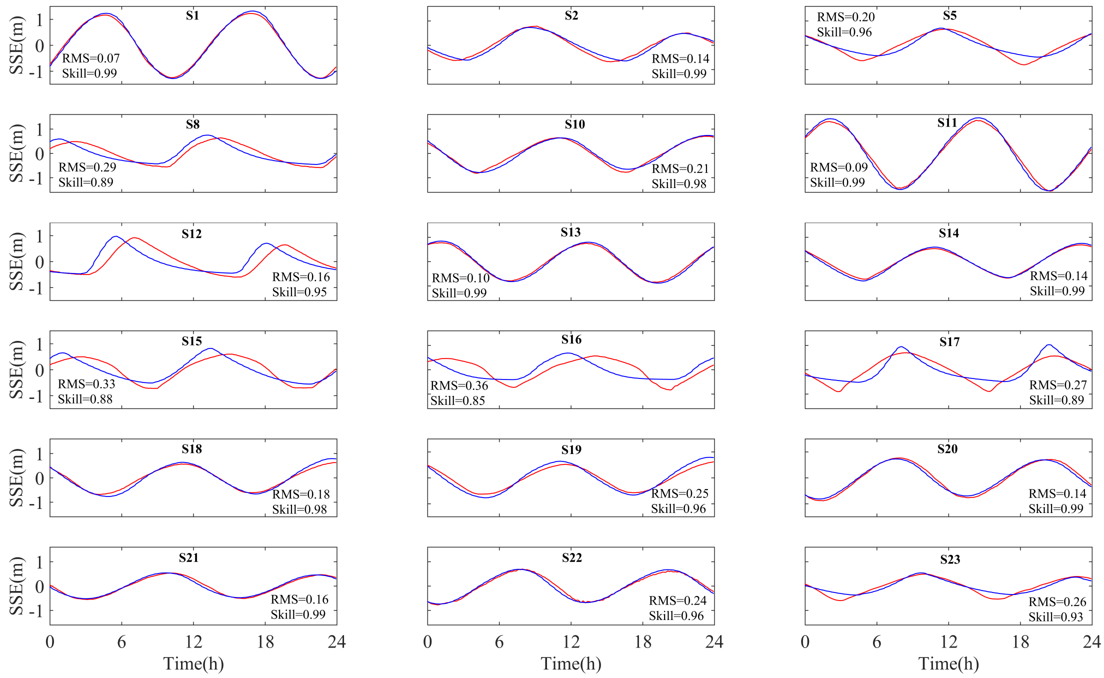

Figure 5.5: Comparison between simulated and observed Ria de Aveiro SSE time series in the frame of hydrodynamic calibration procedure (red line: data; blue line: model). Statistical results (RMS error (m) and Skill) are also presented.

the skill values are higher than 0.90. In 13 of 18 stations (S1, S2, S5, S10, S11, S12, S13, S14, S18, S19, S20, S21 and S22), the skill values are higher than 0.95, which is considered an excellent agreement between model simulations and observations.

From the analysis of Figure 5.6 is verified that M_2 and S_2 are the most important harmonic constituents in the lagoon, representing approximately 90% of the tidal energy in Ria de Aveiro, in agreement with Dias et al. (1999). As for the time series discussed above, the reproduction of the tidal constituents shows higher disagreement at the upstream stations. From the analysis of these results is found that the mean amplitude difference for the M_2 constituent is about 10 cm, while the mean phase difference is about 10°, which corresponds to a 20 minutes difference in tidal wave arrival. For the S_2 constituent, the mean amplitude and phase difference is approximately 5 cm and 15°, respectively, representing an average delay of about 43 minutes.

Despite some uncertainties, the overall results showed an excellent agreement between model simulations and observations at the stations located at the lagoon central area, and good agreement at the upstream stations.

Besides the calibration, the hydrodynamic model was also validated by comparing model simulations with observations for January 2018. The procedure was carried out without any change in the tidal input characteristics referred in the calibration

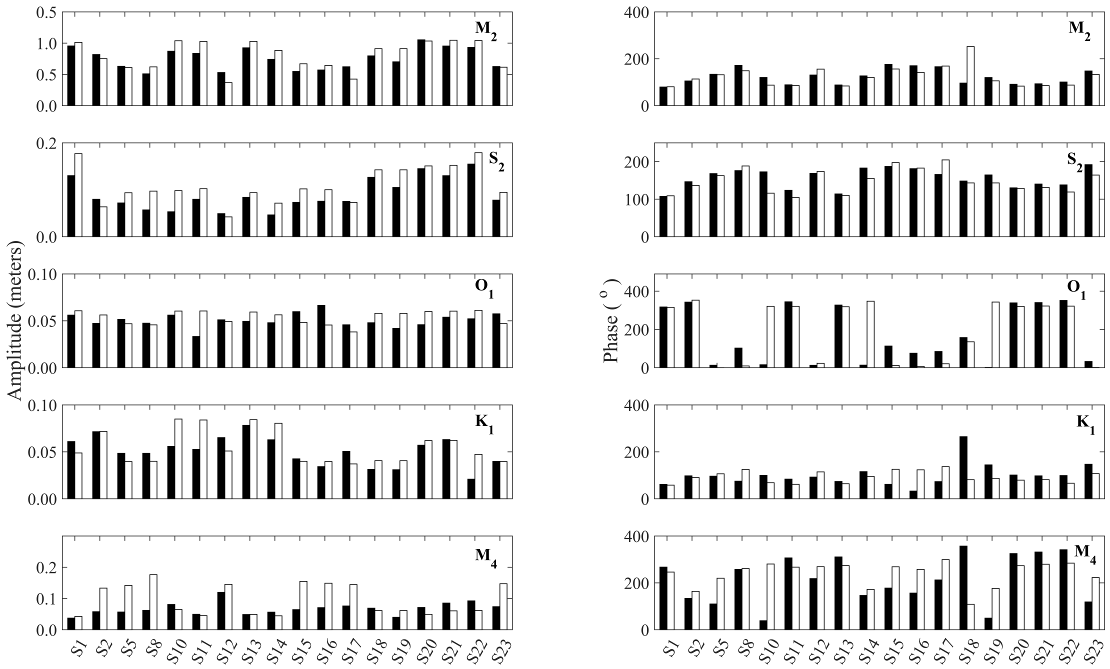

Figure 5.6: Comparison between simulated and observed Ria de Aveiro's amplitude and phase for the major semi-diurnal and diurnal constituents. The black and white bars represent the observed and predicted values, respectively.

procedure. Also, the Manning coefficients were not modified.

From statistical results depicted in Table 5.1, which summarizes the statistical results of hydrodynamic model validation, is found that RMS values are lower than 10% of the local amplitude for all stations under analysis, and that the Skill value is always higher than 0.90, representing a very good model accuracy.

This type of models (2-D finite element model) were widely implemented in Ria de Aveiro (Picado et al., 2009; Vaz, 2012; Lopes, 2016). The results achieved in this hydrodynamic model implementation are better than those obtained by Picado et al. (2009) and Vaz (2012), and slightly worse comparing with Lopes (2016). The mean RMS error obtained in this study was 19.9 cm, which is lower than 25.9 and 24.6 cm obtained by Picado et al. (2009) and Vaz (2012), and slightly higher comparing with Lopes (2016) implementation (18.2 cm). Note that Lopes (2016) included in the numerical grid a larger area of intertidal regions, the lagoon margins and the existing protection structures, which may explain the results obtained.

These results demonstrate that the model accurately reproduces the tidal wave propagation along Ria de Aveiro, and therefore can be considered suitable to predict tidal propagation along this lagoon. Under these conditions, very good inputs are available to force the water quality model.

Table 5.1: Model accuracy in reproducing observed SSE as characterized by means of RMS (m) and Skill values at selected Ria de Aveiro stations.

Station	RMS (m)	Skill
S2	0.13	0.98
S5	0.25	0.92
S9	0.12	0.99
S10	0.17	0.96
S18	0.07	0.99

5.3.1.2 Rias Baixas

The visual comparison between simulated and observed SSE is depicted in Figure 5.7. The blue line corresponds to model simulations, while red line regards to observations. RMS errors are lower than 7 centimeters for all stations, corresponding to a relative error of about 2% of local tidal amplitude, and skill values higher than 0.99. These statistical results, as described in section 5.2.2, indicate excellent agreement between simulated and observed SSE.

In Figure 5.8 is depicted the comparison between simulated and observed amplitude and phase of the major semi-diurnal and diurnal constituents in the stations considered in the calibration procedure. Similarity to Ria de Aveiro, and in agreement with Ruiz-Villarreal et al. (2002), M_2 and S_2 are the main harmonic constituents, representing more than 90% of the Rias Baixas tidal energy. The analysis of Figure 5.8 shows that hydrodynamic models reproduces with accuracy the amplitude and phase of the major harmonic constituents.

The maximum amplitude difference for M_2 is observed at VP station in Ria de Vigo, with a value of 1.06 centimetres. In stations AP and PP, the amplitude difference is 0.99 and 0.36 centimetres, respectively. The mean M_2 phase difference between datasets is 1.47°, which corresponds to less than 3 minutes difference between observed and simulated tidal wave phase. Regarding to S_2, the mean amplitude between observed data and model results is about 7.9 centimetres, while the phase difference is 3.83°, corresponding to 7.6 minutes.

Table 5.2 summarizes the statistical results of the hydrodynamic model validation at stations AP, PP and VP. These have the same order of magnitude than in calibration, indicating an excellent agreement between simulated and observed SSE (Dias et al., 2009). Therefore, the tidal wave propagation is well reproduced by the model, which is therefore suitable to study hydrodynamic processes in the Rias Baixas, but also to provide a good reproduction of physical dynamics, which governs the biogeochemical

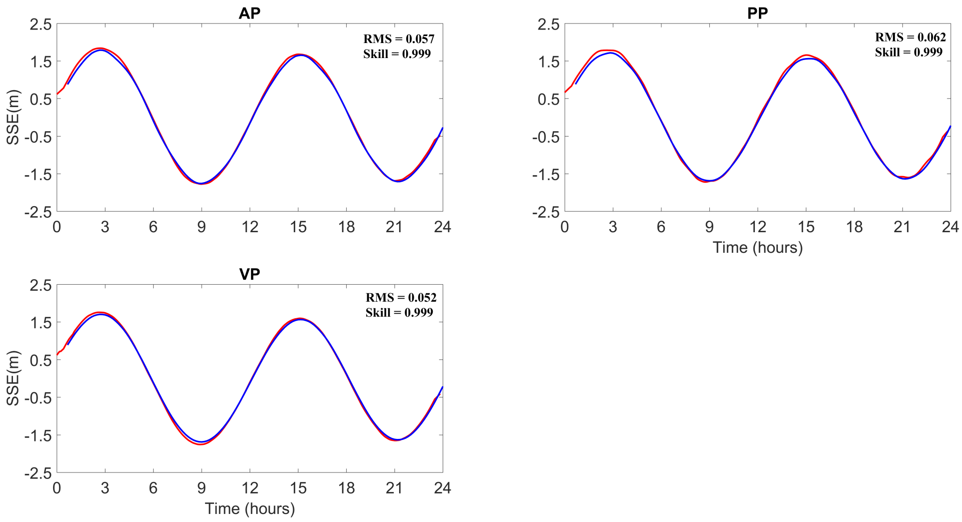

Figure 5.7: Comparison between simulated and observed Rias Baixas SSE time series in the frame of hydrodynamic calibration procedure (red line: data; blue line: model). Statistical results (RMS error and Skill) are also presented.

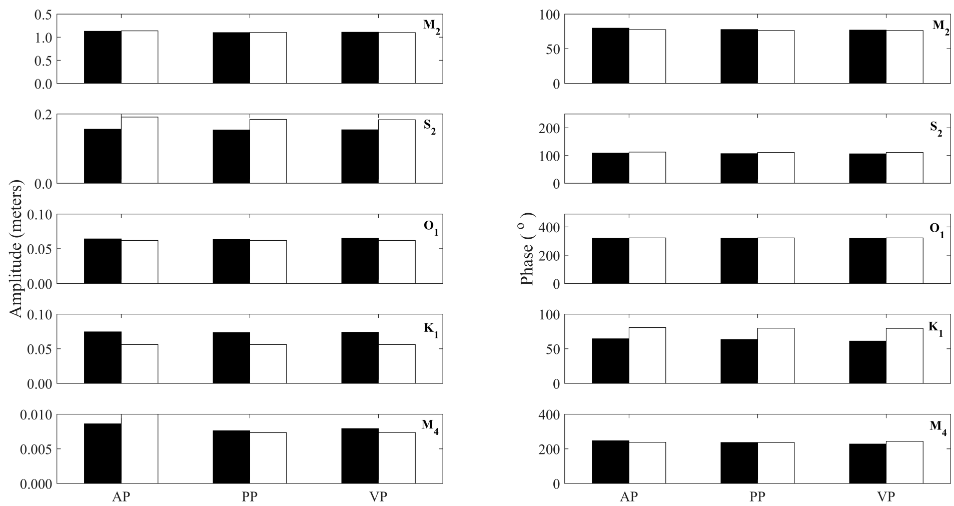

Figure 5.8: Comparison between simulated and observed Rias Baixas amplitude and phase for the major harmonic constituents. The black and white bars represent the observed and simulated values, respectively.

Table 5.2: Model accuracy in reproducing observed SSE as characterized by means of the RMS (m), Skill values and BIAS at AP, PP and VP stations.

Station	RMS (m)	Skill
AP	0.061	0.999
PP	0.056	0.999
VP	0.059	0.999

processes.

The results of this model configuration are similar to those found in previous implementations, such as Sousa (2013) and Des et al. (2019). Sousa (2013) obtained RMS errors for stations AP and VP of 0.06 and 0.05 m, respectively, while RMS errors of 0.05 m for stations PP and VP and 0.04 m for AP were computed by Des et al. (2019). Therefore the model application developed in this work reproduces accurately the hydrodynamic along Rias Baixas.

5.3.2 Water Quality Models Calibration and Validation

5.3.2.1 Ria de Aveiro

Following the methodology developed for the hydrodynamic model calibration, the water quality model was also calibrated comparing model simulations and observations for water temperature, salinity, pH and chlorophyll *a* concentration.

Comparison between simulated and measured water temperature (Figure 5.9) shows a very good agreement. The RMS errors are lower than 10% of mean local temperature in all stations, with a minimum for S5 station (about 3%). The RMS ranges between 5 and 6% of mean water temperature in stations S13, S21, S24 and S25, ranging between 7 and 8% in stations S9 and S11. Station S9, where less accurate results is depicted, is an upstream station, located in a narrow and shallow channel, where the heat fluxes are more challenging to model.

The discrepancies found may be due to uncertainties in river and ocean water temperatures imposed at the open boundaries. In the water temperature modelling several other variables can cause inaccuracies, as for example limitations in cloud cover variations (in this work was imposed a constant value, representing the mean value during the simulation periods). According to these results, the heat transport processes in Ria de Aveiro may be considered well reproduced by the model, resulting in accurate water temperature distribution predictions.

The comparison between simulated and measured salinity is depicted in Figure 5.10, showing an overall good agreement. The RMS errors are lower than 5% of the mean local salinity in all stations considered. These excellent results may be related with the period of sampling, as during summer the freshwater influence is minimum, leading to small salinity variations over time. Following these results, is assumed that the model accurately reproduces the salt transport along the lagoon. But is should be pointed out that in this case the validation procedure will be more important, in order to assess the model accuracy under different conditions.

Figure 5.11 shows the comparison between simulations and observations for chlorophyll *a* concentration (left side) and pH (right side). Due to data limitations, stations S5, S11 and S14 are the only with data available to calibrate these variables. The RMS error for S11 is 2.17 μg/L, corresponding to 35% of the mean local concentration. For S5, in Ílhavo channel, the RMS error is lower than 1.00 μg/L, representing an accuracy of 23%. Finally, for S14, the mean error is about 1.56 μg/L, which corresponds to an accuracy of 32%. As expected, the model deviations for primary productivity are higher than those obtained for water temperature and salinity, since there are some additional local processes, which are hard to predict, leading to model uncertainties. In detail, some processes are predicted with limitations or cannot be considered in the modelling efforts, such as: deficit estimation of the benthic and sediment processes; agriculture fields in the margins of the lagoon causing the water nutrient enrichment; invasive plant species modifying the productivity patterns as well as the light penetration in water column.

Regarding pH, the RMS errors are 0.15, 0.21 and 0.42 for S11, S5 and S14, corresponding to a 2, 3 and 5% of mean local pH. Therefore, the agreement between simulations and data can be considered excellent. Concerning to the comparison between simulated and observed dissolved oxygen concentration time series (Figure 5.12), the model is able to reproduce the tidal cycle, presenting RMS errors of 0.51, 1.37 and 0.35 mgL^{-1} for stations S5, S11 and S14, respectively. Due to the lack of more data available, this is the only comparison between observed and simulated dissolved oxygen concentration.

As mentioned in the methodology section, due to restrictions in data availability, the pH and chlorophyll *a* concentration were only validated by comparing the seasonal variability of the model simulations and *in situ* data.

The monthly comparisons between simulated and measured water temperature and salinity are presented in Figures 5.13 and 5.14. Figure 5.13 revealed a good agreement between predicted and measured water temperature. In general, validation results are better than those obtained in the calibration procedure. For Stations S2, S5 and S9 the error is 7% of the mean local water temperature, while a 6% error was found for station

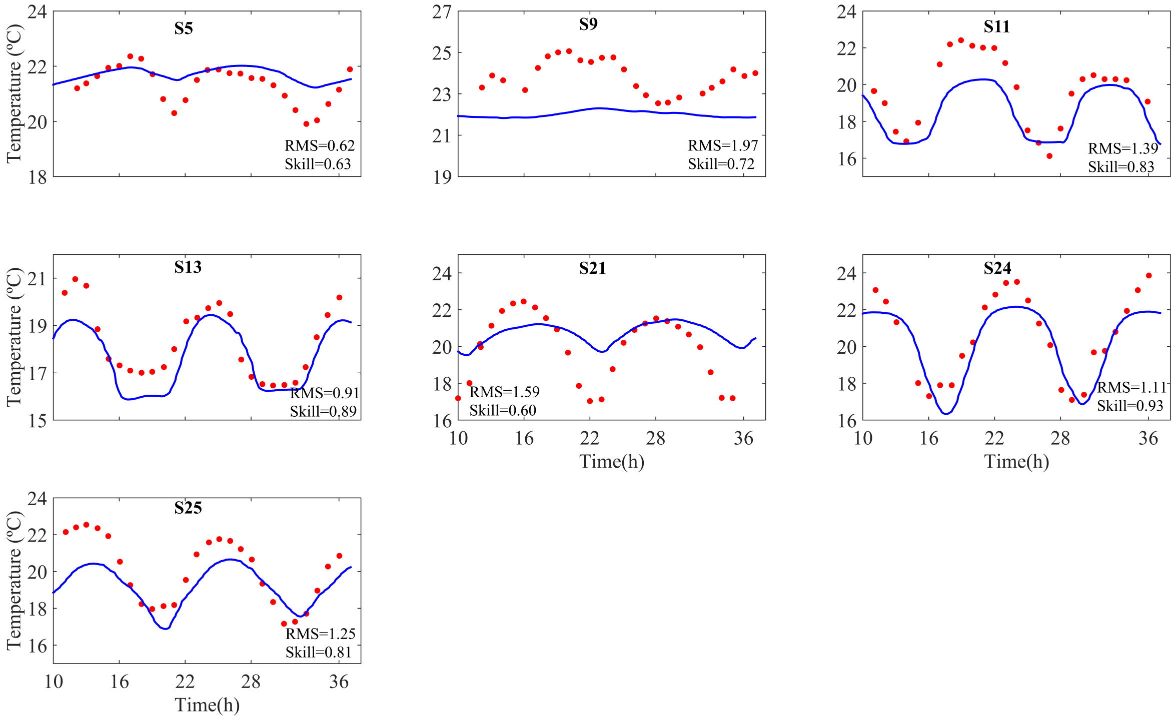

Figure 5.9: Comparison between simulated and observed Ria de Aveiro water temperature time series, in the frame of the water quality calibration procedure (red dots: data; blue line: model).Statistical results (RMS error (°C) and Skill) are also presented.

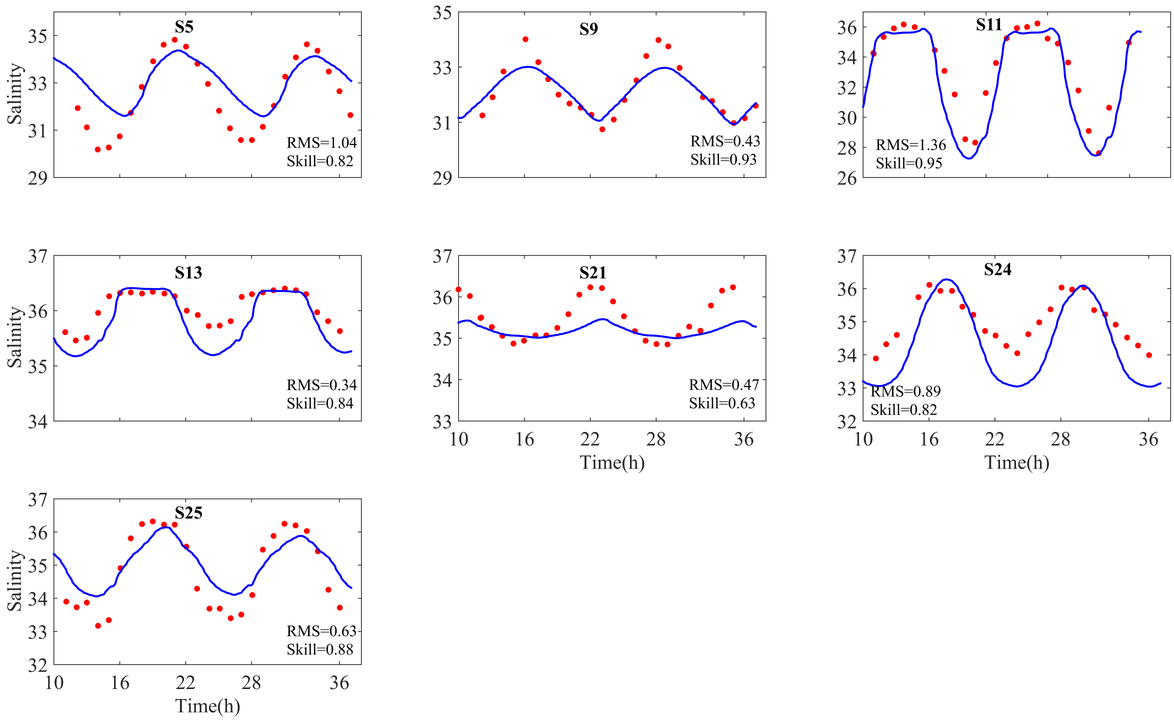

Figure 5.10: Comparison between simulated and observed Ria de Aveiro salinity time series, in the frame of the water quality calibration procedure (red dots: data; blue solid line: model). Statistical results (RMS error and Skill) are also presented.

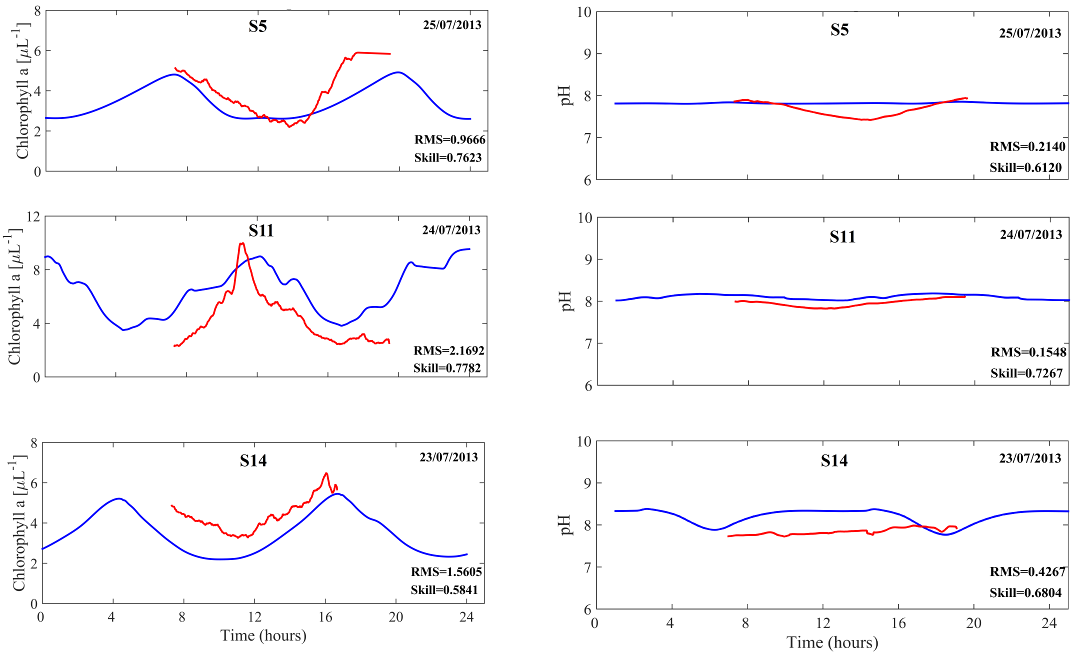

Figure 5.11: Comparison between simulated and observed Ria de Aveiro chlorophyll *a* concentration and pH time series, in the frame of the water quality calibration procedure (red line: data; blue line: model). Statistical results (RMS error and Skill) are also presented.

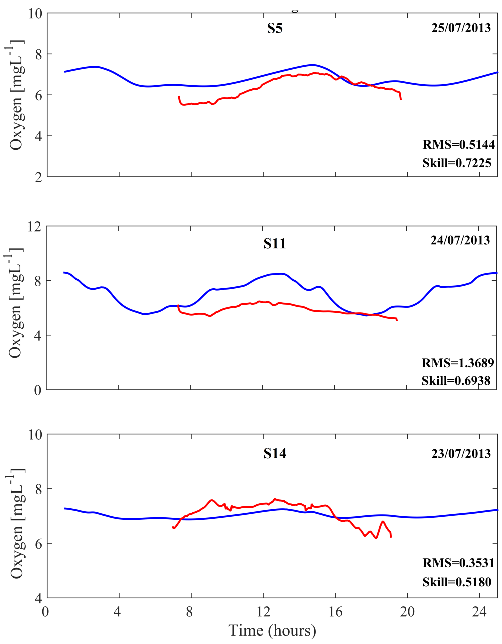

Figure 5.12: Comparison between simulated and observed Ria de Aveiro dissolved oxygen concentration time series, in the frame of the water quality calibration procedure (red line: data; blue line: model). Statistical results (RMS error (mg/L) and Skill) are also presented.

S10, which represents an excellent agreement between simulations and observations. In station S18 the agreement is considered very good, considering the RMS as 16% of the local mean water temperature. Those excellent results may be explained by the atmospheric forcing, which has a high temporal resolution (10 min).

Contrarily to the results obtained for water temperature model validation, the calibration results for salinity (Figure 5.14) are better than those obtained in validation. For stations S5 and S9 the RMS error is lower than 10% of the local mean salinity, with the salinity range accurately reproduced. For stations 2 and 10, the RMS errors range from 17% to 33%. The salinity temporal evolution is well represented by the model, but the mean value is lower than observed. The RMS error is higher than 50% of the local mean salinity for station S18. This station is located near the Vouga river, and therefore the salt transport in this region is strongly dependent on the imposed boundary conditions (freshwater inflow predictions), which an uncertainty associated.

Despite the inaccuracies described, they were in line with the best results from other model implementations for Ria de Aveiro (Dias and Lopes, 2006; Azevedo, 2018), and consequently the salt and heat transport models may be considered validated. Therefore, considering the main aims of this study, the numerical model was found to accurately reproduce the salt and heat transport processes in Ria de Aveiro.

Figures 5.15, 5.16, 5.17 and 5.18 compare the simulated and observed spatio-temporal variability of water temperature, salinity, chlorophyll *a* concentration and pH at selected locations along lagoon. Black dots correspond to observations, while in grey are depicted the daily simulated lower and upper limit values.

The analysis of Figures 5.15 to 5.18 shows that model reproduces the seasonal patterns as well as the mean values of all biotic and abiotic variables in this study. Specifically, it should be depicted that the simulations present the same patterns and mean values previously described for all variables. Nevertheless, the model performance is also quantitatively assessed based on different statistical measures in Figure 5.19.

Regarding the RMS error, all the variables present values lower than 15% of local amplitude. The skill accuracy for water temperature, salinity and chlorophyll *a* ranges between good and excellent. For pH, the skill results are less accurate due to the absence of a typical temporal pattern, making difficult to assess the quality of temporal predictions evolution.

The Nash Sutcliffe Model Efficiency ranges from good to excellent for water temperature, salinity and chlorophyll *a* concentration. The pH predictions have lower accuracy as this variable has low seasonal changes, and its pattern is not as well defined as for the other variables, leading to the decrease of model efficiency. The model bias shows a trend to slightly overestimate salinity (positive results). Regarding to chlorophyll *a*

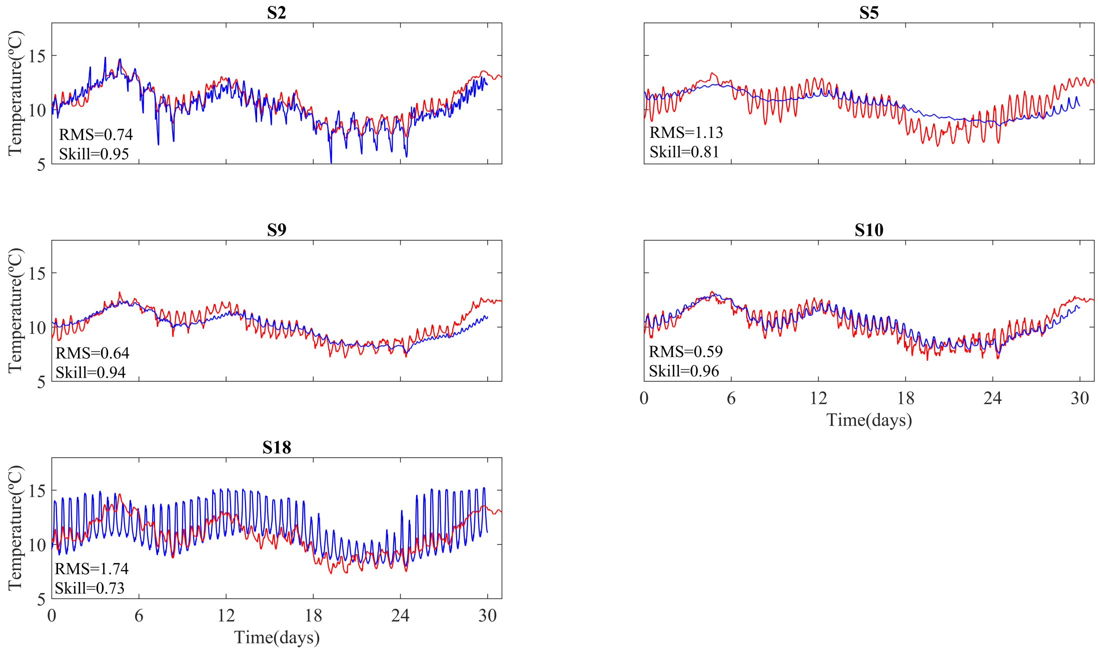

Figure 5.13: Comparison between simulated and observed Ria de Aveiro water temperature time series, in the frame of the water quality validation procedure (red line: data; blue line: model). Statistical results (RMS error (°C) and Skill) are also presented.

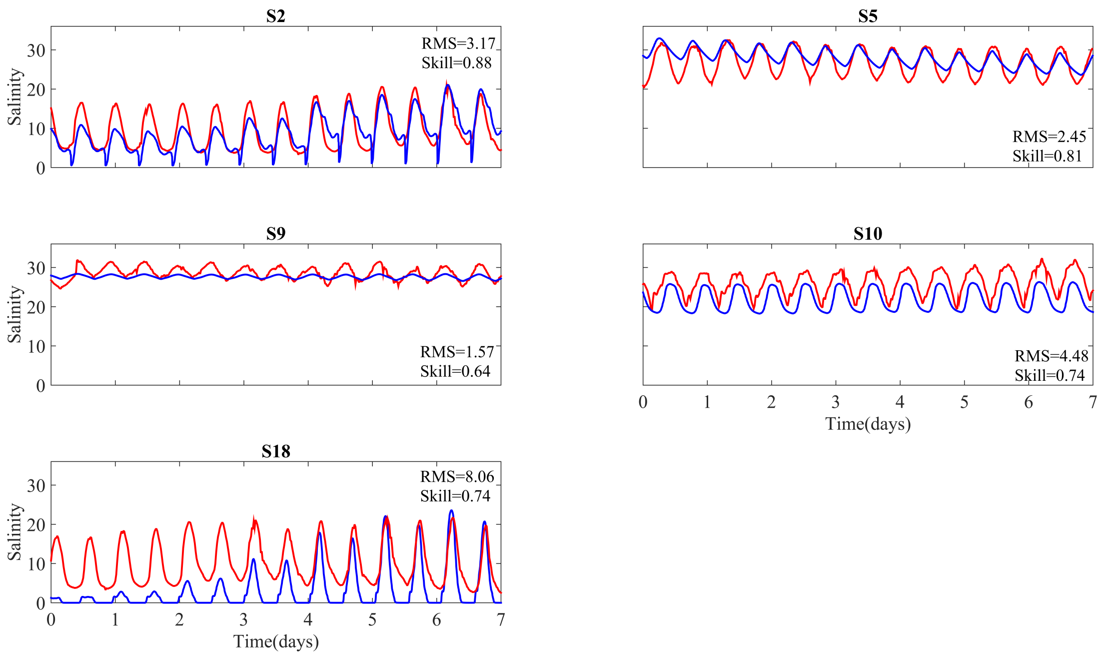

Figure 5.14: Comparison between simulated and observed salinity Ria de Aveiro time series, in the frame of the water quality validation procedure (red line: data; blue line: model). Statistical results (RMS error and Skill) are also presented.

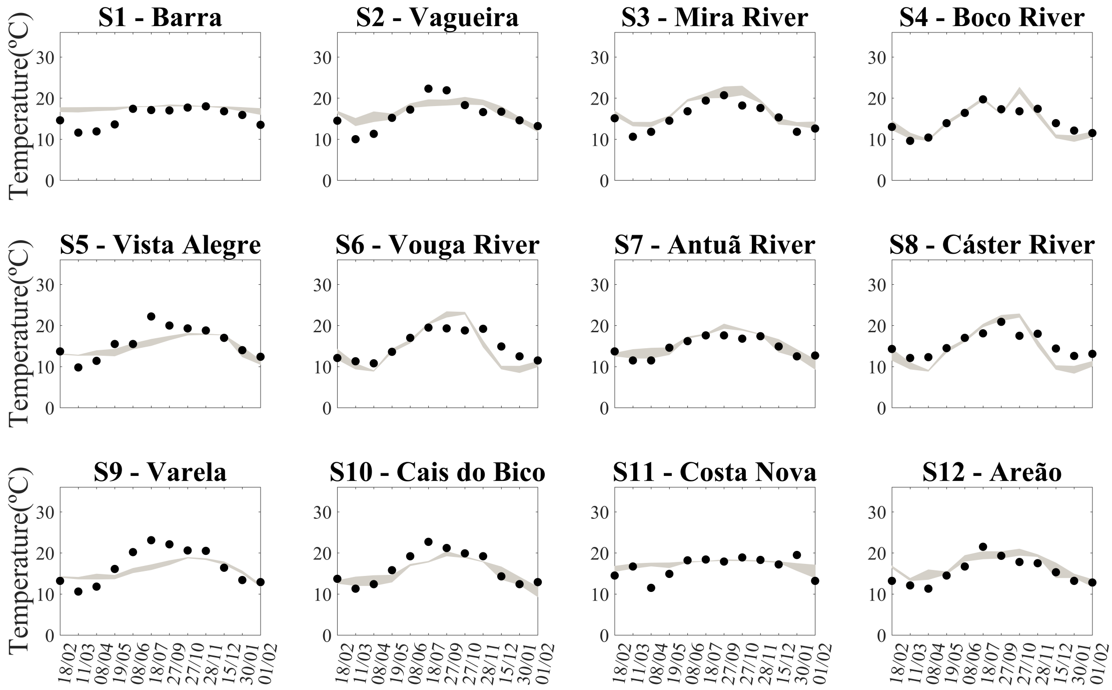

Figure 5.15: Annual evolution of simulated (grey line) and observed (points) Ria de Aveiro water temperature at different lagoon stations.

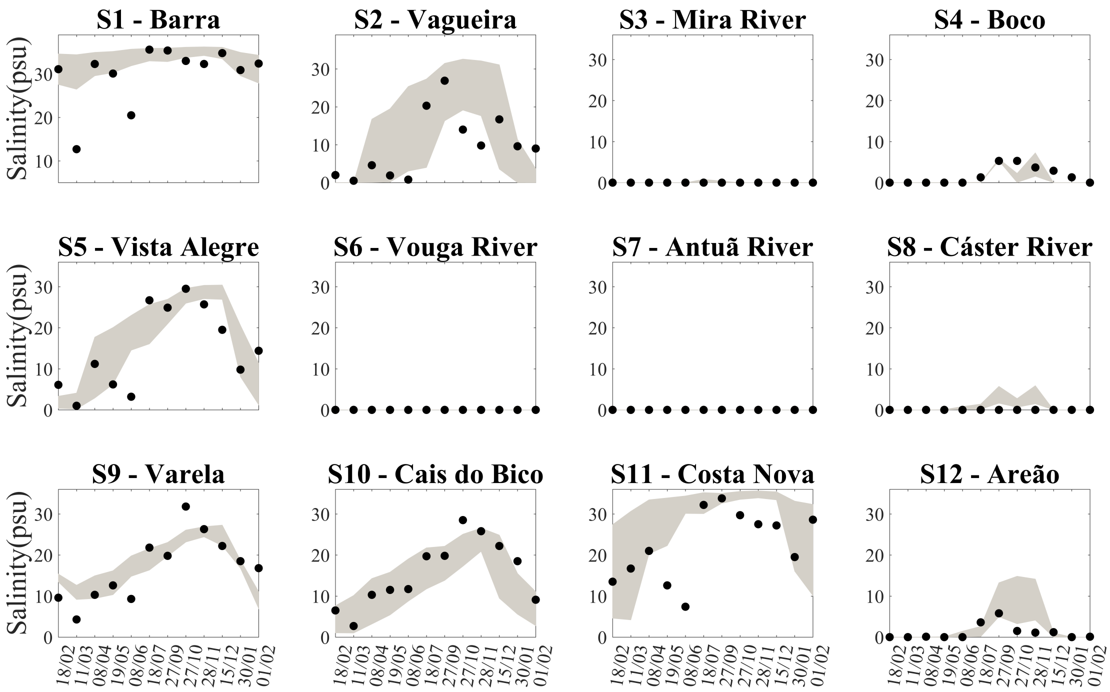

Figure 5.16: Annual evolution of simulated (grey line) and observed (points) Ria de Aveiro salinity at different lagoon stations.

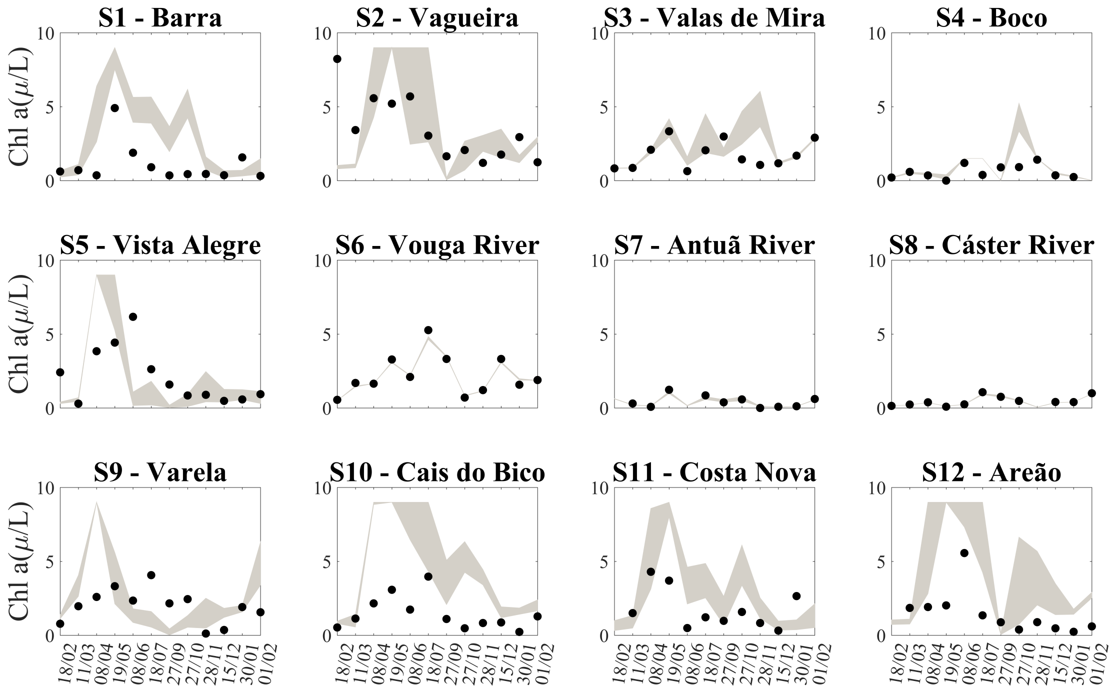

Figure 5.17: Annual evolution of simulated (grey line) and observed (points) Ria de Aveiro chlorophyll *a* concentration at different lagoon stations.

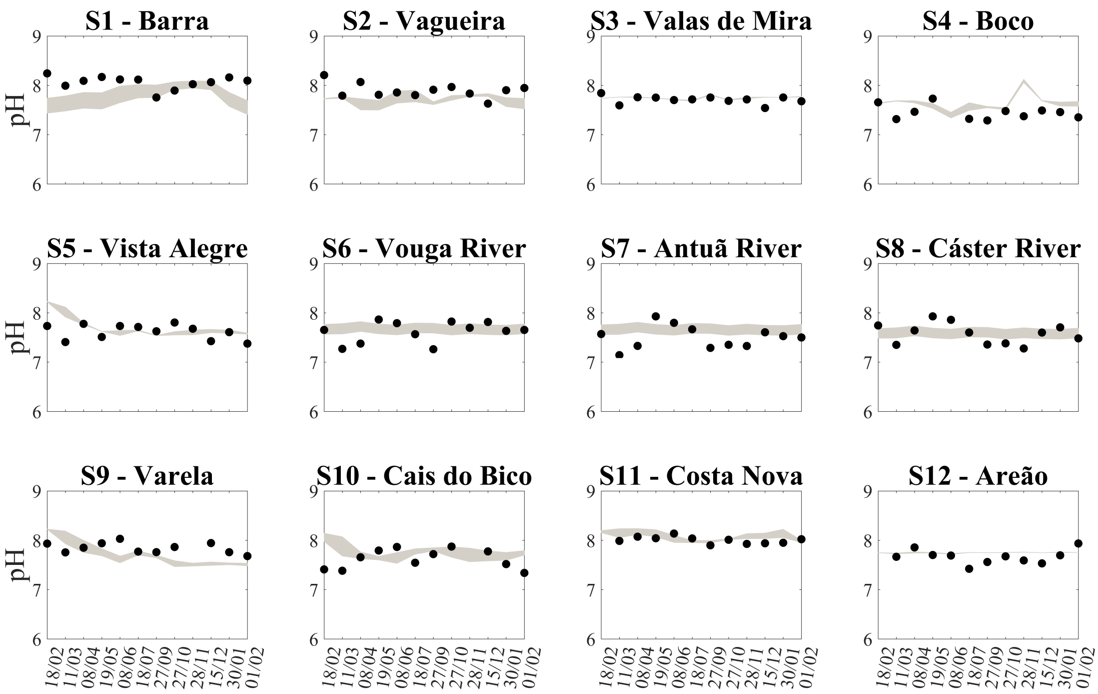

Figure 5.18: Annual evolution of simulated (grey line) and observed (points) Ria de Aveiro pH at different lagoon stations.

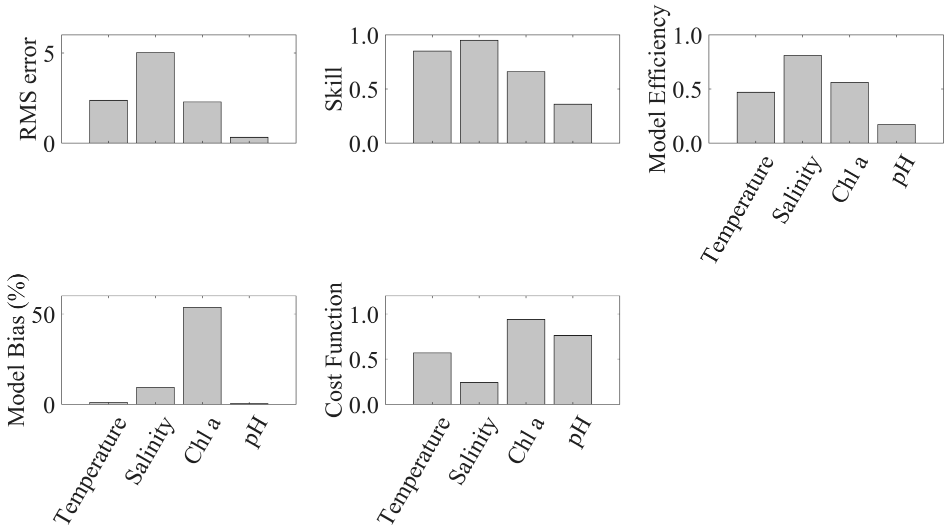

Figure 5.19: Model performance summary statistics, for Ria de Aveiro.

concentration, the overestimation is very well marked leading to low accurate results. The cost function reveals a very good fit between simulations and data, for all variables in analysis.

A summary of basic model data fit metrics (following Allen et al. (2007)) for the time-based dynamics of water temperature, salinity, phytoplankton and pH reveals that the model reproduces with accuracy all variables in study. It also indicates that model performance slightly deteriorates from salinity and water temperature to chlorophyll *a* concentration and finally to pH. However, all evaluated variables reached good to excellent results, showing that the model performs well in capturing the temporal dynamics along Ria de Aveiro's lagoon. Henceforward, this application of Delft3D hydrodynamic and water quality models can be used as a tool to achieve the objectives proposed in this study.

5.3.2.2 Rias Baixas

As mentioned in the methodology section, Rias Baixas water quality model was calibrated comparing observations and model simulations of time series and vertical profiles for water temperature, salinity, dissolved oxygen, pH and chlorophyll *a* concentration.

Figure 5.20 represents the time series comparison between the simulated and measured surface water temperature at MM, AM1, AM2, VM1 and VM2 stations. The results depicted show a good agreement between simulations and observations, revealing RMS errors lower than 10% of the mean temperature for all stations. Stations MM, VM1, VM2 and AM2 present errors lower than 8% (6.5%, 3.7%, 5.5% and 7.2%, re-

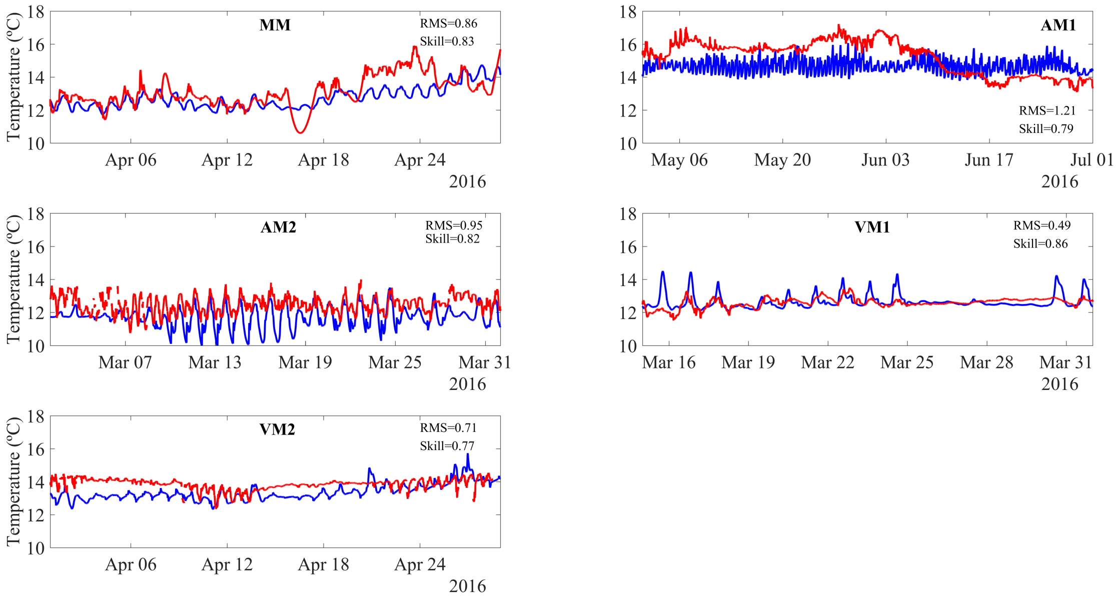

Figure 5.20: Comparison between simulated and observed Rias Baixas surface water temperature time series, in the frame of the water quality calibration procedure (red line: data; blue line: model). Statistical results (RMS error (°C) and Skill) are also presented.

spectively). Although within the range considered "excellent", the RMS error in AM1 is 8.1% of the mean local water temperature. The small discrepancies found may be due to uncertainties imposing river water temperatures at the boundary. Here, due to data limitations, the source of rivers water temperature is not *in situ* data or model predictions, but typical values for the season are considered.

The comparison between simulated and measured surface salinity is depicted in Figure 5.21. In general, the calibration results show a good agreement between simulations and measurements. The RMS errors in the four stations analysed is below 1. The MM station, in Ria de Muros, presents the better salinity reproduction with a mean error of 0.35, which corresponds to 0.98% of the local mean salinity, followed by VM1, AM1 and VM2 stations with relative errors of 2.67%, 1.91% and 2.87%, respectively. The good results achieved in this calibration procedure are certainly related with the good temporal resolution of the freshwater inflow data imposed in the model.

Figure 5.22 represents the comparison between simulated and observed water chlorophyll *a* concentration time series for stations AM1 and VM1. As expectable, this variable is a very challenging to model, and therefore the model accuracy is lower comparing to that obtained for water temperature and salinity. However, RMS errors of 0.27 and 1.42 μgL^{-1} were obtained in stations AM1 and VM1, respectively.

Despite the good model reproduction for surface temperature and salinity, it should be pointed out that the vertical processes are also very important to reproduce. In

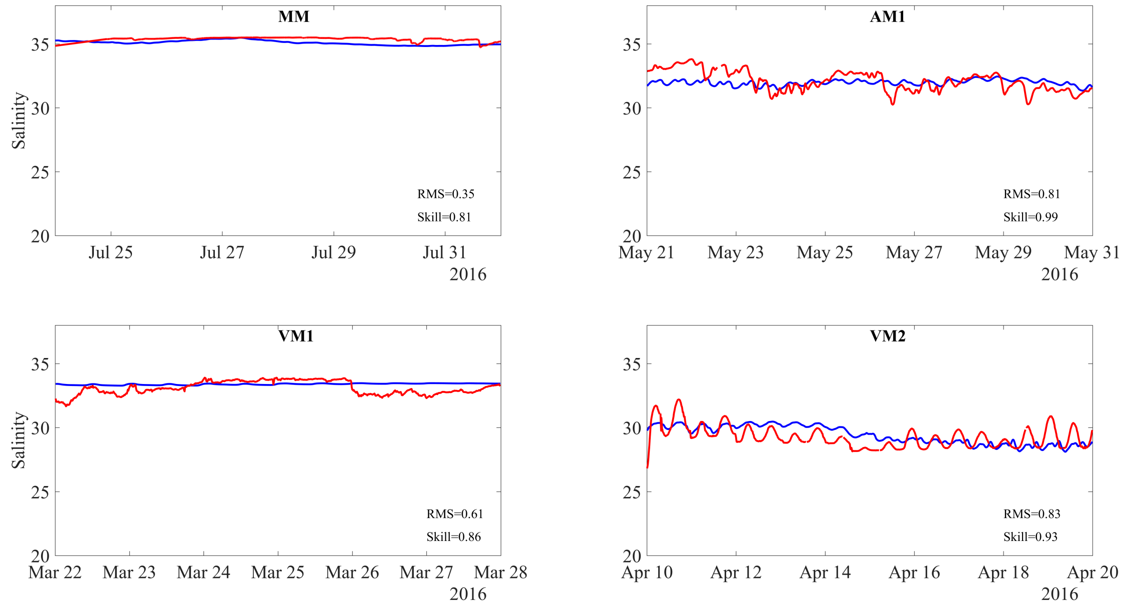

Figure 5.21: Comparison between predicted and observed Rias Baixas surface salinity time series, in the frame of the water quality calibration procedure (red line: data; blue line: model). Statistical results (RMS error and Skill) are also presented.

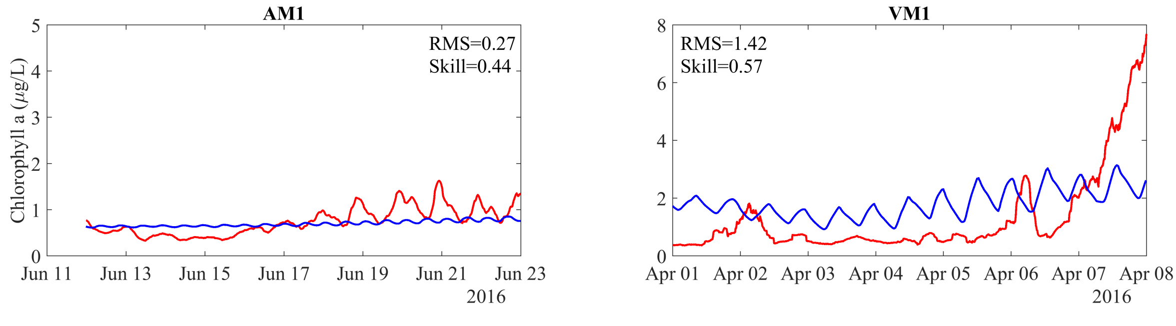

Figure 5.22: Comparison between simulated and observed Rias Baixas surface chlorophyll a concentration time series, in the frame of the water quality calibration procedure (red line: data; blue line: model). Statistical results (RMS error (μg/L) and Skill) are also presented.

Figures 5.23 and 5.24 are represented the simulated and measured water temperature and salinity vertical profiles for particular dates (March 21st and 22nd). In general, Figure 5.23 shows that model slightly overestimates water temperature measurements (positive Bias) at stations V1, P1, P2, A1, A2, M1, M2 and M3, nonetheless the upper layer thermodynamics and vertical stratification of thermohaline properties are well reproduced by the model. RMS errors between model simulations and measurements ranges from 0.1°C in P3 station to 0.7°C in V3, revealing a very good agreement between data and model simulations. Regarding the salinity profiles (Figure 5.24), small differences were observed for stations close to the inlets (stations with index 1), increasing towards the estuaries heads. Nonetheless, the highest RMS error is 1.81 (in station V3), which corresponds to an error lower than 6% of the mean salinity values. In station M1, where the lowest RMS is depicted, the relative error is lower than 0.75% of the local mean salinity. Therefore, results suggest that model adequately reproduces the salinity vertical structure, including the halocline characteristics of Rias Baixas. This implementation has average SSE, water temperature and salinity errors with the same order of magnitude of those obtained by Sousa (2013) and Des et al. (2019). The mean RMS errors for water temperature and salinity are 0.38° C and 0.63, respectively. Des et al. (2019) computed a mean RMS error of 0.74°C for water temperature and 0.68 for salinity. Additionally, Sousa (2013) obtained a mean RMS error of 0.36 comparing the vertical profiles of simulated and observed salinity.

The comparison between predicted and measured dissolved oxygen concentration profiles (Figure 5.25) reveals that the model tends to slightly underestimate the measurements (negatives BIAS at stations V1, V2, P2, P3, A1, M1 and M2), in which the mean BIAS deviation is -0.058 mgL^{-1}. RMS error ranges from 0.33 at station M3 and 0.92 mgL^{-1} at station P2, which is considered a good agreement between measurements and predictions, since dissolved oxygen is a fairly difficult variable to predict because there are many processes driven its concentration, such as the discretization of the model open boundaries, primary production and respiration processes. Since there is no significant vertical variation of pH (Figure 5.26), this variable is less challenging to model because is extremely dependent on the inputs of alkalinity and total inorganic carbon. Nevertheless, the statistical results evidences a model overestimation of pH, with a mean RMS error of 0.21.

As performed for Ria de Aveiro, the model ability to reproduce the seasonal variability was used to validate the water quality model. Therefore, model simulations of water temperature (Figure 5.27), salinity (Figure 5.28), dissolved oxygen concentration (Figure 5.29) and pH (Figure 5.30), for surface and bottom layers were compared with data provided by Intecmar. Additionally, the model performance is also quantitatively

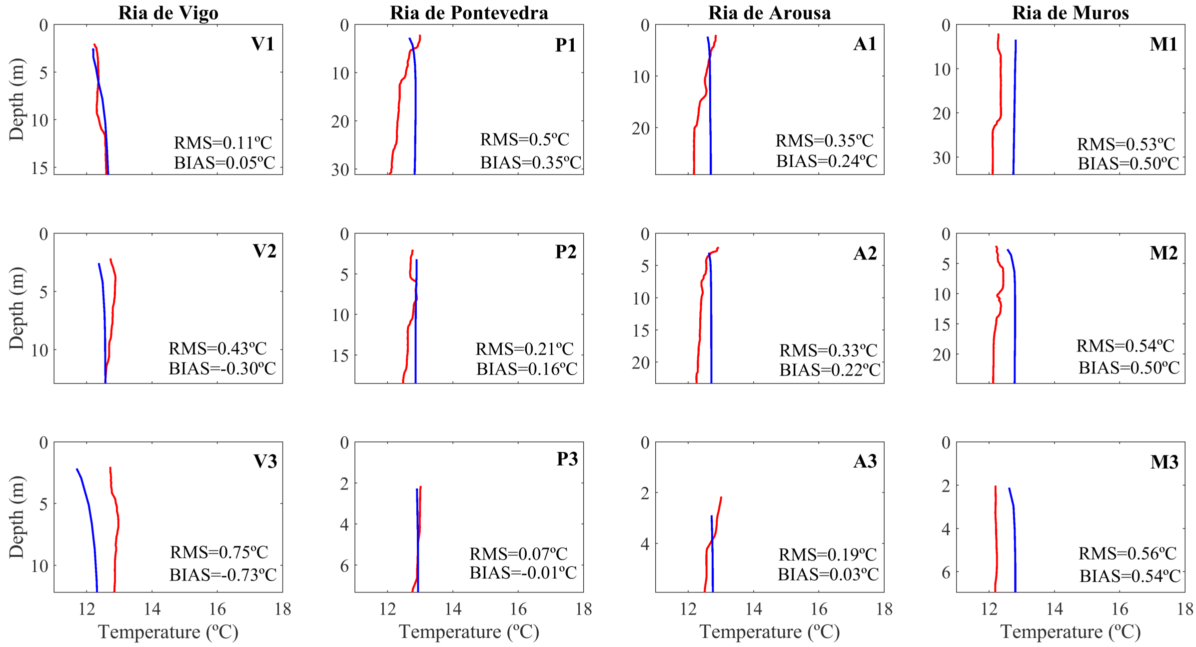

Figure 5.23: Simulated Rias Baixas water temperature profiles comparison with Intecmar profiles (`http://www.intecmar.gal/`), for 2016 (red line: data; blue line: model). Statistical results (RMS error (°C) and Bias (°C)) are also presented.

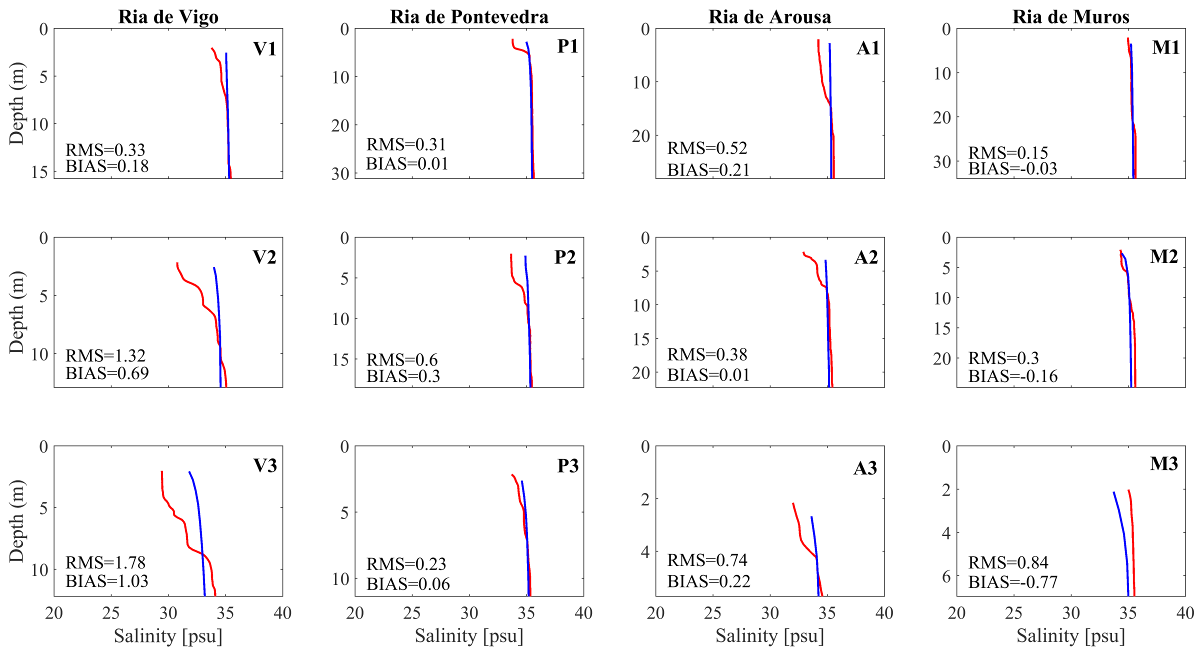

Figure 5.24: Simulated Rias Baixas salinity profiles comparison with Intecmar profiles (`http://www.intecmar.gal/`), for 2016 (red line: data; blue line: model). Statistical results (RMS error and Bias) are also presented.

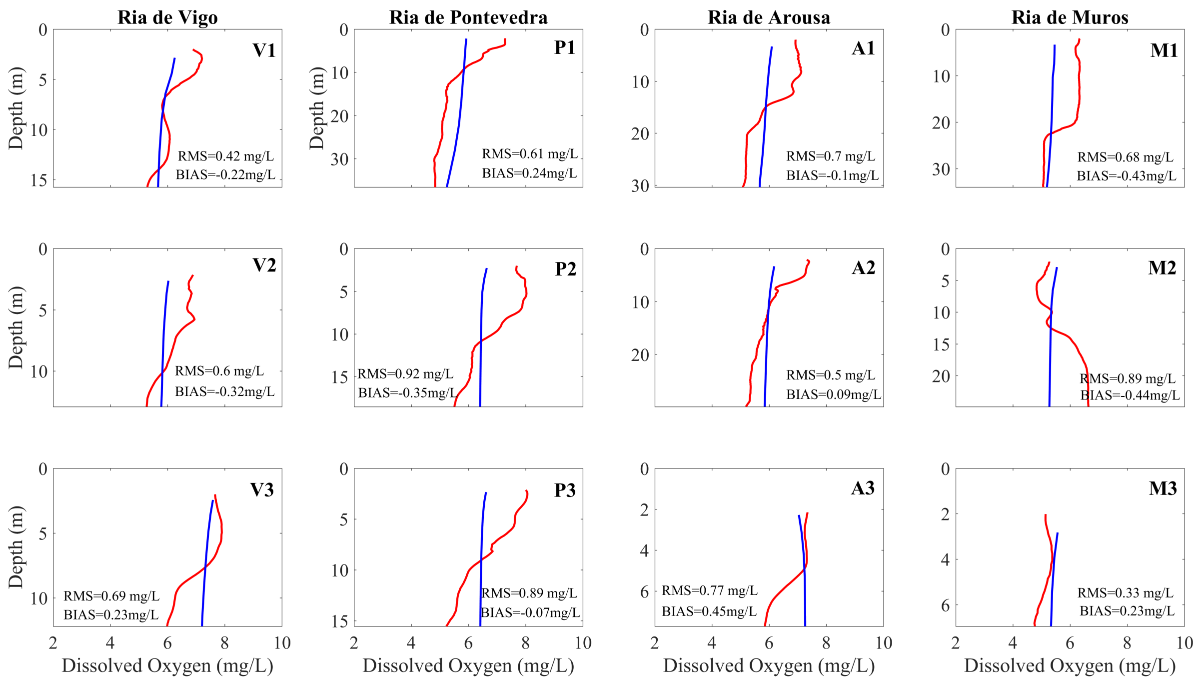

Figure 5.25: Simulated Rias Baixas dissolved oxygen profiles comparison with Intecmar profiles (`http://www.intecmar.gal/`), for 2016 (red line: data; blue line: model). Statistical results (RMS error (mg/L) and BIAS (mg/L)) are also presented.

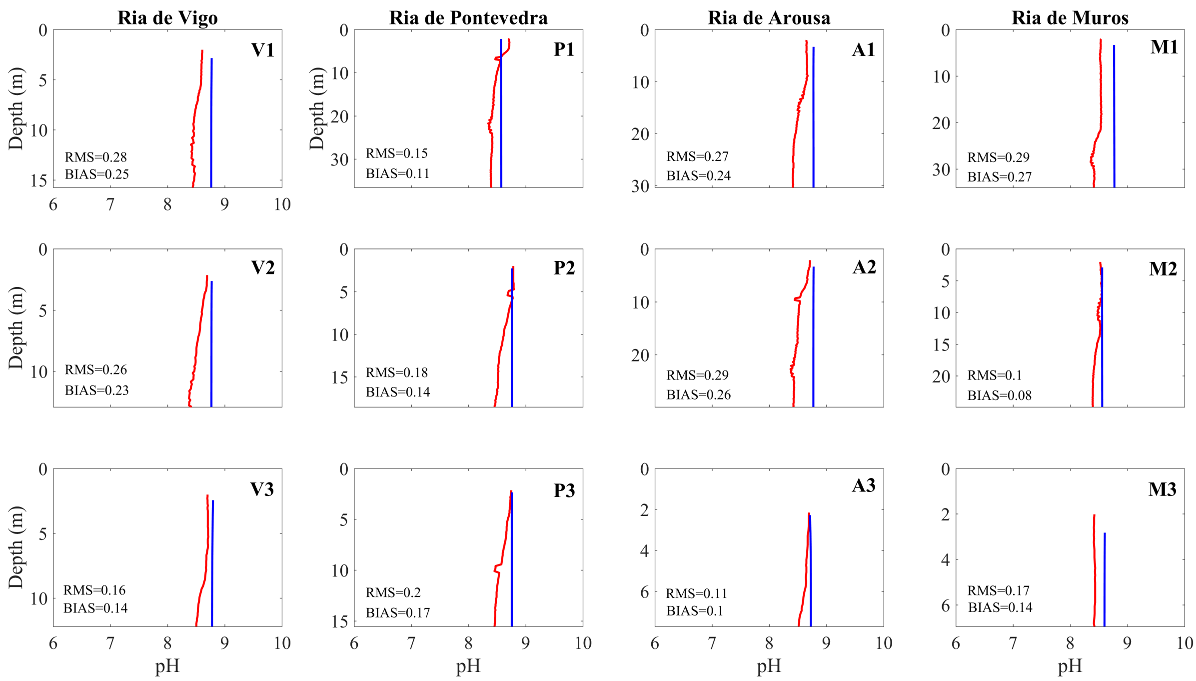

Figure 5.26: Simulated Rias Baixas pH profiles comparison with Intecmar profiles (`http://www.intecmar.gal/`), for 2016 (red line: data; blue line: model). Statistical results (RMS error and BIAS) are also presented.

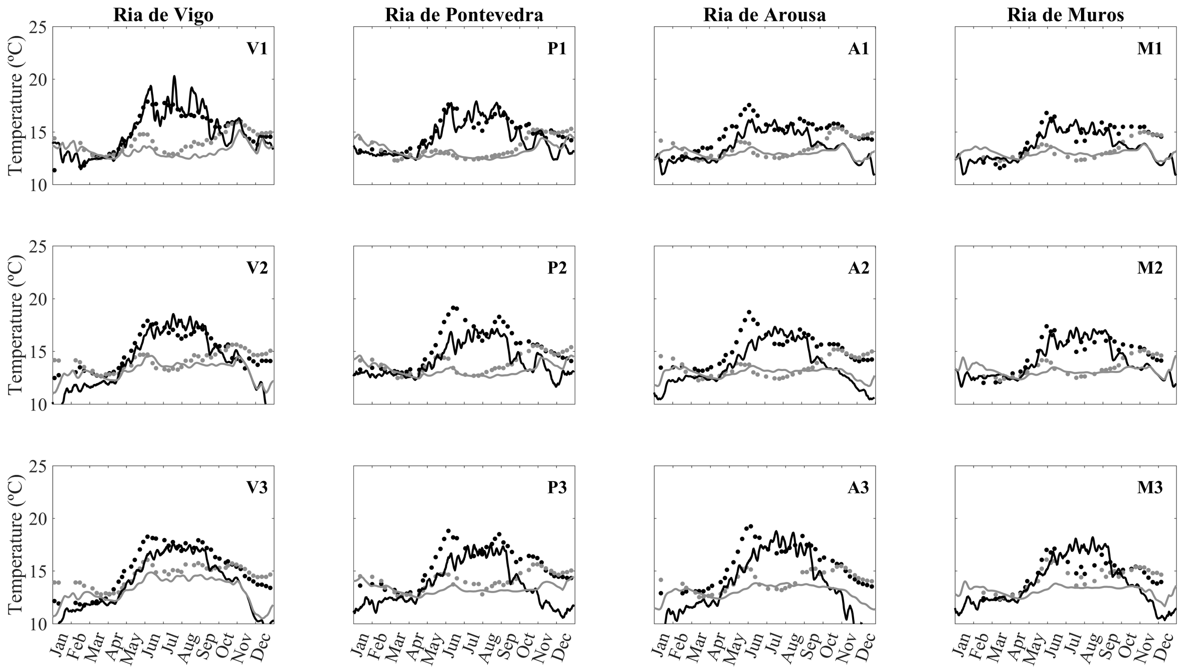

Figure 5.27: Annual evolution of simulated (lines) and observed (points) surface (black) and bottom (gray) water temperature at different Rias Baixas stations.

assessed based on different statistical measurements. Table 5.3 shows the statistical results of the comparison between simulated and observed spatio-temporal variability of surface and bottom water temperature and salinity at selected locations along Rias Baixas.

Analysis of Figures 5.27, 5.28, 5.29, 5.30, summarized in Table 5.3, shows that model reproduces the mean values and the seasonal patterns of water temperature, salinity, dissolved oxygen and pH. RMS errors present values lower than 15% of the local mean value, for all variables. Regarding to water temperature, the mean RMS is 1.6°C at the surface and 1.09°C at the bottom. The model presents a tendency to underestimate the measurements (5.9% at the surface and 5.5% at the bottom), which is considered excellent under Allen et al. (2007) criterion. The errors in the surface salinity prediction are slightly higher. The average RMS error at the surface is below 2.5, with the exception of station V3. However, the model reproduce inaccurately the low surface salinity due to high rainfall events and/or high freshwater inflow, which was concentrated in the thin surface layer. In the bottom, the mean RMS error is at the same order of magnitude (0.44) than those obtained in the remaining stations. As expected, the model reproduces better the thermohaline processes in oceanic stations (stations with index 1). The water temperature and salinity predictions reached good to excellent agreement, showing that the model performs well in capturing the temporal dynamics along Rias Baixas.

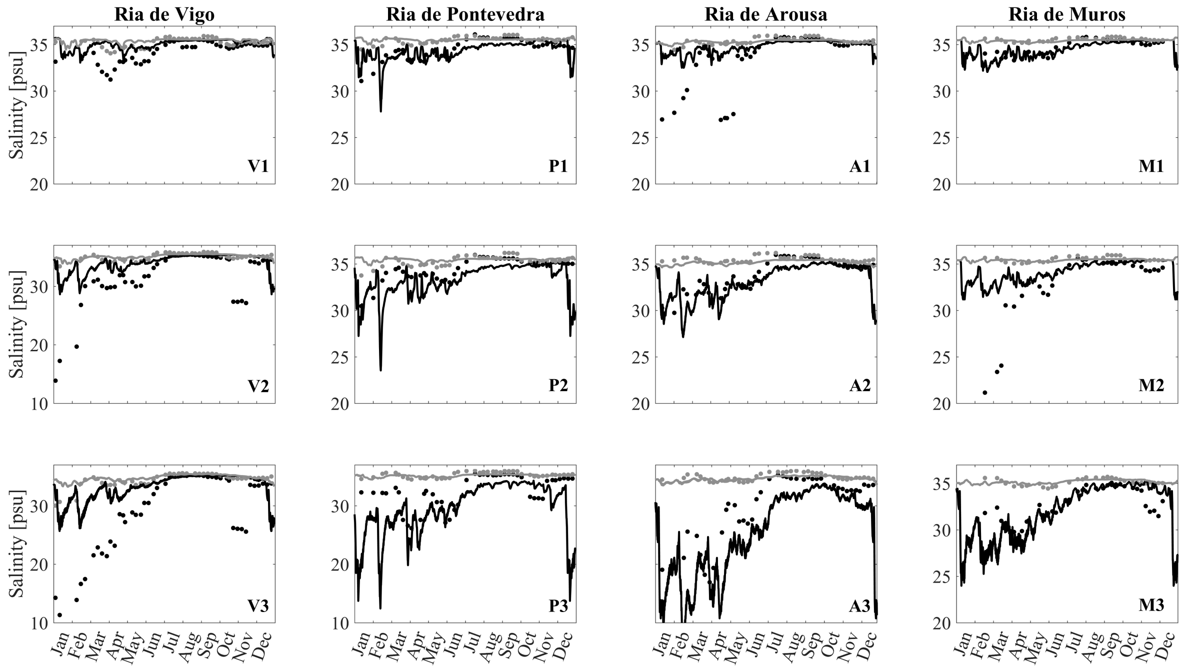

Figure 5.28: Annual evolution of simulated (lines) and observed (points) surface (black) and bottom (gray) salinity at different Rias Baixas stations.

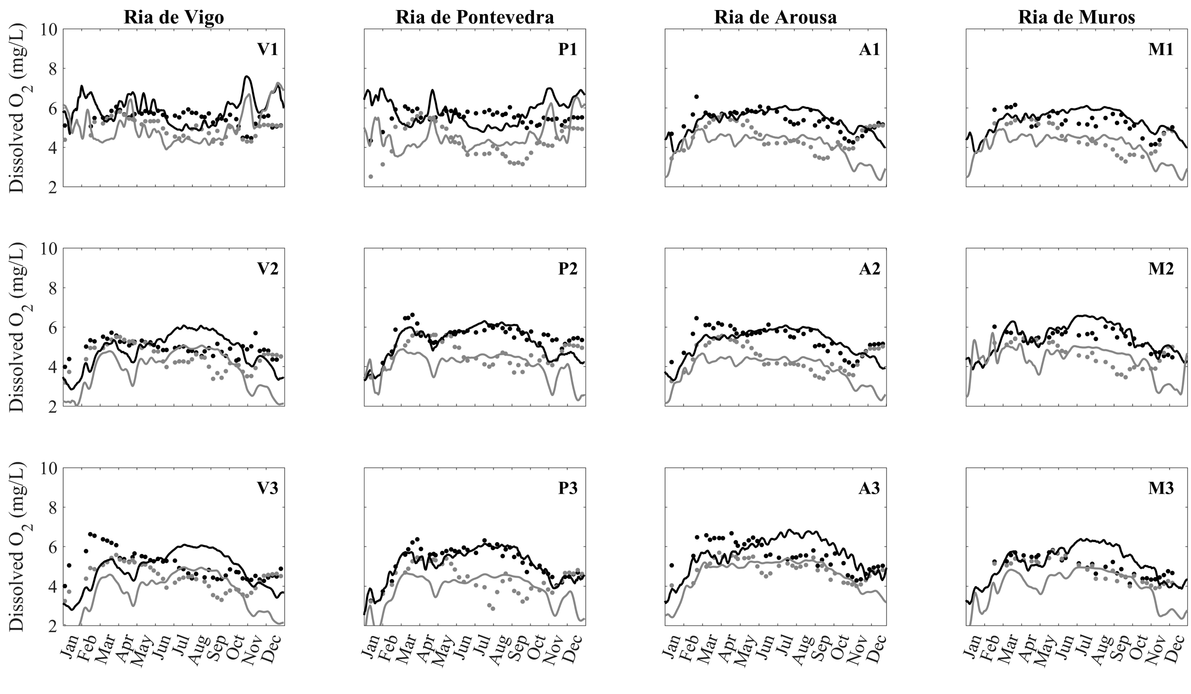

Figure 5.29: Annual evolution of simulated (lines) and observed (points) surface (black) and bottom (gray) dissolved oxygen at different Rias Baixas stations.

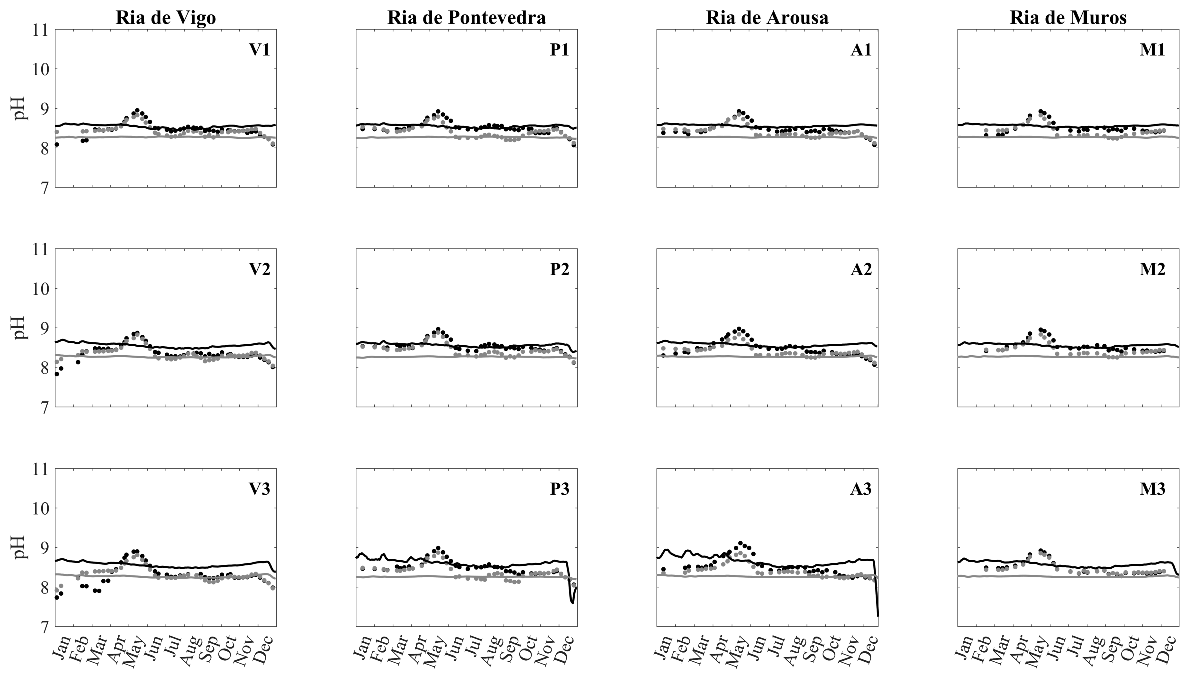

Figure 5.30: Annual evolution of simulated (lines) and observed (points) surface (black) and bottom (gray) pH at different Rias Baixas stations.

Figure 5.29 shows that the model reproduces the differences in dissolved oxygen concentration between the surface and the bottom, as well as the seasonal variability of this variable. The statistical results prove that the model reproduces the seasonal mean values and the seasonal variations. In detail, the mean RMS errors are 0.8 mgL^{-1} and 1.0 mgL^{-1} at the surface and bottom, respectively. The maximum RMS error is depicted at the surface at station M1 (1.55 mgL^{-1}). The Bias analysis reveals that the model tends to overestimate dissolved oxygen concentration in the oceanic stations (the mean Bias on these locations is 0.49 mgL^{-1} at the surface and 0.22 mgL^{-1} at the bottom). The mean Bias in riverine stations (V3, P3, A3 and M3) is 0.08 mgL^{-1} and -0.45 mgL^{-1} at surface and bottom, respectively.

Regarding to pH (Figure 5.30), the model reproduces the mean value as well as the vertical gradient. However, it was unable to reproduce the spring peak which occurs at all stations. Excepting this punctual inaccuracy, the model reproduces horizontal and vertical patterns of pH, depicting mean RMS errors of 0.22 and 0.21 at surface and bottom, respectively. The Bias analysis suggests that the model overestimates the pH at the surface (mean Bias of 0.10) and underestimates in the bottom (mean Bias of 0.14).

The model performance is also quantitatively evaluated based on different statistical measures in Figure 5.31, as performed in Ria de Aveiro water quality model validation procedure. Maximum RMS errors are observed in surface salinity and in surface and

Table 5.3: Model accuracy in reproducing seasonal variability of measured water temperature(°C), salinity, dissolved oxygen (mg/L) and pH as characterized by the Bias and the RMS calculated at 12 stations along Rias Baixas.

Station	**Temperature**		**Salinity**		**DO**		**pH**	
	RMS	**Bias**	**RMS**	**Bias**	**RMS**	**Bias**	**RMS**	**Bias**
V1 – Surface	0.96	-0.01	1.33	0.92	1.05	0.47	0.27	0.07
V1 – Bottom	1.07	-0.86	0.50	0.27	0.93	0.08	0.21	-0.16
V2 – Surface	1.51	-0.79	5.00	2.61	0.84	-0.03	0.29	0.19
V2 – Bottom	1.44	-0.96	0.51	0.12	1.19	-0.54	0.18	-0.08
V3 – Surface	1.71	-1.39	6.96	4.29	1.10	-0.14	0.38	0.26
V3 – Bottom	1.51	-1.32	1.05	0.38	1.27	-0.67	0.19	-0.05
P1 – Surface	1.10	-0.51	0.90	-0.31	0.93	0.25	0.16	0.04
P1 – Bottom	0.73	-0.33	0.36	0.02	0.94	0.24	0.20	-0.13
P2 – Surface	1.67	-1.29	1.84	-1.23	0.53	-0.23	0.15	0.03
P2 – Bottom	0.95	-0.67	0.50	0.14	1.06	-0.60	0.23	-0.17
P3 – Surface	2.18	-1.79	4.86	-2.78	0.36	-0.08	0.21	0.10
P3 – Bottom	1.06	-0.81	0.41	-0.16	1.02	-0.41	0.21	-0.12
A1 – Surface	1.53	-1.31	2.72	1.19	0.49	0.03	0.19	0.09
A1 – Bottom	1.10	-0.63	0.33	-0.05	1.05	-0.49	0.21	-0.14
A2 – Surface	1.93	-1.46	1.42	-0.76	0.59	-0.09	0.23	0.09
A2 – Bottom	1.26	-0.62	0.43	-0.33	1.02	-0.54	0.20	-0.14
A3 – Surface	2.44	-1.85	5.23	-3.98	0.86	0.17	0.27	0.14
A3 – Bottom	1.44	-1.04	0.56	-0.28	0.55	-0.15	0.22	-0.13
M1 – Surface	1.63	0.39	0.52	-0.14	1.55	1.23	0.17	0.03
M1 – Bottom	0.80	-0.27	0.21	-0.13	1.45	1.03	0.22	-0.16
M2 – Surface	1.17	-0.43	3.18	1.47	0.54	0.28	0.16	0.01
M2 – Bottom	0.94	-0.48	0.25	-0.09	0.96	0.28	0.22	-0.17
M3 – Surface	1.60	-0.41	1.64	-0.14	0.80	0.38	0.19	0.10
M3 – Bottom	1.54	-1.59	0.27	0.08	0.88	-0.58	0.24	-0.20

bottom water temperature. These variables presents higher RMS errors because they have higher seasonal variability comparing with DO and pH. The skill accuracy for water temperature, salinity and pH ranges between good and very good, while for DO, the temporal predictions evolution are represented with less accuracy.

The Nash Sutcliffe Model Efficiency ranges from good (surface DO) and excellent (surface water temperature, surface and bottom salinity and bottom DO). The results at bottom water temperature, and surface and bottom pH are considered very good according to Allen et al. (2007) criteria. As already analysed in the previous chapters, the model shows a trend underestimate water temperature. The cost function reveals a very good agreement between simulations and data for all variables in analysis.

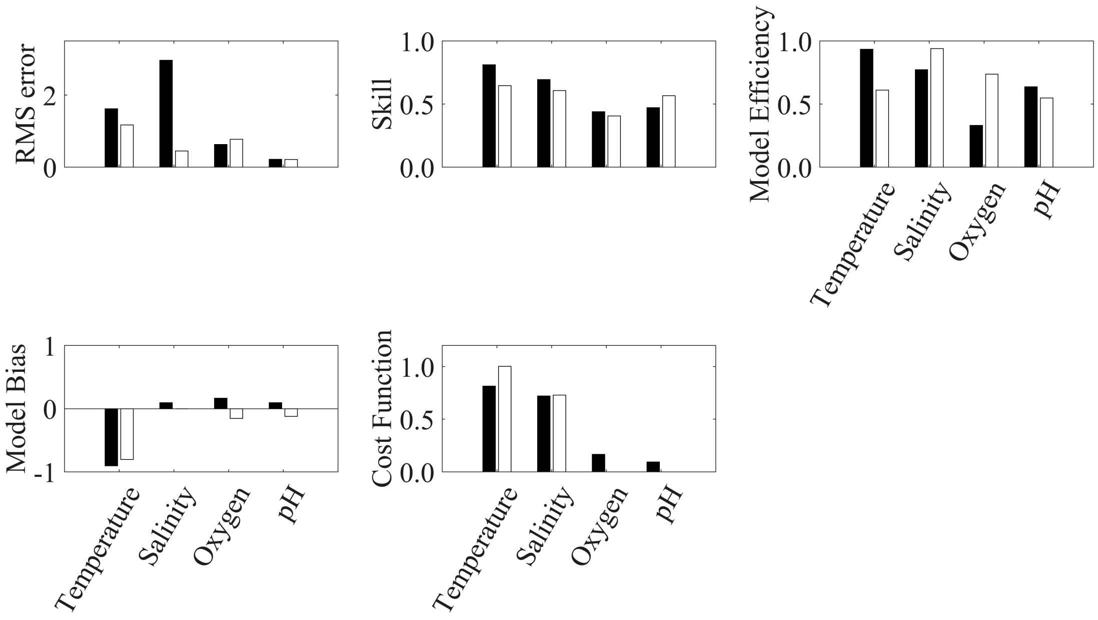

Figure 5.31: Model performance summary statistics, for Rias Baixas. The black and white bars represent the statistical results for surface and bottom, respectively.

5.4 Conclusions

The present chapter aimed to present the implementation, calibration and validation of the coupled circulation and biogeochemical models for Ria de Aveiro and Rias Baixas, which was successfully achieved. Here, two different modelling approaches were followed: 2-D finite element model with an unstructured grid for Ria de Aveiro, and 3-D finite difference discretisation model for Rias Baixas. Results indicate:

- A very good agreement between simulated and measured SSE for both coastal systems, revealing that model accurately reproduces tidal processes;

- Ria de Aveiro salt and heat transport are well described due to the high spatial resolution provided by the numerical grid and high temporal resolution of the atmospheric data imposed;

- The reproduction of the biogeochemical processes in Ria de Aveiro revealed to be a very challenging and demanding task. Despite all the constraints, an integrated model accounting for the coupled biogeochemical renovation processes and fluxes of carbon and macro-nutrients along the shallow tidally-dominated Ria de Aveiro lagoon has been developed;

- The Ria de Aveiro model spatial and temporal resolution assures good conditions to represent the seasonal variability, but also the short-term transient forcing triggered by tides, freshwater inflows and atmospheric processes, providing a detailed representation of the hydrodynamic and transport processes along a topographically-complex system;

- Regarding Rias Baixas, vertical profiles show a good agreement between simulated and measured water temperature, salinity, oxygen and pH, revealing the model accuracy to reproduce the upper layer thermodynamics and vertical stratification, but also the oxygen and pH horizontal and vertical processes;

- In general, for both coastal systems, the highest errors in water temperature were found during summer, while for salinity, DO and pH they occur during winter, due to the rivers impact in the coastal systems.

Additionally, the achievement of the objectives proposed in this chapter (i.e. the implementation of the models) was the longest and most complicated task of this thesis, showing that water quality modelling is a very demanding challenge, since the properties to be simulated strongly depend on each other and on several environmental factors, such as tidal propagation, rivers inflow, nutrients loads, water-air interaction and trophic processes. Despite these difficulties, the modelling tools here presented have been successfully developed and implemented for the first time in Ria de Aveiro and Rias Baixas.

Notwithstanding, in next chapters these model configurations will be used to study physical, chemical and biological characteristics of the study areas, in order to achieve the main goal of this work: identifying preferential sites to ensure aquaculture expansion.

Chapter 6

New Insights About the Primary Production Dependence on Biotic and Abiotic Factors: Ria de Aveiro Case Study

6.1 Introduction

Although the Ria de Aveiro hydrodynamics is tidally dominated (Dias et al., 1999), the significant volume of freshwater usually flowing into the lagoon during the wet seasons, particularly during rainy years, leads to unpredicted seasonal variations of water temperature and salinity, but also nutrient and phytoplankton communities abundance and activity. The complex mixing between salt and fresh waters turns essential to better understand the seasonal local dynamic and interactions between biotic and abiotic variables. The study of water temperature, salinity, pH and chlorophyll a concentration is crucial, since they are key environmental variables which influence several other water properties and biogeochemical processes in Ria de Aveiro lagoon, such as the phytoplankton communities spatial and temporal variability.

The water temperature is an important physical variable since it plays an important role in the chemical and biological processes, as the degradation rates of organic and inorganic matter, bacterial activity and metabolic rates of phytoplankton communities. According to Dias et al. (2009), beyond the major influence of seasonal variations of the radiative fluxes, short-term tidal influence determines both horizontal and vertical water temperature profiles.

Regarding salinity distribution, the head of the Ria de Aveiro channels is generally characterized by riverine input and low salinity, and therefore typical longitudinal estuarine salinity gradients characterize each of the main lagoon channels. In summer, under low freshwater inflow, salt water propagates further upstream and oceanic saline water is found at the extreme ends of the lagoon, and the main lagoon channels are mostly filled with high saline water (Dias et al., 2001; Vaz and Dias, 2008).

The longitudinal chlorophyll *a* concentration and pH gradients are not so well defined as for water temperature and salinity. These variables are ruled, not only by oceanic, river and atmosphere inputs, but also by local processes. The distribution of phytoplankton communities in the lagoon evidences maximum biomasses located between the second half of the lagoon channels and their heads. Contrarily, the minimum values are observed at the lower channels. A strong gradient is found in the central areas of the lagoon, characterizing the transition between the oceanic and fluvial influence zones (Lopes et al., 2005, 2015).

As result of the aforementioned reasons, the Ria de Aveiro lagoon was extensively studied under biological and chemical perspectives, sometimes supported in primary modelling tools (section 1.3.1). However, according to the revision of the state of the art performed in section 1.3.1, there is still a lack of information about the main limiting abiotic factors affecting the growth and mortality of planktonic microalgae, which are actually one of the major issues that need to be clarified. Additionally, there are severe limitations on the knowledge about the biomass distribution dependence on river's freshwater inflow and on Atlantic Ocean salt water propagation.

At an international level, these topics are being researched using advanced water quality numerical models, that are effective tools to evaluate nutrients and phytoplankton communities dynamics. For example, Jiang and Xia (2018) used a hydrodynamic-biogeochemical model to understand the nutrient and phytoplankton variability in the Chesapeake Bay outflow plume and the dominant environmental drivers, concluding that the plume is mostly nitrogen-limited because of the relatively low estuarine DIN export. Pesce et al. (2018) assessed the climate change impacts on nutrients and primary production in the Zero river basin in Italy. Their results suggest that the ecological impact of modified loads and warmer temperatures will likely increase the frequency of eutrophication events in summer, with higher peaks of phytoplanktonic biomass, and modifications in the phytoplankton composition. Béjaoui et al. (2017) developed a 3-D coupled physical-biogeochemical model in order to understand and quantitatively assess the hydrobiological functioning and nutrients budget in the Bizerte Lagoon (Tunisia). The authors found that primary production is co-limited by phosphorus and nitrogen and is highest in the inner part of the lagoon, due to the combined effects of high-water residence time and high nutrient inputs from the boundary.

In this context, the objective of this chapter is to apply the last generation water quality model developed to characterize and assess the temporal and spatial evolution of water temperature, salinity, pH and chlorophyll *a* concentration in the Ria de Aveiro (Chapters 4 and 5), aiming to bring new insights on primary production dependence on biotic and abiotic factors. An innovative approach to analyse and interpret the variations of abiotic conditions and primary production in lagoon ecosystems is therefore used, integrating analysis of *in situ* data and numerical model simulations of local biophysics. The data collection was carried out during 1 year in 12 stations distributed through the main channels, including the connection with the 6 lagoon boundaries (ocean and 5 rivers).

6.2 Methodology

This study comprises two different approaches to evaluate the variations of biotic and abiotic conditions and primary production in Ria de Aveiro: analysis of *in situ* data resulting from local monitoring and of numerical model simulations of local biophysics.

6.2.1 Sampling

Water samples were collected monthly from February 2016 to February 2017, except in August due to logistic difficulties, in 12 stations strategically located along the main lagoon channels (black dots of Figure 6.1). These sampling locations were chosen considering their very distinct characteristics, such as tidal/river influence, freshwater inflow, rate of sediment resuspension and phytoplankton biomass. Therefore, they represent different hydrological, hydrodynamic and biological conditions, assuring an adequate spatial coverage of the lagoon. The precise location of the sampling stations is depicted in Table 6.1, and their respective pictures is showed in Figure 6.2. The field monitoring was performed during morning period, from to 8 am to 13 pm of 01/02/2016, 18/02, 11/03, 08/04, 19/05, 08/06, 18/07, 27/09, 27/10, 28/11, 15/12 and 30/01/2017, during ebb tidal conditions.

The samples were taken, stored in plastic bottles and kept in the dark, and refrigerated until their analysis in the laboratory. Simultaneously, water temperature, salinity and pH were measured *in situ* in each station, with the equipment HQ40D Portable Multi Meter pH meter, thermometer, conductivity meter, salinometer, with an uncertainty error of 0.1 units for temperature, salinity, pH and conductivity.

Chlorophyll *a* concentration was measured by extraction with aqueous acetone and quantified spectrophotometrycally. The detailed description about the procedure to perform pigment extraction is presented along this section. In the laboratory, the filtration of each water sample was carried out using a vacuum filtration device, which

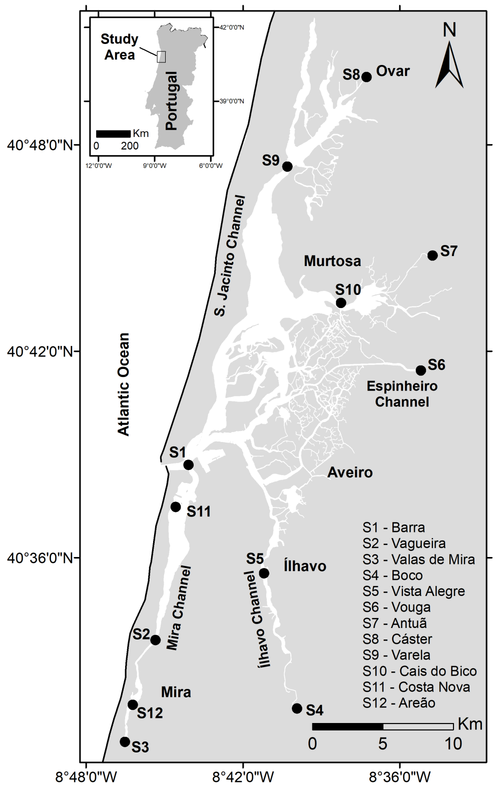

Figure 6.1: Map of Ria de Aveiro lagoon, showing the sampling stations.

Table 6.1: Location of the sampling stations.

Station	**Coordinates**
Station 1 – Barra	40.6460°N, 8.7340°W
Station 2 – Vagueira	40.5603°N; 8.7577°W
Station 3 – Valas de Mira	40.4891°N; 8.7859°W
Station 4 – Boco river	40.5336°N; 8.6669°W
Station 5 – Vista Alegre	40.5881°N; 8.6860°W
Station 6 – Vouga river	40.6730°N; 8.5605°W
Station 7 – Antuã river	40.7491°N; 8.5704°W
Station 8 – Cáster river	40.8479°N; 8.6340°W
Station 9 – Varela	40.7890°N; 8.6718°W
Station 10 – Cais do Bico	40.7286°N; 8.6485°W
Station 11 – Costa Nova	40.6198°N; 8.7488°W
Station 12 – Areão	40.5208°N; 8.7760°W

(A) Station 1 - Barra
(B) Station 2 - Vagueira
(C) Station 3 - Valas de Mira
(D) Station 4 - Boco river
(E) Station 5 - Vista Alegre
(F) Station 6 - Vouga river
(G) Station 7 - Antuã river
(H) Station 8 - Cáster river
(I) Station 9 - Varela
(J) Station 10 - Cais do Bico
(K) Station 11 - Costa Nova
(L) Station 12 - Areão

Figure 6.2: Location of the selected sampling stations.

comprises an air pump, a filter holder with clamp and two erlenmeyers. In order to retain the pigments present in the water samples, glass microfibres filters of 1.2 μm particle retention were used. At this point, let the filters dry out properly revealed to be very important, in order to avoid pigment losses.

Then, the filters were rolled up, transferred to 15 mL tubes and flash freezed using liquid nitrogen. The solvent used as extractor agent was acetone aqueous solution of 90%, which was added to the tubes containing the filters, depending on the number of filters used in the filtering process. The number of filters depended on the amount of particles present in the water samples. When just one filter was used, 4 mL of acetone was added; using two filters, 6 mL of acetone was added; using 3 filters, 8 mL of acetone was needed. Immediately after adding the acetone, the frozen filters were crashed using a glass rod and stored in dark environment at 4°C overnight.

The samples were centrifuged (centrifuge 5804R, Eppendorf) the day after, at 4000 rotations per minute during 10 minutes at 4°C of temperature. After this process, 2 mL of the centrifuged samples were transferred to Eppendorf tubes and stored in a box filled with ice, while the Spectronic GENESYS 6 UV-Visible spectrophotometer was being prepared.

Then, the samples were transferred one by one to optical glass cuvettes and introduced in spectrophotometer, where the absorbances at 630 nm, 647 nm, 664 nm and 750 nm were measured. At the highest wavelength measured (750 nm), the light is no longer absorbed, therefore this wavelength was used as reference. Additionally, the blank sample was composed by 2 mL of 90% acetone.

Following the method applied by Salonen and Sarvala (1995), the chlorophyll *a* concentration is calculated with and without acidification. So, after finishing the measurement of the 12 samples, 12 μL of HCl (0.5M) were added to each sample, and the reading absorbances procedure was repeated. This method is crucial since the samples contain other pigments than chlorophyll *a*, which is determined by the acidification of the regular samples, and re-reading the absorbances at 664 nm and 750 nm. Chlorophyll *a* pigment mainly absorbs radiation between 650 and 700 nm (red) and between 400 and 450 nm (blue) bands of spectrum, therefore the expectable absorption peak is at 664 nm (Consalvey et al., 2005).

So, chlorophyll *a* concentration was measured according to Lorenzen (1967) method, given by:

$$Chl\ a(\mu g/L) = \frac{(AK((A_{664} - A_{750}) - (A_{664\mathrm{a}} - A_{750\mathrm{a}}))\upsilon_a}{V_l L} \tag{6.1}$$

where A is the absorption coefficient of chlorophyll (11.4 g cmL^{-1}), K is the factor to equate the reduction in absorbance to initial chlorophyll concentration (2.25), A_{664} and A_{750} are the sample absorbances at 664 and 750 nm, respectively; A_{664a} and A_{750a} are the samples absorbances at 664 and 750 nm after acidification; V_l is the volume of filtered water; υ_a is the acetone volume used for extraction (mL); L is the path length of the cuvette (1 cm). More details about all the chlorophyll measurement methodology can be found at Lorenzen (1967).

6.2.2 Models Exploitation

Simulations were performed for 18 months (August 1st, 2015 to February 1st, 2017), comprising the period of sampling surveys. The first six months were used for the spin-up of the water quality model. The models configurations, boundaries conditions and the processes and substances selected in the water quality model are as described in Chapter 5. Time series of oxygen concentration, nutrients and growth of phytoplankton as a function of water temperature, were depicted in order to discuss the limiting factors influencing the growth and mortality of plankton communities. Additionally, in order to achieve the complete knowledge about the dynamics of the variables under study their spatial variability (horizontal fields of water temperature, salinity and chlorophyll *a* concentration) is also analyzed from model predictions.

6.3 Results and Discussion

6.3.1 Temporal and spatial evolution of estuarine water temperature, salinity, pH and chlorophyll *a*

In general, water temperature and salinity showed a clear seasonal trend characterized by high temperatures and salinities in summer, a progressive decrease during autumn and early winter due to the decrease of solar radiation and increase of rainfall events, and a renewal in late winter, when heat fluxes return to positive and dry season begins.

Regarding water temperature (Figure 6.3), the minimum value recorded was 9.6°C in S4 (Boco river), observed during late winter (February 18^{th}), while a maximum value of 23.1°C was recorded in June 8^{th} at S9 (Varela, at S. Jacinto channel). The average water temperature during the study period was 15.6°C. The middle areas of the lagoon, namely stations S2, S5, S9 and S10, are more susceptible to larger water temperature ranges, i.e., higher temperatures in summer and lower in winter, because these areas presents low current velocities and high residence time, making them more susceptible to oscillations in heat fluxes, resulting in high heating or cooling, depending on the season. On the other hand, the annual variability is lower in the stations closer to the ocean and river boundaries. The temperature in these stations is ruled by the ocean and river water temperatures, which are less dependent on the heating processes.

Salinity time series, presented in Figure 6.4, show a typical estuarine spatial and temporal pattern, presenting a longitudinal gradient from the river boundaries (stations S3, S4, S6, S7 and S8) to the ocean (S1), with values ranging from 0 to 36. In intermediate stations, such as S2, S5, S9, S10, S11 and S12, salinity fluctuates according to the hydrological conditions of each period. Salinity in these stations is driven by the freshwater discharge and rainfall seasonality, while in S1 salinity ranges between 28 and 34, except in the 2^{nd} and 5^{th} field surveys, when extreme rainfall events took place. In riverine stations (S3, S6, S7 and S8), saline intrusion is not observed. Regarding the temporal variability, salinity exhibited the expected pattern, with higher salinities recorded during the summer period. This highlights the major role of tidal intrusion

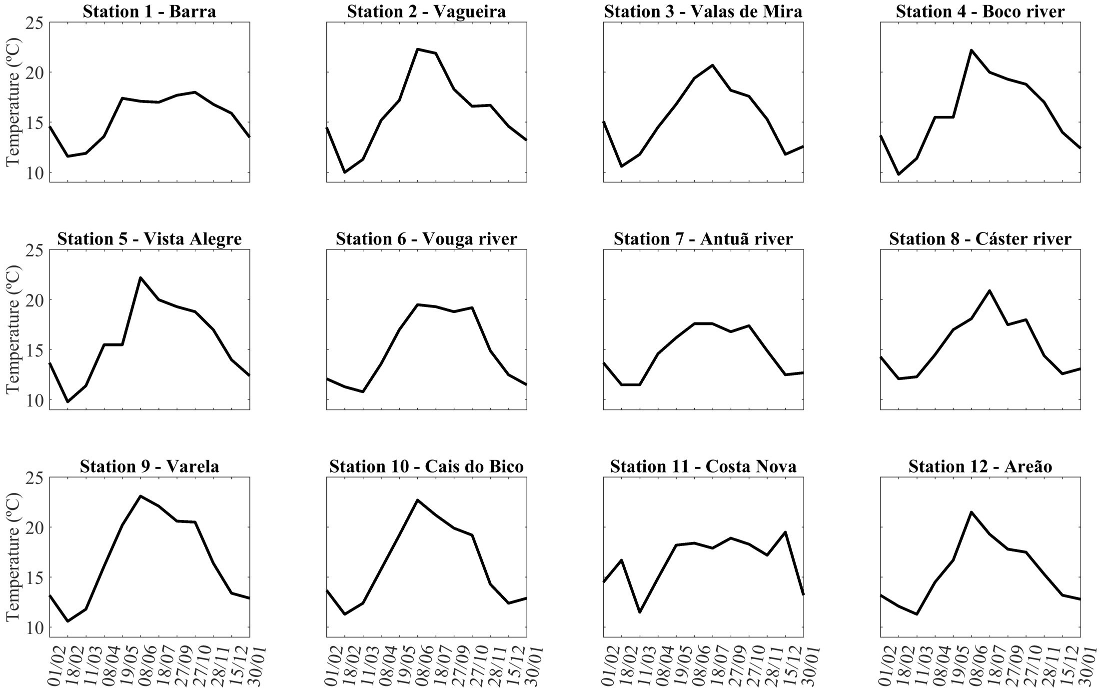

Figure 6.3: Annual evolution of observed water temperature at different lagoon stations.

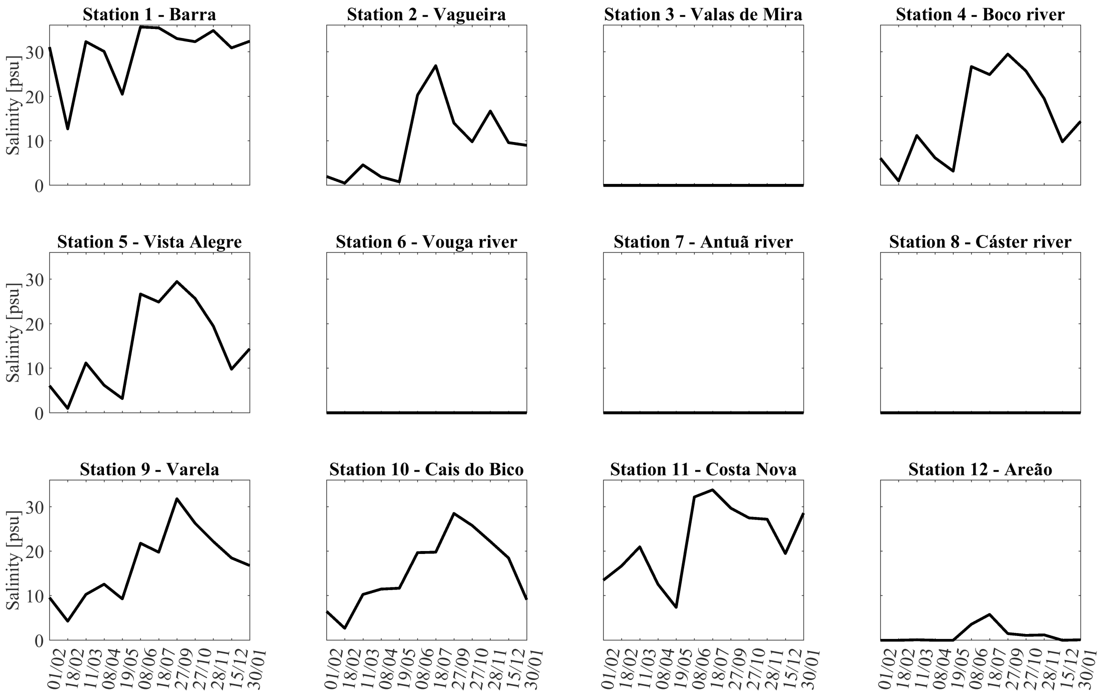

Figure 6.4: Annual evolution of observed salinity at different lagoon stations.

during the dry season, when the penetration of salt water in the lagoon is more evident, in response to lower freshwater inputs.

Chlorophyll *a* time series (Figure 6.5) evidence the development of the characteristic phytoplankton estuarine spring and summer blooms. Here, it is depicted that chlorophyll *a* concentration ranged between 0 and 8.2 μg/L, with values increasing progressively from late winter (February), when surveying started, to late Spring (June), when a spring algae bloom becomes visible in most stations. From summer to late winter, the mean chlorophyll values gradually decreased, due to the decrease of solar radiation, day length and water temperature. In general, maximum phytoplankton biomass values were frequently found in the lagoon's mid areas, namely at S2, S5 and S9 stations, where annual mean chlorophyll a concentration values reached 3.50, 2.09 and 1.97 μg/L, respectively. These lagoon locations are narrow, shallow and characterized by low current velocity, leading to low water renewal rates (Dias et al., 2007). These geomorphologic and hydrodynamic features are favorable to the sustainment of the phytoplankton communities and high photosynthetic activity. Additionally, the resuspension of the microphytobenthos communities presented in the large intertidal mudflats associated with these lagoon's areas is another important contribution to maximum biomass values measured in S2, S5 and S9.

On the other hand, the minimum production rates were found for the regions under the influence of the less important lagoon's freshwater tributaries, Boco, Cáster and Antuã rivers, with values of 0.55, 0.43 and 0.35 μg/L, respectively. Therefore, the main contributor of phytoplankton through the lagoon is Vouga river (S6), with an annual mean concentration of 2.21 μg/L, followed by Mira river with 1.76 μg/L. In the oceanic station (S1) was also observed an expected pattern, with maximum value measured in spring, specifically 4.90 μg/L in the 4$^{\text{th}}$ field survey (08/04/2016). This pattern, along with seasonality, may be explained by an upwelling event that enriches the ocean water with nutrients, stimulating the growth and reproduction of primary producers, once this maximum is not intensely reflected inside the lagoon. The annual mean value was 1.07 μg/L, which is lower than mean concentrations in lagoon's middle areas, and higher than those found in the river boundaries, proves that Ria de Aveiro ecological processes are mainly governed by local hydrodynamic and biogeochemical phenomena.

The pH variability (Figure 6.6) is less marked comparing with the remaining variables under analysis, revealing a smaller deviation from the mean value. However, the annual variability shows an increase in spring season at all stations. pH is one the most important environmental variables for the survival, growth, metabolism and physiology of marine organisms, being controlled by water temperature, dissolved oxygen,

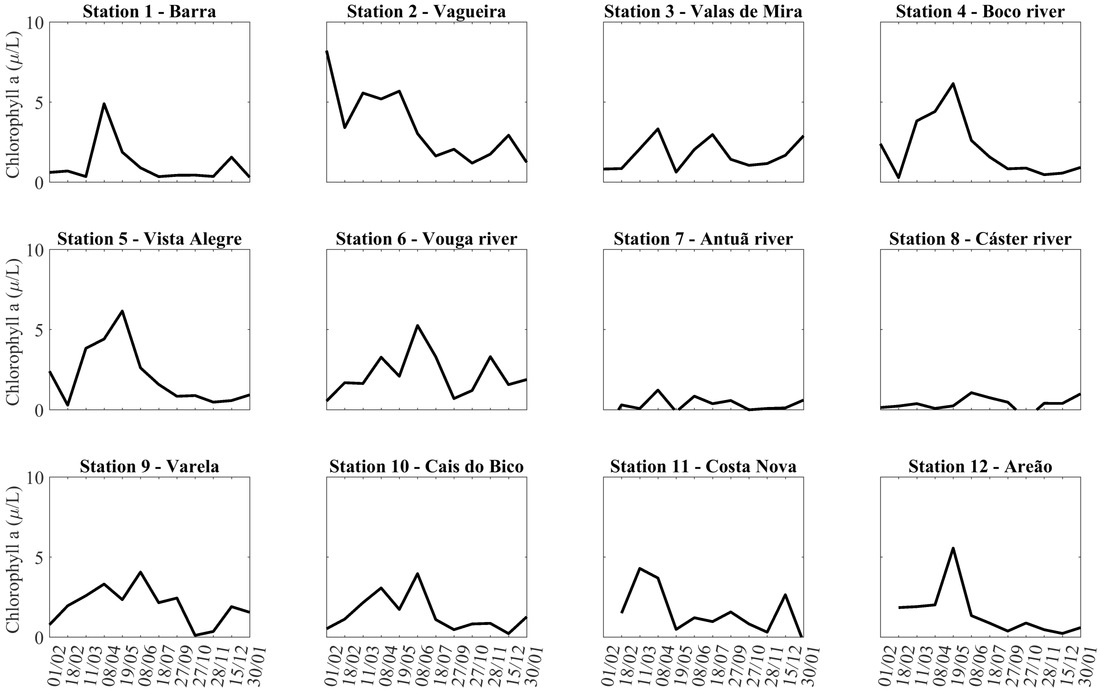

Figure 6.5: Annual evolution of observed chlorophyll *a* concentration at different lagoon stations.

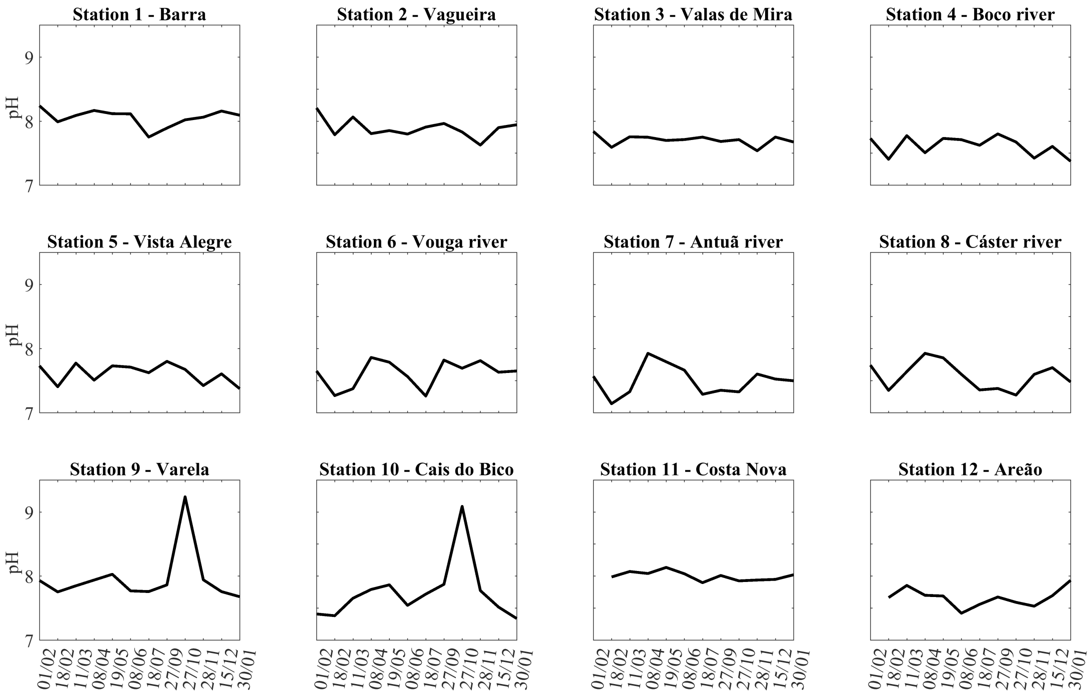

Figure 6.6: Annual evolution of observed pH concentration at different lagoon stations.

organic matter decomposition and photo synthetic activities. Therefore, higher pH values were recorded during early spring, when the water temperature rise motivates phytoplankton photosynthetic activity increasing the carbon dioxide consumption and consequently leading to pH increase (Nassar and Hamed, 2003). The analysis of the spatial variability reveals higher pH values in oceanic stations, and the lowest values in riverine stations, as expected. The alkalinity of seawater is typically higher than for freshwater, which combined with higher phytoplankton activity in middle and oceanic lagoon areas leads to higher pH values at these locations. The annual mean measured pH at S1 (Barra) is 8.05, while the mean pH at river boundaries is 7.56. The maximum measured value is 8.24 in S1. These pH values fall within the most suitable levels for biological productivity, ranging from 7.0 to 8.5 (Abowei, 2010).

Winter and summer mean value of each variable was calculated from model simulations and presented in Figure 6.7, where the upper panel corresponds to winter season, while the summer season is depicted in the lower panel. Considering the low pH dependence found on oceanic and river forcing, this variable does not reveal any gradient or pattern, and for this reason are not presented the respective horizontal fields in Figure 6.7.

From Figure 6.7 A is found that in winter the water temperature has low spatial variability, with slightly higher temperatures observed close to the inlet area (about 15°C). On the other hand, minimum average temperatures about 10°C are found in the upstream areas of S. Jacinto channel. During summer (Figure 6.7 B), a clear longitudinal gradient is observed, and water temperature increases from the inlet towards the head of the channels, ranging from 15°C to 25°C. In this period, the oceanic forcing is more noticeable in water temperature horizontal distribution.

The salinity follows the expected patterns, showing a longitudinal gradient throughout the year. Values close to 36 are found in inlet area, while freshwater (null salinity) is found at the heads of the channels. During winter (Figure 6.7 D), salinity values higher than 30 are confined to the mouth of the lagoon and to the mouth of the S. Jacinto and Mira channels. The summer season (Figure 6.7 C) contrasts with the winter in a large extension of the lagoon, with oceanic water expanding for most the lagoon central area, as well as to the entire S. Jacinto channel, and to the Mira and Ílhavo channels initial stretches.

Regarding chlorophyll *a* concentration spatial distribution, was found a pattern like that observed for salinity. During the spring and summer blooms (Figure 6.7 F), a longitudinal gradient is observed from the inlet to the head of the channels, ranging from 1 to 6 μg/L, respectively. Due to the lower concentrations found during the winter season (Figure 6.7 E), values close to 0 μg/L are observed for most the lagoon. The

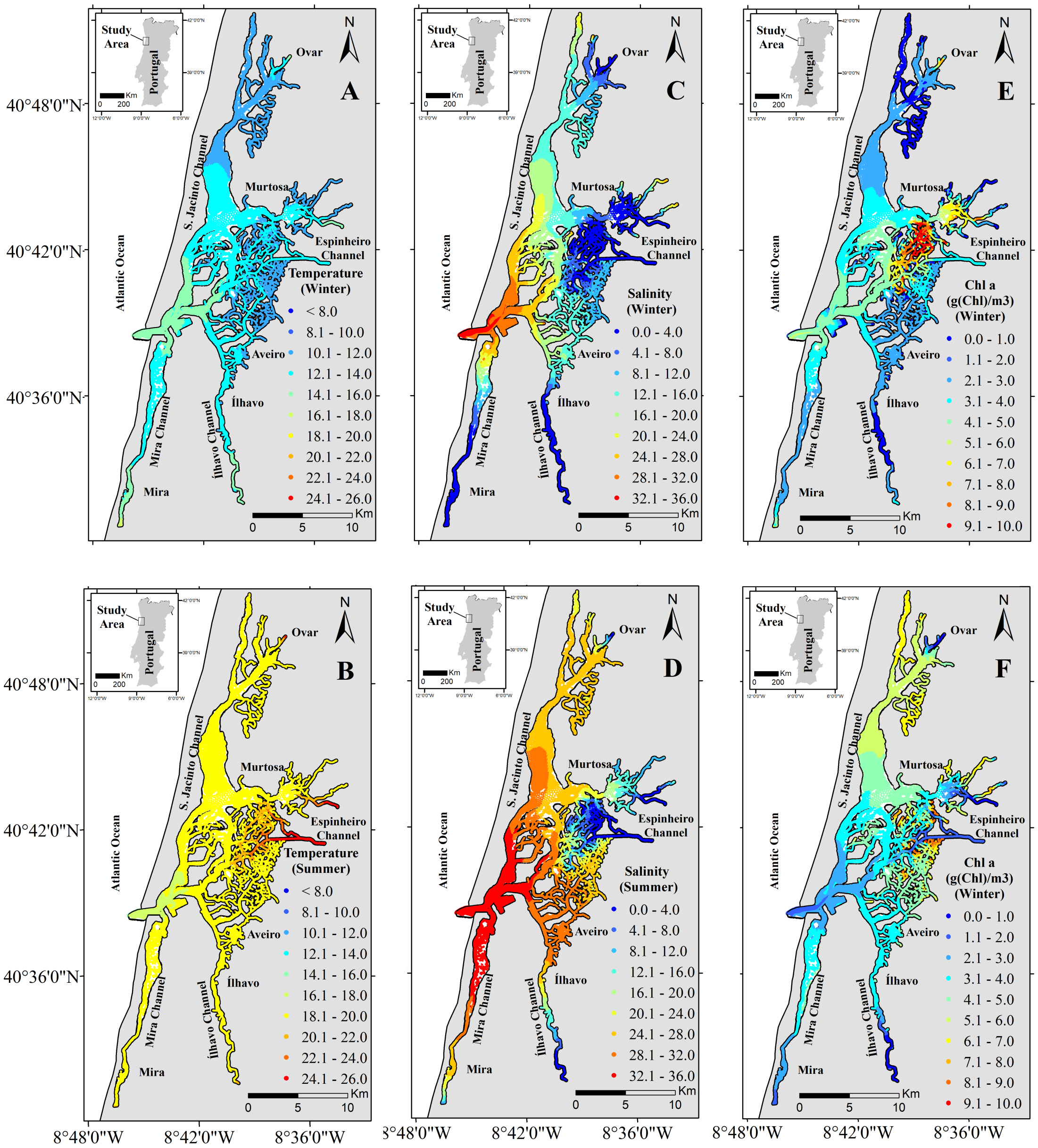

Figure 6.7: Spatial variability of water temperature, salinity and chlorophyll *a* concentration at Ria de Aveiro. A – Water Temperature in Winter; B – Water Temperature in Summer; C – Salinity in Winter; D – Salinity in Summer; E – Chlorophyll *a* concentration in Winter; F – Chlorophyll *a* concentration in Summer.

exceptions are the areas close to the inlet and rivers mouths, as well as Mira channel, where some local processes changes the gradient. This pattern may be explained since the Mira channel is the least dynamic of the four main channels of Ria de Aveiro, once only 10% of the lagoon tidal prism is distributed for this channel. This low tidal prism affects residence time, which is around 15 days (Dias et al., 2007). This high residence time reflects some constrains in the communication between this channel and the mouth of the lagoon, leading to the sustainment of the phytoplankton populations. For this reason, the Mira channel is the most challenging channel to modulate and the most difficult to reproduce water quality or any biotic or abiotic variables.

In summary, water temperature, salinity and chlorophyll *a* concentration show spatial and temporal variability throughout the year. Water temperature and salinity are in line with the expected for estuarine systems. Chlorophyll *a* concentration shows a maximum value in Vagueira (8.23 μg/L) during the first field campaign, on February 1st. This unexpected winter high may evidence the role of the local processes, as well as of the tidal transport mechanism, causing deviations to the expected spatial and temporal variability. Generally, the lowest values were found close to the river mouths, namely in Antuã and Cáster rivers, confirming their poor contribution to biomass (Lopes et al., 2015). These results agree with Bum and Pick (1996) that concluded that areas with high flushing potential, such as rivers with small residence times, limit phytoplankton growth. Due to the higher solar radiation in spring, the light availability enhances the phytoplankton spring bloom, which occurred between April and June in all stations analyzed.

6.3.2 Abiotic factors affecting the growth and mortality of planktonic microalgae

In general, estuarine systems as Ria de Aveiro have three main limiting abiotic factors affecting the growth and mortality of planktonic microalgae: nutrients, light availability and water temperature. Nutrients are involved in reactions of photosynthesis, wherein carbon, phosphorus and nitrogen are considered the most important nutrients controlling the growth of these organisms. Water temperature influences the metabolic rates of organisms and their photosynthetic capacity, while light is the source of energy used by organisms to generate new biomass. Additionally, tidal propagation and estuarine currents are also very important in the pelagic communities distribution (Leal et al., 2015).

The biomass values measured and also simulated by the model are similar to those found in Lopes et al. (2005), and lower than those presented by Almeida et al. (2005) and Lopes et al. (2008) for Ria de Aveiro lagoon, or found for other coastal systems, like for example, the Rias Baixas (Varela et al., 2008), the Urdaibai estuary (García et al., 2010) (Spain) or the Delaware estuary (USA) (Keller et al., 2001).

In agreement with Lopes et al. (2015), this study also indicates that the distribution of phytoplankton concentration in the lagoon evidences maximum values located on the second half of the lagoon channels, during all the year. On the other hand, the minimum values are observed at the river mouths. A well typified longitudinal concentration gradient was found in the central area of the lagoon, characterizing the transition between the oceanic and the riverine influence.

Irigoien and Castel (1997) studied the turbidity influence on Gironde estuary (SW France) and proved that this feature may seriously affect the distribution of chlorophyll pigments and that the photosynthetic activity is reduced as a consequence of the light limitation. Also, Camacho et al. (2014) concluded that the light limitation due to the low availability of solar radiation in the water column in response to turbidity is an important limiting factor for phytoplankton production. Regarding Ria de Aveiro, Lopes et al. (2015) pointed out that light limitation conditions do not affect the phytoplankton growth, although this assumption should be deeply discussed.

Figure 6.8 portraits predicted spatio-temporal variability in the nutrients limitation factor, phytoplankton biomass, DO concentrations and phytoplankton growth as function of water temperature (TFG) at selected locations along the estuarine zone continuum over the year 2016 and early 2017. Nutrient limitation function of 1 means total availability for nutrients uptake by algae, while values close to 0 means that the station is nutrient limited. TFG predicts the water temperature influence on microalgae growth, expressed by: $\upsilon_{\mathrm{t}}{}^{T\text{-}20}$, where υ_{t} is a temperature dependency constant and T is the water temperature. The stations were selected according to their different hydrological conditions: S1 is dominated by oceanic water, while S6 is a riverine station; S12 is a typical estuarine station under the influence of both forcing.

As expected, a seasonal pattern of TFG (lower panel) is observed, in which during spring and summer the water temperature conditions are more favourable to phytoplankton growth, since its metabolic rates and photosynthetic capacity are optimized (Leal et al., 2015). Results also evidences that in S6, due to the large water temperature seasonal variability, the temperature function amplitude is higher comparing with the remaining stations. The extreme cold river water in winter may be the main responsible for the decrease of phytoplankton biomass in winter. These results also suggest that, even in the deepest area of the lagoon (S1), the microalgae have enough light available to generate primary production all year long. As expectable, the amount of radiation is smaller during winter, limiting the phytoplankton growth during this season, in agreement with the findings of Lopes et al. (2015).

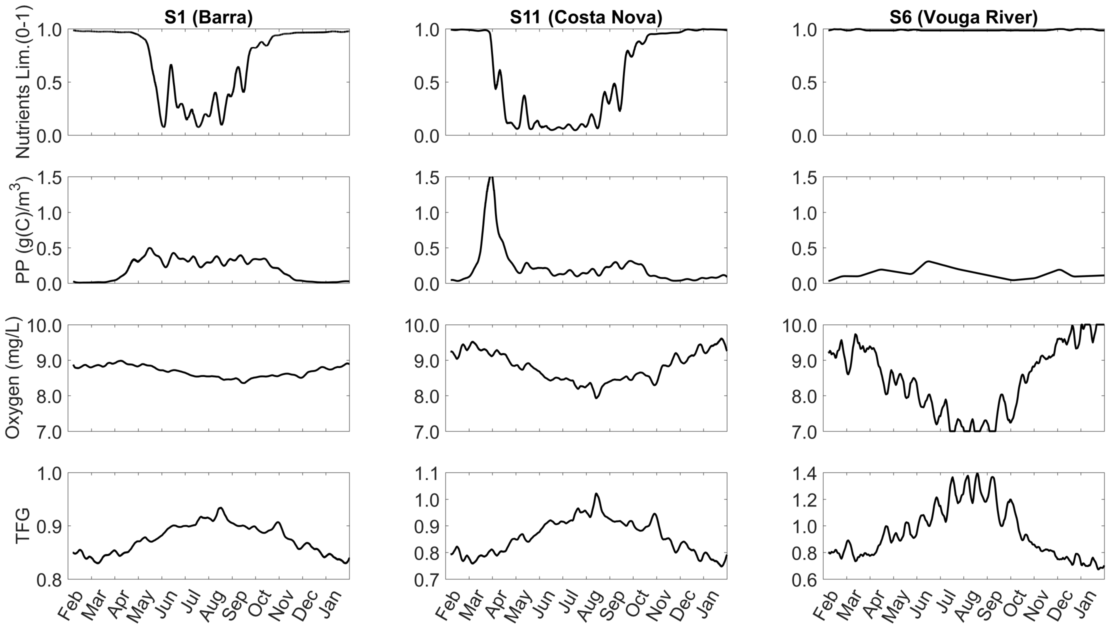

Figure 6.8: Annual evolution of predicted nutrients limitation, biomass and dissolved oxygen at selected Ria de Aveiro stations (S1, S11 and S6).

In general, in the analysed stations, nutrients and DO concentrations show a clear seasonal trend characterized by high values in winter, a progressive decrease during the productive spring and summer periods, and a replenishment of nutrient levels in late summer and autumn.

In spring, the significant nutrient depletion reflects the development of a characteristic phytoplankton spring bloom along the lagoon zone that coincides with periods of low nutrient level. These results suggest a substantial uptake of nutrients by phytoplankton, which causes a drop in nutrients concentration. Those patterns are observed in S1 and S12, however in S6 the nutrients concentration is high and non-limited during entire year. Vouga river, the main tributary in Ria de Aveiro, has a mean freshwater inflow of 50.0 m^3s^{-1} (Vaz et al., 2016), constituting a continuous nutrient supply with very low residence time. These predictions agree with Lessin and Raudsepp (2007) results for Narva Bay (Finland), which showed that areas close to river mouths are characterized by high concentrations of inorganic nitrogen and low phytoplankton concentration due to the high magnitude of hydrodynamic processes.

Regarding biomass, a peak was observed in S12 during March due to the hydrodynamic local processes that occur in the upstream area of Mira channel, which is propagated during ebb to Costa Nova. The occurrence of this unexpected phenomenon in Mira channel was already explained in the previous section.

This shows that nutrients in Ria de Aveiro tend to have riverine origin, being transported to the shallow areas of the lagoon, where they tend to accumulate. Therefore, the high phytoplankton biomass in mid-channel areas reflect not only the nutrients accumulation, but also the increase of irradiance at those areas.

6.4 Conclusions

A complex model accounting for the coupled biogeochemical renovation processes and fluxes of carbon and macro-nutrients along the shallow tidally-dominated Ria de Aveiro lagoon was applied, integrated with *in situ* temperature, salinity pH and chlorophyll *a* concentration data at 12 stations distributed along the lagoon channels. The results give important insights into the dynamics and environmental factors that control the spatial structure and evolution of autotrophic processes. In this context, this study results in an important advance in the ecological modelling in Ria de Aveiro, since it presents the development of an innovative approach integrating analysis of *in situ* data and numerical model predictions of local biophysics. This methodology had never been applied in Ria de Aveiro to evaluate the individual and combined contribution of water temperature, light and nutrients, to the growth of phytoplankton communities. From this chapter, the following conclusions may be drawn:

- According to *in situ* measurements, seasonal and longitudinal variability of biophysical variables is observed. The phytoplankton biomass presents an important seasonal variability, characterized by a spring and summer blooms, in which chlorophyll *a* concentration may exceed 8 μg/L, when environmental conditions are suitable for its growth. The spatial and temporal distribution of primary production extremely depends on phytoplankton inter-relation and on biotic and abiotic factors, but is also strongly influenced by the tidal dynamics, which determines the generation, location and intensity of algae blooms;

- The geomorphologic features of Ria de Aveiro, such as shallow depth and narrowness of the channels, also play a major role in water quality characteristics. The chlorophyll *a* concentration during the spring bloom is more than 1000% higher than the concentration measured during winter season, responding to a water temperature increase of 90%. This tendency is opposite to that for nutrients concentration, revealing the uptake by phytoplankton communities;

- When the lagoon is not light limited (between March and September), the primary production is governed by nutrients variability, being the riverine input the most important natural source. The nutrients depletion caused by phytoplankton uptake is the main limiting factor, during spring and summer seasons. The decrease of nitrogen and phosphate compounds during this period controls the autotrophic organism concentrations, avoiding eutrophication;

- The water temperature also plays a major role in primary production patterns, being responsible for the spring and summer algal bloom. The seasonal variability of primary production is governed mainly by water temperature, limiting the photosynthesis since October to early March;

- In ocean and middle lagoon areas, the nutrients uptake by phytoplankton and other marine organisms is about 90% higher than the nutrients replenishment by ocean and rivers. Near the river mouths, neither light nor the nutrients availability (100% availability in S6) limit phytoplankton enhancement, which depends essentially on hydrodynamic processes, such as high current velocity and very low residence time. Hydrodynamic processes are also responsible for the unpredictable and unexpected local processes, such as those found in the Mira channel;

- Until now, the scientific community believed that phytoplankton development in Ria de Aveiro was always nutrient limited (Lopes et al., 2007b, 2015). However, this study proves that this assumption is not verified during the entire year, but only during spring and summer seasons. In autumn and winter, the nutrients are totally available for phytoplankton growth, but their metabolic rates are inhibited by water temperature. This is also the first study demonstrating that close to mouth of the rivers the phytoplankton growth is limited by hydrodynamic processes.

The *in-situ* data collected within the scope of this study revealed to be crucial to reach the conclusions achieved, since the knowledge about the biomass and the abiotic variables incoming from the ocean and rivers was essential to assess the patterns found in the mid-channel areas. The integrated approach here followed between *in situ* data sampling and the exploitation of the model implementation had generated the necessary conditions to give future response to local economic problems, allowing the identification of best conditions and areas to local aquaculture exploitation, which is assessed in the next two chapters.

The lack of long-term hydrodynamic, physical and biotic variables data with high temporal and spatial resolution consisted is the main limitation of this study. The existence of such a database would be a valuable asset for future studies on the biological and chemical dynamics of the lagoon, but also for the development of more accurate hydrodynamic and water quality models.

Chapter 7

Water Renewal Estimation for Sustainable Aquaculture Development in Ria de Aveiro and Rias Baixas

7.1 Introduction

Finfish and/or shellfish aquaculture sustainability in inshore areas, such as Ria de Aveiro and Rias Baixas, is extremely dependent on the efficiency of the water renewal at the culture sites, since oxygen and nutrients must be continuously supplied to fish and bivalves. On the other hand, excessive organic matter, detritus and excretions resulting from production must be flushed away from the culture sites. Additionally, areas with low flushing rates are more susceptible to water overheating, causing problems to aquaculture production (Boghen, 1989).

Therefore, the evaluation of local hydrodynamic characteristics induced by tidal forcing, river runoff, thermohaline processes, wind and other meteorological forcing is crucial to assess water renewal in coastal systems. In this context, before selecting new sites for aquaculture industry development in Ria de Aveiro and Rias Baixas, it is crucial to know about the hydrodynamic functioning and the flushing potential of these coastal systems.

Water renewal time (WRT) is defined as the time for a significant fraction of water (β) inside a domain of interest to be renewed by waters from outside this domain (Zimmerman, 1976). There are different methodologies to calculate water renewal, such as residence time, flushing time, age of a particle and turnover time. These methods have been widely discussed in the scientific literature, and numerous numerical models have been applied to analyze the water renewal and exchange between estuaries/lagoons and open sea/rivers. For example, Ferrarin et al. (2013) investigated the hydrological regime and renewal capacity of the heavily modified Venice Lagoon using the Shyfem 3-D hydrodynamic model, concluding that sea level rise will increase water renewal time in the central part of the lagoon, where most of the pollutant sources are located. This implies that the area close to the city of Venice and close to the industrial zone will experience the most intense ecological consequences. Umgiesser et al. (2014) focused on hydrodynamics in terms of exchange rates, transport time scale and mixing, in ten Mediterranean lagoons, using the same hydrodynamic model. These authors concluded that tidal action and wind set-up are the main processes controlling water exchange. Previous studies have also focused on some Portuguese and Spanish coastal systems, but from a very different perspective to that explored in this study. Malhadas et al. (2009) used MOHID 3-D model to evaluate the effect of dredging operations in WRT at Óbidos lagoon (Portugal), demonstrating that it can be reduced in about 50% in some areas. A similar work was recently performed by García-Oliva et al. (2018) in Mar Menor (Murcia, Spain), in which the hydrodynamic response of the Mar Menor lagoon to dredging interventions at the inlets was assessed, concluding that dredging operations leads to a homogenization of the WRT along the lagoon.

For the locations where this work is focused, Gómez-Gesteira et al. (2003) and Dale et al. (2004) calculated residence times in Ria de Pontevedra. The first assessed the dependence of the water residence time in Ria of Pontevedra on the seawater inflow and on the river discharge. Dale et al. (2004) evaluated the transient oceanic and tidal contributions to water exchange and residence times. These authors concluded that freshwater input play a minor role in water exchange comparing to periodic upwelling events. When upwelling conditions were observed, a decrease of WRT was verified, while under downwelling favorable conditions, the water retention increased. In Ria de Aveiro, Dias et al. (2001), coupled a hydrodynamic model with a particle tracking model in order to study the dispersion processes and residence time in Ria de Aveiro, predicting a residence time of 2 days in the central area of the lagoon, and more than 2 weeks in the channel's heads. Dias et al. (2007) aimed to identify the main lagoon sources of sediments (ocean or rivers), and determined residence time for this purpose, concluding that in short time scales the oceanic influence is dominant in sediment residence time.

The mixing processes induced by water inflowing from ocean and rivers is more likely to occur in the areas close to the boundaries, therefore it is expectable that WRT progressively increase away from the boundaries. Therefore, water renewal in estuaries and coastal lagoons is a function of distance from the oceanic and river boundaries, depending on boundary fluxes, such as time varying freshwater discharge and tidal fluctuations at the inlet.

The main goal of this chapter is to assess and compare hydrodynamic functioning and WRT in Ria de Aveiro and Rias Baixas, two contrasting systems in which aquaculture has been successfully implemented in the Northwest coast of Iberian Peninsula, aiming to ensure overall management and future developments of aquaculture infrastructures is these coastal systems. A novel procedure to predict residence times was performed under two different seasonal scenarios: summer and winter conditions. Besides, the present work also aims to answer the following questions: (1) what is the best methodology to use in such two different systems, a shallow, narrow and vertical homogeneous coastal lagoon and V-shaped partially stratified estuaries; (2) how aquaculture quality can be estimated in these two coastal systems, assessing the main drivers influencing their water renewal rates.

As mentioned in the Chapter 1, Ria de Aveiro and Rias Baixas are the two most successful coastal systems in the aquaculture industry in the northwestern coast of the Iberian Peninsula, despite their geomorphological and hydrodynamic differences. Furthermore, they are geographically close, once the distance between Ria de Vigo and Ria de Muros is 60 km, and the distance between Ria de Vigo and Ria de Aveiro is about 150 km. The information collected in the scope of Chapter 2 evidenced the geomorphological, hydrodynamic and hydrological differences between Ria de Aveiro and Rias Baixas. In this context, the comparison between their water renewal processes and hydrodynamic functioning is very relevant and will contribute to bring new insights about WRT processes and their influence on aquaculture exploitation in semi-enclosed coastal systems.

7.2 Methodology

The assessment of Ria de Aveiro and Rias Baixas hydrodynamics and thermohaline dynamics is performed in this chapter, in order to predict their water renewal rates, through the analysis of numerical model results.

The estimation of the spatial and temporal distribution of residence time can be performed according to three different modelling approaches: Lagrangian particle tracking (Dias et al., 2007; Brooks et al., 1999); Eulerian tracer advection dispersion (Koutitonsky et al., 2004); or a combination of both methodologies (Burwell et al., 2000). In this study, an Eulerian tracer method is applied, which allows to distinguish between the integral renewal time (IRT) and the local renewal time (LRT). According to Josefson and Rasmussen (2000), IRT is useful for comparative coastal ecosystem studies and LRT is useful to ensure the most appropriate places for localized human interventions in a coastal ecosystem, such as the site of an aquaculture activity, an outfall diffuser site, or an industry cooling water outlet. The Eulerian model track the movement and concentration of a tracer over time, solving the advection, turbulent and molecular diffusions equations. More details about the Eulerian model used in this study can be found in Deltares (2006a).

7.2.1 Models Exploitation and Scenarios

This work is performed coupling an advection-dispersion passive tracer model to calibrated and validated hydrodynamic models for Ria de Aveiro and Rias Baixas.

In order to assess the seasonal variability of the flushing potential, summer and winter scenarios were established for each coastal system. For river flow, typical constant summer and winter freshwater discharges were established (Table 7.1), corresponding to the mean freshwater inflow measured by Meteogalicia database (Rias Baixas) and predicted by the SWIM model (Ria de Aveiro) (Krysanova et al., 2000), during the simulation periods. Here, constant rivers values are used because, in this way, they produce an uniform variation in WRT for the whole simulation period.

The approach followed in this study to estimate the WRT in Ria de Aveiro and Rias Baixas is the dissolved Eulerian tracer method, based on the advection-dispersion of a passive tracer. The applied methodology establishes the initial concentration (C_t) of the passive tracer equal to one (C_t=1) over the entire domain, and C_t=0 at the oceanic and river boundaries. The water with C_t=1 represents the water initially inside the systems, while the concentration C_t=0 represents the water initially outside the systems, i.e., in the Atlantic Ocean and tributary rivers. The decrease of tracers concentration in time and space is a proxy for water renewal originally located inside the domains by water originally outside the domain.

The threshold concentration adopted to a fraction of water be considered renewed (β) is 63% of the initial concentration (Ranasinghe and Pattiaratchi, 1998; Arneborg, 2004; Koutitonsky et al., 2004). The time needed to decrease the concentration below 37% of the initial concentration is considered the LRT for each cell and depth (case of Rias Baixas) of the numerical grid. The estimation of IRT is obtained by averaging the concentrations of all grid cells over the entire domains, at each time, and by associating the IRT to the time when the average concentration drops to 37% of its initial concentration.

The summer scenario was simulated between 01/07/2016 and 30/09/2016, while the winter scenario was simulated between 01/01/2016 and 31/03/2016. A spin-up period of 2 months precedes both simulation periods. The model results were analyzed and horizontal fields of the depth-averaged LRT were depicted, as well as the vertical profiles of LRT, residual velocity and mean water temperature during the simulation

Table 7.1: River discharges values (m^3s^{-1}) considered for Ria de Aveiro and Rias Baixas simulations.

System	River	Winter	Summer
Ria de Aveiro	Valas de Mira	16.6	0.5
	Boco	3.6	0.1
	Vouga	62.1	8.7
	Antuã	22.7	1.4
	Cáster	8.3	0.3
Rias Baixas	Verdugo-Oitavén	60.4	2.7
	Lérez	79.9	3.9
	Ulla	84.7	9.4
	Umia	22.4	1.1
	Tambre	67.2	3.5

periods along the main Rias Baixas axis. The horizontal fields of residual velocity for Ria de Aveiro and Rias Baixas were also computed, however, since the patterns are similar to those found in the literature (Lopes and Dias, 2007; Ruiz-Villarreal et al., 2002; Carballo et al., 2009), the results were not shown in this study, but are mentioned whenever necessary. Residual circulation values were obtained by averaging the predicted velocities during a period of 14 days, 18 hours, 32 minutes and 24 seconds, once this is a multiple period of the tidal constituents M_2 and S_2. With this procedure, the main tidal constituents are filtered, including the constituents related with the spring and neap tidal cycle. Additionally, in order to compare Ria Aveiro and Rias Baixas flushing potential, the IRT was also predicted for both domains.

This study intends to study the seasonal variability of WRT. Therefore, it is essential to frame 2016 into the historical average, in order to understand, if the seasonal variability of water temperature and salinity observed in 2016 is representative of a typical pattern of these variables, avoiding the analysis of an atypical year. In this context, Figure 7.1 shows the comparison between the monthly mean of depth-averaged water temperature (left panel) and salinity (right panel) between 2006 and 2018 (blue dots) and their deviation, with the monthly average for 2016 (black dots), for stations V1, P1, A1 and M1, used for Rias Baixas water quality validation procedure (Figure 5.1 of Chapter 5). The variability of the average water temperature and salinity shows that 2016 can be considered a normal year with values close to the historical mean. Thus, the mean value variability of water temperature and salinity evidences that 2016 is within the average of historical values, being representative of the thermohaline seasonality of Rias Baixas. Due to the lack of historical data for Ria de Aveiro, this analysis was not performed for the Portuguese lagoon.

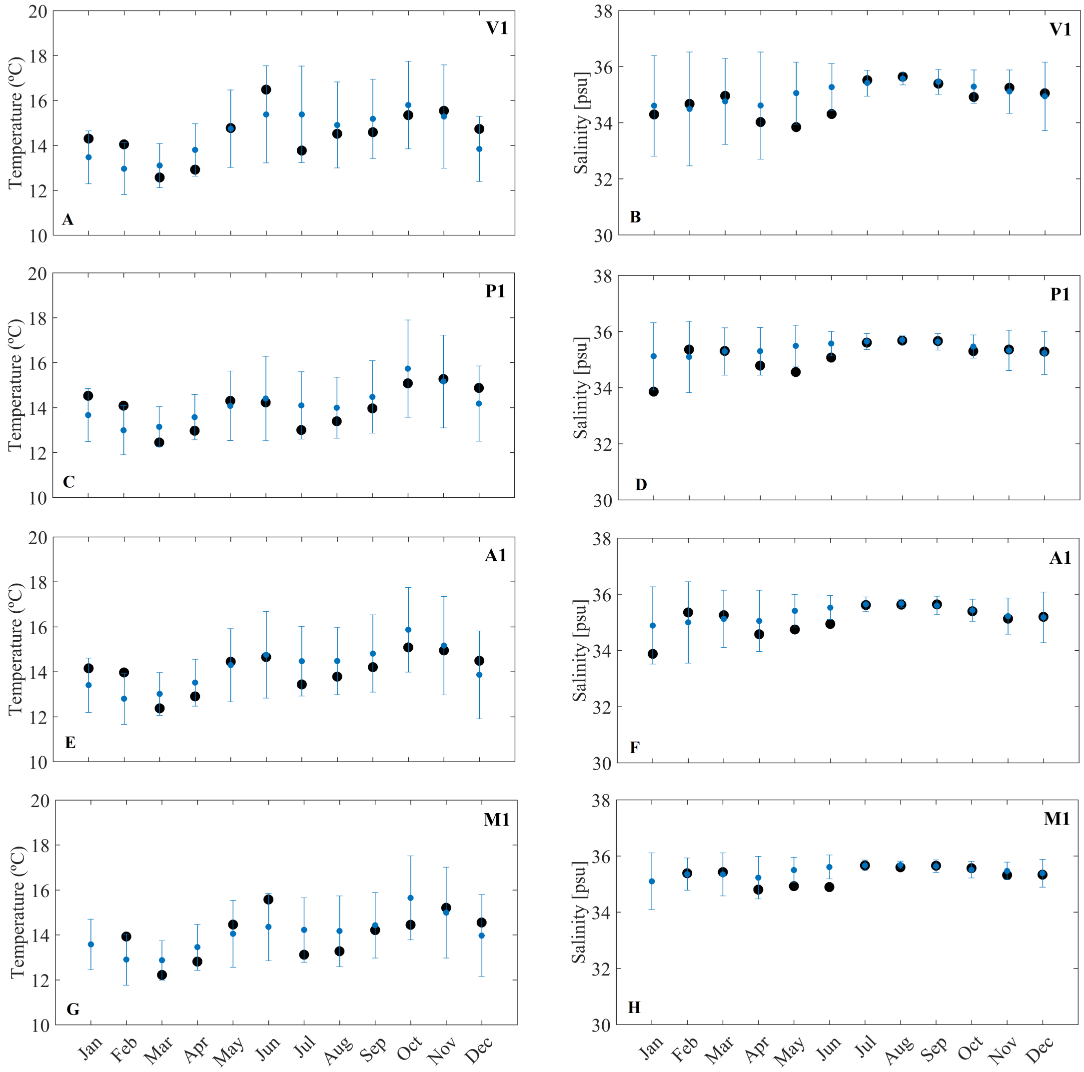

Figure 7.1: Comparison of the historical data of Rias Baixas water temperature (A, C, E and G) and salinity (B, D, F and H), with the monthly average values for 2016 (black dots).

7.3 Results

7.3.1 LRT

The LRT spatial distribution in Ria de Aveiro and Rias Baixas (Figure 7.2) was predicted using the dissolved tracer method previously outlined. The effects of seasonal discharge conditions at river boundaries on the LRT were depicted by imposing two different discharge conditions in both study areas, as well as the effects of seasonal thermohaline processes.

For Ria de Aveiro, the maximum LRT values were predicted in S. Jacinto channel

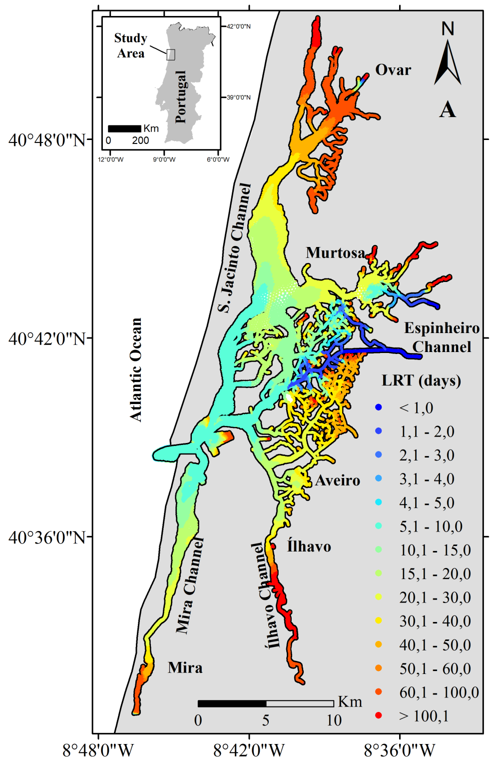

(A) Ria de Aveiro - Summer

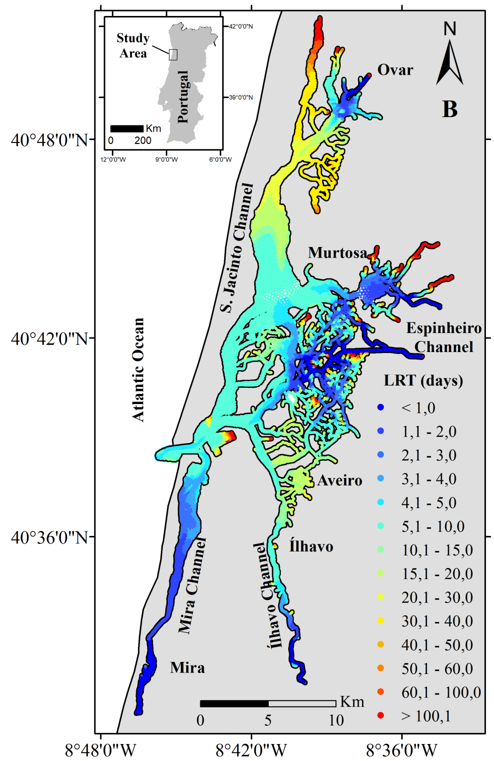

(B) Ria de Aveiro - Winter

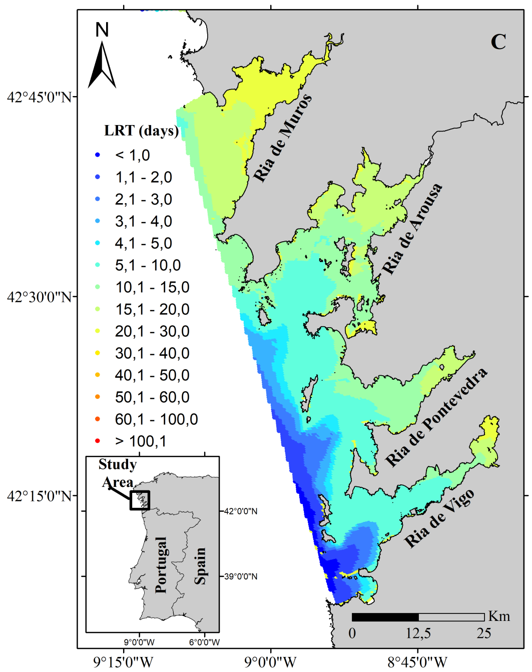

(C) Rias Baixas - Summer

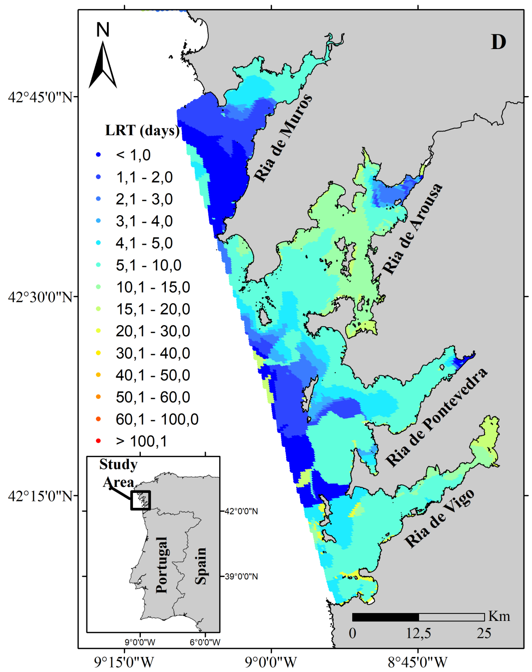

(D) Rias Baixas - Winter

Figure 7.2: Spatial distribution of the depth-averaged LRT in Ria de Aveiro (A, B) and Rias Baixas (C, D) for summer (A, C) and winter (B, D) seasons, respectively.

head and in the mid-area of Ílhavo channel (more than 100 days), under low freshwater scenario (Figure 7.2 A). These areas present a minimum downstream residual velocity, with an order of magnitude of 10^{-4} ms^{-1}, suggesting a relationship between residual velocity and LRT. With the exception of Vouga river mouth, the maximum renewal rates occur at inlet area, S. Jacinto and Mira channels (between 4 and 5 days), responding to maximum downstream residual velocities of approximately 8 cms^{-1}, in these areas. This result reveals that properties advected with water tend to move oceanward, reflecting the tidal asymmetries patterns and ebb dominance in central area of Ria de Aveiro (Lopes and Dias, 2014), suggesting that Ria de Aveiro tends to export water properties to the ocean, which may benefit aquaculture exploitation.

As expected, the renewal times are considerably reduced in response to higher freshwater discharges, and the best water renewal conditions are observed under winter conditions, corresponding to high freshwater discharge from Vouga, Antuã, Cáster, Valas de Mira and Boco rivers (Figure 7.2 B). In this case, the renewal times in the middle area and head of Mira and Espinheiro channels are lower than at the inlet, since the initial concentration present in these channels is pushed to the inlet area due to the high downstream residual velocity found in these areas. In fact, the LRT in the inlet is identical both under winter and summer conditions (about 4-5 days). This reveals that the overall fluxes at inlet area are not affected by the seasonal variations of freshwater discharge in the lagoon, considering that tide is the main process inducing water renewal in the area. The inner tracer concentrations that are "pushed" to the inlet area by tidal and river flow actions are responsible for the LRT values in Ria de Aveiro's inlet, following the lagoon's outflow tendency. Lopes and Dias (2007) predicted a lower residence time for inlet area (1 day), due to the differences in the methodology approach: Lopes and Dias (2007) used a Lagrangian particle tracking module. Under high freshwater inflow, the magnitude of lagoon's residual velocities is strongly modified, influencing LRT. In fact, Ria de Aveiro mean residual circulation almost doubles its intensity (91%) under high freshwater inflow, promoting a decrease in LRT.

These results show that the main differences in the renewal rates are found from the main-channel to channel heads, where Ria de Aveiro geomorphology is very complex, characterized by very shallow and narrow channels, and where freshwater inflow is important. Contrarily, from mid-channel to inlet area, the seasonal variability of LRT is low, revealing no variations in the water renewal rates due to thermohaline processes. Therefore, the dynamics of Ria de Aveiro is basically determined by longitudinal advection, and highly dependent on the inflows from the open boundaries.

Next, the patterns found for Rias Baixas are analyzed from the 3-D hydrodynamic and thermohaline points of views, since there are estuaries with classification different from Ria de Aveiro, turning the analysis more complex and extensive.

The distribution of LRT for Rias Baixas under the summer scenario (Figure 7.2 C) reveals a longitudinal gradient in the four estuaries, which is more pronounced at Rias de Vigo and de Arousa, due to their geomorphologic features. Ria de Arousa has the highest surface area (239 km^2), being necessary a larger number of tidal cycles to promote water dilution (Abdelrhman, 2005). The lower water renewal condition in the upstream area of Ria de Vigo (San Símon Bay) during summer period (about 40 days) is due to the narrowing geometry associated to low water depths, which promotes water retention in these areas. This inhibits water exchange with the downstream area of Ria de Vigo, requiring a larger number of tidal cycles to decrease the initial tracer concentration. This pattern is in accordance with Montero et al. (1999) findings, which also denoted Lagrangian particle retention in this area of Ria de Vigo. During winter season (Figure 7.2 D), the water renewal values are reduced, and maximum values were predicted in the mid-channel estuary areas (about 10 days). A maximum LRT of 17 days is observed in upstream area of Ria de Vigo (San Simón Bay). The longitudinal gradient of LRT reflects the spatial variability of depth-averaged residual velocity in Rias Baixas (order of magnitude of 10^{-1} ms^{-1} close to Rias inlets, and 10^{-2} ms^{-1} in the upstream areas).

A very important characteristic of Rias Baixas LRT is that renewal rates are higher in the southern than in the northern part of the inlets for both scenarios. This pattern is related to residual velocity, which shows a more intense incoming current through the southern mouths, and more intense outgoing current through the northern mouths (Carballo et al., 2009; Montero et al., 1999). However, near Rias Baixas inlets there are seasonal changes not explained by hydrodynamic processes. In this context, axial (along-channels) sections are plotted in Figure 7.3, to analyze in detail the water column structure of LRT, and the processes governing water renewal in partially mixed estuaries in comparison with a vertical homogeneous case (Ria de Aveiro).

Figure 7.3 evidences the importance of stratification and the associated gravitational circulation on water renewal rates. During summer scenario (Figures 7.3 A, 7.3 C, 7.3 E and 7.3 G) a significant vertical gradient of LRT is depicted, with low water renewal rates at surface layers. Figure 7.4 depicts the vertical profile of the residual velocity along the Rias axis, showing the presence of two-layered circulation, where water penetrates into Rias Baixas through deeper layers and leaves the estuaries close to the surface. In summer season, the increase of thermal stratification, due to surface solar heating and intense upwelling episodes that introduce shelf colder waters in deeper layers, retards vertical mixing and dilution in the bottom layers. During this

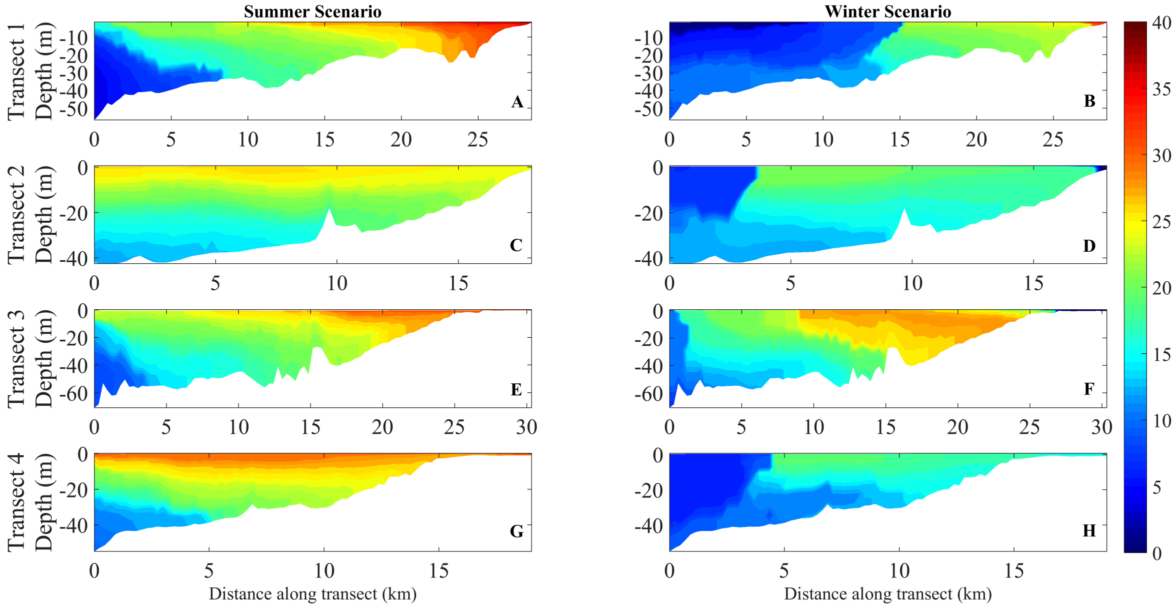

Figure 7.3: Vertical profiles of LRT (days) along the Rias main axis. T1 (Ria de Vigo) – A and B; T2 (Ria de Pontevedra) – C and D; T3 (Ria de Arousa) – E and F; T4 (Ria de Muros) – G and H.

period, the stratification slows down the estuarine circulation pattern, due to lower upstream and downstream residual velocities (Figures 7.4 A, 7.4 C, 7.4 E and 7.4 G). Across-channel currents between Ria de Vigo mouths are responsible for the positive residual velocities depicted in the surface layers around this area (Figure 7.4 A and B), as also depicted by Montero et al. (1999).

In winter, the horizontal and vertical distribution of LRT (Figures 7.3 B, 7.3 D, 7.3 F and 7.3 H) is more homogeneous, in response to the water surface cooling that induces convective mixing. During this period, the maximum values observed at bottom layers are lower than 10 days. Under this scenario, the bottom upstream and the surface downstream residual velocities (Figures 7.4 B, 7.4 D, 7.4 F and 7.4 H) increase, making the estuarine circulation more efficient, and improving the water renewal rates. Another important feature is that, during winter, the estuaries are divided into two contrasting zones: one more homogeneous and with low LRT values, near the mouths; and another more stratified located from the middle to upstream areas of the estuaries, characterized by higher LRT values, caused by the higher freshwater inflow. Therefore, this stratified wedge is proportional to the volume of freshwater discharged in these estuaries. In Ria de Arousa, where river flow is more important, this stratified wedge extends throughout the estuary; the opposite phenomenon is depicted in Ria de Vigo.

During summer, residence times are lower at the bottom as result of thermal stratification, causing water to penetrate the estuaries through the deepest layers. However,

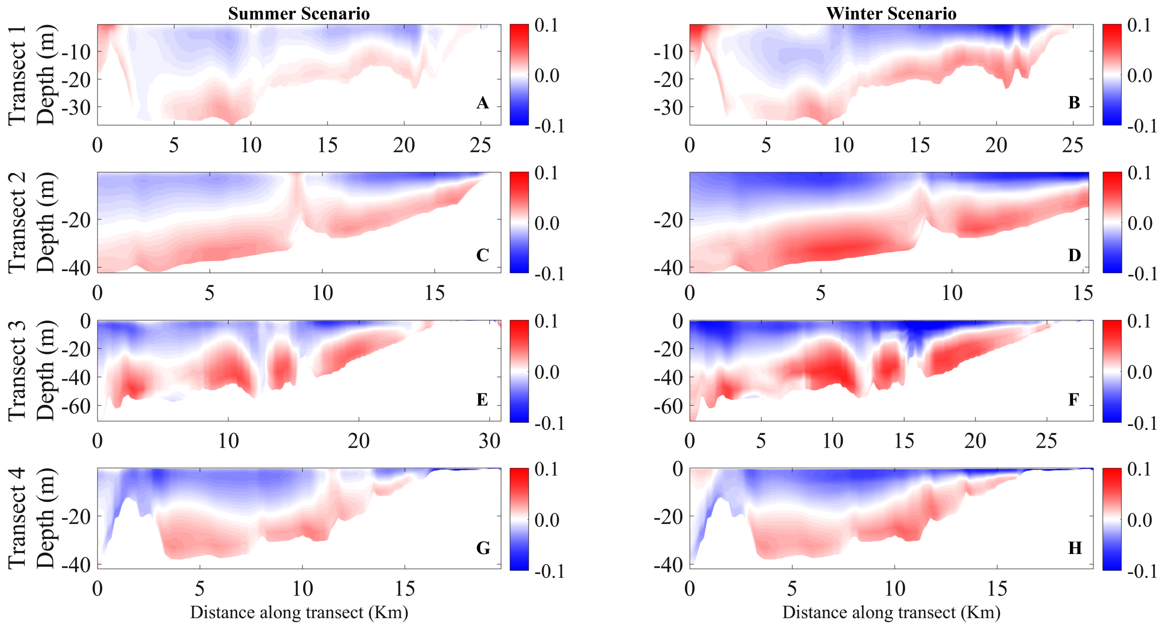

Figure 7.4: Vertical profiles of residual velocity component (ms^{-1}) along the Rias main axis. T1 (Ria de Vigo) – A and B; T2 (Ria de Pontevedra) – C and D; T3 (Ria de Arousa) – E and F; T4 (Ria de Muros) – G and H.

during winter, the tracer concentration starts to decrease in the upper layers, indicating that the stratification patterns are modified by winter thermohaline conditions, influencing the water renewal rates. In order to verify this important seasonal characteristic, Figure 7.5 represents the average water temperature simulated during the winter period. Figure 7.5 depicts a thermal inversion during winter (Figure 7.5 B, 7.5 D, 7.5 F and 7.5 H), resulting in warmer waters near the bottom, proving that the differences in vertical LRT patterns during winter are caused by the change in the vertical gradient of water temperature. These results are in agreement with the findings of Alvarez et al. (2005).

During winter, the downwelling processes noticed along the NW Iberian coast, caused by southern winds, induce the generation of thermal inversions (Alvarez et al., 2005). This seasonal thermohaline characteristic changes the water renewal processes, increasing the renewal rates in the surface layers, revealing an opposite pattern than found for the summer season. During summer (Figure 7.5 A, 7.5 C, 7.5 E and 7.5 G), when upwelling is prevalent, a strong thermal stratification is depicted, which retards vertical mixing and induces high LRT at surface layers.

Considering the previous results, the water column stratification processes play a major role in Rias Baixas water renewal patterns. On other hand, in Ria de Aveiro lagoon, the advective processes driven by tidal and river inflow actions governs water renewal. In fact, the low Rias Baixas freshwater inflow confined to the surface layers

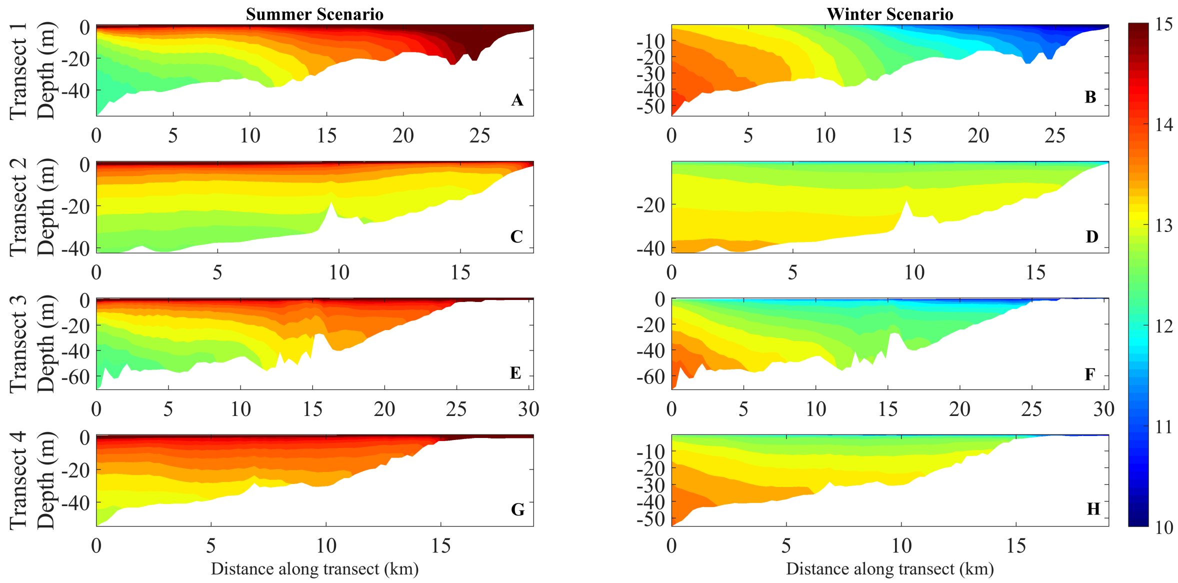

Figure 7.5: Vertical profiles of water temperature (°C) along the Rias main axis. T1 (Ria de Vigo) – A and B; T2 (Ria de Pontevedra) – C and D; T3 (Ria de Arousa) – E and F; T4 (Ria de Muros) – G and H.

combined with thermal stratification causes high local renewal times. The water that penetrates into the estuaries through the bottom layers is renewed with less efficiency during summer, due to the higher stability of the water column, which retards mixing processes.

7.3.2 IRT

The IRT results (Figure 7.6) corroborate the previously observed LRT patterns (Figure 7.2), showing higher renewal rates in Rias Baixas during entire year, while in Ria de Aveiro water renewal is inhibited during summer. Therefore, in theory, Rias Baixas have better hydrodynamic conditions for aquaculture production. In detail (Table 7.2), Ria de Aveiro integral renewal time ranges from 9.7 to 27.6 days from winter to summer. During high-stratified summer conditions, Ria de Pontevedra shows the lowest integral renewal time (16.0 days), followed by Ria de Muros with 18.8 days. The summer IRT for Ria de Vigo and Ria de Arousa are very similar, 23.1 and 21.0 days, respectively. During winter, Ria de Arousa shows the highest IRT (23.3 days), followed by Ria de Vigo with 17.3 days. Finally, Ria de Muros and Ria de Pontevedra presents an IRT of about 11.3 and 14.2 days, respectively. As observed in Figure 7.6, at the beginning of each tidal cycle, the concentration rapidly decreases to a temporary minimum (tidal oscillations observed in Figure 7.6), as the ebb flush out the water outside the estuaries. This tidal signature is more pronounced in Ria de Aveiro. During flood, the tracer concentration increases due to the partial return of

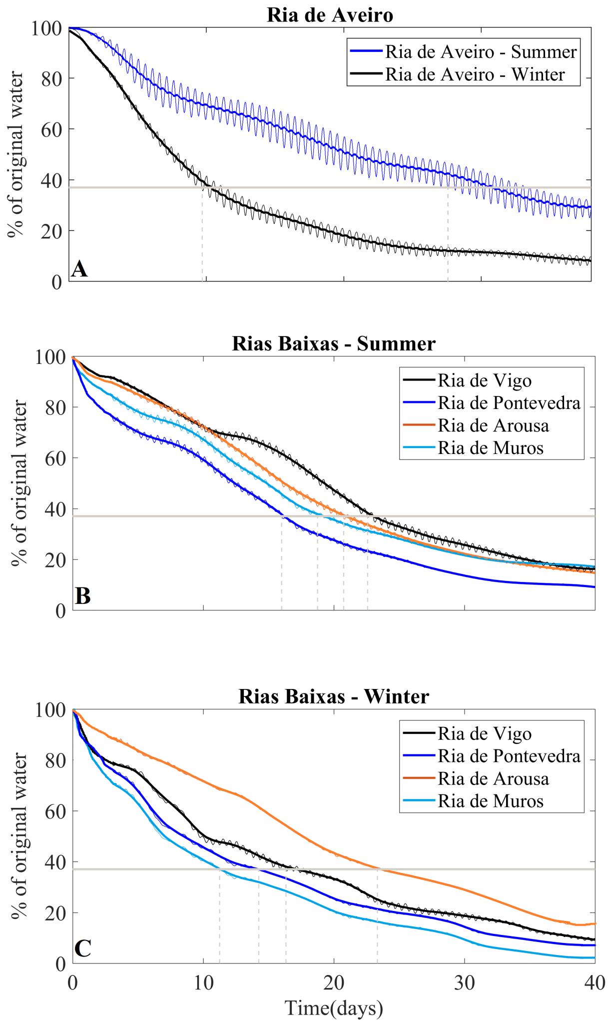

Figure 7.6: Percentage of original water remaining in Ria de Aveiro (A) and Rias Baixas (B, C) as a function of time. Vertical gray line represents the time when average concentration drops to 37% of its initial concentration.

the water that moved downstream during the previous ebb, and returns during the next flood. Both Ria de Aveiro and Rias Baixas flushed the water away very fast during the first days, since the water near the open sea boundary rapidly exits the system. The flushing rates decrease after the first few days and follow a long term exponential pattern.

7.4 Discussion

The local renewal and integral renewal times depend on various factors, such as tidal forcing, freshwater inflow, stratification processes driven by water temperature and salinity changes, and wind stress triggering upwelling or downwelling events. Tide

Table 7.2: IRT values (days) predicted for Ria de Aveiro and Rias Baixas, for both scenarios.

System	Winter	Summer
Ria de Aveiro	9.7	27.6
Ria de Vigo	17.3	23.1
Ria de Pontevedra	14.2	16.0
Ria de Arousa	23.3	21.0
Ria de Muros	11.3	18.8

is the main responsible for water flushing in Ria de Aveiro and Rias Baixas. The residence times difference between Ria de Aveiro and Rias Baixas is explained by local hydrodynamic and thermohaline processes, but also by their geomorphological characteristics. The shallow and narrow channels of the Ria de Aveiro tend to generate water retention in upstream areas, in opposition with a deep and wide geometry of Rias Baixas, with higher inflow and outflow fluxes. In fact, Dias (2001), Picado et al. (2009) and Valentim (2012) studied the Ria de Aveiro tidal asymmetry, and concluded that the lower and central parts of the lagoon, where lower LRT values are depicted, are ebb dominated, while the remote upstream zones are flood dominated. Flood dominant areas tend to accumulate material (water, sediments, pollutants, etc.) in their channels, whereas ebb dominant areas tend to flush properties seaward. The LRT horizontal pattern of Ria de Aveiro during summer, when the relative importance of tide is higher, is similar to the pattern found by Picado et al. (2009) and Valentim (2012) for tidal asymmetry.

Over the years, different methodologies to predict residence time have been followed in Ria de Aveiro, resulting in different residence time values. However, in this study, the patterns obtained by Dias (2001) and Dias et al. (2007) are confirmed. Therefore, Ria de Aveiro can be divided in three different distinct areas: (1) inlet area characterized by strong ocean influence, where water renewal is favourable for aquaculture practices during the entire year; (2) mid-channel areas, where LRT changes very fast under the influence of both forcings; (3) a third area at the far end of the Mira, S. Jacinto and Ílhavo channels characterized by unsuitable water renewal conditions for aquaculture production in summer and suitable under high freshwater inflow conditions, in winter. Nevertheless, high freshwater inflow may not benefit aquaculture production, since these locations are under low salinity and high turbidity conditions during these periods.

The combined effect of Rias Baixas local forcing results in very different spatial patterns comparing with Ria de Aveiro lagoon. During summer period, when upwelling takes place, the longitudinal gradient of LRT is negligible (is maximum in Ria de Aveiro, during this period). On the other hand, the vertical gradient of LRT is very important and governed by thermohaline processes. Despite the water renewal is considered suitable for aquaculture development over the entire domain (absolute LRT values lower than for Ria de Aveiro), the water renewal rates increase with depth. Under high river run-off, thermohaline processes also govern Rias Baixas WRT, in opposition to the advective features governing WRT at the Ria de Aveiro, which is typical in a well-mixed coastal system. During winter, Rias Baixas are divided into two different areas: a first area, close to the inlets, where thermal inversion enhances convective mixing; and a second area where, the contribution of salinity maintains the pattern observed in summer.

The LRT results, which are very relevant to assess the ecological, chemical and biological functioning of an estuary or lagoon (Abdelrhman, 2005), suggest that Rias Baixas have better hydrodynamic conditions and water renewal rates than Ria de Aveiro for sustainable aquaculture development. This important characteristic may be the basis for the intensive mussels production in Rias Baixas, with a production of 250 $\times$ 10^6 kg year^{-1}. In Rias Baixas, the areas where water is retained for more than 30 days are confined to a few enclosed bays of Ria de Arousa and Ria de Vigo. Indeed, the majority of aquaculture sites are located in areas with good water renewal both in Ria de Aveiro and Rias Baixas, which denotes the importance of renewal rates for local farmers.

The hydrodynamic suitability for Ria de Aveiro aquaculture exploitation, based on the analysis of LRT results, decreases in the upstream direction. From the middle channels to the head of Mira, S. Jacinto and Ílhavo channels, the water renewal conditions may not be suitable for aquaculture production. Concerning to Rias Baixas, excepting the upstream area of San Simón bay, water exchange seems to be adequate for aquaculture practices.

The geomorphological differences between both coastal systems are the main feature governing the average residence time. In Ria de Aveiro, high water retention is caused by its shallow and narrow channels which inhibits water exchange, in accordance with tidal asymmetry described by Dias (2001), Picado et al. (2009) and Valentim (2012). In contrast, the wide and deep estuaries of Rias Baixas promote water exchange, as a consequence of higher tidal prisms.

The differences in the mechanisms governing water renewal in Ria de Aveiro and Rias Baixas are a consequence of the differences in their stratification: a homogenized lagoon in opposition to a partially mixed estuarine system. Water exchange in Ria de Aveiro is ruled by advective processes, in which the freshwater inflow is the responsible for the seasonal variations. Contrarily, freshwater inflow play a minor role in Rias Baixas water exchange in comparison with the stratification events, in accordance with Dale et al. (2004). When water column is stratified (during summer due to solar heating combined with upwelling events, or in winter due to vertical salinity gradients from mid to upper estuaries), water exchange is retarded. On the other hand, when estuaries are well mixed (which occurs in winter, close to the inlets), water is renewed very fast.

Therefore, despite both systems have identical seasonal variability, their water renewal dynamics are ruled by different mechanisms depending on their geomorphology, freshwater inflow and vertical structure, constituting different challenges and concerns to the farmers.

These results aim to demonstrate the importance of numerical models in the estimation of the environmental factors ruling aquaculture. To study and compare a single variable in two contrasting systems, it was necessary to apply two different methodologies, which encompass the main processes of each estuarine system. In this study, the implementation of a 2-D model proved to be enough to study Ria de Aveiro water renewal processes, while for the Rias Baixas a more complex 3-D model revealed to be crucial for studying water renewal processes. Therefore, aquaculture quality in Ria de Aveiro, based on water renewal rates can be estimated assessing the variability of the inflow patterns (tidal amplitude (spring and neap tide) and freshwater inflow variations), while in Rias Baixas the vertical structure of the environmental variables may govern the aquaculture quality.

7.5 Conclusions

The main objective of this study was to assess the hydrodynamic functioning and thermohaline processes in two contrasting coastal systems (Ria de Aveiro and Rias Baixas), in order to investigate the water renewal rates for aquaculture purposes. Numerical simulations were conducted testing two scenarios: summer and winter.

In this context, the results obtained from this analysis indicate the following:

- Generally, water renewal rates in Rias Baixas are more suitable than in Ria de Aveiro;

- Water renewal rates are improved under winter conditions, for both coastal systems;

- Ria de Aveiro seasonal variability is governed by freshwater inflow seasonality, while variations in the vertical patterns of water temperature and salinity rules the

Rias Baixas LRT seasonal variability;

- Therefore, Ria de Aveiro LRT is governed by advective processes, while vertical thermohaline processes drive water renewal in Rias Baixas;

- Based on these results, Rias Baixas water renewal conditions are suitable for aquaculture practices, while the far end of S. Jacinto , Mira and Ílhavo channels are characterized by unsuitable water renewal conditions for aquaculture production;

- Areas where water is renewed with less efficiency may experience accumulation of detritus and organic matter inherent to production. Additionally, the natural food supply may be also inhibited.

Here, it were depicted different effects for different estuarine systems depending on estuary classification as a homogeneous (Ria de Aveiro), or partially mixed estuary (Rias Baixas), on the local geomorphology and on the local forcing. The combination of these effects is variable and specific to each coastal system, which reveals the importance of using a baroclinic 3-D model to study Rias Baixas hydrodynamic functioning, while a 2-D model to evaluate Ria de Aveiro water renewal proved to be efficient.

Finally, water renewal depends on several processes such as: tidal forcing and distortion, freshwater inflow, wind-driven processes (upwelling and downwelling events), water temperature and salinity variability. Therefore, the knowledge about hydrodynamic functioning and the flushing potential of the estuarine systems seems to be very important to select new sites for the development of an aquaculture farm.

The knowledge acquired in this chapter is important for the achievement of the main goal of this thesis, which consists in the application of a water quality model to predict aquaculture quality, assessing the spatial and temporal distribution of other geomorphological, chemical and biological variables (next chapter).

Chapter 8

A Habitat Suitability Model for Aquaculture Site Selection: Ria de Aveiro and Rias Baixas

8.1 Introduction

The strong and fast growing of aquaculture practices reflects on significant environmental impacts and in new challenges on management and planning in coastal areas, where these are deeply reported and debated in the literature. For example, Kalantzi and Karakassis (2006) and Mantzavrakos et al. (2007) assessed the sediment organic enrichment and eutrophication due to fish farming; beyond others, chemical pollution from heavy metals, organic and pharmaceuticals such as antibiotics was measured by Sapkota et al. (2008) and Lai and Lin (2009); Pusceddu et al. (2007) and Vezzulli et al. (2008) studied the alterations on biodiversity and ecological status of endemic species populations.

These types of stressors reinforces the need for sustainable practices to be considered during the early stages of planning and management of the different types of aquaculture activities. This chapter aims to present some results that can contribute to sustainable aquaculture activities in Ria de Aveiro and Rias Baixas, once the determination of the areas where natural conditions are suitable is essential for the development of sustainable operations in order to mitigate environmental stress and social conflicts, enhance economic development and promote sustainability in aquaculture sector, which is concretely defined by Boyd and Schmittou (1999) as the locations 'where ecological and economic viability persist indefinitely'.

In this chapter the analysis of a large database of geomorphologic, hydrodynamic and biogeochemical variables is presented, in order to characterize the spatial and temporal variability of fish and bivalves aquaculture suitability in Ria de Aveiro and Rias Baixas, through the development of a methodology consisting in the integration of the numerical modelling results into a habitat suitability model.

In this context, this chapter aims to fulfill the main objective of this thesis: identify preferential sites to ensure aquaculture expansion and proper operation in a sustainable manner,with minimal environmental impact and fairly low-cost, under optimal hydrodynamic and water quality conditions in Ria de Aveiro (Portugal) and Rias Baixas (Spain). The achievement of this objectives constitutes an important step forward in the planning of Ria de Aveiro and Rias Baixas human activities, green economy and environmental sustainability, in accordance with the strategic objective defined by European Union (EU) for the period 2014-2020. EU encouraged the member countries to increase and diversify the aquaculture production, in order to satisfy the growing demand and local development. In this chapter, a habitat suitability model is developed exploring the relationship between the key geomorphological, hydrodynamic and biogeochemical variables governing aquaculture and the spatial and temporal fish and bivalves production suitability.

8.2 Methodology

The habitat suitability estimation for fish and bivalves farming at Ria de Aveiro and Rias Baixas is computed in three main steps, which are described in detail in this section. Firstly, the hydrodynamic, morphological, chemical and biological variables affecting fish and bivalves are identified. Secondly, variable suitability functions (VSF) are defined to estimate the suitability of a location according to each variable. In third place, the VSF's are integrated into a weighted geometric mean, assessing the site habitat suitability (HS).

8.2.1 Variable Suitable Functions (VSF)

The model variables affecting fish and bivalves cultures were chosen according to the literature review performed in section 1.3.4, which comprise geomorphological, hydrodynamic and biochemical variables. Therefore, the input variables for HS model are water depth, current velocity, summer LRT (when the less favourable conditions are predicted (Chapter 7)), water temperature, salinity, pH, dissolved oxygen, Trophic index (TRIX) and chlorophyll *a* concentration.

The variables used for HS model are self explanatory except, TRIX. This index is calculated in order to determine the eutrophication level of a certain area and to assess the water quality, based on a formulation adopted by Vollenweider et al. (1998), given by:

$$TRIX = \frac{Log_{10}(PO_4 \times TN \times Chla \times D\%O_2) + a}{b} \tag{8.1}$$

where PO_4 is total inorganic phosporus, as $P\text{-}PO_4$, in μgL^{-1}; TN is the dissolved organic nitrogen ($N\text{-}NO_3 + N\text{-}NO_2 + N\text{-}NH_4$), as μgL^{-1}; $D\%O_2$ is the % deviation of the oxygen concentration from saturation conditions; *Chl a* is the chlorophyll a concentration as μgL^{-1}. The parameters a=1.5 and b=1.2 are scale coefficients, defined by Giovanardi and Vollenweider (2004) in order to stablish the lower limit value of the index and also to fix the scale range from 0 to 10. Table 8.1, adapted from Fiori et al. (2016), details TRIX values and the corresponding trophic state and water quality conditions.

In order to assess the site suitability regarding to local geomorphology, hydrodynamics, physics and biogeochemistry, variable suitable functions were defined (Ortigosa et al., 2000; Vincenzi et al., 2006). For each specific variable, the suitability is expressed by a Suitability Index (SI) defined on a scale between 0 and 1, in which 1 is a suitable habitat and 0 represents an unsuitable habitat (Vincenzi et al., 2006).

Table 8.1: Reference values of the trophic index (TRIX) and corresponding water quality and trophic conditions.

Conditions	**TRIX values**	**State**	**Water quality conditions**
Oligotrophic	TRIX $<$ 4	Elevated	Low water productivity High water transparency No water colors anomalies Oxygen oversaturation in the bottom
	4 $<$ TRIX $<$ 5	Good	Moderate water productivity Ocasional water turbidity Ocasional water color anomalies Ocasional hypoxia events in the bottom
Mesotrophic	5 $<$ TRIX $<$ 6	Medium	High water productivity Low water transparency Frequent water colors anomalies Hypoxia and anoxia events in the bottom Benthic communities stress
Eutrophic	TRIX $>$ 6	Poor	Strongly water productivity High water turbidity Persistent water colors anomalies Hypoxia and anoxia in the bottom Mortality of benthic communities Strong decrease of biodiversity

VSF's (Figure 8.1) are non-linear functions generated by the knowledge acquired in section 1.3.4. Ria de Aveiro and Rias Baixas have the same VSF relationship between model variables and suitability index (SI) for all descriptors, excepting for bathymetry, due to the type of production that already exists in both coastal systems. In Ria de Aveiro (Figure 8.1 A dark dashed gray), inshore bivalves production takes place in shallow areas, including intertidal ones, while in Rias Baixas (Figure 8.1 A light gray), the bivalves cages are permanently covered by water. From a theoretical point of view, bivalves production in Rias Baixas is optimized when the ropes reach their maximum length allowed by law - 12 meters. Therefore, SI is considered maximum for depths $\geq$ 12 meters.

8.2.2 Habitat Suitability Model

Multi-criteria techniques are used to combine and aggregate contributing variables into a spatially variable (x and y coordinates) Suitability Index ($SI_{(x,y)}$). Therefore, the $\mathrm{SI}_{(x,y)}$ is computed as the weighted geometric mean of VSF's, which converts the original data (outputs from the hydrodynamic and water quality models) to standardized aquaculture suitability scores (Arnold et al., 2000; Vincenzi et al., 2006; Silva et al., 2011), as described in Equation 8.2:

$$SI_{(\mathrm{x,y})} = \left(\prod_{i=1}^{9} VSF_i^{w_i} \right)^{\frac{1}{\sum_{i=1...9}^{w_i}}} \tag{8.2}$$

where VSF_i are the spatially variables modified into suitability index (Figure 8.1); w_i are the weights corresponding to the relative importance of each descriptor; and i=1...9 is an index identifying the corresponding input variables.

A weighted geometric mean is applied (Silva et al., 1999; Vincenzi et al., 2006), where to each variable is assigned a weight to indicate relative importance, introducing some subjectivity and ambiguity to the habitat model. Here, the criterion weights were estimated following the pairwise comparison method (Saaty, 1977). In summary, each criterion is compared to all the others and a value between 1 and 9 is allocated according their relative importance (Table 8.2).

In this study the pairwise comparison matrix for fish and bivalves was built (Table 8.3). Table 8.4 presents the criterion weights, that were computed from the pairwise matrix.

According to Lawson (2013), dissolved oxygen is the main limiting factor for fish culture in estuaries and lagoons, since these are areas with high rates of biological activity, with a high DO demand. For that reason, DO is considered the descriptor

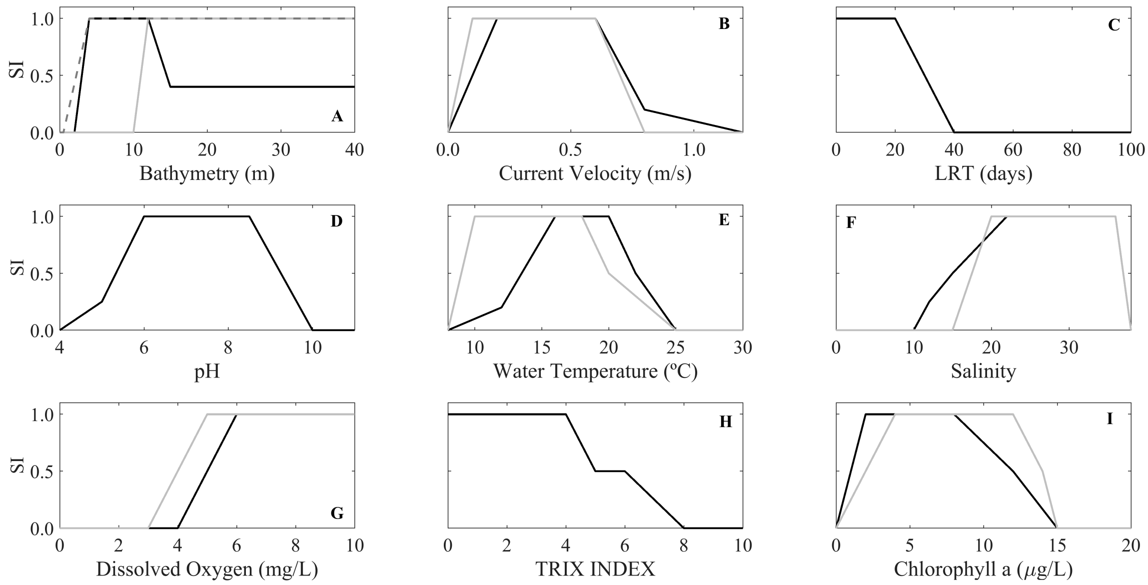

Figure 8.1: The VSF relationships between model variables and suitability for fish (black) and bivalves (gray) production, for the descriptors selected: (A) bathymetry, (B) velocity, (C) LRT, (D) water temperature, (E) salinity, (F) pH, (G) oxygen, (H) chlorophyll a, (I) TRIX index. Light gray line at sub-figure (A) corresponds to Rias Baixas, while dashed dark gray line corresponds to Ria de Aveiro. Same VSF relationships adopted for fish and bivalves: only the black line is shown (Sub-figures (C), (D) and (H)).

with higher relative weight, followed by water temperature, which highly influence fish breathing and growth. The seasonal and spatial dynamics of water temperature also influence other descriptors, such as dissolved oxygen, since the increase of water temperature enhances bacteria activity (including pathogenic), and consequently make DO to decrease (Lawson, 2013). Then, hydrodynamics (LRT and current velocity) follows dissolved oxygen and water temperature, since fish is extremely dependent on the efficiency of the water renewal, since detritus and excretions inherent to production must be flushed away from the culture sites. Then, batymetry and salinity have similar weight, and smaller weights have been set for chlorophyll *a* concentration, TRIX and pH.

Regarding to bivalves, according with the findings of Melià et al. (2004), the maximum relative weight has been assigned to the hydrodynamic regime (LRT and current velocity), as they play a major role in determining growth processes of filter-feeder organisms by influencing water temperature, phytoplankton, nutrient circulation and DO dynamics. Chlorophyll *a*, as phytoplankton indicator, is the main source of food avoiding chemical feeding, reducing the production costs. Dissolved oxygen is also a key factor for bivalve growth, as described in the last paragraph. A very relevant, though smaller, weight is given to bathymetry and salinity, and further smaller weights have been assigned for the remaining parameters, TRIX and pH.

The use of the geometric mean implies that, if a site is unsuitable with respect to one parameter ($VSF_{x,y}$=0), the overall suitability index ($SI_{(x,y)}$) is 0 regardless of the $VSF_{x,y}$ value for the other variables (Vincenzi et al., 2006; Soniat and Brody, 1988). This provides a distinct advantage over other type of models (Perez et al., 2005; Dubois and Habbane, 2002), which computes $SI_{(x,y)}$ using an arithmetic mean.

The numerical model results (one year simulations, after 6 months of snip-up) were converted into a suitability index ($SI_{(x,y)}$), for each time step of hydrodynamic and water quality models. Then, the percentage of time (POT) that the specimens (fish or bivalves) are comfortable in the environment ($SI > 0.6$) was assessed. Finally, this percentage of occurrence was converted in a final Suitability Index according to the following equation.

$$SI = \begin{cases} 0, & \text{if } POT \leq 25\%. \\ 0.025 \times POT - 0.625, & \text{if } 25\% < POT < 65\%. \\ 1, & \text{if } POT \geq 65\%. \end{cases} \tag{8.3}$$

The final aquaculture suitability was scored in Unsuitable, Medium, Good and Suitable according the intervals presented in Table 8.5.

Numerical simulations were performed for 18 months (July 1st of 2015 to January 1st of 2017), in which the period between July 1st, 2015 and January 1st, 2016 was the water quality model spin-up. Hydrodynamic and water quality models configurations described in Chapter 5 were used in order to achieve the main goal of this chapter. The model results were analyzed and horizontal fields of the selected descriptors (depth-averaged) were depicted, for both study areas, as well as the spatial distribution of the depth-average aquaculture suitability in Ria de Aveiro and Rias Baixas. Vertical

Table 8.2: Importance scale of pairwise comparison.

Importance Scale	Definition
1	Equal importance
2	Equal to moderate importance
3	Moderate importance
4	Moderate to strong importance
5	Strong importance
6	Strong to very strong importance
7	Very strong importance
8	Very strong to extremely strong importance
9	Extreme importance

Table 8.3: Pairwise comparison matrix for aquaculture suitability criteria.

		Bathymetry	Velocity	LRT	pH	Temperature	Salinity	Oxygen	TRIX	Chlorophyll a
Fish	Bathymetry	1	1/2	1/3	2	1/3	1	1/3	1	1
	Velocity	2	1	1/2	3	1/2	2	1/2	2	3
	LRT	3	2	1	4	1	3	1	5	5
	pH	1/2	1/3	1/4	1	1/5	1/2	1/5	1	1
	Temperature	3	2	1	5	1	3	1	6	6
	Salinity	1	1/2	1/3	2	1/3	1	1/4	1	1
	Oxygen	3	2	1	5	1	4	1	6	6
	TRIX	1	1/2	1/5	1	1/6	1	1/6	1	1
	Chlorophyll a	1	1/3	1/5	1	1/6	1	1/6	1	1
		Bathymetry	Velocity	LRT	pH	Temperature	Salinity	Oxygen	TRIX	Chlorophyll a
Bivalve	Bathymetry	1	1/2	1/2	2	1/2	1	1/2	2	1/2
	Velocity	2	1	1/2	4	1	3	1	5	1
	LRT	2	2	1	4	1	3	1	5	1
	pH	1/2	1/4	1/4	1	1/3	1/2	1/3	1/2	1/3
	Temperature	2	1	1	3	1	3	2	3	1
	Salinity	1	1/3	1/3	2	1/3	1	1/2	1	1/2
	Oxygen	2	1	1	3	1/2	2	1	3	1/2
	TRIX	1/2	1/5	1/5	2	1/3	1	1/3	1	1/4
	Chlorophyll a	2	1	1	3	1	2	2	4	1

Table 8.4: Criterion weights obtained from the pairwise comparison matrix.

Criterion	Weight	
	Fish	Bivalve
Bathymetry	5.84	7.60
Velocity	11.30	16.54
LRT	19.84	17.89
pH	3.88	3.57
Temperature	21.82	15.20
Salinity	5.78	6.25
Oxygen	22.60	12.52
TRIX	4.70	5.19
Chlorophyll *a*	4.57	15.20

Table 8.5: Score for the aquaculture suitability index.

SI	Suitability Score
$0.00 \leq \text{SI} < 0.40$	Unsuitable
$0.40 \leq \text{SI} < 0.60$	Medium
$0.60 \leq \text{SI} < 0.80$	Good
$0.80 \leq \text{SI} \leq 1.00$	Suitable

profiles of Rias Baixas suitability score were carried out along the main axis of the Rias, as already performed in Chapter 7. Moreover, temporal evolution of the suitability score was also computed, by averaging the suitability scores in the grid cells, at each model time step.

8.3 Results

8.3.1 Habitat Suitability Model

The spatial maps of selected descriptors for fish and bivalves aquaculture exploitation in Ria de Aveiro, illustrated in Figures 8.2 and 8.3, are based on the individual criteria previously defined, ranging between unsuitable and suitable scores for aquaculture exploitation.

As widely mentioned during this thesis, Ria de Aveiro has a complex geometry characterized by shallow and narrow channels. For this reason, the intertidal and the shallow areas of the channel's margins are excluded for fish cultures (Figure 8.2(A)). From the hydrodynamic point of view, Ria de Aveiro has a good range of water velocity for fish production (Figure 8.2(B)), excepting the channels margins, from mid to upper

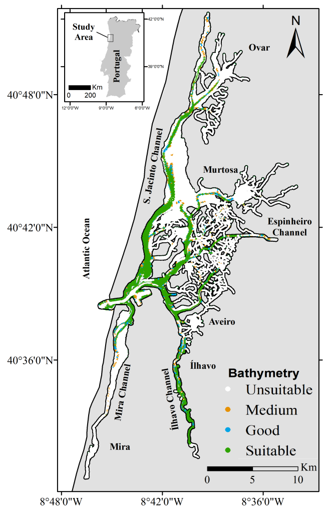

(A) Bathymetry

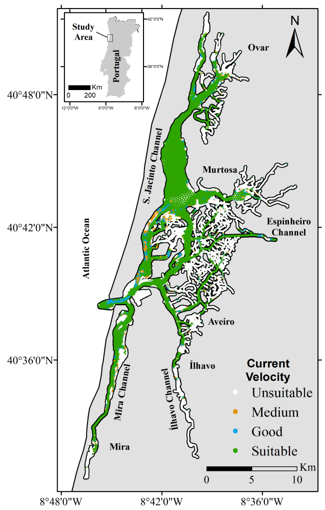

(B) Velocity

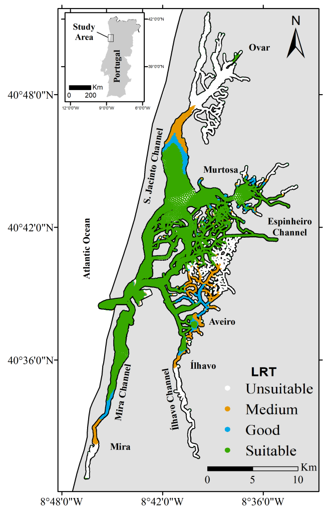

(C) LRT

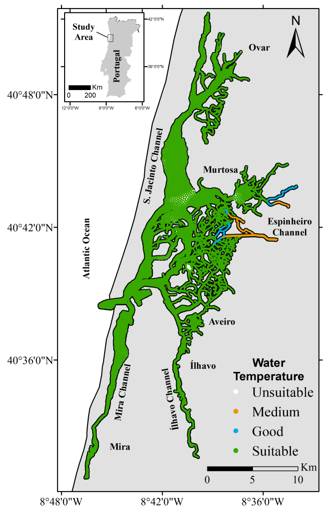

(D) Water Temperature

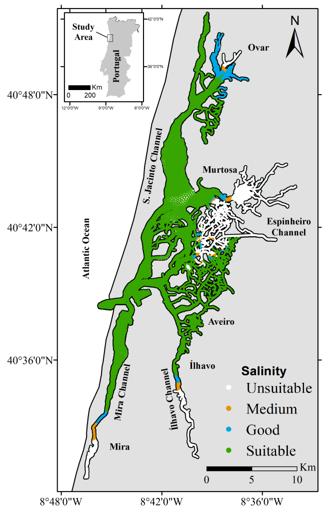

(E) Salinity

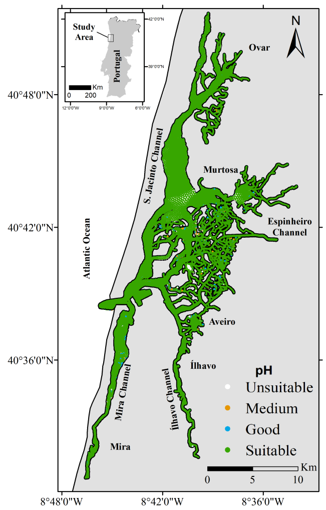

(F) pH

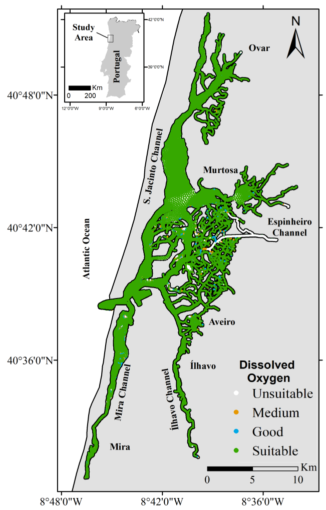

(G) Oxygen

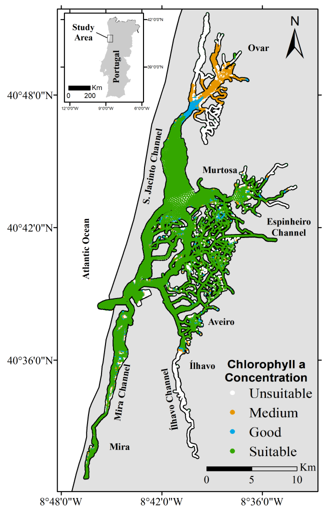

(H) Chlorophyll *a*

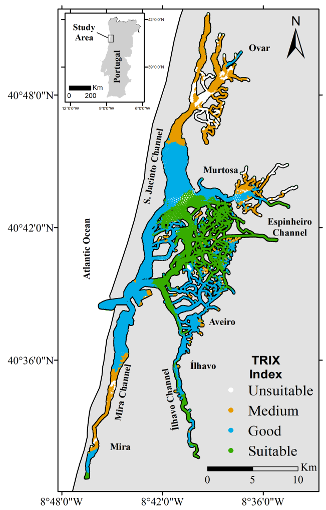

(I) TRIX

Figure 8.2: Maps of descriptors classification for fish culture at Ria de Aveiro: (A) bathymetry, (B) velocity, (C) LRT, (D) water temperature, (E) salinity, (F) pH, (G) oxygen, (H) chlorophyll *a*, (I) TRIX index.

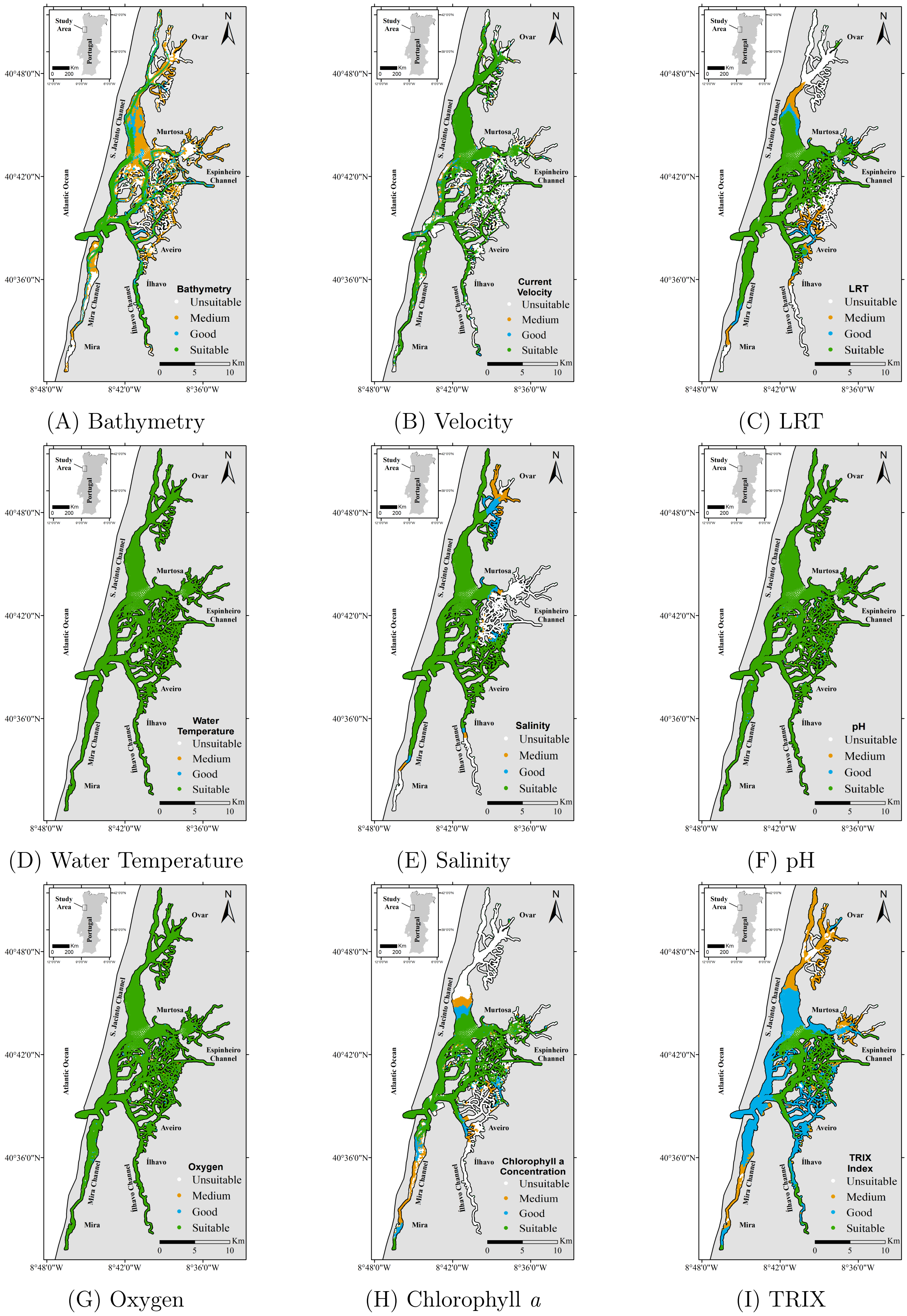

(A) Bathymetry (B) Velocity (C) LRT

(D) Water Temperature (E) Salinity (F) pH

(G) Oxygen (H) Chlorophyll *a* (I) TRIX

Figure 8.3: Maps of descriptors classification for bivalves culture at Ria de Aveiro: (A) bathymetry, (B) velocity, (C) LRT, (D) water temperature, (E) salinity, (F) pH, (G) oxygen, (H) chlorophyll *a*, (I) TRIX index.

Ílhavo channel (which is the most limited channel regarding to water velocity) and the central area of the lagoon. The hydrodynamic suitability for fish culture at Ria de Aveiro, based on LRT results studied in Chapter 7 (Figure 8.2(C)), decreases in the upstream direction. From the middle to the head of Mira, S. Jacinto and Ílhavo channels, water renewal conditions are not suitable for aquaculture practices, for the reasons depicted in the previous chapter. The exception is the Espinheiro channel, because even under summer conditions, the freshwater inflow is enough to flush the water away to other channels and onto the coast. This analysis is also valid for bivalves, once the ranges of LRT adopted here are the same for both cultures (Figure 8.1).

Water temperature (Figure 8.2(D)) provides information on suitable conditions for fish cultures, at the percentile of occurrence adopted in this study. The lagoon has suitable water temperature during the entire year, excepting close to Vouga river, which presents medium suitability. However, some shallow areas, with low current velocity, are susceptible to overheating for short periods during the summer, leading to an increase of bacterial activity and consequently oxygen depletion. The fish production in these areas is limited by bathymetry and water velocity descriptors, despite not limited by water temperature in the analyzed percentile. Salinity is highly favourable for fish culture from inlet to mid-channels areas. The suitability index, based on salinity descriptor, decreases where the influence of freshwater sources within the lagoon increases (Figure 8.2(E)). Areas that are permanently influenced by river action, where salinity decreases down to 10, fish uses more dissolved oxygen for respiration, which cause an increase in their metabolic rates (Nebel et al., 2005).

The pH and dissolved oxygen concentration at the analyzed POT does not limit fish (Figures 8.2 (F) and (G)) and bivalves (Figures 8.3 (F) and (G)) cultures. Regarding to chlorophyll *a* concentration, fish cultures are limited from mid to the upstream area of the Ílhavo channel, which is characterized by high turbidity levels, which increase the limitation by light of phytoplankton growth. Some medium suitability and unsuitable areas are located in the upstream S. Jacinto channel. TRIX descriptor (Figure 8.3(I)), which has the same suitability ranges for fish and bivalves (Figure 8.1), indicates as suitable those areas under the influence of the freshwater outflow from Vouga river. Good conditions are predicted at the lagoon west-central area and at Ílhavo channel. In the upstream areas of S. Jacinto and Mira channels, medium suitability is found from the TRIX descriptor results.

Regarding to bivalve culture, bathymetry descriptor (Figure 8.3(A)) provides a wider range of suitable conditions comparing with fish production, since some oysters cages are located in shallow and/or intertidal areas of the Mira channel. In this context, the majority of areas classified as unsuitable for fish cultures, are classified as medium suitability areas for bivalves production. Water velocity (Figure 8.3(B)) presents a pattern similar to that obtained for fish culture. The main difference is the slight increase of suitable areas in the channels margins, due to difference in the *VSF* between fish and bivalves: SI=1 from 0.2 to 0.6 ms^{-1} for fish cultures and from 0.1 to 0.6 ms^{-1} for bivalves.

Concerning water temperature, the model predicts total suitability for bivalves production (Figure 8.3(D)). Salinity descriptor, presented in Figure 8.3(E), depicts a pattern similar to that found for fish cultures. The unsuitable areas are those with high freshwater influence (upstream areas of Ílhavo, Mira and Espinheiro channels, Laranjo bay and in Cáster river mouth).

Similarity to water temperature, dissolved oxygen is suitable for bivalves production in the whole area of the lagoon, since both variables are highly related to each other. Chlorophyll *a*, which is one of the most important variables for this type of aquaculture, since it provides food to bivalves, is limited from middle to the upstream areas of S. Jacinto and Ílhavo channels, where the most turbid areas are characterized by the presence of muddy sediments.

Maps of descriptors for favourable conditions for the Rias Baixas fish farm (Figure 8.4), anticipate that the pelagic characteristics of the estuarine system may not be adequate for aquaculture practices. As analyzed in the previous chapter, good water renewal rates are depicted for Rias Baixas (Figure 8.4 (C)), constituting suitable LRT conditions for fish cages presences, except in the upstream areas of Ria de Vigo (San Simon bay) where unsuitable areas are identified, and at the upstream areas of Ria de Arousa (good and medium scores). Together with LRT, salinity (Figure 8.4 (E)), pH (Figure 8.4 (F)) and chlorophyll *a* (Figure 8.4 (H)) conditions are suitable for finfish cultures. The high depths observed in the main channels of Rias Baixas (Figure 8.3 (A)) make exploitation expensive, giving to these locations medium suitability (SI=0.4).

In opposition, fish cultures at Ria Baixas are mainly limited by water temperature (Figure 8.4 (D)), which is lower than desirable for this type of practices. Additionally, tidal currents (Figure 8.4 (B)) are frequently lower than 0.1 ms^{-1}, mainly in Rias de Pontevedra and Muros, which is lower than the desirable for aquaculture practices (Katavić and Dadić, 2000). Furthermore, the model results for dissolved oxygen (Figure 8.4 (G)) reflect the processes already noticed in Chapter 3, in which periods of low oxygen concentration or even hypoxia events are depicted in Rias Baixas, strongly disadvantaging fish cultures, which are very sensitive to low DO concentrations (Lawson, 2013). Finally, TRIX (Figure 8.4 (I)) does not prevent production, ranging from medium and good conditions for fish and bivalves farming.

The selected descriptors for bivalve cultures foresees good results for the final suitability maps. Once LRT, pH and TRIX were already analyzed in the previous paragraphs, the Rias Baixas bivalves production is only inhibited by local geomorphology (Figure 8.5 (A)) at the upstream areas of rias and some enclosed bays at Rias de Vigo and de Arousa, characterized by low water depth, and by low current velocity (Figure 8.5 (B)) in the main channel margins. The remaining descriptors presents suitable conditions for bivalves culture.

Final outputs from the fish suitability model for Ria de Aveiro and Rias Baixas (Figure 8.6) present very different results. The Ria de Aveiro fish suitability model (Figure 8.6 A) indicates that 22% of the lagoon area is classified as suitable for sustainable fish culture. The areas considered "good" and "medium" are about 4% of the total Ria de Aveiro. The suitable areas are mainly located in the main channels axis, from the inlet to mid-channel areas. In the channel margins, the low depth, low current velocity and high water retention preclude the fish culture. In the Mira, S. Jacinto and Ílhavo channel upstream areas, chlorophyll *a* concentration, salinity together with high local residence times make those areas unsuitable.

Rias Baixas fish suitability model (Figure 8.6 C) confirms that there is an absence of in-water pelagic fish cultures. Due to high water depth and intense upwelling events, Rias Baixas water temperature is lower than desirable for high fish growth rates. The most produced fish species in the Iberian peninsula, such as sea bass and sea bream, have ideal growth rates between 18-24°C (Egna and Boyd, 1997). The yearly mean water temperature of Rias Baixas is 13.34°C, which is considerably lower than the fish comfort zones, which would inhibit their growth.

Furthermore, the high depth locations may influence the equipment and materials used for moorings, which increase the implementation and maintenance costs. During maintenance procedure, if diving inspections are necessary, deep sites may present a problem, requiring specific training and professional and expensive gear for working at higher depths. The exceptions are areas classified as medium and good in middle and upstream areas of Ria de Vigo, close to Ria de Muros head and in two sheltered bays in Ria de Arousa.

The vertical profiles determined for fish suitability model in the main-axis of the Rias (Figure 8.7 A, C, E and G) reinforce and confirm the depth-averaged results. Medium score for fish cultures is only observed in the top layers of Ria de Vigo main channel, and in San Simon bay region of Ria de Vigo.

Concerning to bivalves, for the Ria de Aveiro lagoon, due to their higher resilience and adaptability to the environment, the *SI* model predicts a larger exploitable area (Figure 8.6 B). The unsuitable areas for bivalves production are confined to channels margins, narrow channels in the central area of the lagoon, upstream area of S. Jacinto

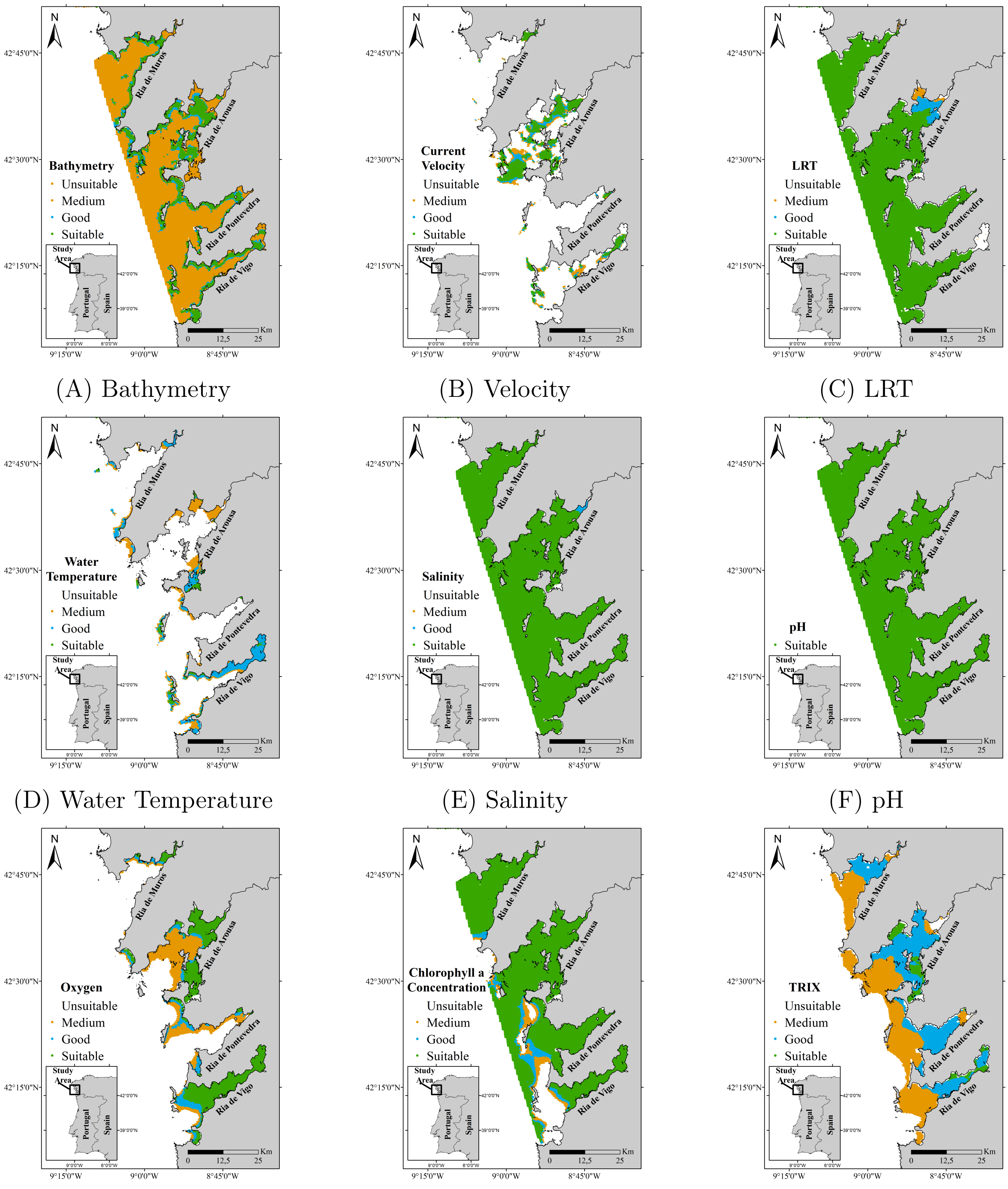

(A) Bathymetry (B) Velocity (C) LRT

(D) Water Temperature (E) Salinity (F) pH

(G) Oxygen (H) Chlorophyll *a* (I) TRIX

Figure 8.4: Maps of descriptors classification for fish culture at Rias Baixas: (A) bathymetry, (B) velocity, (C) LRT, (D) water temperature, (E) salinity, (F) pH, (G) oxygen, (H) chlorophyll *a*, (I) TRIX index.

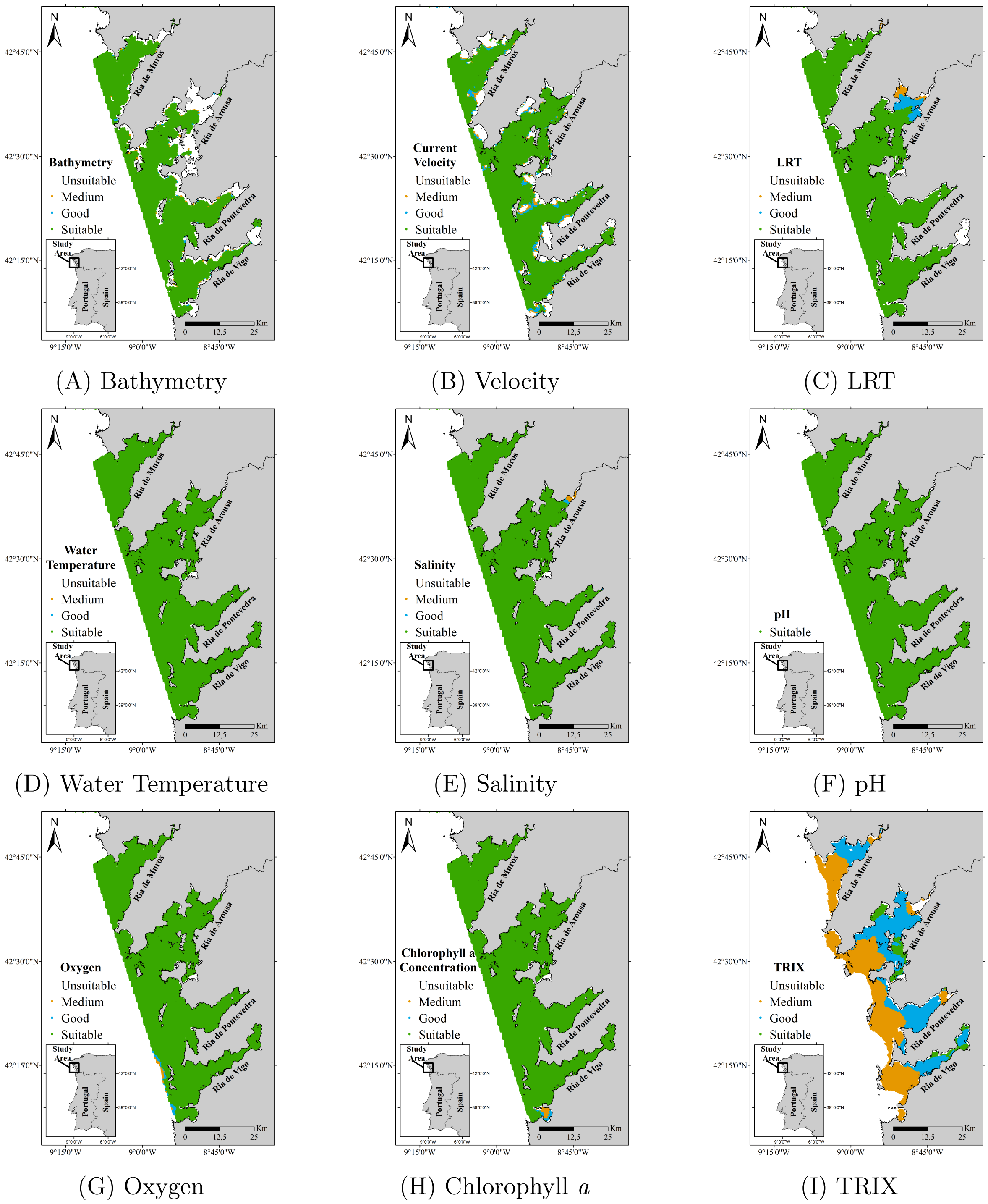

(A) Bathymetry (B) Velocity (C) LRT

(D) Water Temperature (E) Salinity (F) pH

(G) Oxygen (H) Chlorophyll *a* (I) TRIX

Figure 8.5: Maps of descriptors classification for bivalves culture at Rias Baixas: (A) bathymetry, (B) velocity, (C) LRT, (D) water temperature, (E) salinity, (F) pH, (G) oxygen, (H) chlorophyll *a*, (I) TRIX index.

channel, and from middle to upstream areas of the Ílhavo channel, which are characterized by high LRT and low current velocity that inhibits the supply of oxygen and nutrients, and the dilution of excess organic matter inherent to the production. In fact, about 31% of the lagoon is considered suitable for bivalves production, located from inlet to the middle of S. Jacinto, Mira, Espinheiro and Ílhavo channels. In the boundary between suitable and unsuitable model predictions, good and medium suitability areas are depicted, comprising 12.1% and 5.5% of the lagoon total area, respectively.

Regarding Rias Baixas, the habitat suitability model results are in accordance with the high production in the region, which is the largest area of mussel *Mytilus galloprovincialis* in Spain, with more than 90% of the total country production. Generally, Rias Baixas (Figure 8.6 D) are very suitable (62.3% of the total area) for bivalve production, in particular for *Mytilus galloprovincialis*. The unsuitable areas are confined to their margins, upstream areas of Ria de Vigo (San Simon Bay) and of Ria de Arousa. Medium suitability (8.9% of the Rias area) regions are mainly located at upstream areas of Ria de Muros and Ria de Pontevedra, and in the southern bay of Ria de Arousa. It should be pointed out that about 85% of the 3266 mussel rafts present in the Rias Baixas are concentrated in areas predicted as suitable, and 15% in areas considered Medium and Good. None of the actual aquaculture sites are located in areas considered unsuitable by the model.

The vertical profiles (Figure 8.7 B, D, F and H) show that the model predicts unsuitable areas for aquaculture practices in bottom layers close to the inlets for three main reasons: low water temperatures as consequence of intense upwelling events; high water depth; and low dissolved oxygen concentrations due to the vertical processes analysed in Chapter 3. However, these unsuitable areas predicted by the model does not affect mussels production, once the mussel rafts ropes have a maximum length of 12 meters, which is lower than the depths considered unsuitable by the model (Ria de Vigo: from 18.6 m; Ria de Pontevedra: from 38.9 m; Ria de Arousa: from 22.1 m; Ria de Muros: from 28.7 m). In upstream areas of the estuaries, the "unsuitable" score regions are vertically homogeneous. These regions are limited by different descriptors: upstream area of Ria de Vigo is limited by LRT; close to Ulla river (Ria de Arousa), TRIX limits bivalves production, while the remaining unsuitable area of Ria de Arousa is caused by depths lower than 10 meters; bathymetry also limits the exploitation in the upstream areas of Rias de Pontevedra and Muros.

As important as knowing the most and least suitable locations for aquaculture, it is also important the knowledge about the seasons when farmers need to be more careful with their production. In this context, Figure 8.8 depicts the time series of suitability scores for fish and bivalves for Ria de Aveiro (Figure 8.8 A and B) and for

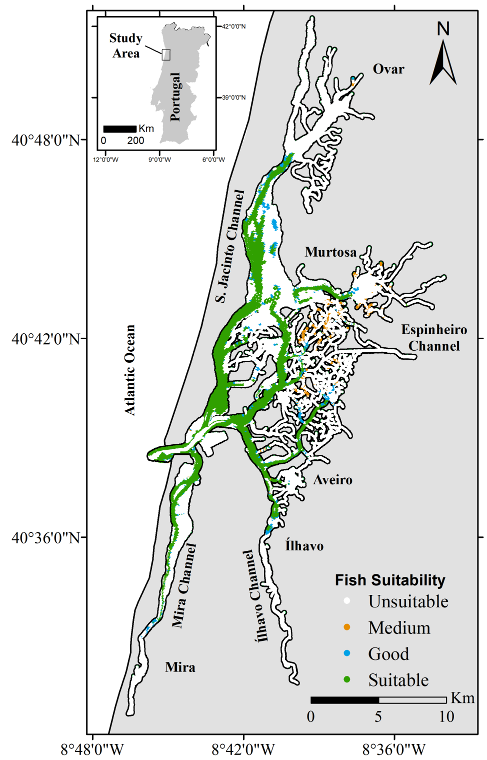

(A) Ria de Aveiro - Fish

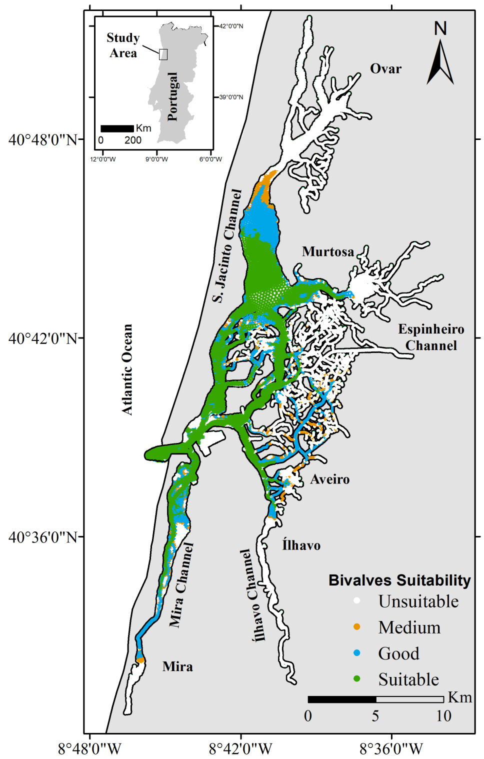

(B) Ria de Aveiro - Bivalves

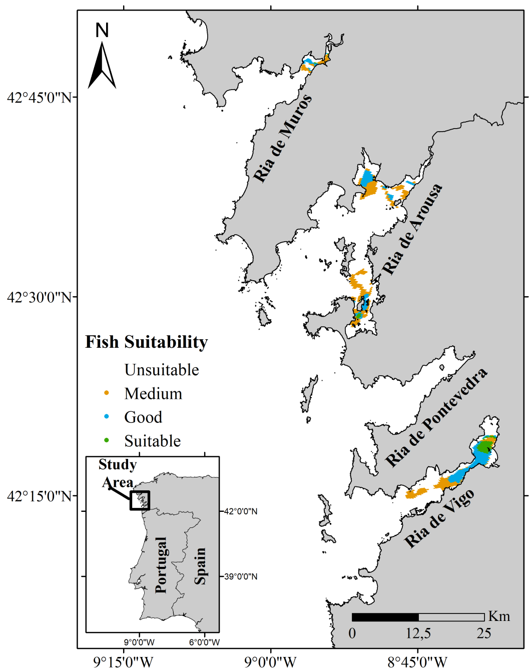

(C) Rias Baixas - Fish

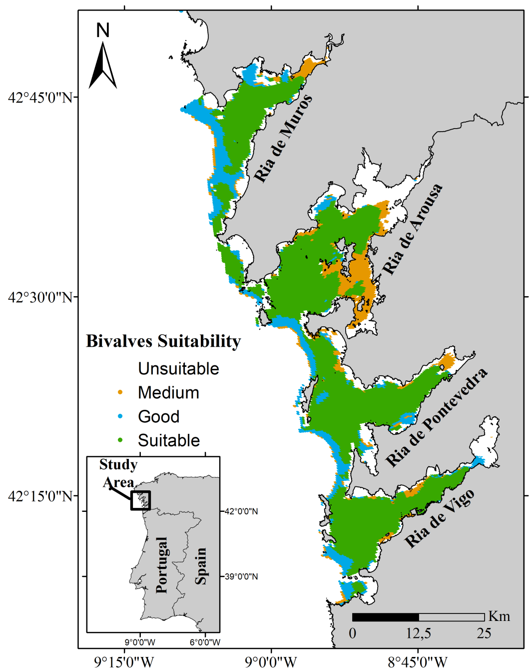

(D) Rias Baixas - Bivalves

Figure 8.6: Spatial distribution of the depth-averaged local aquaculture suitability in Ria de Aveiro and Rias Baixas for: (A) fish at Ria de Aveiro; (B) bivalves at Ria de Aveiro, (C) fish at Rias Baixas; and (D) bivalves at Rias Baixas.

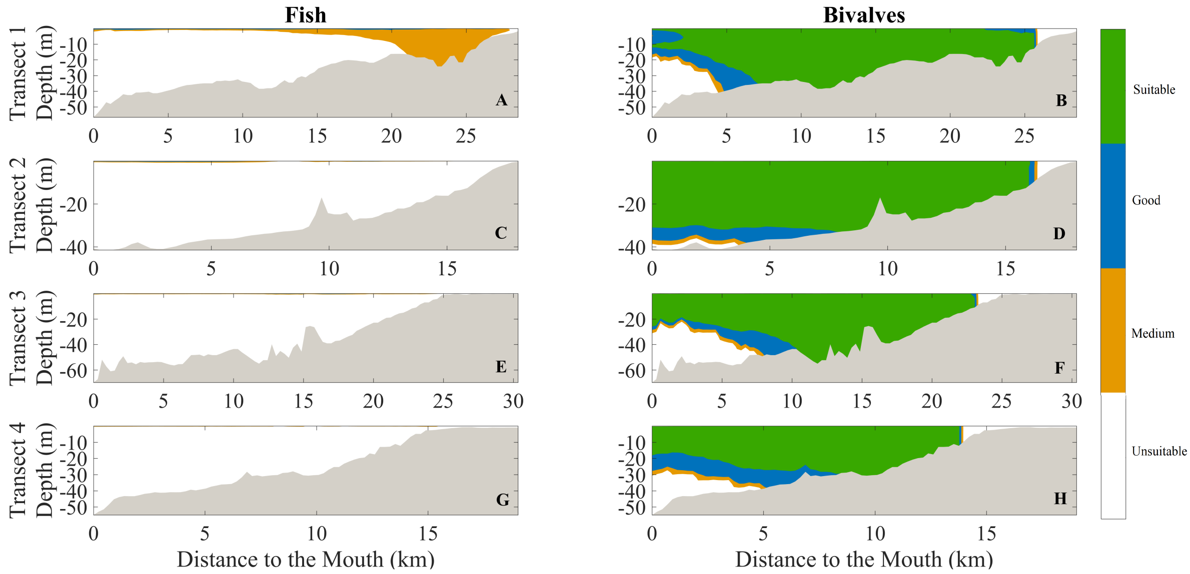

Figure 8.7: Vertical profiles of aquaculture suitability for fish (A, C, E and G) and bivalves (B, D, F and H) along the Rias main axis.

Rias Baixas (Figure 8.8 C, D, E and F). For the Ria de Aveiro, the seasonal variability is different depending on the type of production, fish or bivalves. The fish production in Ria de Aveiro (Figure 8.8 A) is optimized from September to November, when the estuarine water is still enriched with nutrients and phytoplankton due to the biotic summer events, but the water temperature has already decreased leading to higher dissolved oxygen concentrations. On the other hand, during winter, Ria de Aveiro water temperature decreased enough to inhibit fish growth rates. Furthermore, high freshwater inflow leads to salinities below 20 from middle to the upstream areas of the lagoon's channels. Regarding bivalves (Figure 8.8 B), higher values of suitability scores are computed during spring phytoplankton blooms. This effect is more strongly observed in bivalves SI than in fish SI, because this descriptor has a high relative importance for bivalves (w_i=15.20) and low for fish (w_i=4.57), since phytoplankton is the main source of food of bivalves. The absence of phytoplankton from December to March inhibits bivalves production in Ria de Aveiro, due to the low access to natural food.

In Rias Baixas, fish suitability score (Figure 8.8 C) is generally low. The model results predicts minimum suitability scores during summer due to the low dissolved oxygen concentration, and in some cases hypoxia events, in accordance with the results achieved in Chapter 3. Since dissolved oxygen concentration is the main driver of fish recruitment (w_i=22.60), this may affect the implementation of fish cultures. During winter, when oxygen concentrations are replenished, suitable score increases. Figure 8.8 D depicts the time series of suitability scores predicted for bivalves in Rias

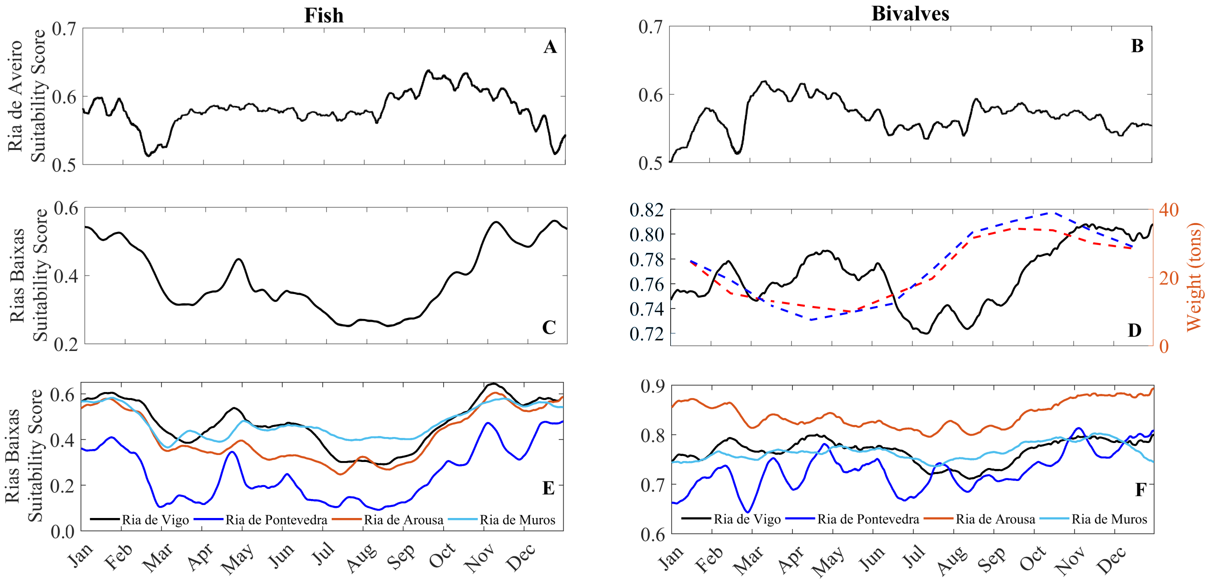

Figure 8.8: Integral suitability score for fish and bivalves in Ria de Aveiro and Rias Baixas. A - Fish suitability for Ria de Aveiro; B - Bivalves suitability for Ria de Aveiro; D - Fish suitability for Rias Baixas; D - Bivalves suitability for Rias Baixas. Red and blue dashed lines corresponds to *Mytilus galloprovincialis* in 2017 and 2018, respectively; E - Fish suitability for each estuary of Rias Baixas; F - Bivalves suitability for each estuary of Rias Baixas.

Baixas (black line), but also the temporal evolution of *Mytilus galloprovincialis* production in Rias Baixas for 2017 (red dashed line) and 2018 (blue dashed line). The model results predict high suitability scores during spring, as consequence of the typical phytoplankton bloom, decreasing from May to August, and increasing again until November, when the maximum score is achieved. During the upwelling season, the bivalves fed and grew, reaching the late autumn/early winter with the desired production conditions.

The comparison of model results with the real production weight in 2017 and 2018, shows agreement between measurements and predictions. The model indicates maximum production in November, while the data shows that it occurs in October. The main discrepancy occurs during spring, when model predicts high suitability that is not confirmed by production weight data.

The temporal evolution of suitability score for each ria individually is depicted in Figure 8.8 E and F. The temporal variability pattern depicted in Figures 8.8 C and D is also observed in each ria individually (Figures 8.8 E and F). Ria de Vigo is considered by the model as the best estuary for fish production, while Ria de Arousa is the most suitable location for bivalves cages, confirming the local distribution of mussels cages. In fact, Ria de Arousa is responsible for 69% of the total Rias Baixas production (2318 rafts). On the other hand, the model confers to Ria de Pontevedra the less suitable condition for fish and bivalves exploitation.

8.4 Discussion

Marine aquaculture has experienced gradual increase at a worldwide scale in the last century, and is expected to be further developed due to a combined effect of the decrease of wild stock and increase of human population. These global concerns ultimately demands a sustainable development of aquaculture practices. Therefore, guidelines for management strategies were defined for the period 2014-2020 by European Union to increase and diversify the marine food production in order to satisfy the growing demand and local development. Following the aim of these guidelines, this work addressed to set and map the potentially suitable areas for fish and bivalves cultures, according to a selection of descriptors based on geomorphological, hydrodynamic and water quality conditions, including the individual and integrated analysis of each descriptor.

As analyzed in the previous chapter, the definition of suitable areas for aquaculture exploitation is highly related with the different geomorphological, hydrological and biogeochemical processes of Ria de Aveiro and Rias Baixas. First of all, aquaculture expansion at Ria de Aveiro is highly inhibited by its geomorphology (low depth, high intertidal flats and narrowness of the channels). However, these characteristics trigger higher water temperatures, making Ria de Aveiro suitable for fish cages implementation, in opposition with deep V-shaped estuaries, which water temperature is more than 3°C below the desirable threshold for fish production. The local vertical structure, a homogeneous water column in opposition to a partially mixed estuarine system, also influences fish suitability. The strong vertical gradient of water temperature and the low oxygen concentration from mid-water column to the bottom of Rias Baixas (predicted by the model in accordance with the measurements analyzed in Chapter 3), disallow fish inshore aquaculture. Results for Ria de Aveiro fish and bivalves suitability indicate that the upstream areas of the lagoon are the most vulnerable from the water quality point of view, in agreement with Lopes et al. (2005) findings. This pattern also highlights the importance of advective processes in the water quality of Ria de Aveiro, in opposition to Rias Baixas dynamics, where vertical gradients are more important than the horizontal.

The hydrodynamic and water quality models simulate changes during a year in water quality conditions, while the observed data is collected at discrete periods and exposed to natural and anthropogenic impacts, most of the times with unknown extension in time and space. This fact coupled with the natural uncertainties of the water quality model helps to explain the uncertainties observed in Figure 8.8 D.

Generally, Rias Baixas offer excellent conditions for bivalves aquaculture, while Ria de Aveiro offers relatively suitable conditions both for fish and bivalves cultures. Nevertheless, in agreement with other studies for different coastal systems (Perez et al., 2005; Vincenzi et al., 2006; Longdill et al., 2008; Silva et al., 2011), the existence of several uses and users of the marine environment may restrict the implementation of aquaculture in the locations that are considered suitable by the model developed. Therefore, important social-economic constraints, such as water sports, recreational navigation, fishing activities, port areas, natural reserves, etc., should take place with the least conflict as possible with aquaculture activities. In this context, all the stakeholders and users interests should be taken into account in the coastal plans managements, in order to integrate all the possible conflicting uses (McKindsey et al., 2006).

The validation of the inferred habitat suitability for aquaculture exploitation, considering all the selected descriptors, was performed against data on the presence/absence of aquaculture in both coastal systems. This cross-validation revealed that the areas presently under aquaculture exploitation strongly match with medium to highly favourable areas regarding the habitat suitability for aquaculture exploitation, inferred from model results. This validation is more precise for the Rias Baixas once the *Mytilus galloprovincialis* production is inshore and totally dependent on the water quality conditions. Here, 100% of mussel cages are in areas considered medium, good and suitable by the model.

The extension of suitable, good and medium areas for fish or bivalves production does not estimate physical, ecological, social and production carrying capacities, but identify location where this carrying capacity may be optimized if the sustainability is maintained. The assessment of the upper limits of aquaculture production given the environmental limits and social acceptability for natural ecosystem and the social functions, requires more information and data about the local economy, social development of the region and stocking densities.

Despite the present habitat model portraits the usefulness of this type of methodologies as a planning tool for aquaculture management, the final model should be subjected to discussion between scientific community and stakeholders, from the following point of views: (1) firstly, this study is based on physical, thermohaline and ecological characteristics of the water column, however there are some additional exogenous or endogenous factors influencing fish or bivalves growth: type of sediment, bottom slope, pollutants, pathogens, predators and competitors and other forms of natural or anthropogenic disturbance (Vincenzi et al., 2006); (2) some ambiguity/subjectivity in the application of *VSF* relationships and in the criterion weights obtained from the pairwise comparison matrix. Despite these eventual uncertainties, the *VSF* relationships are crucial for the multi-criteria evaluation technique and for the integration of several datasets. From the literature, there are almost no standardised datasets of suitability or sustainability descriptors for coastal or inshore aquaculture, beyond those presented in several studies that also adopts ambiguity in their studies (Vincenzi et al., 2006; Silva et al., 2011). Nevertheless, this information is necessary for the establishment and implementation of the habitat model.

In this context, the methodology adopted in the scope of this study may be a helpful tool to marine area planning and management, not providing a definitive answer to a given problem, but generating outputs from a wide range of data and information (Perez et al., 2005), that can support and assist the decision making process.

Foreseeing the potentialities of future complementary work to increase the knowledge already acquired in this chapter, the main suggestions are the following: (1) perform a sensitivity analysis of parameters weights w_i, since they are probably the most critical and subjective step of the habitat model; (2) test different percentiles (Equation 8.3) and different POT values (higher and lower than the value assumed in this study - 0.6); (3) assess the influence of extreme events on aquaculture suitability, such as the high freshwater inflow for different return periods: 2, 10 and 100 years (Lopes et al., 2014), or storm-surge occurrences; (4) replicate the methodology developed in this chapter to evaluate the response of the habitat suitability model to different scenarios of sea level rise, studying future conditions under climate change through the methodology developed here.

Moreover, particularly in Ria de Aveiro, dredging operations are being carried out in order to improve the safety of navigable channels, which may change the water fluxes and current velocities, as already occurred in the past (Costa, 2016). Therefore, as most thermohaline and ecological processes are based on hydrodynamics, define dredging scenarios may provide an important overview about the anthropogenic effects on aquaculture production.

8.5 Conclusions

This study focused on the identification of the most suitable and sustainable locations for inshore aquaculture management support within Ria de Aveiro and Rias Baixas. The analysis performed is only based on natural conditions, excluding the uses and users layers, as well as anthropogenic impacts. Identifying suitable and productive sites is crucial to guarantee environmental sustainability and economic development of aquaculture settlement. Particularly in Ria de Aveiro, which is under international protection by Natura 2000 network, and is classified as Special Protection Area (SPA) by the Birds Directive, the results achieved in this chapter might be integrated with the maps of the protected areas, in order to maintain the ecosystem healthy, even with the expected growth of aquaculture.

The results achieved in this chapter allowed to draw the following main conclusions:

- Ria de Aveiro lagoon is more suitable for fish cultures than Rias Baixas. Indeed, settlement of fish cages in the Spanish estuaries is not recommended by the habitat suitability model;

- Despite the good conditions for bivalves production in Ria de Aveiro, the habitat model confers to Rias Baixas an excellent location for these practices;

- In accordance with the conclusions achieved in Chapter 7, aquaculture in Ria de Aveiro is mainly limited by geomorphological (low depth, intertidal flats and narrowness) and hydrodynamic characteristics (LRT descriptor limits from mid-channels to upstream areas of lagoon areas). On the other hand, fish aquaculture in Rias Baixas is limited by thermohaline processes and by the vertical gradients of dissolved oxygen promoted by the development of summer stratification (in agreement with Chapter 3 results).

- So, the differences in the mechanisms governing water quality conditions in Ria de Aveiro and Rias Baixas, and consequently aquaculture suitability, result from the differences in coastal system stratification, a vertical homogeneous, shallow and narrow lagoon, in opposition to estuaries partially mixed, deep and with a V-shaped geometry;

- Habitat suitability model suggests that fish and bivalves production in Ria de Aveiro is under-explored, since suitability conditions do not reflect the number of companies operating in the region. These results are in line with the European Union's strategies for the coming decades, attributing to Portugal the necessity for investment in aquaculture sector in order to respond to a population with high fish consumption per capita (60 kg/year);

- Rias Baixas habitat suitability model confirms the strong presence and exploitation of shellfish in the region. Additionally, the unsuitability for fish cultures is corroborated by the absence of companies producing pelagic fish.

The numerical modelling approach combined with the multi-critera evaluation technique allowed to consider a high number of hardly compatible variables, integrating them in order to generate outputs that are very useful for coastal mangers and investors. Therefore, this work shows that the methodology developed here for this two Iberian coastal systems is effective for the identification of the optimal sites for the exploitation of aquaculture species. This tool can be replicated and/or adapted in future studies for other estuaries, lagoons or other semi-enclosed bays.

The methodology implemented and described is efficient for increase the knowledge about the environmental conditions to proper aquaculture exploitation, in order to target new investments and give clairvoyance in the decision-making process. Therefore, the mapping obtained in this chapter may be a very effectual tool to plan and design fish and bivalves concessions. However, these results need a certain level of criticism, since the models are build and developed based on the best available information and are a simplification of natural complex systems.

Chapter 9

Final Conclusions and Future Work

The main goal of this thesis was to identify the suitable locations of fish and bivalves cultures expansion in Ria de Aveiro and Rias Baixas, based on the principles of sustainability and on the environmental conditions favourable to their development. To achieve this specific objective, four numerical models were implemented: two hydrodynamic models (one for each coastal system), which formed the basis for the implementation of two additional water quality models. Moreover, a habitat model was also developed to integrate and convert the numerical model results into maps of aquaculture suitability. Although, summary conclusions were presented at the end of each chapter, an overview of the main conclusions and some future work suggestions are summarized in this final chapter.

Chapter 2, besides characterizing the study areas, provides insights about the types of aquaculture that are carried out in each of the coastal system, allowing to draw two main conclusions: Ria de Aveiro aquaculture is under-exploited, while *Mytilus galloprovincialis* production in Rias Baixas is extensive and highly productive. Through the characterization performed in this chapter, it was realized that was necessary to study the vertical dynamics of the Rias Baixas (due to vertical distribution of the mussels (Duarte et al., 2008)), besides the horizontal processes.

In this context, an assessment of vertical profiles of water temperature, salinity, density, irradiance and dissolved oxygen concentration data was carried out in Chapter 3, in order to evaluate the influence of water column stratification in environmental factors that rules *Mytilus galloprovincialis* production. The results show that there is a strong relationship between the seasonal variability of water column stratification and the vertical gradients of dissolved oxygen and irradiance, proving that stratification causes hypoxia and low primary production in bottom layers of the estuaries. However, these environmental phenomena does not highly affect mussels exploitation, since the oxygen and phytoplankton depletion occurs for depths higher than 20 meters, where production no longer takes place (maximum length of mussel rafts ropes is 12 meters). Data analysis shows that mussels may have higher growth rates between 2 and 15 meters deep.

The modelling system Delft 3-D was used to study the hydrodynamic and biogeochemical processes in Ria de Aveiro and Rias Baixas (Chapter 4). Calibration and validation results (Chapter 5) of hydrodynamic and water quality models evidence that they accurately reproduce both the horizontal and vertical processes (case of Rias Baixas) within the coastal systems, highlighting their adequate application (2-D model application in Ria de Aveiro *vs* 3-D model in Rias Baixas) to characterize their local dynamics and processes.

One year sampling, with monthly periodicity, of water temperature, salinity, pH and chlorophyll *a* concentration at 12 stations distributed within Ria de Aveiro, was performed in the scope of Chapter 6. The resulting dataset is the best available for Ria de Aveiro lagoon, and was essential to achieve the objectives of this thesis. The analysis of this dataset allowed the study of seasonal and longitudinal variability of biophysical variables, but also the data necessary to perform the validation procedure of Ria de Aveiro water quality model. The Delft3D model was firstly applied to integrate *in situ* data with modelling results, in order to assess primary production dependence on biotic and abiotic factors. Results evidence that when the lagoon is not light limited (between March and September), the primary production is governed by nutrients variability. During these periods, the nutrients depletion caused by phytoplankton uptake limits lagoon primary production. These results provide an update of Ria de Aveiro biogeochemical knowledge, since scientific community (Lopes et al., 2007a, 2015) classified Ria de Aveiro as nutrient limited during the entire year. This chapter also demonstrates for the fist time, that hydrodynamic processes are the main limiting factor of primary production close to rivers mouth.

In Chapter 7 the assessment and comparison of Ria de Aveiro and Rias Baixas hydrodynamic functioning and water renewal times were carried out, under two different scenarios: summer and winter conditions. The results for both coastal systems show that water renewal rates are higher during winter season. Despite Ria de Aveiro and Rias Baixas have similar LRT seasonal patterns, they are governed by different phenomena: advective processes govern water exchange in Ria de Aveiro, while renewal rates are governed by the water column stratification in Rias Baixas, reflecting the differences in their estuarine classification: a homogeneous lagoon in opposition to partially mixed estuarine systems. Additionally, Rias Baixas have better hydrodynamic conditions and water renewal rates than Ria de Aveiro. The complex geomorphology of Ria de Aveiro promotes water retention from mid to upstream channels areas. These results are very important in the estimation of aquaculture quality in coastal and estuarine systems, since the supply of food (nutrients and phytoplankton) and oxygen to culture sites is highly dependent on water renewal rates (Boghen, 1989). Furthermore, LRT is one of the most important environmental descriptors for the implementation of the suitability habitat model, allowing the identification of favourable locations for aquaculture exploitation.

Finally, in Chapter 8, high resolution maps for fish and bivalves suitability for Ria de Aveiro and Rias Baixas were determined, based on the integration of the numerical models results with a habitat suitability model implementation. Maps evidences that upstream areas of Ria de Aveiro channels are unsuitable both for fish and bivalves cultures, while the suitable areas are located in the central area of the channels (away from the intertidal areas). The model also predicts higher suitability areas for bivalves production (31%), comparing with fish (22%). Regarding Rias Baixas, maps show more extreme patterns: almost total suitability for bivalves exploitation, and almost total unsuitability for fish production. Indeed, the validation of this habitat suitability model was carried out against data on the presence/absence of aquaculture in Ria de Aveiro and Rias Baixas. Areas currently under aquaculture exploitation overall matched with medium, good and suitable areas predicted by the habitat suitability model. Ria de Aveiro has a wide area where aquaculture is strongly limited by local geomorphology: low depth hinders fish cultures; narrow and shallow channels cause higher water retention. Fish production in Rias Baixas is highly limited by low water temperature (annual average of 13.3°C) and dissolved oxygen concentration (concentrations below 3 mg/L at the bottom layers). As widely discussed throughout the thesis, Ria de Aveiro and Rias Baixas are two very distinct coastal systems, and the habitat model was able to respond appropriately to both systems dynamics, proving their suitability for different coastal systems, from different regions.

Attending these results, the mapping of aquaculture suitability in Ria de Aveiro and Rias Baixas regions was successfully achieved by applying a habitat suitability conceptual model. However, it should be highlighted that the results obtained here have an uncertainty associated, and must be evaluated with certain level of criticism. In fact, it is recognized among the scientific community that there is an underlying uncertainty associated to the estimation of suitable areas based on habitat models (Silva et al., 1999; Vincenzi et al., 2006; Perez et al., 2005; Dubois and Habbane, 2002). Potential uncertainties can derive from different sources: biogeochemical variables are quite difficult to model, since they strongly depend on each other; water quality models are based on flows and volumes generated by hydrodynamic models, which accuracy depends on the precision of bathymetric data measurements, on model parametrizations and on the grid resolution (Lopes, 2016); some ambiguity on the appliance of the ranges of environmental variables considered suitable and unsuitable for aquaculture, and on the relative weight considered for each descriptor. Furthermore, in coastal systems like Ria de Aveiro and Rias Baixas, there are complex and important interactions between water column and bottom sediments. The processes occurring in the sediment layers were over-parametrized, constituting one of the most important limitations of this study. Finally, the lack of available data made difficult and time consuming the calibration and validation procedures of Ria de Aveiro water quality model.

Despite the model limitations above mentioned, the methodological approach followed in the scope of this study produced reliable results on identifying the suitable areas for aquaculture production, and can be applied to other estuaries/ lagoons/ lakes/ rivers worldwide. Particularly, part of the methodology assembled here is being reproduced within the AquiMap project (`http://aquimap.myscispot.eu/`), in order to assess aquaculture suitability in 11 estuaries and lagoons (Minho, Lima, Mondego, Tagus, Mira, Sado estuaries and Ria de Aveiro, Óbidos, Albufeira, Alvor and Ria Formosa lagoons) along Portuguese coast, for several types of fish and bivalves species.

Finally, this thesis demonstrated the usefulness of numerical models on supporting the management and planning programs, moving towards sustainability, which is highlighted by different national and international organizations. The achievement of the main goal of this study seems to be a very important contribution to the sustainable territorial planning and environmental management of Ria de Aveiro and Rias Baixas, enabling the adequate targeting of new investments, promoting a sustainable development of the economy of the sea and ensuring the good ecological status of the estuarine environment, as stipulated for example in Portuguese Maritime Spatial Planning (PSOEM). This study proves to be an important step forward in the planning of human activities, green economy and environmental sustainability, in agreement with the strategic objectives defined by European Union for the current period, which aim to increase and diversify the aquaculture production in a sustainable manner, in order to satisfy the growing demand and local development. In this context, the results achieved here should be integrated with the interests of the lagoonal and estuarine uses and users, to achieve a sustainable balance between the environmental, economic, social and leisure sectors.

Concerning to future work, more tests about habitat suitability model should be done, such as a sensitivity analysis on the relative weights of each descriptor. The exploitation of different threshold values of POT may also provide additional detailed information about the model behaviour. Furthermore, the evaluation of aquaculture suitability under extreme events (high freshwater inflow, storm surges, heat waves and sea level rise projections) may also give news insights about the most vulnerable areas in these coastal systems. Finally, future work to be performed consists on the dissemination of the thesis results by local communities and territorial managers.

As final remarks, this thesis comprised a multidisciplinary approach in two contrasting coastal system, contributing to deep the knowledge about water quality status and to target aquaculture exploitation, through the integration between *in situ* data analysis and numerical model approaches. The overall initial goals were successfully achieved despite the above-mentioned supplementary work that may improve the methodology applied.

References

Abdelrhman, M. A. (2005). Simplified modeling of flushing and residence times in 42 embayments in New England, USA, with special attention to Greenwich Bay, Rhode Island. *Estuarine, Coastal and Shelf Science*, 62(1-2):339–351.

Abowei, J. F. N. (2010). Salinity, dissolved oxygen, pH and surface water temperature conditions in Nkoro River, Niger Delta, Nigeria. *Advance Journal of Food Science and Technology*, 2(1):36–40.

Aguilar-Manjarrez, J. and Ross, L. G. (1995). Geographical information system (GIS) environmental models for aquaculture development in Sinaloa State, Mexico. *Aquaculture International*, 3(2):103–115.

Alarcon, J. F. and Villanueva, M. L. (2001). Using Geographic Information Systems as a site selection tool for aquaculture. *Aquaculture 2001: Book of Abstracts*, World Aquaculture Society, Louisiana State University, Balton Rouge, LA, USA, 7 pp.

Allen, J. I., Holt, J. T., Blackford, J., and Proctor, R. (2007). Error quantification of a high-resolution coupled hydrodynamic-ecosystem coastal-ocean model: Part 2. Chlorophyll-a, nutrients and SPM. *Journal of Marine Systems*, 68(3-4):381–404.

Almeida, M. A., Cunha, M. A., and Alcântara, F. (2005). Relationship of bacterioplankton production with primary production and respiration in a shallow estuarine system (Ria de Aveiro, NW Portugal). *Microbiological Research*, 160(3):315–328.

Alonso-Pérez, F., Ysebaert, T., and Castro, C. (2010). Effects of suspended mussel culture on benthic–pelagic coupling in a coastal upwelling system (Ría de Vigo, NW Iberian Peninsula). *Journal of Experimental Marine Biology and Ecology*, 382(2):96–107.

Alvarez, I., Decastro, M., Gomez-Gesteira, M., and Prego, R. (2005). Inter-and intra-annual analysis of the salinity and temperature evolution in the Galician Rías Baixas–ocean boundary (northwest Spain). *Journal of Geophysical Research: Oceans*, 110(C4):1–14.

Alvarez, I., DeCastro, M., Gomez-Gesteira, M., and Prego, R. (2006). Hydrographic behavior of the Galician Rias Baixas (NW Spain) under the spring intrusion of the Miño River. *Journal of Marine Systems*, 60(1-2):144–152.

Alvarez, I., Dias, J. M., deCastro, M., Vaz, N., Sousa, M. C., and Gómez-Gesteira, M. (2013). Influence of upwelling events on the estuaries of the north-western coast of the Iberian Peninsula. *Marine and Freshwater Research*, 64(12):1123–1134.

Álvarez-Salgado, X. A., Gago, J., Mıguez, B. M., Gilcoto, M., and Pérez, F. F. (2000). Surface waters of the NW Iberian margin: Upwelling on the shelf versus outwelling of upwelled waters from the Rıas Baixas. *Estuarine, Coastal and Shelf Science*, 51(6):821–837.

Álvarez-Salgado, X. A., Rosón, G., Pérez, F. F., Figueiras, F. G., and Pazos, Y. (1996). Nitrogen cycling in an estuarine upwelling system, the Ria de Arousa (NW Spain). I. Short-time-scale patterns of hydrodynamic and biogeochemical circulation. *Marine Ecology Progress Series*, 135:259–273.

AMRia/CPU (2006). Plano Intermunicipal de Ordenamento da Ria de Aveiro – Relatório do Plano, versão final (Intermunicipal Plan for the Ria de Aveiro – Plan Report, final version), CPU Urbanistas e Arquitectos LDA, Association of the municipalities of the Ria de Aveiro, Portugal, Aveiro.

Aneiros, F., Rubal, M., Troncoso, J. S., and Bañón, R. (2015). Subtidal benthic megafauna in a productive and highly urbanised semi-enclosed bay (Ría de Vigo, NW Iberian Peninsula). *Continental Shelf Research*, 110:16–24.

Anjum, N. A., Ahmad, I., Válega, M., Pacheco, M., Figueira, E., Duarte, A. C., and Pereira, E. (2012). Salt marsh macrophyte Phragmites australis strategies assessment for its dominance in mercury-contaminated coastal lagoon (Ria de Aveiro, Portugal). *Environmental Science and Pollution Research*, 19(7):2879–2888.

Araujo, I. (2006). Sea level variability: examples from the Atlantic coast of Europe. PhD thesis, School of the National Oceanography Centre, Southampton, UK, 216 pp.

Arid, H., Moudni, H., Orbi, A., Talbaoui, M., Lakhdar Idrissi, J., Massik, Z., Masski, H., Littaye, A., and Paoli, R. (2005). Remote sensing and GIS for Integrated Management of Aquaculture potentialities. *European Space Agency (Special Publication)*, 584:121–129.

Arndt, S., Lacroix, G., Gypens, N., Regnier, P., and Lancelot, C. (2011). Nutrient dynamics and phytoplankton development along an estuary–coastal zone continuum: a model study. *Journal of Marine Systems*, 84(3-4):49–66.

Arneborg, L. (2004). Turnover times for the water above sill level in Gullmar Fjord. *Continental Shelf Research*, 24(4-5):443–460.

Arnold, W. S., White, M. W., Norris, H. A., and Berrigan, M. E. (2000). Hard clam (*Mercenaria spp.*) aquaculture in Florida, USA: geographic information system applications to lease site selection. *Aquacultural Engineering*, 23(1-3):203–231.

Arsenault, D. J. and Himmelman, J. H. (1998). Spawning of the Iceland scallop (*Chlamys islandica*) in the northern Gulf of St. Lawrence and its relationship to temperature and phytoplankton abundance. *Veliger*, 41(2):180–185.

Asokan, P. K., Laxmilatha, P., Surendranath, V. G., and Sivadasan, M. P. (2011). Site selection for mussel culture. *Central Marine Fisheries Research Institute*, 7:19–26.

Azevedo, A. (2018). Intertidal seagrass modelling in a mesotidal coastal lagoon. PhD thesis, University of Aveiro, 219 pp.

Azevedo, A., Sousa, A. I., Lencart e Silva, J. D., Dias, J. M., and Lillebø, A. I. (2013). Application of the generic DPSIR framework to seagrass communities of Ria de Aveiro: a better understanding of this coastal lagoon. *Journal of Coastal Research*, SI 65:19–24.

Baluyut, E. A. and Balnyme, E. (1995). Aquaculture systems and practices: a selected review. Daya Publishing House, 90 pp.

Béjaoui, B., Solidoro, C., Harzallah, A., Chevalier, C., Chapelle, A., Zaaboub, N., and Aleya, L. (2017). 3D modeling of phytoplankton seasonal variation and nutrient budget in a southern Mediterranean Lagoon. *Marine Pollution Bulletin*, 114(2):962–976.

Bermúdez, M., Pietrzak, J. D., Cea, L., Puertas, J., Stelling, G. S., and De Boer, G. J. (2013). A numerical study of mixing and stratification dynamics in the ría de Arousa estuary (NW Spain) during summer. *Proceeding Coastal Dynamic*, France, 24-28 June:161–172.

Boghen, A. D. (1989). Cold-water aquaculture in Atlantic Canada. Canadian Institute for Research on Regional Development Moncton, Canada, 410 pp.

Boyd, C. E. and Schmittou, H. (1999). Achievement of sustainable aquaculture through environmental management. *Aquaculture Economics & Management*, 3(1):59–69.

Boyd, C. E. and Tucker, C. S. (2012). Pond aquaculture water quality management. Springer Science & Business Media, 700 pp.

Brooks, D. A., Baca, M. W., and Lo, Y. T. (1999). Tidal circulation and residence time in a macrotidal estuary: Cobscook Bay, Maine. *Estuarine, Coastal and Shelf Science*, 49(5):647–665.

Brown, P. and Hutchings, L. (1987). The development and decline of phytoplankton blooms in the southern Benguela upwelling system. 2. Nutrient relationships. *South African Journal of Marine Science*, 5(1):393–409.

Bum, B. K. and Pick, F. R. (1996). Factors regulating phytoplankton and zooplankton biomass in temperate rivers. *Limnology and Oceanography*, 41(7):1572–1577.

Burwell, D., Vincent, M., Luther, M., and Galperin, B. (2000). Modeling residence times: Eulerian vs Lagrangian. *Estuarine and Coastal Modeling*, VA:995–1009.

Camacho, R. A., Martin, J. L., Watson, B., Paul, M. J., Zheng, L., and Stribling, J. B. (2014). Modeling the factors controlling phytoplankton in the St. Louis Bay Estuary, Mississippi and evaluating estuarine responses to nutrient load modifications. *Journal of Environmental Engineering*, 141(3):04014067.

Carballo, R., Iglesias, G., and Castro, A. (2009). Residual circulation in the Ria de Muros (NW Spain): a 3D numerical model study. *Journal of Marine Systems*, 75(1-2):116–130.

Cardia, F. and Lovatelli, A. (2015). Aquaculture operations in floating HDPE cages: a field handbook. FAO Fisheries and Aquaculture Technical Paper, 152 pp.

Castro, M. d., Álvarez, I., Varela, M., Prego, R., and Gómez-Gesteira, M. (2006). Miño River dams discharge on neighbor Galician Rias Baixas (NW Iberian Peninsula): Hydrological, chemical and biological changes in water column. *Estuarine, Coastal and Shelf Science*, 70(1-2):52–62.

Cerco, C. F. and Cole, T. (1993). Three-dimensional eutrophication model of Chesapeake Bay. Technical report. *Journal of Engineering*, 119(6):1006–1025.

Cerejo, M. and Dias, J. M. (2007). Tidal transport and dispersal of marine toxic microalgae in a shallow, temperate coastal lagoon. *Marine Environmental Research*, 63(4):313–340.

Cermeno, P., Maranón, E., Pérez, V., Serret, P., Fernández, E., and Castro, C. G. (2006). Phytoplankton size structure and primary production in a highly dynamic coastal ecosystem (Ría de Vigo, NW-Spain): Seasonal and short-time scale variability. *Estuarine, Coastal and Shelf Science*, 67(1-2):251–266.

Consalvey, M., Perkins, R. G., Paterson, D. M., and Underwood, G. J. C. (2005). PAM fluorescence: a beginners guide for benthic diatomists. *Diatom Research*, 20(1):1–22.

Corner, R. A., Brooker, A. J., Telfer, T., and Ross, L. G. (2006). A fully integrated GIS-based model of particulate waste distribution from marine fish-cage sites. *Aquaculture*, 258(1-4):299–311.

Costa, S. M. (2016). Suspended sediments in Ria de Aveiro: Present and future dynamics. PhD thesis, University of Aveiro, 205 pp.

Culberson, S. D. and Piedrahita, R. H. (1996). Aquaculture pond ecosystem model: temperature and dissolved oxygen prediction—mechanism and application. *Ecological Modelling*, 89(1-3):231–258.

da Silva, J. F. and Duck, R. W. (2001). Historical changes of bottom topography and tidal amplitude in the Ria de Aveiro, Portugal trends for future evolution. *Climate Research*, 18(1-2):17–24.

Dahms, H. U. (2014). The grand challenges in marine pollution research. *Frontiers in Marine Science*, 1:1–5.

Dale, A. W., Prego, R., Millward, G. E., and Gómez-Gesteira, M. (2004). Transient oceanic and tidal contributions to water exchange and residence times in a coastal upwelling system in the NE Atlantic: the Pontevedra Ria, Galicia. *Marine Pollution Bulletin*, 49(3):235–248.

deCastro, M., Gomez-Gesteira, M., Alvarez, I., and Prego, R. (2004). Negative estuarine circulation in the Ria of Pontevedra (NW Spain). *Estuarine, Coastal and Shelf Science*, 60(2):301–312.

DeCastro, M., Gómez-Gesteira, M., Prego, R., Taboada, J. J., Montero, P., Herbello, P., and Pérez-Villar, V. (2000). Wind and tidal influence on water circulation in a Galician ria (NW Spain). *Estuarine, Coastal and Shelf Science*, 51(2):161–176.

Deltares (2006a). Delft3D-Flow user manual. Delft, the Netherlands, 684 pp.

Deltares (2006b). Delft3D-WAQ user manual. Delft, the Netherlands, 392 pp.

Deltares (2018). Delft3D Flexible Mesh Suite user manual . Delft, the Netherlands, 470 pp.

DeMenocal, P., Ortiz, J., Guilderson, T., and Sarnthein, M. (2000). Coherent high- and low-latitude climate variability during the holocene warm period. *Science*, 288(5474):2198–2202.

Des, M., deCastro, M., Sousa, M. C., Dias, J. M., and Gómez-Gesteira, M. (2019). Hydrodynamics of river plume intrusion into an adjacent estuary: The Minho River and Ria de Vigo. *Journal of Marine Systems*, 189:87–97.

Dias, J. M. (2001). Contribution to the study of the Ria de Aveiro hydrodynamics. PhD thesis, University of Aveiro, 288 pp.

Dias, J. M., Abrantes, I., and Rocha, F. (2007). Suspended particulate matter sources and residence time in a mesotidal lagoon. *Journal of Coastal Research*, SI 50:1034–1039.

Dias, J. M. and Fernandes, E. H. (2006). Tidal and subtidal propagation in two atlantic estuaries: Patos lagoon (Brazil) and Ria de Aveiro lagoon (Portugal). *Journal of Coastal Research*, SI 39:1422–1426.

Dias, J. M. and Lopes, J. F. (2006). Implementation and assessment of hydrodynamic, salt and heat transport models: the case of Ria de Aveiro Lagoon (Portugal). *Environmental Modelling & Software*, 21(1):1–15.

Dias, J. M., Lopes, J. F., and Dekeyser, I. (1999). Hydrological characterisation of Ria de Aveiro, Portugal, in early summer. *Oceanologica Acta*, 22(5):473–485.

Dias, J. M., Lopes, J. F., and Dekeyser, I. (2000). Tidal propagation in Ria de Aveiro lagoon, Portugal. *Physics and Chemistry of the Earth, Part B: Hydrology, Oceans and Atmosphere*, 25(4):369–374.

Dias, J. M., Lopes, J. F., and Dekeyser, I. (2001). Lagrangian transport of particles in Ria de Aveiro lagoon, Portugal. *Physics and Chemistry of the Earth, Part B: Hydrology, Oceans and Atmosphere*, 26(9):721–727.

Dias, J. M., Lopes, J. F., and Dekeyser, I. (2003). A numerical system to study the transport properties in the Ria de Aveiro lagoon. *Ocean Dynamics*, 53(3):220–231.

Dias, J. M. and Mariano, S. (2011). Numerical modelling of hydrodynamic changes induced by a jetty extension: the case of Ria de Aveiro (Portugal). *Journal of Coastal Research*, SI 64:1008–1012.

Dias, J. M. and Picado, A. (2011). Impact of morphologic anthropogenic and natural changes in estuarine tidal dynamics. *Journal of Coastal Research*, SI 64:1490–1494.

Dias, J. M., Sousa, M. C., Bertin, X., Fortunato, A. B., and Oliveira, A. (2009). Numerical modeling of the impact of the Ancão Inlet relocation (Ria Formosa, Portugal). *Environmental Modelling & Software*, 24(6):711–725.

Díaz, P. A., Álvarez, G., Varela, D., Pérez-Santos, I., Díaz, M., Molinet, C., Seguel, M., Aguilera-Belmonte, A., Guzmán, L., Uribe, E., Rengel, J., Hernandez, C., Segura, C., and Figueroa, R. I. (2019). Impacts of harmful algal blooms on the aquaculture industry: Chile as a case study. *Perspectives in Phycology*, 6(1-2):39–50.

Doval, M. D., Nogueira, E., and Pérez, F. F. (1998). Spatio-temporal variability of the thermohaline and biogeochemical properties and dissolved organic carbon in a coastal embayment affected by upwelling: the Ria de Vigo (NW Spain). *Journal of Marine Systems*, 14(1-2):135–150.

Duarte, P., Labarta, U., and Fernández-Reiriz, M. J. (2008). Modelling local food depletion effects in mussel rafts of Galician Rias. *Aquaculture*, 274(2-4):300–312.

Duarte, P., Meneses, R., Hawkins, A., Zhu, M., Fang, J., and Grant, J. (2003). Mathematical modelling to assess the carrying capacity for multi-species culture within coastal waters. *Ecological Modelling*, 168(1-2):109–143.

Dubois, J. M. and Habbane, M. (2002). Methodology of Regional aquaculture zoning using the aid of teledetection in IRS. *The Canadian Geographer*, 46(2):172–185.

Egna, H. S. and Boyd, C. E. (1997). Dynamics of pond aquaculture. CRC press, 472 pp.

Fernández-Reiriz, M. J., Labarta, U., and Babarro, J. M. F. (2001). Relaciones funcionales del comportamiento alimentario del mejillón (*Mytillus galloprovincialis*) en relación al seston natural en las rías gallegas. *Acuicultura y Desarrollo Sostenible.*, Consejería de Ganaderia, Agricultura y Pesca, Santander:296–300.

Ferrarin, C., Ghezzo, M., Umgiesser, G., Tagliapietra, D., Camatti, E., Zaggia, L., and Sarretta, A. (2013). Assessing hydrological effects of human interventions on coastal systems: numerical applications to the Venice Lagoon. *Hydrology and Earth System Sciences*, 17(5):1733.

Ferreira, J. G., Hawkins, A. J. S., Monteiro, P., Moore, H., Edwards, A., Goven, R., Lourenco, P., Mellor, A., Nunes, J. P., and Ramos, L. (2007). SMILE-sustainable mariculture in northern Irish lough ecosystems: assessment of carrying capacity for environmentally sustainable shellfish culture in Carlingford Lough, Strangford Lough, Belfast Lough, Larne Lough and Lough Foyle. Institute of Marine Research, 98 pp.

Ferreira, J. G., Simas, T., Nobre, A., Silva, M. C., Shifferegger, K., and Lencarrt-Silva, J. (2003). Identification of sensitive areas and vulnerable zones in transitional and coastal portuguese systems: application of the united states national estuarine eutrophication assessment to the Minho, Lima, Douro, Ria de Aveiro, Mondego, Tagus, Sado, Mira, Ria Formosa and Guadiana systems. INAG, 151 pp.

Figueiras, F., Gómez, E., Nogueira, E., and Villarino, M. (1996). Selection of Gymnodinium catenatum under downwelling conditions in the Ria de Vigo. *In Yasumoto, T., Oshima, Y & Fubkuyo, Y (eds)*, Intergovernmental Oceanographic Comission of UNESCO, Paris:215–218.

Figueiras, F. and Ríos, A. (1993). Phytoplankton succession, red tides and the hydrographic regime in the Rias Bajas of Galicia. *Developments in Marine Biology*, 5th International conference on toxic marine phytoplankton:239–244.

Figueiras, F. G., Jones, K. J., Mosquera, A. M., Alvarez-Salgado, X. A., Edwards, A., and MacDougall, N. (1994). Red tide assemblage formation in an estuarine upwelling ecosystem: Ria de Vigo. *Journal of Plankton Research*, 16(7):857–878.

Figueiras, F. G., Labarta, U., and Reiriz, M. J. F. (2002). Coastal upwelling, primary production and mussel growth in the Rías Baixas of Galicia. *Hydrobiologia*, 484(1-3):121–131.

Fiori, E., Zavatarelli, M., Pinardi, N., Mazziotti, C., and Ferrari, C. R. (2016). Observed and simulated trophic index (TRIX) values for the Adriatic Sea basin. *Natural Hazards and Earth System Sciences*, 16(9):2043–2054.

Fiúza, A., Hamann, M., Ambar, I., del Rıéo, G. D., González, N., and Cabanas, J. M. (1998). Water masses and their circulation off western Iberia during May 1993. *Deep Sea Research Part I: Oceanographic Research Papers*, 45(7):1127–1160.

Fortunato, A. B., Rodrigues, M., Dias, J. M., Lopes, C. L., and Oliveira, A. (2013). Generating inundation maps for a coastal lagoon: a case study in the Ria de Aveiro (Portugal). *Ocean Engineering*, 64:60–71.

Froján, M., Castro, C. G., Zúñiga, D., Arbones, B., Alonso-Pérez, F., and Figueiras, F. G. (2018). Mussel farming impact on pelagic production and respiration rates in a coastal upwelling embayment (Ría de Vigo, NW Spain). *Estuarine, Coastal and Shelf Science*, 204:130–139.

Fry, V. A. and Aubrey, D. G. (1990). Tidal velocity asymmetries and bedload transport in shallow embayments. *Estuarine, Coastal and Shelf Science*, 30(5):453–473.

García, A., Juanes, J. A., Álvarez, C., Revilla, J. A., and Medina, R. (2010). Assesment of the response of a shallow macrotidal estuary to changes in hydrological and wastewater inputs through numerical modelling. *Ecological Modelling*, 221(8):1194–1208.

García-Moreiras, I., Delgado, C., Martínez-Carreño, N., García-Gil, S., and Sobrino, C. M. (2019). Climate and vegetation changes in coastal ecosystems during the Middle Pleniglacial and the early Holocene: Two multi-proxy, high-resolution records from Ría de Vigo (NW Iberia). *Global and Planetary Change*, 176:100–122.

García-Oliva, M., Pérez-Ruzafa, Á., Umgiesser, G., McKiver, W., Ghezzo, M., De Pascalis, F., and Marcos, C. (2018). Assessing the hydrodynamic response of the Mar Menor Lagoon to dredging inlets interventions through numerical modelling. *Water*, 10(7):959.

Gibbs, M. M., James, M. R., Pickmere, S. E., Woods, P. H., Shakespeare, B. S., Hickman, R. W., and Illingworth, J. (1991). Hydrodynamic and water column properties at six stations associated with mussel farming in Pelorus Sound, 1984–85. *New Zealand Journal of Marine and Freshwater Research*, 25(3):239–254.

Gimpel, A., Stelzenmüller, V., Töpsch, S., Galparsoro, I., Gubbins, M., Miller, D., Murillas, A., Murray, A. G., Pınarbaşı, K., Roca, G., and Watret, R. (2018). A GIS-based tool for an integrated assessment of spatial planning trade-offs with aquaculture. *Science of the Total Environment*, 627:1644–1655.

Giovanardi, F. and Vollenweider, R. A. (2004). Trophic conditions of marine coastal waters: experience in applying the Trophic Index TRIX to two areas of the Adriatic and Tyrrhenian seas. *Journal of Limnology*, 63(2):199–218.

Gómez-Gesteira, M., deCastro, M., and Prego, R. (2003). Dependence of the water residence time in Ria of Pontevedra (NW Spain) on the seawater inflow and the river discharge. *Estuarine, Coastal and Shelf Science*, 58(3):567–573.

Gómez-Gesteira, M., DeCastro, M., Prego, R., and Pérez-Villar, V. (2001). An unusual two layered tidal circulation induced by stratification and wind in the Rıa of Pontevedra (NW Spain). *Estuarine, Coastal and Shelf Science*, 52(5):555–563.

Guneroglu, A., Kose, E., Eruz, C., Basar, E., and Erkebay, S. (2005). Use of geographic information system (GIS) to select fish cage farming sites in Surmene Bay, Black Sea. *Israeli Journal of Aquaculture*, 57(2):81–89.

Handisyde, N. T., Ross, L. G., Badjeck, M. C., and Allison, E. H. (2014). The effects of climate change on world aquaculture: a global perspective. Aquaculture and Fish Genetics Research Programme, Stirling Institute of Aquaculture. Final Technical Report, DFID, Stirling, 151 pp.

Hanson, R. B., Alvarez-Ossorio, M. T., Cal, R., Campos, M. J., Roman, M., Santiago, G., Varela, M., and Yoder, J. A. (1986). Plankton response following a spring upwelling event in the Ria de Arosa, Spain. *Marine Ecology Progress Series*, 32:101–113.

Hwang, J., Kim, S., Seo, Y., Lee, K., Park, C., Choi, Y., Kim, D., Gilad, A. A., and Choi, J. (2018). Mechanisms of salinity control in sea bass. *Biotechnology and Bioprocess Engineering*, 23:271–277.

Ibarra, E. and Prego, R. (1997). La Ria de Pontevedra: Revisión de su conocimiento. *Monografıas de Quımica Oceanográfica*, 1:55–87.

Iglesias, G. and Carballo, R. (2009). Seasonality of the circulation in the Ría de Muros (NW Spain). *Journal of Marine Systems*, 78(1):94–108.

Iglesias, G. and Carballo, R. (2010). Effects of high winds on the circulation of the using a mixed open boundary condition: the Ría de Muros, Spain. *Environmental Modelling & Software*, 25(4):455–466.

Iglesias, G., Carballo, R., and Castro, A. (2008). Baroclinic modelling and analysis of tide-and wind-induced circulation in the Ría de Muros (NW Spain). *Journal of Marine Systems*, 74(1-2):475–484.

Irigoien, X. and Castel, J. (1997). Light limitation and distribution of chlorophyll pigments in a highly turbid estuary: the Gironde (SW France). *Estuarine, Coastal and Shelf Science*, 44(4):507–517.

Jayanthi, M., Thirumurthy, S., Muralidhar, M., and Ravichandran, P. (2018). Impact of shrimp aquaculture development on important ecosystems in India. *Global Environmental Change*, 52:10–21.

Jiang, L. and Xia, M. (2018). Modeling investigation of the nutrient and phytoplankton variability in the Chesapeake Bay outflow plume. *Progress in Oceanography*, 162:290–302.

Josefson, A. B. and Rasmussen, B. (2000). Nutrient retention by benthic macrofaunal biomass of Danish estuaries: importance of nutrient load and residence time. *Estuarine, Coastal and Shelf Science*, 50(2):205–216.

Kalantzi, I. and Karakassis, I. (2006). Benthic impacts of fish farming: meta-analysis of community and geochemical data. *Marine Pollution Bulletin*, 52(5):484–493.

Katavić, I. and Dadić, V. (2000). Environmental consideration of mariculture: A case from Croatia. *Periodicum Biologorum*, 102(1):23–30.

Keller, A., Taylor, C., Oviatt, C., Dorrington, T., Holcombe, G., and Reed, L. (2001). Phytoplankton production patterns in Massachusetts Bay and the absence of the 1998 winter–spring bloom. *Marine Biology*, 138(5):1051–1062.

Koutitonsky, V. G., Guyondet, T., St-Hilaire, A., Courtenay, S. C., and Bohgen, A. (2004). Water renewal estimates for aquaculture developments in the Richibucto estuary, Canada. *Estuaries*, 27(5):839–850.

Krysanova, V., Wechsung, F., Arnold, J., Srinivasan, R., and Williams, J. (2000). SWIM (soil and water integrated model) user manual, Potsdam Institute for Climate Impact Research, 239 pp.

Lai, H. and Lin, J. (2009). Degradation of oxolinic acid and flumequine in aquaculture pond waters and sediments. *Chemosphere*, 75(4):462–468.

Laing, I. and Spencer, B. (2006). Bivalve cultivation: criteria for selecting a site. Science series, Technical report no. 136, 33 pp.

Lawson, T. (2013). Fundamentals of aquacultural engineering. Springer Science & Business Media, 355 pp.

Lawson, T. B. (1995). Water quality and environmental requirements. *Aquacultural Engineering*, Springer:12–39.

Leal, M. C., Jesus, B., Ezequiel, J., Calado, R., Rocha, R. J. M., Cartaxana, P., and Serôdio, J. (2015). Concurrent imaging of chlorophyll fluorescence, chlorophyll a content and green fluorescent proteins-like proteins of symbiotic cnidarians. *Marine Ecology*, 36(3):572–584.

Lessin, G. and Raudsepp, U. (2007). Modelling the spatial distribution of phytoplankton and inorganic nitrogen in Narva Bay, southeastern Gulf of Finland, in the biologically active period. *Ecological Modelling*, 201(3-4):348–358.

Li, M., Zhong, L., and Boicourt, W. C. (2005). Simulations of Chesapeake Bay estuary: Sensitivity to turbulence mixing parameterizations and comparison with observations. *Journal of Geophysical Research: Oceans*, 110(C12):1–22.

Longdill, P. C., Healy, T. R., and Black, K. P. (2008). An integrated GIS approach for sustainable aquaculture management area site selection. *Ocean & Coastal Management*, 51(8-9):612–624.

Lopes, C. B., Lillebø, A. I., Dias, J. M., Pereira, E., Vale, C., and Duarte, A. C. (2007a). Nutrient dynamics and seasonal succession of phytoplankton assemblages in a Southern European Estuary: Ria de Aveiro, Portugal. *Estuarine, Coastal and Shelf Science*, 71(3-4):480–490.

Lopes, C. B., Pereira, M. E., Vale, C., Lillebø, A. I., Pardal, M. Â., and Duarte, A. C. (2007b). Assessment of spatial environmental quality status in Ria de Aveiro (Portugal). *Scientia Marina*, 71(2):293–304.

Lopes, C. L. (2016). Flood risk assessment in Ria de Aveiro under present and future scenarios. PhD thesis, University of Aveiro, 224 pp.

Lopes, C. L., Alvarez, I., and Dias, J. M. (2014). Ria de Aveiro marginal flooding: dependence on oceanic and fluvial drivers and on morphological evolution. *Avances en ciencias de la tierra*, (5):23–31.

Lopes, C. L., Azevedo, A., and Dias, J. M. (2013). Flooding assessment under sea level rise scenarios: Ria de Aveiro case study. *Journal of Coastal Research*, SI 65:766–772.

Lopes, C. L. and Dias, J. M. (2014). Influence of mean sea level rise on tidal dynamics of the Ria de Aveiro lagoon, Portugal. *Journal of Coastal Research*, SI 70:574–580.

Lopes, C. L., Silva, P. A., Dias, J. M., Rocha, A., Picado, A., Plecha, S., and Fortunato, A. B. (2011). Local sea level change scenarios for the end of the 21st century and potential physical impacts in the lower Ria de Aveiro (Portugal). *Continental Shelf Research*, 31(14):1515–1526.

Lopes, J. F., Almeida, M. A., and Cunha, M. A. (2010). Modelling the ecological patterns of a temperate lagoon in a very wet spring season. *Ecological Modelling*, 221(19):2302–2322.

Lopes, J. F. and Dias, J. M. (2007). Residual circulation and sediment distribution in the Ria de Aveiro lagoon, Portugal. *Journal of Marine Systems*, 68(3-4):507–528.

Lopes, J. F., Dias, J. M., Cardoso, A. C., and Silva, C. (2005). The water quality of the Ria de Aveiro lagoon, Portugal: From the observations to the implementation of a numerical model. *Marine Environmental Research*, 60(5):594–628.

Lopes, J. F., Dias, J. M., and Dekeyser, I. (2001). Influence of tides and river inputs on suspended sediment transport in the Ria de Aveiro lagoon, Portugal. *Physics and Chemistry of the Earth, Part B: Hydrology, Oceans and Atmosphere*, 26(9):729–734.

Lopes, J. F., Dias, J. M., and Dekeyser, I. (2006). Numerical modelling of cohesive sediments transport in the Ria de Aveiro lagoon, Portugal. *Journal of Hydrology*, 319(1-4):176–198.

Lopes, J. F. and Silva, C. (2006). Temporal and spatial distribution of dissolved oxygen in the Ria de Aveiro lagoon. *Ecological Modelling*, 197(1-2):67–88.

Lopes, J. F., Silva, C. I., and Cardoso, A. C. (2008). Validation of a water quality model for the Ria de Aveiro lagoon, Portugal. *Environmental Modelling & Software*, 23(4):479–494.

Lopes, J. F., Vaz, N., Vaz, L., Ferreira, J. A., and Dias, J. M. (2015). Assessing the state of the lower level of the trophic web of a temperate lagoon, in situations of light or nutrient stress: a modeling study. *Ecological Modelling*, 313:59–76.

Lorenzen, C. J. (1967). Determination of chlorophyll and pheo-pigments: spectrophotometric equations. *Limnology and Oceanography*, 12(2):343–346.

MacKenzie, A. L. and Gillespie, P. A. (1986). Plankton ecology and productivity, nutrient chemistry, and hydrography of Tasman Bay, New Zealand, 1982–1984. *New Zealand Journal of Marine and Freshwater Research*, 20(3):365–395.

MacKenzie, L. and Adamson, J. (2004). Water column stratification and the spatial and temporal distribution of phytoplankton biomass in Tasman Bay, New Zealand: implications for aquaculture. *New Zealand Journal of Marine and Freshwater Research*, 38(4):705–728.

Malhadas, M. S., Silva, A., Leitão, P. C., and Neves, R. (2009). Effect of the bathymetric changes on the hydrodynamic and residence time in Óbidos Lagoon (Portugal). *Journal of Coastal Research*, SI 56:549–553.

Mantzavrakos, E., Kornaros, M., Lyberatos, G., and Kaspiris, P. (2007). Impacts of a marine fish farm in Argolikos Gulf (Greece) on the water column and the sediment. *Desalination*, 210(1-3):110–124.

MAOT/INAG (2012). Revisão do Plano de Ordenamento da Orla Costeira Ovar – Marinha Grande, Fase 1: Relatório 2, Volume I – Caracterização e Diagnóstico Prospetivo (Review of Coastal Zone Management Plan Ovar – Marinha Grande), 188 pp.

Maréchal, D. (2004). A soil-based approach to rainfall-runoff modelling in ungauged catchments for England and Wales. PhD thesis, Cranfield University, 145 pp.

Margalef, R. (1956). Estructura y dinámica de la "purga de mar" en la Ría de Vigo. *Investigacion Pesquera*, V:113–134.

Margalef, R. and Fraga, F. (1979). Estudio y explotación del mar en galicia. *Investigacion Pesquera*, 5:255–263.

McKindsey, C. W., Thetmeyer, H., Landry, T., and Silvert, W. (2006). Review of recent carrying capacity models for bivalve culture and recommendations for research and management. *Aquaculture*, 261(2):451–462.

Melià, P., De Leo, G. A., and Gatto, M. (2004). Density and temperature-dependence of vital rates in the Manila clam *Tapes philippinarum*: a stochastic demographic model. *Marine Ecology Progress Series*, 272:153–164.

Mendes, R., Vaz, N., and Dias, J. M. (2011). Numerical modeling changes induced by the low lying areas adjacent to Ria de Aveiro. *Journal of Coastal Research*, SI 64:1125–1129.

Montero, P., Gómez-Gesteira, M., Taboada, J. J., Ruiz-Villarreal, M., Santos, A. M. P., Neves, R., Prego, R., and Pérez-Villar, V. (1999). On residual circulation of the Ria of Vigo, using a 3-D baroclinic model. *Scientia Marina*, 65(1):277–289.

Moreira, M. H., Queiroga, H., Machado, M. M., and Cunha, M. R. (1993). Environmental gradients in a southern Europe estuarine system: Ria de Aveiro, Portugal implications for soft bottom macrofauna colonization. *Netherland Journal of Aquatic Ecology*, 27(2-4):465–482.

Morgado, F., Queiroga, H., Melo, F., and Sorbe, J. (2003). Zooplankton abundance in a coastal station off the Ria de Aveiro inlet (north-western Portugal): relations with tidal and day/night cycles. *Acta Oceanologica*, 24:175–181.

Nash, J. E. and Sutcliffe, J. V. (1970). River flow forecasting through conceptual models part I—A discussion of principles. *Journal of Hydrology*, 10(3):282–290.

Nassar, M. Z. and Hamed, M. A. (2003). Phytoplankton standing crop and species diversity in relation to some water characteristics of Suez Bay (Red Sea), Egypt. *Egyptian Journal of Aquatic Biology & Fisheries*, 7(3):25–48.

Nebel, C., Romestand, B., Nègre-Sadargues, G., Grousset, E., Aujoulat, F., Bacal, J., Bonhomme, F., and Charmantier, G. (2005). Differential freshwater adaptation in juvenile sea-bass *Dicentrarchus labrax*: involvement of gills and urinary system. *Journal of Experimental Biology*, 208(20):3859–3871.

O'Donncha, F., James, S. C., and Ragnoli, E. (2017). Modelling study of the effects of suspended aquaculture installations on tidal stream generation in Cobscook Bay. *Renewable Energy*, 102:65–76.

Oliveira, A., Fortunato, A. B., and Dias, J. M. (2006). Numerical modeling of the Aveiro inlet dynamics. *Proceedings of 30th International Conference on Coastal Engineering*, World Scientific Publishing Co:3282–3294.

Ortigosa, G. R., De Leo, G. A., and Gatto, M. (2000). VVF: integrating modelling and GIS in a software tool for habitat suitability assessment. *Environmental Modelling & Software*, 15(1):1–12.

Otero, P., Ruiz-Villarreal, M., and Peliz, A. (2008). Variability of river plumes off Northwest Iberia in response to wind events. *Journal of Marine Systems*, 72(1-4):238–255.

Otto, L. (1975). Oceanography of the Ria de Arosa (NW-Spain). Leiden University, Leiden, 210 pp.

Outeiro, L., Byron, C., and Angelini, R. (2018). Ecosystem maturity as a proxy of mussel aquaculture carrying capacity in Ria de Arousa (NW Spain): A food web modeling perspective. *Aquaculture*, 496:270–284.

Pawlowicz, R., Beardsley, B., and Lentz, S. (2002). Classical tidal harmonic analysis including error estimates in MATLAB using T_TIDE. *Computers & Geosciences*, 28(8):929–937.

Pereira, C., Salvador, S., Arrojado, C., Silva, Y., Santos, A. L., Cunha, Â., Gomes, N., and Almeida, A. (2011). Evaluating seasonal dynamics of bacterial communities in marine fish aquaculture: a preliminary study before applying phage therapy. *Journal of Environmental Monitoring*, 13(4):1053–1058.

Pérez, F. F., Alvarezsalgado, X., Rosón, G., and Ríos, A. F. (1992). Carbonic-calcium system, nutrients and total organic nitrogen in continental runoff to the Galician Rias Baixas, NW Spain. *Acta Oceanologica*, 15(6):595–602.

Perez, O. M., Telfer, T. C., and Ross, L. G. (2005). Geographical information systems-based models for offshore floating marine fish cage aquaculture site selection in Tenerife, Canary Islands. *Aquaculture Research*, 36(10):946–961.

Pesce, M., Critto, A., Torresan, S., Giubilato, E., Santini, M., Zirino, A., Ouyang, W., and Marcomini, A. (2018). Modelling climate change impacts on nutrients and primary production in coastal waters. *Science of the Total Environment*, 628:919–937.

Picado, A., Dias, J. M., and Fortunato, A. B. (2009). Effect of flooding the salt pans in the Ria de Aveiro. *Journal of Coastal Research*, SI 56:1395–1399.

Picado, A., Dias, J. M., and Fortunato, A. B. (2010). Tidal changes in estuarine systems induced by local geomorphologic modifications. *Continental Shelf Research*, 30(17):1854–1864.

Picado, A., Silva, P. A., Fortunato, A. B., and Dias, J. M. (2011). Particle tracking-modeling of morphologic changes in the Ria de Aveiro. *Journal of Coastal Research*, SI 64:1560–1564.

Piedracoba, S., Álvarez-Salgado, X. A., Labarta, U., Fernández-Reiriz, M. J., Gómez, B., and Balseiro, C. (2014). Water flows through mussel rafts and their relationship with wind speed in a coastal embayment (Ría de Ares-Betanzos, NW Spain). *Continental Shelf Research*, 75:1–14.

Pitcher, G. C., Figueiras, F. G., Hickey, B. M., and Moita, M. T. (2010). The physical oceanography of upwelling systems and the development of harmful algal blooms. *Progress in Oceanography*, 85(1-2):5–32.

Platt, T., Fuentes-Yaco, C., and Frank, K. T. (2003). Marine ecology: spring algal bloom and larval fish survival. *Nature*, 423(6938):398.

Plecha, S. (2011). Contribution to the study of the Ria de Aveiro inlet morphodynamics. PhD thesis, University of Aveiro, 163 pp.

Plew, D. R. (2011). Shellfish farm-induced changes to tidal circulation in an embayment, and implications for seston depletion. *Aquaculture Environment Interactions*, 1(3):201–214.

Prego, R., Dale, A. W., Decastro, M., Gómez-Gesteira, M., Taboada, J. J., Montero, P., Villareal, M. R., and Pérez-Villar, V. (2001). Hydrography of the Pontevedra Ria: Intra-annual spatial and temporal variability in a Galician coastal system (NW Spain). *Journal of Geophysical Research: Oceans*, 106(C9):19845–19857.

Prego, R. and Fraga, F. (1992). A simple model to calculate the residual flows in a Spanish ria. Hydrographic consequences in the Ria of Vigo. *Estuarine, Coastal and Shelf Science*, 34(6):603–615.

Pusceddu, A., Fraschetti, S., Mirto, S., Holmer, M., and Danovaro, R. (2007). Effects of intensive mariculture on sediment biochemistry. *Ecological Applications*, 17(5):1366–1378.

Ranasinghe, R. and Pattiaratchi, C. (1998). Flushing characteristics of a seasonally-open tidal inlet: a numerical study. *Journal of Coastal Research*, 14(4):1405–1421.

Randall, D. J. and Tsui, T. K. N. (2006). Tribute to RG Boutilier: Acid–base transfer across fish gills. *Journal of Experimental Biology*, 209(7):1179–1184.

Raposo, C., Matos, J., and Monteiro, A. (2012). Plano de Gestão das Bacias Hidrográficas dos rios Vouga, Mondego e Lis Integradas na Região Hidrográfica 4: Parte 2–Caracterização da Região Hidrográfica. Administração da região Hidrográfica do Centro IP, Coimbra, 215 pp.

Ray, R. D. (1999). A global ocean tide model from TOPEX/POSEIDON altimetry: GOT99. 2. National Aeronautics and Space Administration, 66 pp.

Rebelo, J. E. (1992). The ichthyofauna and abiotic hydrological environment of the Ria de Aveiro, Portugal. *Estuaries*, 15(3):403–413.

Rippeth, T. P. and Simpson, J. H. (1996). The frequency and duration of episodes of complete vertical mixing in the Clyde Sea. *Continental Shelf Research*, 16(7):933–947.

Rodrigues, A. M., Quintino, V., Sampaio, L., Freitas, R., and Neves, R. (2011). Benthic biodiversity patterns in Ria de Aveiro, Western Portugal: Environmental-biological relationships. *Estuarine, Coastal and Shelf Science*, 95(2-3):338–348.

Rodrigues, M., Oliveira, A., Queiroga, H., Fortunato, A. B., and Zhang, Y. J. (2009). Three-dimensional modeling of the lower trophic levels in the Ria de Aveiro (Portugal). *Ecological Modelling*, 220(9-10):1274–1290.

Rosón, G., Álvarez-Salgado, X. A., and Pérez, F. F. (1997). A non-stationary box model to determine residual fluxes in a partially mixed estuary, based on both thermohaline properties: application to the Ria de Arousa (NW Spain). *Estuarine, Coastal and Shelf Science*, 44(3):249–262.

Rosón, G., Pérez, F. F., Alvarez-Salgado, X. A., and Figueiras, F. G. (1995). Variation of both thermohaline and chemical properties in an estuarine upwelling ecosystem: Ria de Arousa; I. Time evolution. *Estuarine, Coastal and Shelf Science*, 41(2):195–213.

Ross, L. G., Mendoza, E. A., and Beveridge, M. C. M. (1993). The application of geographical information systems to site selection for coastal aquaculture: an example based on salmonid cage culture. *Aquaculture*, 112(2-3):165–178.

Ruiz-Villarreal, M., Montero, P., Taboada, J. J., Prego, R., Leitao, P. C., and Pérez-Villar, V. (2002). Hydrodynamic model study of the Ria de Pontevedra under estuarine conditions. *Estuarine, Coastal and Shelf Science*, 54(1):101–113.

Saaty, T. L. (1977). A scaling method for priorities in hierarchical structures. *Journal of Mathematical Psychology*, 15(3):234–281.

Salonen, K. and Sarvala, J. (1995). Field manual for the determination of chlorophyll and primary production in Lake Tanganyika research. Finfish International Development Agency, Food and Agriculture Organization of the United Nations, 20 pp.

Santos, L., Vaz, L., Gomes, N. C. M., Vaz, N., Dias, J. M., Cunha, Â., and Almeida, A. (2014). Impact of freshwater inflow on bacterial abundance and activity in the estuarine system Ria de Aveiro. *Estuarine, Coastal and Shelf Science*, 138:107–120.

Sapkota, A., Sapkota, A. R., Kucharski, M., Burke, J., McKenzie, S., Walker, P., and Lawrence, R. (2008). Aquaculture practices and potential human health risks: current knowledge and future priorities. *Environment International*, 34(8):1215–1226.

Seeyave, S., Probyn, T., Álvarez-Salgado, X. A., Figueiras, F. G., Purdie, D. A., Barton, E. D., and Lucas, M. (2013). Nitrogen uptake of phytoplankton assemblages under contrasting upwelling and downwelling conditions: The Ría de Vigo, NW Iberia. *Estuarine, Coastal and Shelf Science*, 124:1–12.

Shepard, S., Beukers-Stewart, B., Hiddink, J. G., Brand, A. R., and Kaiser, M. J. (2010). Environmental variables and their influence on growth of the great scallop (*Pecten maximus*) in the English Channel. *Marine Biology*, 157:91–97.

Silva, C., Ferreira, J. G., Bricker, S. B., DelValls, T. A., Martín-Díaz, M. L., and Yáñez, E. (2011). Site selection for shellfish aquaculture by means of GIS and farm-scale models, with an emphasis on data-poor environments. *Aquaculture*, 318(3-4):444–457.

Silva, C., Olivarí, R., and Yany, G. (1999). Aquaculture site selection using a geographical information system. *Investigaciones marinas*, 27:93–99.

Silva, J. F., Duck, R., and Catarino, J. (2004). Seagrasses and sediment response to changing physical forcing in a coastal lagoon. *Hydrology and Earth Sciences*, 8(2):151–159.

Simpson, J. H. and Bowers, D. (1981). Models of stratification and frontal movement in shelf seas. *Deep Sea Research Part A. Oceanographic Research Papers*, 28(7):727–738.

Simpson, J. H., Crisp, D. J., and Hearn, C. (1981). The shelf-sea fronts: implications of their existence and behaviour. *Philosophical Transactions of the Royal Society of London*, 302(1472):531–546.

Simpson, J. H., Hughes, D. H., and Morris, N. C. G. (1977). The relation of the seasonal stratification to tidal mixing on the continental shelf. *A voyage of discovery*, Supplement of Deep-Sea Research:327–340.

Simpson, J. H., Sharples, J., and Rippeth, T. P. (1991). A prescriptive model of stratification induced by freshwater runoff. *Estuarine, Coastal and Shelf Science*, 33(1):23–35.

Skogen, M. D., Eknes, M., Asplin, L. C., and Sandvik, A. D. (2009). Modelling the environmental effects of fish farming in a Norwegian fjord. *Aquaculture*, 298(1-2):70–75.

Sobrino, C. M., García-Moreiras, I., Castro, Y., Carreño, N. M., de Blas, E., Rodríguez, C. F., Judd, A., and García-Gil, S. (2014). Climate and anthropogenic factors influencing an estuarine ecosystem from NW Iberia: new high resolution multiproxy analyses from San Simón Bay (Ría de Vigo). *Quaternary Science Reviews*, 93:11–33.

Soniat, T. M. and Brody, M. S. (1988). Field validation of a habitat suitability index model for the American oyster. *Estuaries*, 11(2):87–95.

Sousa, M. C. (2013). Modelling the Minho river plume intrusion into the Rias Baixas. PhD thesis, University of Aveiro, 136 pp.

Sousa, M. C., Mendes, R., Alvarez, I., Vaz, N., Gomez-Gesteira, M., and Dias, J. M. (2014a). Unusual circulation patterns of the rias Baixas induced by Minho Freshwater Intrusion (NW of the Iberian Peninsula). *PloS One*, 9(11):e112587.

Sousa, M. C., Ribeiro, A. S., Des, M., Mendes, R., Alvarez, I., Gomez-Gesteira, M., and Dias, J. M. (2018). Integrated high-resolution numerical model for the NW Iberian Peninsula coast and main estuarine systems. *Journal of Coastal Research*, SI 85:66–70.

Sousa, M. C., Vaz, N., Alvarez, I., Gomez-Gesteira, M., and Dias, J. M. (2014b). Modeling the Minho River plume intrusion into the Rias Baixas (NW Iberian Peninsula). *Continental Shelf Research*, 85:30–41.

Stalnacke, P., I Lillebø, A., and D Gooch, G. (2016). Coastal Lagoons in Europe: Integrated Water Resource Strategies. IWA Publishing, 256 pp.

Summerfelt, S. T., Vinci, B. J., Tucker, C., and Hargreaves, J. (2008). Better management practices for recirculating aquaculture systems. *Environmental Best Management Practices for Aquaculture*, Wiley Blackwell, Oxford, UK:389–426.

Tabuada, M. (2009). Aquacultura: estudo das condições ambientais internas de uma instalação. PhD thesis, Instituto Politécnico do Porto, 169 pp.

Torres-López, S., Álvarez-Salgado, X. A., and Varela, R. A. (2005). Offshore export versus *in situ* fractionated mineralization: a 1-D model of the fate of the primary production of the Rías Baixas (Galicia, NW Spain). *Journal of Marine Systems*, 54(1-4):175–193.

Trainer, V. L., Pitcher, G. C., Reguera, B., and Smayda, T. J. (2010). The distribution and impacts of harmful algal bloom species in eastern boundary upwelling systems. *Progress in Oceanography*, 85(1-2):33–52.

Trites, R. (1995). Physical oceanographic features of Letang Inlet including evaluation and results from a numerical model. Canadian technical report of hydrography and ocean sciences No. 163, 61 pp.

Umgiesser, G., Ferrarin, C., Cucco, A., De Pascalis, F., Bellafiore, D., Ghezzo, M., and Bajo, M. (2014). Comparative hydrodynamics of 10 Mediterranean lagoons by means of numerical modeling. *Journal of Geophysical Research: Oceans*, 119(4):2212–2226.

Valentim, J. M. (2012). Hydrodynamic Effects in Ria de Aveiro and Tagus Estuary Salt Marshes. Msc thesis, University of Aveiro, 81 pp.

Varela, M., Prego, R., and Pazos, Y. (2008). Spatial and temporal variability of phytoplankton biomass, primary production and community structure in the Pontevedra Ria (NW Iberian Peninsula): oceanographic periods and possible response to environmental changes. *Marine Biology*, 154(3):483–499.

Vaz, L. (2012). Hydrodynamic study of the wave effect in the Aveiro inlet. Msc thesis, University of Aveiro, 64 pp.

Vaz, L., Mateus, M., Serôdio, J., Dias, J. M., and Vaz, N. (2016). Primary production of the benthic microalgae in the bottom sediments of Ria de Aveiro lagoon. *Journal of Coastal Research*, SI 75:178–182.

Vaz, N. and Dias, J. M. (2008). Hydrographic characterization of an estuarine tidal channel. *Journal of Marine Systems*, 70(1-2):168–181.

Vaz, N., Dias, J. M., and Leitão, P. C. (2009). Three-dimensional modelling of a tidal channel: the Espinheiro Channel (Portugal). *Continental Shelf Research*, 29(1):29–41.

Vezzulli, L., Moreno, M., Marin, V., Pezzati, E., Bartoli, M., and Fabiano, M. (2008). Organic waste impact of capture-based Atlantic bluefin tuna aquaculture at an exposed site in the Mediterranean Sea. *Estuarine, Coastal and Shelf Science*, 78(2):369–384.

Vincenzi, S., Caramori, G., Rossi, R., and De Leo, G. A. (2006). A GIS-based habitat suitability model for commercial yield estimation of Tapes philippinarum in a Mediterranean coastal lagoon (Sacca di Goro, Italy). *Ecological Modelling*, 193(1-2):90–104.

Vollenweider, R. A., Giovanardi, F., Montanari, G., and Rinaldi, A. (1998). Characterization of the trophic conditions of marine coastal waters with special reference to the NW Adriatic Sea: proposal for a trophic scale, turbidity and generalized water quality index. *Environmetrics*, 9(3):329–357.

Warner, J. C., Geyer, W. R., and Lerczak, J. A. (2005). Numerical modeling of an estuary: A comprehensive skill assessment. *Journal of Geophysical Research: Oceans*, 110(C5):1–13.

Wiles, P. J., van Duren, L. A., Häse, C., Larsen, J., and Simpson, J. H. (2006). Stratification and mixing in the Limfjorden in relation to mussel culture. *Journal of Marine Systems*, 60(1-2):129–143.

Willmott, C. J. (1981). On the validation of models. *Physical geography*, 2(2):184–194.

Wool, T. A., Ambrose, R. B., Martin, J. L., Comer, E. A., and Tech, T. (2006). Water quality analysis simulation program (WASP). User's Manual, 268 pp.

Zeng, T. Q., Dorman, F., Ogburn, D., Derwent, L., and Williams, R. (2003). Aquaculture management with geographical information systems (GIS) in NSW fisheries, Australia. *Coastal GIS*, 1:454–66.

Zimmerman, J. T. F. (1976). Mixing and flushing of tidal embayments in the western Dutch Wadden Sea part I: Distribution of salinity and calculation of mixing time scales. *Netherlands Journal of Sea Research*, 10(2):149–191.